
UNIVERSITY OF KWAZULU-NATAL
SCHOOL OF MECHANICAL ENGINEERING
HOWARD COLLEGE

In fulfilment of the degree of
Master of Science in Mechanical Engineering
at the University of KwaZulu-Natal.

<p>PART CLAMPING AND FIXTURE GEOMETRIC ADAPTABILITY FOR RECONFIGURABLE ASSEMBLY SYSTEMS</p>
--

Christian Ivan Basson
216076946

November 2017

As the candidate's supervisor, I agree to the submission of this dissertation.

Dissertation Supervisor: Prof. Glen Bright

Dissertation Co-Supervisor: Dr. Anthony Walker

Declaration of Plagiarism

As the Candidate's Supervisor, I agree to the submission of this dissertation.

Signed:

Date:

Prof. Glen Bright

As the Candidate's Co-Supervisor, I agree to the submission of this dissertation.

Signed:

Date:

Dr. Anthony Walker

I declare this dissertation has not previously been submitted for any degree in this or any other university, and it is the student's (MSc. Eng. Christian Ivan Basson) own original work.

Signed: Date:

Christian Ivan Basson

I, Christian Ivan Basson, declare that:

- i. The research reported in the dissertation, except where otherwise indicated, and is my original work.
- ii. The dissertation has not been previously submitted for any degree or examination at any other university.
- iii. The dissertation does not contain other persons' data, pictures, graphs or information, except where specifically acknowledged as being referenced from sources.
- iv. The dissertation does not contain other persons' writing unless specifically acknowledged as being sourced from other researchers. Sources have been paraphrased to present general information that was attributed to the referenced citation. Exact wording and phrases have been directly quoted and referenced from source.
- v. In circumstance of any publication
- vi. The dissertation does not contain text, graphics, and tables that are replicated or/and duplicated from any source unless specifically acknowledged, and the source being detailed in the dissertation and/or reference sections.

Signed:

Date:

Declaration of Publications

Details of contribution to peer-reviewed publications that include research presented in the dissertation. The undersigned agree that the following submissions were made and accepted as described and that the content therein is contained in this research.

Publication 1 (Accepted): ICINCO 2017

Basson, C. Bright, G. & Walker, A., “Investigating geometric adaptability for flexible grippers in reconfigurable assembly systems”, *14th International Conference on Informatics in Control, Automation and Robotics*. Published July 2017, 6 Pages, 2017.

The paper was accepted in July 2017 in the Madrid, Spain.

Christian Basson was the lead author of this paper and conducted all research and experimentation under the supervision of Professor Glen Bright and Doctor Anthony Walker.

Publication 2 (Published): M2VIP 2017

Basson, C. Bright, G. & Walker, A., “Investigating geometric adaptability for flexible grippers in reconfigurable assembly systems”, *2017 IEEE 24TH International Conference on Mechatronics and Machine Vision in Practice (M2VIP2017)*. Published November 2017, 6 Pages, 2015.

The paper was published and presented in November 2017 in the Auckland, New Zealand.

Christian Basson was the lead author of this paper and conducted all research and experimentation under the supervision of Professor Glen Bright and Doctor Anthony Walker.

Publication 3 (Published): PRASA-RobMech 2015

Basson, C. Bright, G. & Walker, A., “Analysis of Flexible End-Effector for Geometric Conformity in Reconfigurable Assembly Systems”, *2015 PRASA-RobMech International Conference*. Published November 2017, 6 Pages, 2017.

The paper was published and presented in November 2017 in the Bloemfontein, South Africa.

Christian Basson was the lead author of this paper and conducted all research and experimentation under the supervision of Professor Glen Bright and Doctor Anthony Walker.

Publication 4 (Submitted): SAJIE 2017

Basson, C. Bright, G. & Walker, A., “Testing flexible grippers for geometric and surface grasping conformity in reconfigurable assembly systems”, *The South African Journal of Industrial Engineering*. Submitted November 2017, 15 Pages, 2017.

The paper was submitted in November 2017 in Stellenbosch, South Africa.

Christian Basson was the lead author of this paper and conducted all research and experimentation under the supervision of Professor Glen Bright and Doctor Anthony Walker.

Signed: Date: Mr. Christian Ivan Basson

Signed: Date: Prof. Glen Bright

Signed: Date: Dr. Anthony John Walker

Preface

A biologically inspired robotic gripper based on the Fin Ray Effect[®] was investigated to establish conformity properties for the performance of a robotic gripper system. As a result, the study established the optimization of self-adjusting end-effectors. The gripper system design focused on the force response application to the conformity of the gripper fingers. The gripper system design was simulated and empirically tested.

Signed:

Date:

Dedication

The dissertation is dedicated to those who inspired it and to those who will not read it.

“Necessity is the mother of invention”

~ Plato ~

Acknowledgements

- The work presented in the dissertation was carried out under the supervision of Prof. Glen Bright and Dr. Anthony Walker of the School of Mechanical Engineering, Howard College, University of KwaZulu-Natal.
- The author wishes to thank the “Blue Sky Research Grant” under the grant number 91339.
- In addition, acknowledgement is given to the National Research Foundation (NRF) towards this research. Opinions expressed and conclusions arrived at, are those of the authors and not necessarily to be attributed to the NRF.
- The author’s special thanks are extended to the staff of UKZN for the opportunity to present my work.
- The author would like to offer special thanks to Mr. I.E. Basson and Mrs. H. Basson for the encouragement and motivation throughout the progress of the project.
- The author would also like to express gratitude to Mr. S.E. Basson for always providing inspiration to always improve.

Abstract

The Fourth Industrial Revolution is leading towards cyber-physical systems which justified research efforts in pursuing efficient production systems incorporating flexible grippers. Due to the complexity of assembly processes, reconfigurable assembly systems have received considerable attention in recent years. The demand for the intricate task and complicated operations, demands the need for efficient robotic manipulators that are required to manoeuvre and grasp objects effectively. Investigations were performed to understand the requirements of efficient gripping systems and existing gripping methods. A biologically inspired robotic gripper was investigated to establish conformity properties for the performance of a robotic gripper system. The Fin Ray Effect[®] was selected as a possible approach to improve effective gripping and reduce slippage of component handling with regards to pick and place procedures of assembly processes. As a result, the study established the optimization of self-adjusting end-effectors. The gripper system design was simulated and empirically tested.

The impact of gripping surface compliance and geometric conformity was investigated. The gripper system design focused on the response of load applied to the conformity mechanism called the Fin Ray Effect[®]. The appendages were simulated to determine the deflection properties and stress distribution through a finite element analysis. The simulation proved that the configuration of rib structures of the appendages affected the conformity to an applied force representing an object in contact. The system was tested in real time operation and required a control system to produce an active performance of the system. A mass loading test was performed on the gripper system. The repeatability and mass handling range was determined. A dynamic operation was tested on the gripper to determine force versus time properties throughout the grasping movement for a pick and place procedure. The fluctuating forces generated through experimentation was related to the Lagrangian model describing forces experienced by a moving object. The research promoted scientific contribution to the investigation, analysis, and design of intelligent gripping systems that can potentially be implemented in the operational processes of on-demand production lines for reconfigurable assembly systems.

Keywords — Flexibility, Shape Conformity, Adaptability, Material Handling, Force Feedback, Force-Time Characteristics

Acronyms

AMS	Advanced Manufacturing Systems
RMS	Reconfigurable Manufacturing System
RAS	Reconfigurable Assembly Systems
PLC	Programmable Logic Controller
ABS	Acrylonitrile Butadiene Styrene
FRE	Fin Ray Effect®
AC	Alternating Current
DC	Direct Current
LIB	Lithium-Ion Battery
LiPo	Lithium-Ion Polymer
ISO	International Organisation of Standard
DH	Denavit Hartenberg
FANUC	Fuji Automatic Numerical Control
DOF	Degrees of Freedom
RoboDK	Robot Development Kit
HTM	Homogeneous Transformation Matrix
JM	Jacobian Matrix
R/C	Remote Control
PFS	Piezo-electric Force Sensor
FSR	Force Sensitive Resistor
NEMA	National Electrical Manufacturers Association
CAD	Computer Aided Drawing
FEA	Finite Element Analysis

Nomenclature

FUNDAMENTAL MECHANICS

<u>Symbol</u>	<u>Description</u>	<u>SI-unit</u>
F	Force	N
μ_s	Static Friction Coefficient	-
μ_k	Kinetic Friction Coefficient	-
g	Gravitational acceleration constant	m/s ²
SF	Safety Factor	-
M	Moment	N/m
L	Length	M
m	Mass	kg
I	2 nd Moment of Area	m ⁴
R	Radial Distance	M
W	Weight	N
a, b, c	Dimensions of length	m

FUNDAMENTAL STATISTICS

<u>Symbol</u>	<u>Description</u>	<u>SI-unit</u>
$\bar{X}, \bar{Y}, \bar{Z}$	Position Average	m
N	Number of Position Commands	-
i	Number of Iterations	-
$\bar{X}_c, \bar{Y}_c, \bar{Z}_c$	Position Commands	m
$\bar{X}_R, \bar{Y}_R, \bar{Z}_R$	Reached Position	m
l_i	Normal Length of Positions	m
\bar{l}	Normal Average Length of Positions	m
S_L	Standard Deviation	m
RP_L	Repeatability for Three Dimensions	mm / %

DENAVID-HARTENBERG MODEL

<u>Symbol</u>	<u>Description</u>	<u>SI-unit</u>
H_i	Denavit-Hartenberg Matrix	-
a_i	Link Length	m
α_i	Link Twist	rad / θ
d_i	Link Offset	m
θ_i	Joint Angle	rad / θ
$c\theta_i$	Cos Factor for Joint Angle	cos(θ_i)
$s\theta_i$	Sin Factor for Joint Angle	sin(θ_i)
$c\alpha_i$	Cos Factor for Link Twist	cos(α_i)
$s\alpha_i$	Sin Factor for Link Twist	sin(α_i)
T_n	Transformation Matrix	-
q_i	Position Vector	m
s_x, s_y, s_z	Relative Position to x-axis	m
n_x, n_y, n_z	Relative Position to y-axis	m
a_x, a_y, a_z	Relative Position to z-axis	m
P_x, P_y, P_z	End-effector Position	m

JACOBIAN MATRIX AND LANGRANGIAN FORCE MODEL

<u>Symbol</u>	<u>Description</u>	<u>SI-unit</u>
X	Displacement Vector Matrix	-
\dot{X}	Velocity Vector Matrix	-
\ddot{X}	Acceleration Vector Matrix	-
J	Displacement Jacobian Matrix	-
\dot{J}	Velocity Jacobian Matrix	-
\ddot{J}	Acceleration Jacobian Matrix	-
Q	Displacement Vector	m
\dot{Q}	Velocity Vector	m/s
\ddot{Q}	Acceleration Vector	m/s ²
$a(q)$	Definite Inertia Matrix	N
$b(q)$	Centripetal Forces	N
$c(q)$	Coriolis Forces	N
$g(q)$	Gravitational Forces	N
τ	Vector of Actuator Torques	N

TABLE OF CONTENTS

1	Introduction.....	1
1.1	Introduction.....	1
1.2	Background and Context of Study	1
1.3	Industrial Example for Flexible Gripping Application	2
1.4	Problem Statement	3
1.5	Overview	4
1.6	Research Questions	5
1.7	Hypothesis.....	6
1.8	Objectives	6
1.9	Description and General Methodology	7
1.10	Layout of Study.....	7
1.10.1	Scope.....	7
1.10.2	Layout	7
1.10.3	Target Audience.....	8
1.11	Conclusion	8
2	Literature Review.....	9
2.1	Introduction.....	9
2.2	Review of Traditional Fixturing Methods.....	10
2.3	Review of Flexible Fixture and Gripping Technology	12
2.3.1	Flexible Shape Gripping	13
2.3.2	Magnetic Gripping	14
2.3.3	Gripping by Jamming of Granular Material.....	15
2.3.4	Pin Matrix Gripping.....	16
2.3.5	Dry Adhesive Gripping	17
2.3.6	Electro-adhesive Gripping	18
2.3.7	Dextrous Gripping.....	19
2.3.8	Vacuum Gripping.....	20
2.3.9	Gripping Through the Fin Ray Effect®	21
2.4	Micro-Gripping	23
2.5	Quantifying Fixture Performance and Efficiency	24
2.6	Summary of Flexible Gripper Selection	25
2.7	Mechanical and Electronic Design	26
2.8	Typical Sensor System and Sensor Feedback Loop	27

2.9	Conclusion	28
3	Theory	29
3.1	Introduction.....	29
3.2	Gripping Force and Payload	29
3.2.1	Introduction.....	29
3.2.2	Determining Gripping Force.....	30
3.3	Precision Placement, Precise Location Control, and Repeatability	33
3.3.1	Introduction.....	33
3.3.2	Statistical Measurement	34
3.4	Kinematics of Robotic Arm	35
3.4.1	Introduction.....	35
3.4.2	Forward Kinematics: Denavit-Hartenberg (DH) Convention.....	36
3.5	The Fin Ray Effect®	37
3.5.1	Introduction.....	37
3.5.2	Fish Ray Effect® Mechanism	37
3.6	Conclusion	38
4	Methodology	39
4.1	Introduction.....	39
4.2	Research and Development.....	39
4.2.1	Specifications and Benchmark.....	39
4.2.2	Robotic Arm Selection.....	40
4.2.3	End effector Selection.....	41
4.2.4	Design Procedure	41
4.2.5	Simulation Procedure.....	42
4.3	Experimental Procedure.....	42
4.3.1	Test Specimen, Test Rig, and Apparatus	42
4.3.2	Configuration for Geometric Adaptability.....	43
4.3.3	Configuration for Precision and Repeatability.....	43
4.4	Data Capturing and Recording.....	43
4.4.1	Data Capturing Method.....	43
4.4.2	Results Interpretation	44
4.5	Conclusion	44
5	System Conceptual Design	45
5.1	Introduction.....	45

5.2	System Specifications	45
5.2.1	Types of States	45
5.2.2	Types of Grasps	46
5.2.3	Forces in Grasps.....	47
5.2.4	Grasp Stability	47
5.2.5	Sensing in Object Handling	48
5.2.6	Safety in Grasps	48
5.2.7	Repeatability	48
5.3	System Proposal and System Integration.....	49
5.4	Robotic Arm Concept Selection	51
5.4.1	Robotic Arm Selection.....	51
5.4.2	Path Planning for Operation.....	53
5.4.3	Kinematic and Dynamic Model Describing Forces Acting on Gripper.....	54
5.5	End Effector Concept Development	59
5.5.1	Gripper Selection	59
5.5.2	Material Selection	60
5.5.3	Finger Gripper Concept Model	60
5.5.4	Gripping Modes	61
5.6	Specimen Design	62
5.6.1	Specimen Geometry	62
5.7	Electronic Control	63
5.7.1	Pseudocode	63
5.7.2	Force Feedback Control	64
5.7.3	System Circuit Diagram Layout	64
5.7.4	Motor Selection.....	65
5.7.5	Motion Transmission Selection	66
5.7.6	Sensor Selection.....	66
5.8	Conclusion	68
6	System Embodiment Design.....	69
6.1	Introduction.....	69
6.2	Mechanical Design.....	69
6.2.1	3-Finger Gripper	69
6.2.2	4-Finger Gripper	71
6.3	Electronic Design.....	73
6.3.1	Microcontroller Board Layout	73
6.3.2	Sensory System Schematic	74

6.3.3	Motor Push-Button Control Schematic	74
6.4	System Proposed Budget and Energy Audit	75
6.5	Conclusion	75
7	System Computer Aided Simulation.....	77
7.1	Introduction.....	77
7.2	Simulation Procedure.....	77
7.3	Simulation Results	79
7.4	Conclusion	83
8	Manufacturing and Assembly	85
8.1	Introduction.....	85
8.2	3D Printing.....	85
8.3	3-D Printing of Appendages	86
8.4	Part Assembly	87
8.5	Electronic Assembly	88
8.6	Final Assembly onto Robotic Arm	89
8.7	Conclusion	90
9	Testing and Validation	91
9.1	Introduction.....	91
9.2	Safety Preparation for Experimentation.....	91
9.3	Test Preparation	92
9.4	Sensor Calibration.....	93
9.5	Path Plan for Robotic Arm.....	95
9.6	Dynamic Data Interpretation.....	95
9.7	Test Phase 1: Static Holding Mass Test Procedure.....	96
9.8	Test Phase 2: Dynamic Holding Force Test Procedure	98
9.8.1	Dynamic Test Run – Specimen: Cricket Ball	99
9.8.2	Dynamic Test Run for 3-Finger Gripper – Specimen: Sphere.....	100
9.8.3	Dynamic Test Run for 4-Finger Gripper – Specimen: Sphere.....	100
9.9	Test Phase 3: Dynamic and Static Visual Testing Procedure for Miscellaneous Parts.....	101
9.9.1	Test Specimen Weights.....	101
9.9.2	3-Finger Dynamic and Static Visual Testing Procedure.....	102
9.9.3	4-Finger Dynamic and Static Visual Testing Procedure.....	104
9.10	Conclusion	105
10	Results and Discussion	107

10.1	Introduction.....	107
10.2	Result Discussion.....	107
10.2.1	Appendage Conformity FEA Simulation.....	107
10.2.2	Test Phase 1: Static Holding Mass Test Procedure Results	108
10.2.3	Test Phase 2: Dynamic Holding Force Test Results	109
10.2.4	Test Phase 3: Dynamic and Static Visual Test Results	115
10.2.5	Summary of Gripper Test Performance	116
10.3	Industrial Application of Research	116
10.4	Scientific Contribution.....	117
10.5	Conclusion	117
11	Conclusion and Recommendations.....	119
11.1	Conclusion	119
11.2	Recommendations.....	120
	References.....	123
	APPENDIX A: Selection Criteria.....	A
	APPENDIX A.1: Flexible Gripping Technologies: Selection Matrix	A
	APPENDIX A.2: Flexible Gripping Technologies: Quality Function Deployment	B
	APPENDIX A.3: Proposed Budget for Gripper System.....	C
	APPENDIX A.4: Energy Audit	D
	APPENDIX B: Design.....	E
	APPENDIX B.1: 3-Finger Gripper Assembly	E
	APPENDIX B.2: 3-Finger Gripper Exploded View	F
	APPENDIX B.3: 4-Finger Assembly	G
	APPENDIX B.4: 4-Finger Exploded View	H
	APPENDIX B.5: Gripper Parts and Components.....	I
	APPENDIX B.6: Electronic Parts Catalogue Details	W
	APPENDIX B.7: Electronic Design	Z
	APPENDIX C: Simulation	BB
	APPENDIX C.1: Concept Design Simulation: Geometry 1 ABS Plastic.....	BB
	APPENDIX C.2: Concept Design Simulation: Geometry 1 NYLON	CC
	APPENDIX C.3: Concept Design Simulation: Geometry 2 ABS Plastic.....	DD
	APPENDIX C.4: Concept Design Simulation: Geometry 2 NYLON	EE
	APPENDIX C.5: Concept Design Simulation: Geometry 3 ABS Plastic.....	FF

APPENDIX C.6: Concept Design Simulation: Geometry 3 NYLON	GG
APPENDIX C.7: Concept Design Simulation: Geometry 4 ABS Plastic.....	HH
APPENDIX C.8: Concept Design Simulation: Geometry 4 NYLON	II
APPENDIX D: Testing.....	JJ
APPENDIX D.1: Sensor Calibration Data	JJ
APPENDIX D.2: Test Phase 1: Test Mass	KK
APPENDIX D.3: Test Phase 1: 3-Finger - Geometry 1.....	LL
APPENDIX D.4: Test Phase 1: 3- Finger - Geometry 2.....	LL
APPENDIX D.5: Test Phase 1: 3-Finger - Geometry 3.....	MM
APPENDIX D.6: Test Phase 1: 3-Finger - Geometry 4.....	MM
APPENDIX D.7: Test Phase 1: 4-Finger - Geometry 1.....	NN
APPENDIX D.8: Test Phase 1: 4-Finger - Geometry 2.....	NN
APPENDIX D.9: Test Phase 1: 4-Finger - Geometry 3.....	OO
APPENDIX D.10: Test Phase 1: 4-Finger - Geometry 4.....	OO
APPENDIX D.11: Test Phase 2: 4-Finger –Geometry 4 Initial Test Cricket Ball	PP
APPENDIX D.12: Test Phase 2: 3-Finger - Geometry 1.....	QQ
APPENDIX D.13: Test Phase 2: 3-Finger - Geometry 2.....	SS
APPENDIX D.14: Test Phase 2: 3-Finger - Geometry 3.....	UU
APPENDIX D.15: Test Phase 2: 3-Finger - Geometry 4.....	VV
APPENDIX D.16: Test Phase 2: 4-Finger - Geometry 1.....	XX
APPENDIX D.17: Test Phase 2: 4-Finger - Geometry 2.....	ZZ
APPENDIX D.18: Test Phase 2: 4-Finger - Geometry 3.....	AAA
APPENDIX D.19: Test Phase 2: 4-Finger - Geometry 4.....	CCC
APPENDIX E: System Code	EEE
APPENDIX E.1: Conceptual Path Planning Code	EEE
APPENDIX E.2: Sensor System Arduino® Code	FFF
APPENDIX E.3: Motor Push-Button Control Arduino® Code.....	GGG

List of Figures

Figure 1: Versatile robots in Tesla factory [3]	2
Figure 2: Simulation of hand grips [6]	3
Figure 3: Robotiq [®] adaptive gripper [8]	5
Figure 4: THIRA gripper [9]	5
Figure 5: Performance versus flexibility [11]	10
Figure 6: Schunk [®] 2-finger gripper [14]	12
Figure 7: Schunk [®] 3-finger gripper [14]	12
Figure 8: Festo's FlexShapeGripper [®] [16]	13
Figure 9: GOUDSMIT [®] Magnetic Gripper - Friction	15
Figure 10: Empire Robotics VERSABALL [®] - 65" head [19]	16
Figure 11: MATRIX Form Adapting Clamp System [®] [22]	16
Figure 12: Directional suction cups based on gecko feet [23]	18
Figure 13: Electro-adhesive gripping [27]	19
Figure 14: Volver fingers gripper [30]	19
Figure 15: Robotiq Adaptive Gripper [®] [8]	20
Figure 16: SCHMALZ [®] FXP-SVK 442 3R18 Vacuum gripper [32]	21
Figure 17: THIRA gripper [9]	22
Figure 18: FESTO's MultiChoice Gripper [®] [33]	22
Figure 19: Micro-gripping techniques [34]	23
Figure 20: Gripper system procedure	26
Figure 21: Gripper mechanical system outline	26
Figure 22: Typical sensor feedback loop	28
Figure 23: Feedback and control of gripper system	28
Figure 24: Friction force required for two and 3-fingered gripper [43]	30
Figure 25: Length shown in gripping geometry [43]	30
Figure 26: Gripping point L versus overhanging H [43]	31
Figure 27: Moments in all direction [43]	31
Figure 28: Moment of inertia all z -directions [43]	32
Figure 29: Allowable load torque [43]	33
Figure 30: Allowable thrust load [43]	33
Figure 31: Repeatability and accuracy [45]	34
Figure 32: Kinematic link and joint parameters [47]	36
Figure 33: Mechanism of the Fin Ray Effect [®] [48]	38
Figure 34: Robotic arm selection	41

Figure 35: Linkage a) and screw b) driven actuation gripping types.....	41
Figure 36: States and actions in object handling [50]	46
Figure 37: Typical grasps with grasp-type grippers [50]	47
Figure 38: Forces in grasps for gripping [50]	47
Figure 39: Gripper system conceptual model.	50
Figure 40: Conceptual closed-loop robotic system setup.	51
Figure 41: Visual representation of 6-DOF robotic arm [52]	52
Figure 42: BCN3D MOVEO robotic arm [53]	52
Figure 43: FANUC M-10iA robotic arm [54]	53
Figure 44: Experimental path plan.....	54
Figure 45: Assembly path plan.	54
Figure 46: Geometrical dimensions of the M-10iA [54]	55
Figure 47: The joint orientation of the M-10iA [54].....	55
Figure 48: Coordinate reference frames for M-10iA robotic arm [55]	56
Figure 49: Force attributes of a moving object [58]	58
Figure 50: BCN3D MOVEO gripper [53]	59
Figure 51: Dual fin gripper [59].....	59
Figure 52: Tri-max gripper [60].....	60
Figure 53: Rib structure design for appendages.....	61
Figure 54: 4-Finger gripper and 3-finger gripper design	61
Figure 55: Gripping modes for gripper system [33]	62
Figure 56: Specimen 1 – Design cube	62
Figure 57: Specimen 2 – Mass holder.....	63
Figure 58: Pseudocode for gripper system.....	63
Figure 59: Force sensor feedback loop	64
Figure 60: TB-6560 motor controller circuit diagram [62].....	65
Figure 61: Operation of the strain gauge.	67
Figure 62: Piezoelectric force sensor	67
Figure 63: Force sensitive resistor	67
Figure 64: FlexiForce pressure sensors.....	68
Figure 65: Assembly of 3-Finger gripper design	70
Figure 66: Exploded view and BOM of 3-finger gripper system	71
Figure 67: Assembly of 4-Finger gripper design	71
Figure 68: Exploded view and BOM of 3-finger gripper system	72
Figure 69: Design dimensions for NEMA 17 motor housing [70]	73
Figure 70: ARDUINO MEGA 2560 board layout [71]	73
Figure 71: Sensory system schematic	74
Figure 72: Motor push-button control schematic.....	75
Figure 73: Constraints and loads applied to the first Geometry structure.....	78
Figure 74: Convergence of iterative equation solver for linear statics	78
Figure 75: Non-linear iteration history for non-linear statics	79
Figure 76: Load step convergence solver for non-linear statics	79
Figure 77: Geometry 1 deflection and Von Mises stress result visual illustration for linear statics....	80
Figure 78: Geometry 2 deflection and Von Mises stress result visual illustration for linear statics....	80
Figure 79: Geometry 3 deflection and Von Mises stress result visual illustration for linear statics....	81
Figure 80: Geometry 4 deflection and Von Mises stress result visual illustration for linear statics....	81

Figure 81: Geometry 1 deflection and Von Mises stress result visual illustration for non-linear statics	82
Figure 82: Geometry 2 deflection and Von Mises stress result visual illustration for non-linear statics	82
Figure 83: Geometry 3 deflection and Von Mises stress result visual illustration for non-linear statics	83
Figure 84: Geometry 4 deflection and Von Mises stress result visual illustration for non-linear statics	83
Figure 85: Foundation scaffolding of the printed appendages.....	85
Figure 86: Layer build-up of the appendage.....	86
Figure 87: Final manufactured appendages.	86
Figure 88: Hinged type appendages.....	86
Figure 89: Flexible filament appendages.....	87
Figure 90: Unassembled components for gripper system.....	87
Figure 91: Assembled prototype of gripper system.	88
Figure 92: Sensory system assembly	88
Figure 93: Motor push-button control assembly.....	88
Figure 94: Electronic control board	89
Figure 95: Sensor installation	89
Figure 96: Power supply	89
Figure 97: Side view of robot arm and gripper system.....	90
Figure 98: Front view of robot arm and gripper system	90
Figure 99: Mass measurement of sample weights	92
Figure 100: Unloaded 3-finger gripper	92
Figure 101: Loaded 4-finger gripper with mass holder	92
Figure 102: Resistance verse force graph for FSR sensor calibration [73].....	93
Figure 103: Voltage verse force graph of different resistors for FSR sensor calibration [73].....	93
Figure 104: Mass vs voltage calibration graph for Sensor 1.....	94
Figure 105: Mass vs voltage calibration graph for Sensor 2.....	94
Figure 106: Mass vs voltage calibration graph for Sensor 3.....	94
Figure 107: Mass vs voltage calibration graph for Sensor 4.....	94
Figure 108: Pick and place path plan for gripper testing.	95
Figure 109: Gripping performance in terms of a force verse time graph [75]	95
Figure 110: 3-Finger gripper loading sequence 1-3 for mass holding test.....	97
Figure 111: 3-Finger gripper loading sequence 4-6 for mass holding test.....	97
Figure 112: 3-Finger gripper loading sequence 7-9 for mass holding test.....	97
Figure 113: Maximum mass hold for all four geometries for 3-finger gripper.....	97
Figure 114: Maximum mass hold for all four geometries for 4-finger gripper.....	98
Figure 115: Initial dynamic experimental operational test on cricket.....	99
Figure 116: Voltage verse time graph for 4-finger gripper- Cricket ball: Geometry 4.....	99
Figure 117: Dynamic test for 3-finger gripper: Geometry 1, 2, 3 and 4.	100
Figure 118: Dynamic test for 4-finger gripper: Geometry 1, 2, 3 and 4.	100
Figure 119: Test specimen weights.....	102
Figure 120: Visual dynamic and static testing of the 3-finger gripper for Geometry 1.....	102
Figure 121: Visual dynamic and static testing of the 3-finger gripper for Geometry 2.	103
Figure 122: Visual dynamic and static testing of the 3-finger gripper for Geometry 3.....	103

Figure 123: Visual dynamic and static testing of the 3-finger gripper for Geometry 4.....	103
Figure 124: Visual dynamic and static testing of the 4-finger gripper for Geometry 1.....	104
Figure 125: Visual dynamic and static testing of the 3-finger gripper for Geometry 2.....	104
Figure 126: Visual dynamic and static testing of the 3-finger gripper for Geometry 3.....	104
Figure 127: Visual dynamic and static testing of the 3-finger gripper for Geometry 4.....	105
Figure 128: Deflection of shape of Geometry 1,2,3 and 4.....	108
Figure 129: Voltage verse time graph for 3-finger gripper: Geometry 1.....	110
Figure 130: Voltage verse time graph for 3-finger gripper: Geometry 2.....	110
Figure 131: Voltage verse time graph for 3-finger gripper: Geometry 3.....	111
Figure 132: Voltage verse time graph for 3-finger gripper: Geometry 4.....	111
Figure 133: Voltage verse time graph for 4-finger gripper: Geometry 1.....	112
Figure 134: Voltage verse time graph for 4-finger gripper: Geometry 2.....	113
Figure 135: Voltage verse time graph for 4-finger gripper: Geometry 3.....	113
Figure 136: Voltage verse time graph for 4-finger gripper: Geometry 4.....	114

<h2 style="text-align: center;">List of Tables</h2>

Table 1: Representation of traditional gripping methods.....	11
Table 2: Schunk® 2-finger gripper and actuator technical data	11
Table 3: Schunk® 3-finger gripper and actuator technical data	12
Table 4: GOUDSMIT Magnetic Gripper® - Friction Type - #40 mm – 140 N technical data	14
Table 5: Empire Robotics VERSABALL® - 65” head technical data	15
Table 6: Dry adhesive gripping technical data.....	17
Table 7: Electro-adhesive gripping technical data.....	18
Table 8: Robotiq Adaptive Gripper® technical data	20
Table 9: SCHMALZ® FXP-SVK 442 3R18 Vacuum gripper technical data	21
Table 10: TIHRA gripper technical data.....	21
Table 11: FESTO’s MultiChoice Gripper® technical data.....	22
Table 12: Comparative list of specifications for prospective grippers.....	25
Table 13: BCN3D MOVEO robotic arm technical information	52
Table 14: FANUC M-10iA robotic arm technical information	53
Table 15: Geometric inputs for the DH model.	56
Table 16: Mechanical properties of the 3D-printing material.....	60
Table 17: NEMA 17 technical specifications	65
Table 18: 12V DC motor technical specifications.....	66
Table 19: Comparison of motor types.....	66
Table 20: Tabulated results for ABS plastic for linear statics	107
Table 21: Tabulated results for Nylon for linear statics.....	107

Table 22: Tabulated results for ABS plastic for non-linear statics	108
Table 23: Tabulated results for Nylon for non-linear statics	108
Table 24: Summarized results for repeatability and average mass hold of 3-finger gripper	109
Table 25: Summarized results for repeatability and average mass hold of 4-finger gripper	109
Table 26: 3-Finger dynamic grip performance.	109
Table 27: 4-Finger dynamic grip performance.	112
Table 28: Visual dynamic and static testing results of the 3-finger gripper for Geometry 1, 2, 3 and 4.	115
Table 29: Visual dynamic and static testing results of the 4-finger gripper for Geometry 1, 2, 3 and 4.	115
Table 30: 3-Finger gripper performance.....	116
Table 31: 4-Finger gripper performance.....	116

1 Introduction

1.1 Introduction

The background of the problem is described in relation to flexible gripping methods and implementation in the operational environment of Reconfigurable Assembly Systems, (RAS). Flexible end-effectors play a role in increasing efficiency of production in pick and place procedures in Advanced Manufacturing Systems, (AMS). Complex production systems are incorporated across a range of platforms including car manufacturing, the aerospace industry, computer-chip production, etc. The production platforms are described as mixed-product lines that require the handling and assembly of a variety of geometries and shapes. The research provides an overview of applicable flexible gripping systems and requirements for incorporation in RAS. The research question and objectives are expressed in terms of the constraints set out for the project. The layout is described for the project regarding the solution strategy for the problem.

1.2 Background and Context of Study

A demand for high production rate capabilities is observed in modern manufacturing systems. Optimised production systems have become attractive in terms of reduction of assembly costs, reduced production time and maximised profit. The focus has been placed on customizable production and assembly lines. Reconfigurable assembly systems defined by Dymond et al. [1] are required to enable agile market demand response with respect to the capacity and functionality of the production system.

Reconfigurable Assembly Systems, (RAS), described by Savu and Vlase [2], are part of the term called “Factories of the Future” and are also known as Next Generation Manufacturing Systems. Reconfigurable assembly systems have the potential to adapt to market demands making it simpler for smaller and similar industries to compete with product variation in the growing manufacturing markets and, satisfying the requirements of investors and clients. Efficient assembly processes incorporating pick and place procedures are required which involves precise part control and component placement, with the least amount of degrees of freedom. Additionally, adaptable fixtures are mandatory for part geometric conformity, reducing part orientation and grip orientations

The research has applied biologically inspired systems to resolve existing problems. The unique gripper and fixtures could theoretically be implemented in the automation industries. Grippers adapted from biological mechanisms were studied, for example, simulated chameleon tongues, elephant trunks, and octopus tentacles. Other technologies reached out to more sophisticated developments including phenomenon, for example, magnetorheological fluids, dry adhesion, etc. Flexible gripping techniques provide an advantage in modern assembly lines and simulated near perfect conformity. The multi-

functional robotic arm assembly process in Tesla's new Fremont factory demonstrates multi-platform assembly including welding, riveting, bonding and installing shown in Figure 1 [3].

Operational environments were investigated to determine performance criteria for flexible fixtures. The design focused on geometric adaptability and flexibility of the gripper system. Overall human and material safety was considered in the development of the gripper system. The system was designed for intelligent control and object manipulation and consisted of an integrated electronic control system. The experimental procedural firmware was installed for generating empirical data. The advancements and recommendations of grasping mechanisms as well as challenges related to flexibility, adaptability, and sensitivity of self-adjusting grippers/fixtures were summarized to provide a detail description of the problem.



Figure 1: Versatile robots in Tesla factory [3]

1.3 Industrial Example for Flexible Gripping Application

The flexibility of a system is explained as the capability and capacity to accommodate the uncertainty and variable change of the environment of the operation. For the flexibility to maximize efficiency, the system has to respond to the fluctuations in demand in terms of different products. Therefore, flexible systems have to accommodate a variety of products with the high complexity of the design. Mixed-product lines would be an appropriate industrial application for the scenario in which to test the adaptive system. In essence, the technique should be able to accommodate volume demands, mixed component characteristics and factor in complexity.

The aerospace space industry demonstrates an environment where lightweight, intricate designs and unique tasks are required for high production demands. Complicated tasks are required for assembly of mechanisms and the increase of product variety is proportional to assembly complexity. A result of this increase in difficulty of assembly creates a higher demand for supervisory, work and administrative resource requirement. Grenier-Lafond et al. [4] specified conceptualized flexible systems are always in need for more adaptive and efficient assembly lines to handle the demand for production. Economic problems are faced in the necessary handling of the wide variety of workpieces and the elimination of fixture interchange. The challenge was to create a system that:

- Is semi-automated for higher operational production and repeatability.
- Adaptive end effector characteristics are required by the gripper system.
- The system requires handling of various workpieces and masses.
- Improved material handling is required.

The solution was to design a robotic gripping system, integrated with an intelligent sensory feedback system to enable a sense of object orientation and geometric adaptiveness. The system was enabled with incorporation into a precise and repeatable continuous assembly. The following was to be integrated into the system:

- Task categorization for robotic sensory abilities.
- Fast and flexible integration of the system.
- A versatile and robust system design.
- An adaptive semi-autonomous system.

1.4 Problem Statement

Self-adjustable capabilities with regard to precise gripping with flexible, adaptable and sensitive securing properties of flexible fixtures are unknown. A system needs to be developed to fulfil these requirements.

The problem was based on the technological gap presented in the automation industry and assembly systems. The problem was influenced by systematic part family and part geometric change in the assembly process. Additionally, playing a key role as discussed by Trappey et al. [5], was precision and repeatability of object placement. The gripping system could be disrupted by bad behaving gripping and movement control through environmental factor. Path planning and variable location control was assumed as a fixed constraint and was not taken into consideration. The gripping properties of a human hand were modelled as shown in Figure 2 and presented a challenge in the development of appropriate grippers for task handling [6]. The fingers conform to the object's shape and conform to the geometric conditions.

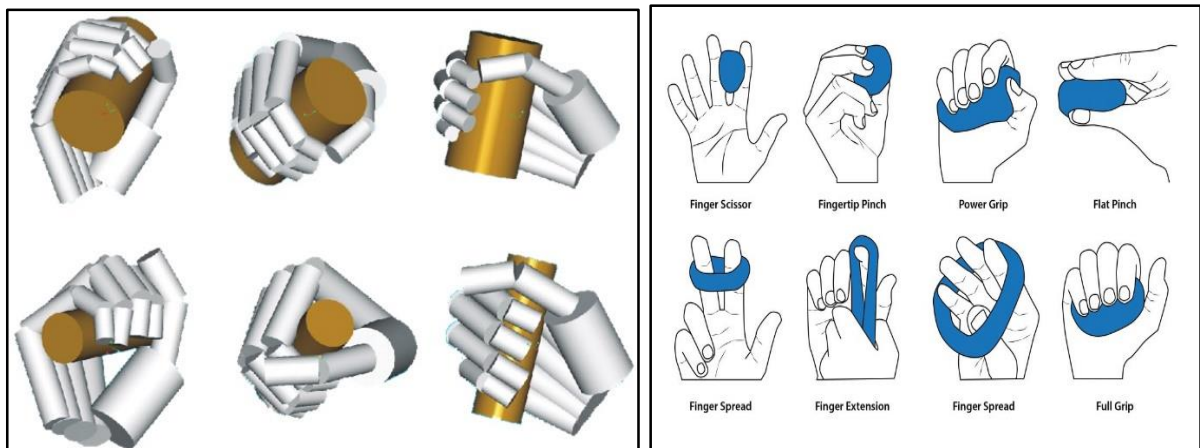


Figure 2: Simulation of hand grips [6]

1.5 Overview

Attention was given to the study of a variety of gripping and fixturing methods applicable in the automation of production and assembly processes. Part handling, placement, and fastening are the general procedures to be studied when looking at different techniques. Subjects that will be revised, which are not practical for the study are conventional mechanical fixtures and micro-gripping. The literature supports studies researched in the field of flexible fixtures and grippers that involve:

- Flexible shape gripping;
- Magnetic gripping;
- Gripping by jamming of granular materials;
- Adaptive bionic gripping;
- Trunk-based gripping;
- Pin-matrix gripping;
- Dry adhesive gripping;
- Electro-adhesive gripping;
- Dextrous gripping;
- Shape adaptable gripping;
- Vacuum gripping;
- Fin Ray gripping.

The system was to be investigated as part of a reconfigurable assembly system and should be, to some extent, applicable to following characteristics of an RMS, defined by Padayachee [7]:

Modularity: The system is required to be composed of common parts to create a variety of products.

Customisation: The system should consist of an open architecture and customized flexibility, including the system's ability to clamp different part families with different geometries.

Convertibility: The interchangeability of the systems tools, software, raw materials, and fixtures, to accommodate different part families.

Scalability: The system's adaptability to the placement and fastening of different component geometries.

Diagnosability: The system's ability to effortlessly detect irregular behaviour.

Self-adjusting placement systems involved the handling of part components to selected locations for further operations in assembly and further processes. The concept behind precise handling was to optimise pickup and placement processes for a jig and fixture. The gripping component should be designed according to the following assumptions:

- The centroid is known and the coordinate position is acquired from previous design processes for components.
- Orientation is known from previous placement to output position of the parts from the previous assembly process.

Part handling and sensitivity to part geometry were evaluated according to effective part gripping and shape conformity. Flexible part grasping was essential, for the reason that operative handling was not sustainable without the conformity properties. The effectiveness of part handling in terms of conformity

was optimised. Optimised gripping systems were researched for example Robotiq's Adaptive gripper seen in Figure 3 [8] and THIRA gripper shown Figure 4 [9].

The process followed a procedure that was repetitive and adjustable to new part geometries experienced by assembly procedure or further processes. A benchmark was developed and was found within previous research. Performance markers/tolerances were established in terms of load gripping force constraints that were applied in fixturing processes.

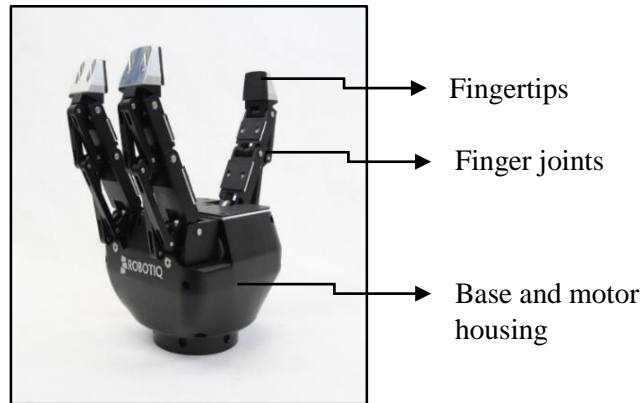


Figure 3: Robotiq[®] adaptive gripper [8]

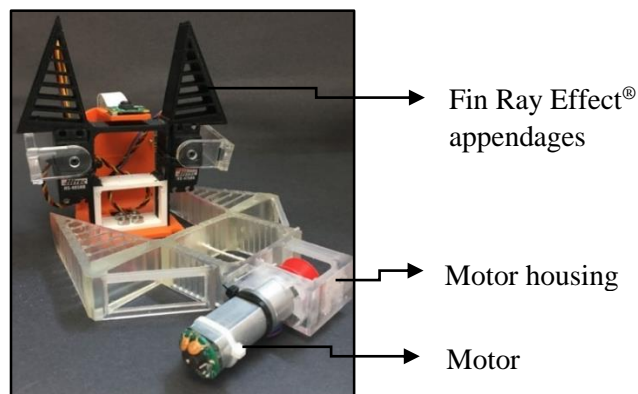


Figure 4: THIRA gripper [9]

1.6 Research Questions

The research question addressed in the project relating to flexible fixtures in reconfigurable assembly systems was:

- Is it possible for flexible fixtures to incorporate self-adjustment characteristics enabling flexible, adaptable and sensitive clamping in reconfigurable assembly systems?

1.7 Hypothesis

The hypothesis relating to flexible gripping in reconfigurable assembly systems was proposed as follows:

- A degree of adjustable grasping in terms of adaptable fixturing is obtained by the adjustment of the type of gripping and characteristic models able to conform to the shape of the intended object to be moved.
- Research proved that developments in adaptable fixture principles in reconfigurable assembly systems were developed to improve performance in production lines.

1.8 Objectives

The dissertation focused on the study and development of adaptable fixturing and gripping systems for reconfigurable assembly systems. The feasibility of the overall system was determined through defining a benchmark based on performance and efficiencies from previously studied grips and fixtures.

1. The objective of the research is to review the field of adaptable fixtures for part component assembly processes. The design specifications are to be investigated and applicability is required for a variety of flexible grippers and fixtures.
2. The intent of the project is to develop performance criteria in terms of object conformity, gripping strength, repeatability, material sensitivity and system integration of a biologically inspired gripping system.
3. A placement and fixture system is to be researched and developed that enables flexibility, adaptability, and sensitivity concerning part families and part geometries. The suggested system is to be evaluated against benchmarks that are established through the literature study and ISO standards for industrial grippers. The validity of the performance of the system is to be researched and investigated.
4. The performance criteria proposed are to be tested according to static holding load and dynamic holding load experimentation and results evaluated through the testing procedure.
5. A theoretical static model is to be developed for the gripping system appendages, through conceptual calculations, computer-aided drawings, and computer-aided simulations. The static model attained would form the basis for the tested model.
6. A gripping system should be designed and manufactured according to the specifications. The performance and validation of integration of the gripper system should be determined.
7. Holding properties, load limits and force control is to be evaluated through grip holding test, static force load test and dynamic force load test. The tests results have to agree to industrial requirements.
8. The system efficiency should be validated through experimental studies of the system. Multiple runs are to be performed in terms of testing and increased accuracy of results for testing are to be generated.

1.9 Description and General Methodology

The methodology of the project according to the objectives are described as follows:

1. A comparative study was examined according to ISO standard according to selecting and developing an adaptive gripping method.
2. A fixturing design was developed from existing technology to incorporate and accommodate an adaptable placement system for pick and place procedures.
3. The selection was performed from fixture benchmark on precision criteria for geometric adaptability gripping of the part.
4. A quantitative test procedure was performed to develop and determine the performance of the system.
5. An empirical and performance study was performed on the system in terms of performance and system compliance with regards to generated specifications.

1.10 Layout of Study

1.10.1 Scope

An adaptable fixture was modelled according to features with reference to part handling, geometric adaptability, part sensitivity, and precision. The gripping device was designed to encompass the ability to secure workpieces or objects permitting to the forces involved in an assembly process. Chan, Benhabib, and Dai et al. [10] proposed the requirements for the specific development of reconfigurable fixtures are the following:

- Modularity: Standard modules should be included in the fixture used for assembly.
- Automatic reconfigurability: The fixture should be reconfigurable according to features included in the gripping device of the robotic arm end-effectors.
- Sensory feedback controllability: Sensory integration and feedback controllability should be included in the system.
- Programmability: The operational system should be programmable without difficulty.

1.10.2 Layout

The layout of the project document was prepared as follows:

1. Introduction: Explanation of dissertation background and framework.
2. Literature study: This will give more information on the subject at hand that has not been handled in the study course.
3. Theory: The theory section will explain the models and how they are applied in the project.
4. System conceptual design: Description and design of conceptual models included in the dissertation.
5. System embodiment development: Complete system design.
6. System computer-aided simulation: This section explains how the computer-aided analysis is done and the reasoning behind it.
7. Validation: This section explains the validation and the experimental process.
8. Results: The results of the experiment are discussed and summarized.

-
9. Cost estimation: All costs involved.
 10. Conclusions and recommendations: Brief description of data compilation and information for improving methodologies and project procedures.

1.10.3 Target Audience

The project was aimed at the following audience (readers, academics, relevant parties) related or have an interest in the following:

- Academic staff, students and relevant parties related to the field of study in accordance with the Exit Level Outcomes pertaining to an MSc dissertation.
- Any person or reader interested in the field of study of Reconfigurable Manufacturing Systems.
- Any areas of interest where the subject of flexible grippers traverses into robotic disciplines, for example, medical practices, manufacturing, etc.

1.11 Conclusion

The chapter introduced the subject matter related to flexible grippers pertaining to reconfigurable manufacturing systems. The problem statement was addressed and objectives elaborated with respect to project outputs, experimentation, and results. The methodology and layout were expressed regarding the presentation of the dissertation. The intended target was provided for the project report. The introduction described the outcomes of the research process for the investigation and development of adaptability properties of flexible grippers for reconfigurable assembly systems.

2 Literature Review

2.1 Introduction

Fixturing and devices contributing to the robotic operation have played the role in replacing human intervention which concerns production. Comparisons between human and robotic assembly cannot be equally compared, as represented in Figure 5. In some instances where tasks that are easy for a human assembler, are quite intricate and almost impossible for a robot arm assembly unit, due to the lack of aptitude [11]. In today's manufacturing industry, the need for reconfigurable assembly systems is far greater for autonomous production. Hence adaptations of parts, products, and processes have to be developed in requirements of robotic and autonomous assembly. Bi, Wang, and Lang [12] emphasized that robots have to be designed to handle and solve complex problems in the assembly process.

The following are recommendations set out for the development in terms of capable robotic systems in terms of industry actions [13]:

- Development of performance measures for assembly.
- Increased use of robots for 'intelligent' fixturing.
- Development of methodologies for human/robot interaction.
- Integration of current industrial grippers with sensors.
- Development of autonomous robot systems capabilities that compare to humans.
- Definition of clear, standard interfaces for grippers.
- Use of robot hand guiding through the teaching process.
- Development of path planning for robotic arms.
- Use of external metrology to support robot system applications.
- Verification of perception systems combined with low-cost gripper tactile sensors.
- Improvement of force control for assembly processes.

The following are recommendations set out for the improvement in terms of capable robotic systems in terms of technological development [13]:

- Adaptive end-effectors.
- More compact end-effectors and end-of-arm sensing.
- Tactile sensing for low-cost grippers.
- Dynamic robot work volumes.
- Tactile based response for robots.

The following requirements and factors determine the type of gripper and capacity of the task to be accomplished:

- Technological requirements: These include the number of the object acquisitions per gripping cycle, time duration depended on the applied force, gripping path and time capacity.
- Effects of the characteristics of the objects: These include the temperature, strength, material type, surface properties, stability, and centre of gravity, tolerance of determined dimensions, design, and mass.
- Factors related to handling equipment: These include connection specifications, axial acceleration, and positional accuracy.
- Factors related to environmental parameters: these include the vibration, humidity, contamination, storage conditions, feeding conditions and clamps, and forces.

The gripping procedure was divided into four phases consisting of part prehension (the ability to grasp an object) and retention (the continuous possession and control of grasping):

- Preparation for contact.
- Establishing the contact between the part surface and gripper surface.
- Fixturing and retention of the part during manipulation.
- The release of the component at the destination.

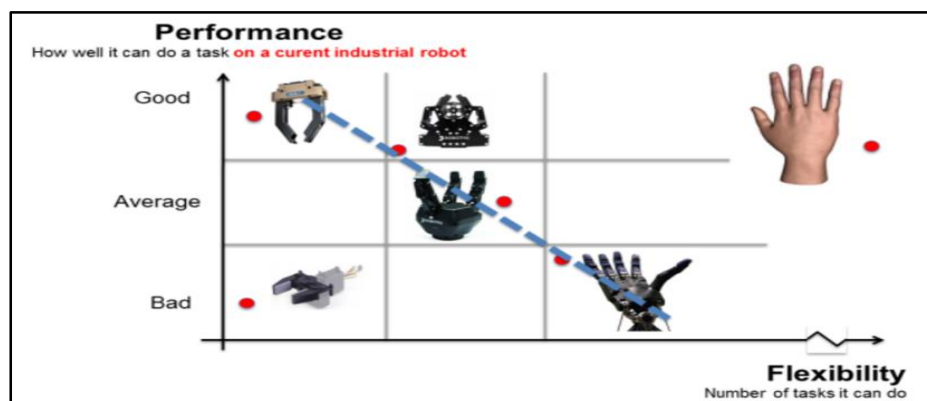


Figure 5: Performance versus flexibility [11]

2.2 Review of Traditional Fixturing Methods

End-effector fixture designs have quite a range of strategies. Developments in the universal robotic hand have led to reconfigurable designs using a wide-range of end-effector manipulators. The key factor is to develop automotive robotic hands that are required to be cost-effective in terms of production speeds. The more effective the system becomes in grasping varying weights, shapes and materials with regard to reconfigurable assembly systems, the more attractive it becomes to the end user.

In the traditional identification of gripping, fixtures can be separated into different classes of fixture groups namely: Impactive, ingressive, contigutive and astrictive. Traditional gripping methods can be sub-classed into two groups namely non-penetrating and penetrating. Penetrating and non-penetrating

designs for traditional grippers are shown in Table 1. The following class description described by Bostelman and Falco [13], explains gripping mechanisms with regards to gripping criteria.

- Impactive gripping methods involves the motion of the gripper jaw impacting against the surface of the component, in producing a gripping force.
- Ingressive gripping in simple terms could be called force-shape gripping where the manipulator contact surface is deformed or even penetrated (intrusive) in which applying direct contact to facilitate gripping.
- Contigutive gripping entails the process of the gripper to be in direct contact with the component surface.
- Astrictive gripping methods involves joining forces between the component surface and gripper surface.

Table 1: Representation of traditional gripping methods

Gripping Method	Non-penetrating	Penetrating
Impactive	Clamping jaws, chucks, collets.	Pincers, pinch mechanisms.
Ingressive	Brush elements, hooks, hook and loop (Velcro).	Needles, pins, hackles.
Contigutive	Chemical adhesion (glues), surface tension forces.	Thermal adhesion.
Astrictive	Electrostatic adhesion.	Magnetic grippers, vacuum suction.

Schunk® presents a 2-finger and 3-finger traditional gripper and can be classified as impactive gripping methods [14]. The traditional grippers investigated by Naidoo, Pillay and Ramnath et al. [15], have limited uses and would to interchangeable according to the work environment chosen. Object manipulation is limited due to geometric constraints of the gripper. The 2-finger illustrated in Figure 6, is limited to square shaped objects. The 3-finger shown in Figure 7, the gripper is limited to cylindrical and round shape objects. Table 2 and Table 3 summarizes the important gripping technical data for the Schunk® grippers investigated:

Table 2: Schunk® 2-finger gripper and actuator technical data

Specification Description	Technical Detail
Stroke Per Jaw	6 mm
Maximum Closing Force	250 N
Maximum Opening Force	270 N
Weight	0.28 kg
Minimum Pressure	250 kPa
Maximum Pressure	800 kPa
Nominal Pressure	600 kPa
Maximum Deflection	0.0031 mm

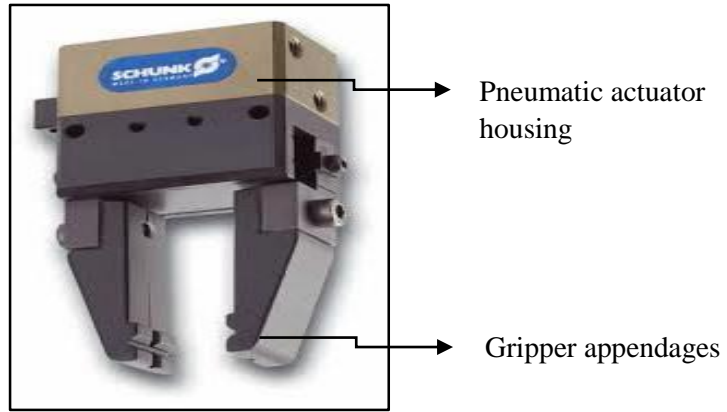


Figure 6: Schunk® 2-finger gripper [14]

Table 3: Schunk® 3-finger gripper and actuator technical data

Specification Description	Technical Detail
Stroke Per Jaw	6 mm
Maximum Closing Force	250 N
Maximum Opening Force	270 N
Weight	0.28 kg
Minimum Pressure	250 kPa
Maximum Pressure	800 kPa
Nominal Pressure	600 kPa
Maximum Deflection	0.036 mm

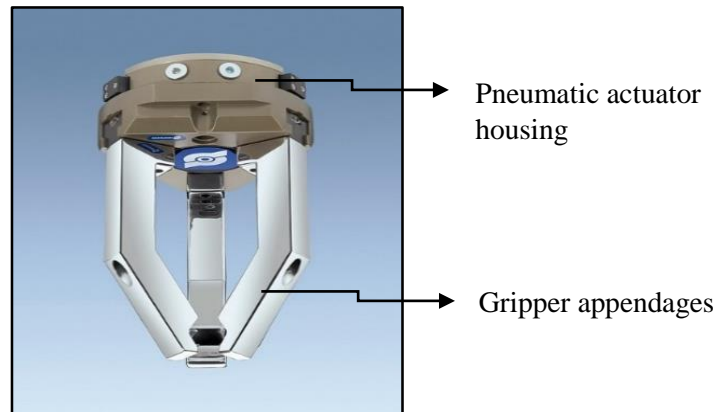


Figure 7: Schunk® 3-finger gripper [14]

2.3 Review of Flexible Fixture and Gripping Technology

Modern industry systems incorporate flexible gripper technologies and are evolving as the need for efficiency and performance increases. Unique tasks and operations must be performed, thus intricate solutions are required. A wide range of gripping solutions have been developed to tackle the needs of reconfigurable assembly lines.

Designated tasks are to be developed that require a change in the workpiece, enabling an adaptable fixturing device that resolves the problem of interchanging fixture head conversions or replacements. Hence, in the future, there will be a requirement for flexible installations which have the ability to automatically adapt to the change in assembly and production line methods. This entails research and development in the field of flexible fixtures and gripping technologies.

2.3.1 *Flexible Shape Gripping*

Kärcher, Moerdijk, and Schrof [16] proposes the flexible shape gripper and is modelled after the mechanics and gripping ability of a chameleon's tongue. Using this biological example to simulate natural gripping of objects, the chameleon can enclose its tongue around its prey by retracting the middle section of the tongue, whilst the outside continues to move forward. The process allows a gripping effect by means of static pressure, due to the surface texture of the tongue, against the movement of the insect being gripped. FESTO® has designed and manufactured a concept model based on this principle called the FlexShapeGripper® as shown in Figure 8.

This gripping device has the ability to pick-up, gather and place objects of different shapes and geometries in one procedure, without needing to alter the mechanism manually. The gripping principle is established by utilizing a silicone cap, flexible to an extent, in order to cover the component to be moved. The cap is previously filled with water, which gives the forming property of the cap. The gripping tool involves using a double-acting cylinder, by which one cylinder controls the flow of air and the other, is filled permanently with water. As with the chameleon tongue, the mechanism is controlled pneumatically when the cap conforms to the shape of the object to be gripped. The high static friction force created from the properties of the silicone material generates a good retaining force on the object. Gripping takes place by hydraulically inverting a silicone bulb. (There is no technical information available for Festo's FlexShapeGripper®).

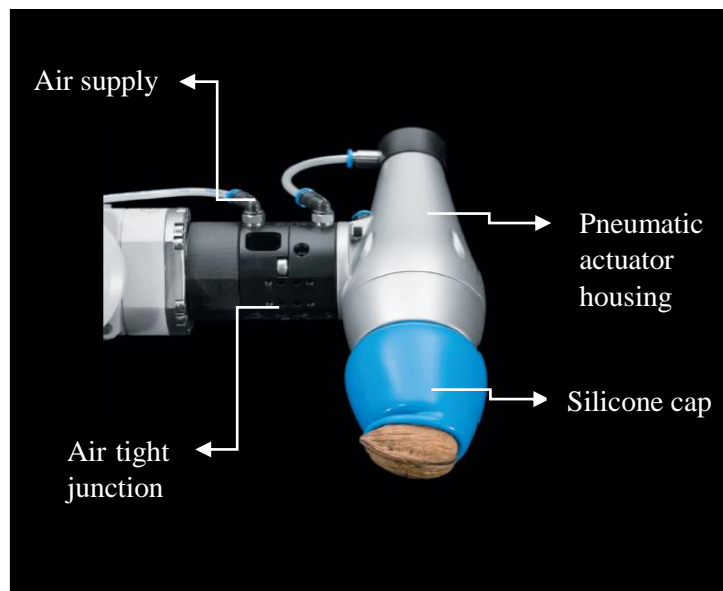


Figure 8: Festo's FlexShapeGripper® [16]

2.3.2 *Magnetic Gripping*

GOUDSMIT® [17] magnetic fixturing devices can be used in reconfigurable assembly systems, especially when used in combination with vacuum grippers. Magnetic gripping devices can hold on to flat surfaces as with sheet metal assembly processes but also perforated surfaces and non-planar objects. Where vacuum technology lacks the tenacity to grip to variable surface textures. Although being limited to ferromagnetic materials, it is quite a robust fixturing device and the properties are shown in Table 4. GOUDSMIT® Magnetic Systems has designed and manufactured a concept model based on this principle called the Goudsmit Magnetic Gripper® as shown in Figure 9.

According to Wadhwa, Lien, and Monkman [18], a magnetic flow path, called magnetic flux, is created when a magnetic contact surface is in touch with the metallic object being grasped. A magnetic force attracts and holds the object against fixture surface until ejection of the part. The magnetomotive force is the driving force in a magnetic circuit, this produces a magnetic flux generated by the coil reluctance.

A drawback to this gripping technique is that robotic arm movement causes a slipping motion of the contact surface between the component and the magnetic gripper if the tangential force of movement is greater than the static force in contact. Therefore, the clamping force is dependent on the static friction coefficient for the magnet to part surface pair.

The versatility of these types of grippers was described to have a simple construction with little to no moving parts, straightforward power supply, and usage, reduction in setups and flexibility with regards to part geometry. High precision is achievable in the placements of components with vacuum gripping and possesses easier assembly production applications.

The magnetic properties of materials do have limits concerning the pre-tension force that is necessary to grasp the component. De-magnetising can occur to the magnetic material used for clamping in relation to the magnetizing force required. Residual magnetism should also be taken into consideration when choosing magnetism as a gripping medium.

Table 4: GOUDSMIT Magnetic Gripper® - Friction Type - #40 mm – 140 N technical data

Specification Description	Technical Detail
Advised working load	47 N
Minimum working sheet thickness	1 mm
Maximum Tear-off force	140 N
Maximum Opening Force	270 N
Weight	0.23 kg
Minimum Pressure	-300 kPa
Maximum Pressure	400 kPa
Maximum Deflection	0 mm

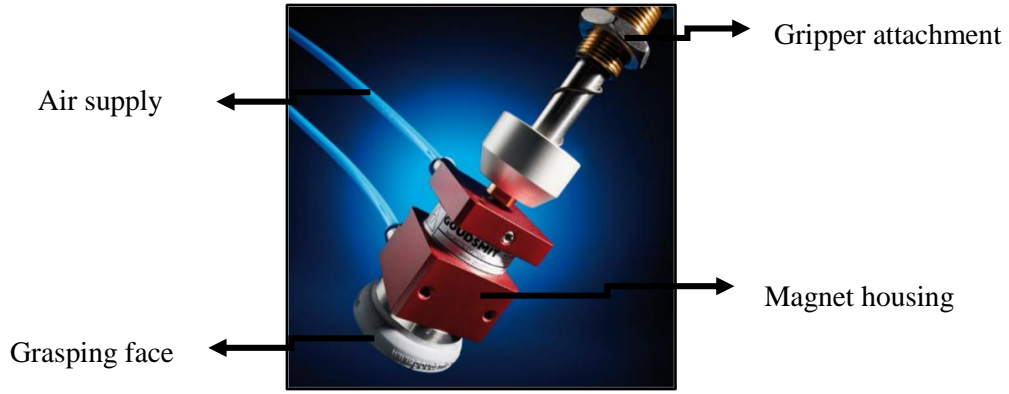


Figure 9: GOUDSMIT® Magnetic Gripper - Friction
Type - #40 mm – 140 N [17]

2.3.3 *Gripping by Jamming of Granular Material*

Empire Robotics [19] developed a manipulator that grips based on the jamming of granular materials. The gripper clamps onto the object by positive and negative pressures by gripping and releasing objects. This unique fixturing device can grasp on to a wide range of shapes and geometries. It is versatile in adapting and conforming to different object shape profiles. By passively conforming to the shape of the object the granular material is then vacuum hardened and grips on by means of negative pressure. The component can be released by reversing this process by means of a positive pressure where thus the gripper itself returns to its original shape. Empire Robotics® has designed and manufactured a concept model based on this principle called the VERSABALL® as shown in Figure 10. The properties of the VERSABALL® shown in Table 5.

The VERSABALL® takes advantage of the gripping mechanism which occurs due to the transition state between fluid and solid properties. The jamming of the object transpires between the membranes that are filled with a granular material. Slight volume contraction of universal gripper results in a friction force, which in turns creates a pinch force on the object. This is due to the evacuation of air from inside gripper reducing the volume. Amend, Brown, Rodenberg, Jaeger, and Lipson [20] defines the shift from fluid-like state to solid state can be classified into three types of modes:

Mode 1: Surface contact in terms of static friction.

Mode 2: By interlocking on to the object it grasps by geometric restraints.

Mode 3: Approximate suction occurs on the surface of the part on contact with gripper surface due to airtight seal achieved after contraction.

Table 5: Empire Robotics VERSABALL® - 65” head technical data

Specification Description	Technical Detail
Weight	3.45 kg
Operating pressure	551.58 kPa
Maximum retention force	88.96 N
Maximum contact force	88.96 N
Pinching pressure	48.26 kPa
Placement precision	7.62 mm
Maximum Deflection	Complete conformity

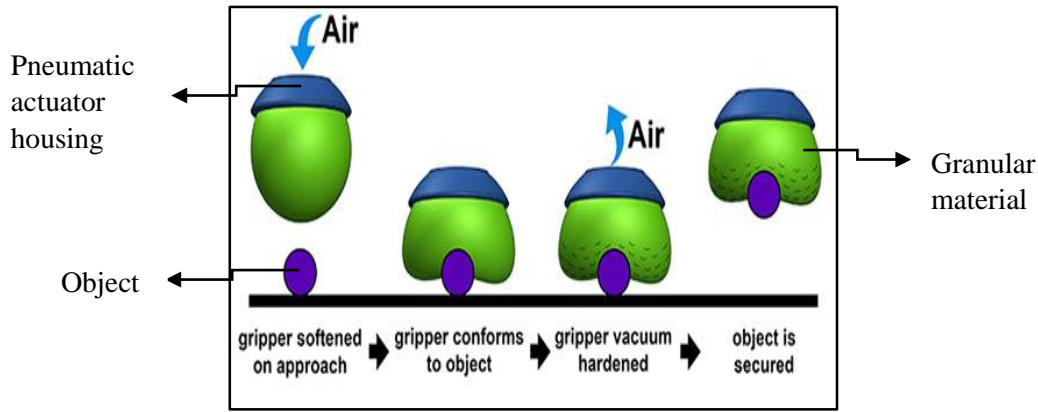


Figure 10: Empire Robotics VERSABALL® - 65" head [19]

The gripper takes advantage of the operational modes. The gripper has the benefit of being able to conform to a variety of different geometries, weights, and material fragility. Also, an advantage would be that the gripper in conjunction with a robotic arm, operates in an open loop without the need for visual feedback and fixture planning.

The disadvantages would be that the gripping behaviour would not be able to be correctly modelled. The result being, that the unknown interaction between the gripper contact and conforming properties in terms of grasping. Jiang, Amend, Lipson and Saxena [21] raised the concern that further investigations would be required to generate predictive models with regards to flow grains and membrane deformation.

2.3.4 *Pin Matrix Gripping*

MATRIX® [22] has developed a clamping system based on the conforming properties of a pincushion as shown in Figure 11. The pin matrix technique adheres to the gripping principle of multiple pins pushing together to form around the shape of the object, conforming to the geometry. Effectively clasping the object, the fixture is sensitive to the material of the object. The pins are controlled as if forming around the object like a fluid, but yet has the required strength capability. Each pin is made of steel and is mechanically controlled by a fluid pressure pushing the pins through each individual socket manipulating the pins individually to be shaped by the counterforce from the object. (There is no technical information available for MATRIX® Pin Matrix System).

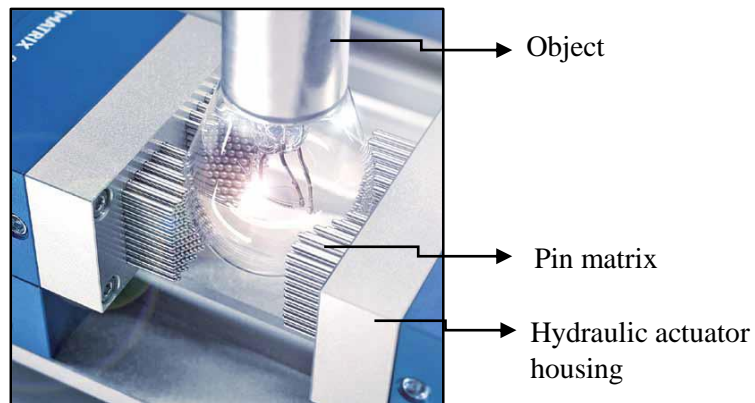


Figure 11: MATRIX Form Adapting Clamp System® [22]

Workpieces are held firmly in place by the pins. Adaptors can be added, including angle connectors, cones and prism supports, and can effectively grip any shape. The bulk support of the unit can absorb vibration and its stiffness properties can be used for further machining processes. When used in conjunction with a robotic arm, the MATRIX[®] pin clamping unit can effectively be used in precise pick-up and placement processes.

The performance of the system benefits from being a flexible shape gripper. The gripper has properties of being cost-effective in terms of reducing production costs. The system can be implemented in any production and automation procedures with regards to gripping, placing and fixturing. The system was used for varying shapes, materials and automated assembly processes.

2.3.5 *Dry Adhesive Gripping*

The gripper mechanism occurrence called dry adhesive gripping, seen in the feet of Gekkota was described by Keijia et al. [23]. Dry adhesive gripping was said to be theorized in the form of glue-like secretions, suction, microscale interlocking, friction, electrostatic forces, capillary adhesion and van der Waals forces. Through the process of experimental elimination, it was found that van der Waal forces were the cause of this grasping effect. “Other properties are also utilized by the gecko namely: Anisotropic (directional forces), force generation in relation to preloading, ease of detachment (peel-zone modelling), material-independence attachment, non-self-adherence and self-cleaning mechanism” [23].

Micro-suction cups employing dry adhesive gripping have been used in the production of dry adhesive tapes and pads. A unique grasping technique called NanoGripteck[®] was developed based on the self-suction ability of negative pressure in a suction cup. NanoGripteck[®] [24] has developed gripping solutions inspired by Gekkota. Table 6 shows the properties of the dry adhesive gripper.

Directional gripping was attained by placing the individual suction cups at an angle of contact. Therefore, when a force is applied in one direction of contact loading occurs on the surface of the pad and when a force is applied in the opposite direction, the grip is released from the surface of contact. Theoretical and experimental magnitudes have been determined by Murphy, Aksak and Sitti [25] in determining gripping angles and gripping forces and are illustrated in Figure 12.

The robotic application for dry adhesive gripping can be added on existing gripping systems or used independently to be an effective gripper discussed by Chary, Das, Tamelier, and Pesika [26]. The gripping method enhances fixtures to the extent of geometric conformation and material sensitivity and can be adaptable to any fixturing method.

Table 6: Dry adhesive gripping technical data

Specification Description	Technical Detail
Weight	0.015 kg
Maximum retention force	42.17 N
Maximum retention pressure	13.5 kPa
Area of contact	0.32 m ²
Placement precision	2 mm
Maximum Deflection	Fully conforms

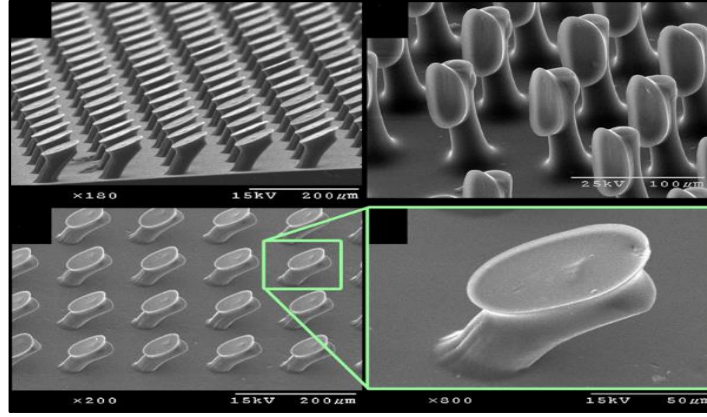


Figure 12: Directional suction cups based on gecko feet [23]

2.3.6 *Electro-adhesive Gripping*

Electro-adhesive gripping is based on the principle of electrostatic actuation, mechanised by intrinsic electro-adhesion force. This gripping technique allows for clasping of fragile objects by means of a two-fingered gripper. Shintake, Rosset, Schubert, Floreano, and Shea [27] introduced a gripper that consists of flat membranes by which the surface adhesion force is applied to in contact with the object being grasped. The holding force generated is high compared to other electro-gripping devices used in (for instance) micro-gripping technologies.

“In principle, electro-adhesion works by applying an electric field to the surface area an elastomer which is sandwiched between two electrodes, the opposite charges generate an electrostatic pressure called Maxwell stress [27].” Fringe fields also develop on the edges of the electrodes, which can cause electro-adhesion in contact with objects as illustrated in Figure 13. As the fields are polarized due to the charged surfaces of the objects attractive forces are generated. This results in a grasping effect of the surface of the gripper.

Electro-adhesive technology has been developed by SRI International® [28] regarding this gripping method. The electro-adhesion technology addresses an extensive range needs in different industries. The gripping method mentioned can grip onto a wide range of materials and has the ability to conform to objects to an extent. Electro-adhesive gripping has high gripping forces in relation to the contact surface. The gripping technology can be adapted to automation processes where gripping and placing is required. Due to the quick release mechanism of electro-adhesion contact, it becomes a comfortable and adaptable fixturing device. Properties are shown in Table 7 of the electro adhesive gripper.

Table 7: Electro-adhesive gripping technical data

Specification Description	Technical Detail
Weight	± 0.10 kg
Maximum retention force	3.5 N
Maximum retention pressure	35 kPa
Area of contact	83.75 mm ²
Placement precision	2 mm
Maximum Deflection	Fully conforms

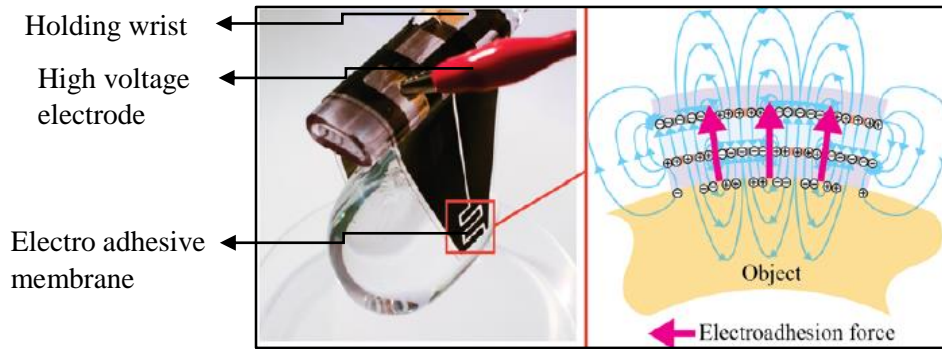


Figure 13: Electro-adhesive gripping [27]

2.3.7 *Dextrous Gripping*

Dextrous manipulation has been one of the most common methods of gripping in the robotics industry. Grippers with dextrous ability, mean the manipulator has grasping functions that are in relation to the capabilities of animal/human hands. Using individual finger appendages as the gripping tool to conform to the shape of the object, either by individual joints bending into different directions or the entire finger shaping by a flexible material. The gripper can consist of two or many fingers. Falco, Marvel, and Messina [29] discussed the industrial applications of an anthropomorphic robot hand in assembly processes.

A dextrous gripper introduced by Tincani, Catalano, Farnioli, Garabini, Grioli, Fantoni and Bicchi [30], proposes a dextrous gripper called Velvet Fingers® as shown in Figure 14. Proposing a two-finger type claw-like structure, and being able to control the adhesion that takes place between the grasping surface and the object in the motion of becoming gripped. The finger consists of two moveable appendages connected by a hinge, making it able to conform to the shape of an object. The clamping faces are made from belts drives enabling the component to travel along rollers over the belts. By enabling push active surfaces, the gripper utilizes tangential forces to push the object between movements from active surfaces in tip grasping to power grasping, which partially shapes around the part. (There is no technical information available for Velvet Fingers®).

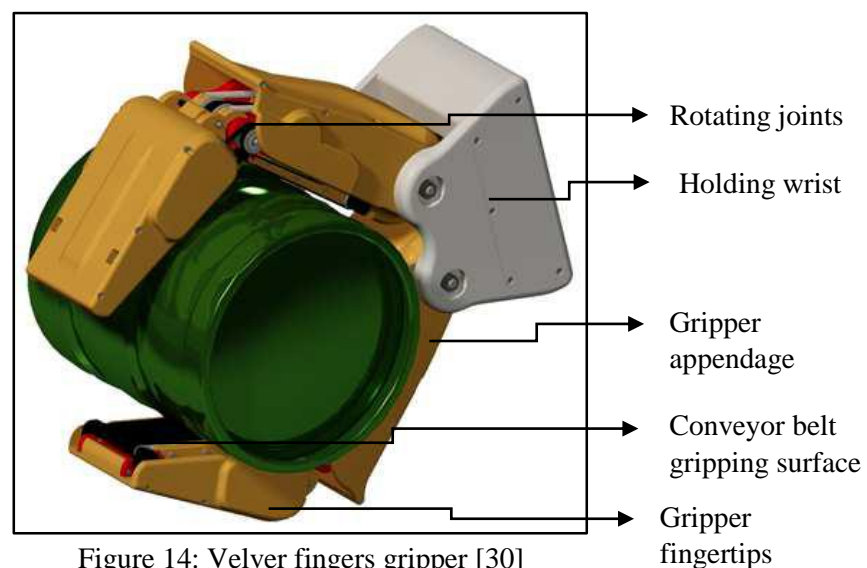


Figure 14: Veller fingers gripper [30]

Robotiq® [8] has developed a 3-finger adaptive gripper. The manipulation system is based on the movement of human fingers. Each appendage is controlled through sectioned links and split into 3 segments. The design simulates the gripping characteristics of hand movements as demonstrated in Figure 15. The gripper is able to form around objects, creating a versatile manipulation system for manufacturing processes. The properties of the adaptive gripper are shown in Table 8.

Table 8: Robotiq Adaptive Gripper® technical data

Specification Description	Technical Detail
Weight	± 2.3 kg
Maximum grip force	60 kN
Maximum encompassed load	10 kg
Maximum fingertip load	2.5 kg
Placement repeatability	0.05 mm
Maximum Deflection	± 0.1 mm (conforms to joints)

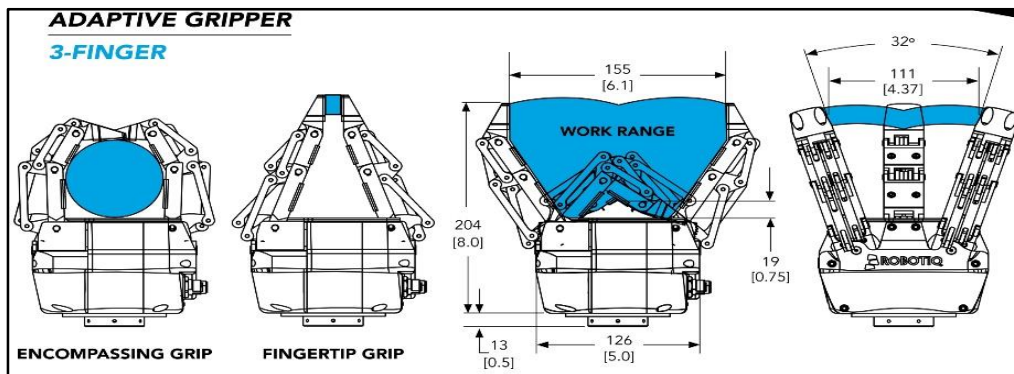


Figure 15: Robotiq Adaptive Gripper® [8]

2.3.8 Vacuum Gripping

Many industrial robots use vacuum technology for part manipulation and fastening structures, especially in sheet metal and glass sheet production environment, due to the flat surfaces of workpieces. Suction gripping comprises of suction cups which come into contact with the part surface, and a vacuum is created either mechanically or pneumatically. Horák and Novotný et al. [31] describes the action of the vacuum that creates a negative pressure, in which a gripping force is a result of this grasping motion.

SCHMALZ® [32] has successfully developed vacuum gripping devices for handling workpieces of different sizes, surface textures, and materials called SCHMALZ Vacuum Gripping Systems® as seen in Figure 16. This design is ideal for robotic processes due to the light weight of this gripping method and can be used for pick and placement of workpieces that do not have a known pick-up position. It is a multi-purpose gripper for industrial and intricate use. Table 9 shows the properties of a selected SCHMALZ® vacuum gripper.

Suction gripping has the advantage that it is cost-effective, effortlessly used and operated, and can be adapted and implemented into any production or automated system. Even though this type of gripping method is quite versatile in industry, it does have drawbacks with the gripping mechanism itself. Individual suction cups have limited suction power on workpieces and need to be used in clusters and there are limitations to part geometry and surface properties as shown in Figure 16.

Table 9: SCHMALZ® FXP-SVK 442 3R18 Vacuum gripper technical data

Specification Description	Technical Detail
Weight	± 2.6 kg
Maximum suction force	0.55 kN
Maximum load	10 kg
Placement precision	± 0.05 mm
Maximum Deflection	Conforms to surface



Figure 16: SCHMALZ® FXP-SVK 442 3R18 Vacuum gripper [32]

2.3.9 *Gripping Through the Fin Ray Effect®*

Research shows a dependability on gripping systems based off on natural phenomenon. The Fin Ray Effect® is based on the mechanical movement of fish fins, as the name explains. The fin shape wraps around the object as the forces are applied to the structure. The incorporation of the Fin Ray Effect® can be proved to be quite useful in handling non-uniform geometric parts in assembly systems. As the part clamping surfaces do not have to be predetermined for the gripping system. The Fin Ray Effect® describes the mechanism occurring in fish fins and was defined in an interchangeable manner.

The TIHRA gripper was a system developed by Crooks, Vukasin, O’Sullivan, Messner, and Rogers [9] incorporating the Fin Ray Effect® as shown in Figure 17. An object can be gripped in terms of the appendages bending around the geometry. The TIHRA was adapted by changing the rib orientation. The parallel ribs are replaced with slightly slanted ribs. The concept proved to be more effective in gripping through extensive experimental results. Table 10 displays the properties of the TIHRA gripper:

Table 10: TIHRA gripper technical data

Specification Description	Technical Detail
Weight	± 1.0 kg
Maximum force	5.49 N
Maximum load	0.56 kg
Placement precision	Not tested
Deflection with 10 kN	16.8 mm

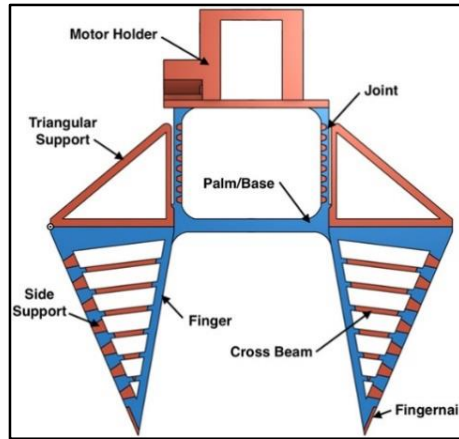


Figure 17: TIHRA gripper [9]

Another unique gripper type is the MultiChoice Gripper®, modelled from the forceps gripping of the thumb, index finger and middle finger. This robotic manipulation has been designed and demonstrated by FESTO® [33], yet again incorporating the Fin Ray Effect®, on three individual appendages. A number of finger elements can vary between two six. The gripper is attached to an articulated robotic arm which supplies the finger elements with three compressed air lines, used for grasping by means of pneumatics as shown in Figure 18. This gripping method enforces both form fitting to the object and applied force by using the finger elements that are made of polyurethane to grab components. The properties of the MultiChoice Gripper are presented in Table 11.

Table 11: FESTO's MultiChoice Gripper® technical data

Specification Description	Technical Detail
Weight	0.66 kg
Maximum operating pressure	800 kPa
Gripper opening stroke	92 mm
Placement precision	± 0.05 mm
Maximum Deflection	Adequate conformity

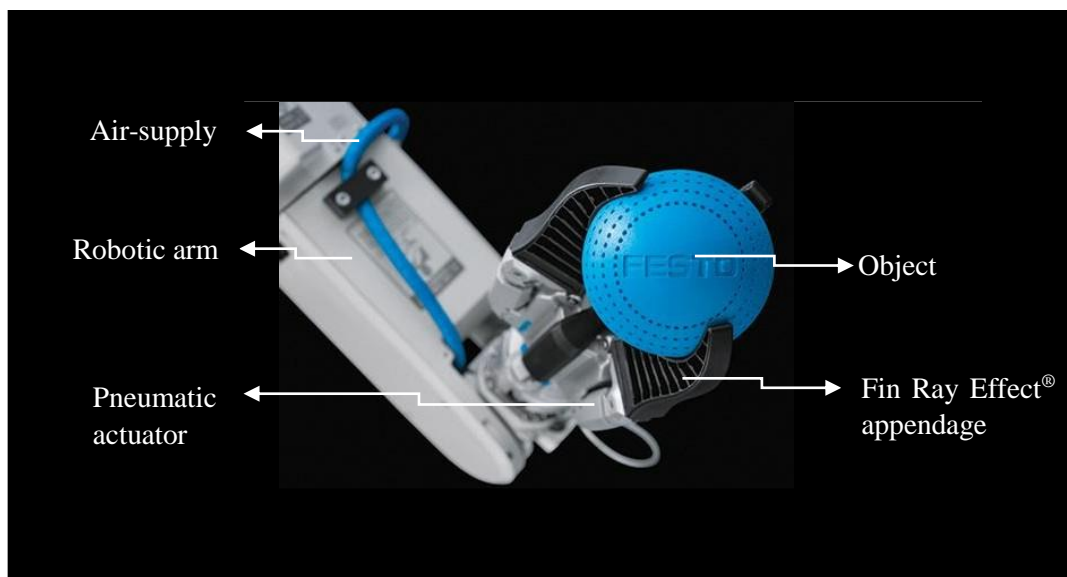


Figure 18: FESTO's MultiChoice Gripper® [33]

2.4 Micro-Gripping

Micro-gripping is concerned with manipulating and handling parts on the micro level, meaning these components are as big as one micrometre to one millimetre. There has been increasing interest in gripping technologies requiring efficient, reliable and flexible grasping of parts on a micro level. The application may be in the fields of micro-robotics, biological manipulations, optical, mechanical or electrical micro-component assembly as described by Lang et al. [34].

Micro-gripping technologies may include a wide range of natural or experimental occurrences and phenomena. The following are just some examples of interesting micro-gripping developments that are being researched. A study done by López-Walle, Gauthier, and Chaillet [35], indicated that cryogenic gripping by freezing a liquid around an object possesses effective grasping properties. Another interesting gripper is a micro-gripper that's been researched by El-Sayed, Abo-Ismael, El-Melegy, Hamzaid, and Osman [36] using piezo-electric bio-morphs, which utilizes piezoelectric materials to apply a force on an object, for gripping purposes. The following are different micro-gripping techniques shown in Figure 19:

- Friction Gripping;
- Form Closure Gripping;
- Vacuum Gripping;
- Electrostatic Gripping;
- Capillary Force Based Gripping;
- Gripping on the Basis of Van der Waals Forces;
- Liquid Solidification Gripping (Cryogenic Gripping);
- Ultrasonic Pressure Gripping;
- Magnetism Based Gripping;
- Optical Pressure Gripping;
- Gripping on the Basis of the Bernoulli Effect;
- Piezo-Electric Gripping;
- Tactile Micro-Gripper.

Micro-gripping possessed potential grasping characteristics for flexible end-effectors but lacked the ability to handle large components. A short introduction was provided in this dissertation as micro-gripping was not part of the scope of the project.

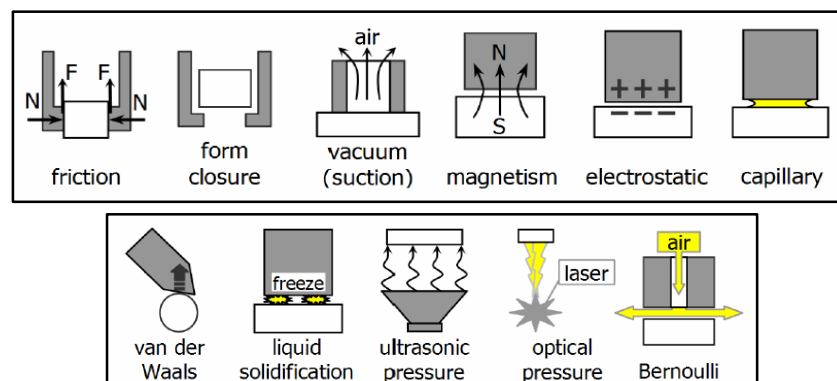


Figure 19: Micro-gripping techniques [34]

2.5 Quantifying Fixture Performance and Efficiency

According to Bouchard et al. [37], it is important to note that using the most suitable gripper method for the grasping process is important and also measuring the performance and efficiency of the gripping device. The function of the gripper device must be known in the automation process to increase process effectiveness. The fixture performance and efficiency must be identified and quantified. When selecting a gripper for the process at hand we consider focusing on technical factors from a process and part perspective. The following factors could give an idea as to which role the gripper:

- A gripping operation required by the gripper to perform during a pick and place procedure.
- Cycle time and speed required for fastening and releasing of the gripper.
- Precision and adaptability required for gripper method.
- Environmental needs and manufacturing industry part manipulation need to take place.
- Part factors include the following: Size, shape, weight and surface type.
- Economic factors and economic restraints on automation process.

After selecting a gripper for the process, the performance and efficiency of the gripper should measure up to selected specification criteria. The following specification criteria give an idea of how the benchmark will be set up for the gripping technique:

- Effective shape conformity, and geometric adaptability.
- Gripping force according to the weight of the object and static force resistant properties.
- Precision gripping and repeatability.
- Sensitivity to material types and surface damage.
- Process integration and adaptability, compared to adjustment with other automation processes.
- Intelligent self-adjusting and flexible properties.

2.6 Summary of Flexible Gripper Selection

A specifications priority has been selected and the flexible grippers mentioned in the literature study were compared accordingly as seen in Table 12. The comparison table provided qualitative information on the gripper techniques researched. A gripper concept was selected and designed from the selection procedure using the disadvantages and advantages in terms of conformity, grip strength, repeatability, sensitivity, integration, and self-adjustment. Selection of flexible gripping technologies was completed through a selection matrix and a quality function deployment. Refer to APPENDIX A.1 - Flexible Gripping Technologies: Selection Matrix. Refer to APPENDIX A.2 - Flexible Gripping Technologies: Quality Function Deployment

Table 12: Comparative list of specifications for prospective grippers

	Effective Shape Conformity	Gripping Strength	Repeatability	Material Sensitivity and Limitation	Process Integration	Self-adjustment
FESTO'S FlexShapeGripper®	Full	Weak	Limited	Any	Limited	Excellent
GOUDSMIT Magnetic Gripper®	Minimal	Moderate	High	Ferro-magnetic	Full	Restricted
Empire Robotics Versaball®	Full	Weak	Limited	Any	Limited	Excellent
MATRIX® Form Adapting Clamp System	Satisfactory	High	Adequate	Any	Full	Excellent
Dry Adhesive Gripping	Satisfactory	Weak	Adequate	Surface limitations	Limited	Excellent
Electro-Adhesive Gripping	Minimal	Weak	Adequate	Surface limitations	Limited	Excellent
Velvet Fingers®	Satisfactory	High	Adequate	Any	Full	Excellent
Robotiq® Adaptive Gripper	Satisfactory	High	High	Any	Full	Excellent
SCHMALZ® Vacuum Gripper	Minimal	Moderate	High	Any	Full	Restricted
TIHRA® Gripper	Satisfactory	Moderate	Limited	Any	Limited	Excellent
FESTO® Multi-Choice Gripper	Satisfactory	High	Adequate	Any	Full	Excellent

2.7 Mechanical and Electronic Design

The optimization of a mechanical system needs data requirements of system performance. A sensor system provides the required performance data and consequently, a benchmark for the system can be developed. Lipot [38] describes the following: “A mechanical system is a set of physical components that convert an input motion and force into a desired output motion and force.”

Mechanical systems have at least three elements: input, process, and output. Illustrated in Figure 20, the mechanical system is described for the designed system:

- The input part of the system is any type of motion and force that drives the mechanical system.
- The process part of the system is where mechanisms are used to convert the input motion and force into an output motion and force.
- The output is the change created in the input motion and force by the mechanism.

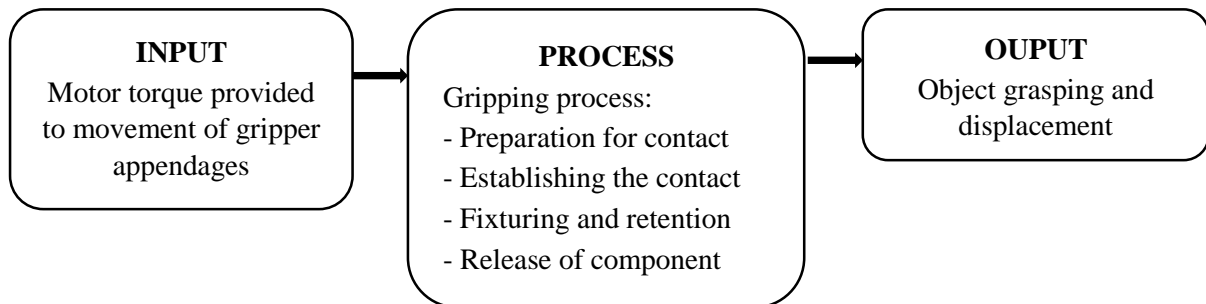


Figure 20: Gripper system procedure

The specific system comprised of a number of subsystems as seen in Figure 21. The design system was divided into subsystems namely: The mechanical structure, the sensory system, actuation, robotic arm, and control system.

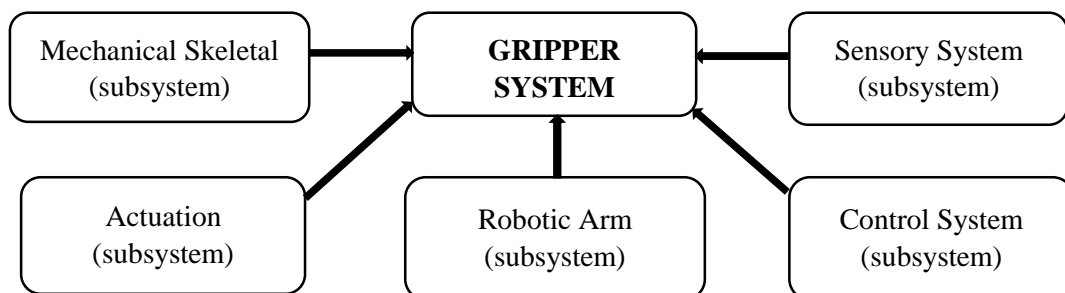


Figure 21: Gripper mechanical system outline

Every fixture system consists of a tool unit, a robot arm, and a control unit. Explained by Prešeren, Avguštin, and Mravlje [39], the mechanical design factors of the gripper system include grip reach, gripping forces, stress distribution, adaptability and grip slippage. A design is proposed by Chiprobot [40], where grip strength of all fingers was simultaneously manipulated with a central motor applying torque to a worm gear. The proposed design reduced the cost compared to grippers with appendages being individually actuated.

The gripping system required to be designed to handle the gravitational forces acting on the object and the forces due to acceleration in the movement to ensure effective grasping. The gripper should also maintain holding pressure due to centripetal forces while in movement. The design should be lightweight not to interfere with the workload capacity of the robotic arm. In addition, the gripping system should also be durable for continuous and repetitive pick and place procedures.

The base material for the gripper's structure was plastic and specifically ABS plastic was selected for ease of manufacturing by means of 3D printing. Steel fasteners, screws and threaded bars, were applicable for all high-stress connections. The method of manufacturing a prototype, as mentioned before, is 3D printing. As an adaption of rapid-prototyping, 3D printing can simply and quickly produce the required components of the design as explained by [41].

An actuation system was designed using a stepper motor, a motor controller, and a micro-controller. The electrical actuation enabled the grasping action of the gripper for grip contact, retention and release of the object to be manipulated. The system was adjusted, dependent on the speed required of the system.

The gripper appendage surface was designed to mimic the geometric conformity of the object. Due to the unique properties of the Fin Ray Effect®, the appendages needed to be designed for rigidity, but also considerations were taken for flexibility. Forces were measured by means of force sensitive resistors to achieve the capability of force control in future research and development. The measurements acquired resembled the forces acting on the gripper fingers.

The final design was considered to incorporate alternative current as the power supply for the gripping unit for integration into an assembly system. An AC to DC converter was considered for ease of implementation on the robotic arms for assembly processes. The prototype design consisted of direct current power supply units.

The section described several mechanical and electronic design considerations that influenced the design process of the gripper system. The section also discussed several design complications that are tackled throughout the research design phase of the project and by other researchers.

2.8 Typical Sensor System and Sensor Feedback Loop

The gripper system described consisted of input, process and output elements in a gripping procedure. The simplified system should allow for control over the force applied to the object in the grasping process. In order to control the force required throughout static and dynamic gripping, the system requires a monitoring and control subsystem as illustrated in Figure 22 and Figure 23. The system was controlled by:

- Using sensors to monitor the input part of the system and feeding the information to a controlling device that makes changes to the input.
- Using sensors to monitor the mechanisms in the process part of the system and feeding the information to a controlling device that makes changes to the input and/or the process part of the system.
- Using sensors to monitor the output part of the system and feeding the information to a controlling device that makes changes to the input and/or the process part of the system.

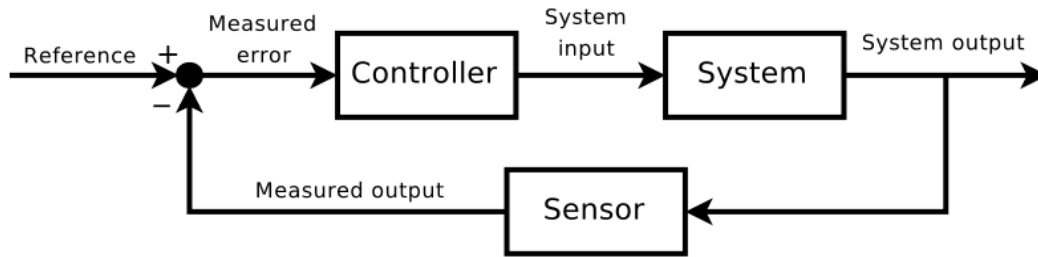


Figure 22: Typical sensor feedback loop

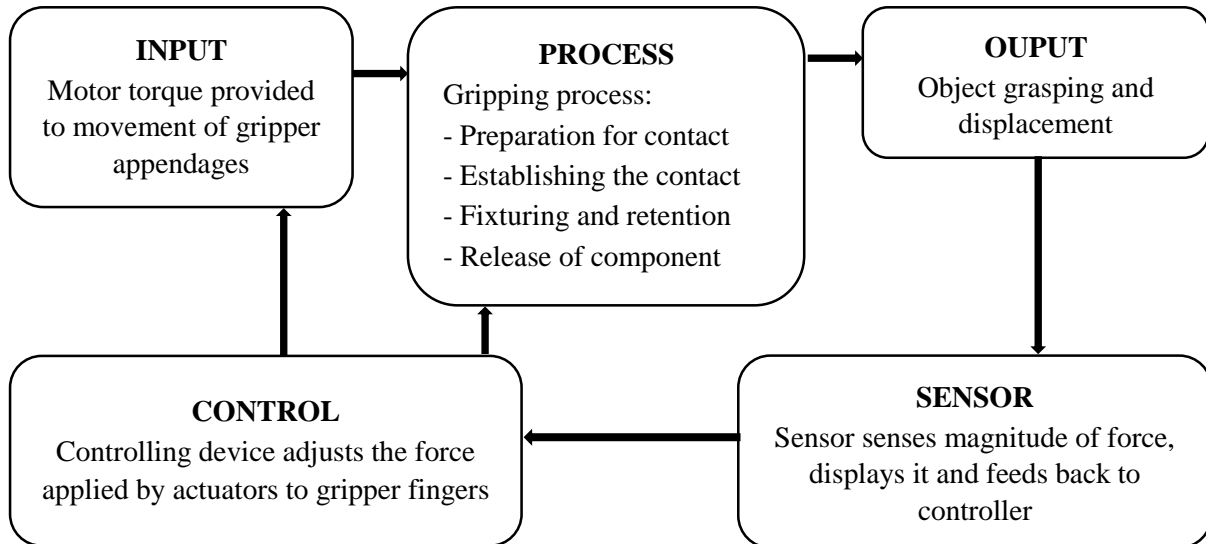


Figure 23: Feedback and control of gripper system

2.9 Conclusion

The section discussed the literature based on previous research completed by other researchers in the field of flexible gripper development in reconfigurable assembly systems. The research undertaken in the literature reviewed and examined initiatives of investigators to overcome challenges in the design and development of flexible grippers. A study generated a variety of solutions and resolved the problem in relation to efficiently gripping an object being incorporated in the production. The study discussed the current situation of grippers in industry and production. An overview description has been examined of basic elements of design including mechanical design, electronic design and sensor system design. The basic elements offer a summary of what the design consists of.

3 Theory

3.1 Introduction

This chapter reviews the forces applicable in gripping mechanisms. The forces required should be incorporated in the strength of the actuation of the appendages. The applied friction forces should be large enough to overcome the maximum forces involved in slipping. Additionally, the force load should be below the threshold able to damage the surface integrity of the object and appendages. The gripper should comply with an ISO standard, with regard to the repeatability of grip retention incorporating the grasping force. Repeatability for grippers are problematic to quantify as a result of the grippers not possessing position control and only the holding force repeatability can be determined. The forces involved in determining the dynamic gripping loads originate from the acceleration parameters occurring through the movement of the robot manipulator. The Denavit-Hartenberg model describes the position of the end-effector attached to the manipulator in terms of joint angular displacement. The position vectors are derived from the DH-matrix model. The Jacobean matrix describes the dynamic motion in terms of acceleration and velocity parameters. The forces are explained through Lagrangian equations, describing force vector components in terms of the acceleration and velocity vectors of the end-effector. Finally, the Fin Ray Effect[®] is reviewed to describe the self-conformity properties of the biologically inspired mechanism.

3.2 Gripping Force and Payload

It is important to determine the gripping force and payload for the gripper as it can affect the working conditions for robotic-arm as well as the end-effector. The payload is generally described as the maximum mass the robotic gripper will be able to support throughout the operation. The payload mass is transformed into a payload force. Bélanger-Barrette et al. [42] describe the grip force as the maximum effort applicable by the manipulator. Payload and gripping force vary for different manufacturing purposes.

3.2.1 Introduction

In determining the gripping force of the robotic manipulator, of which the robotic arm carries a payload, the system was designed with the force constraints in mind. The gripping force is affected by the mass of the payload, the material of the payload in the form of a friction coefficient, the number of fingers on the manipulator, the acceleration of the payload required and the limitation on the actuators.

3.2.2 Determining Gripping Force

Determination of gripping forces is explained by [43]. The gripping force for manipulating an object has to surpass the minimum frictional force, otherwise, the object will slip through the gripping appendages. The necessary gripping force required by the gripper would be about 10 to 20 times the part weight or more. The following equation shows the allowable force required to be above the friction force, to prevent slipping as shown in Figure 24. The gripping force applied must resist the acceleration force due to impact or sudden increase or decrease of velocity on the weight of the object being manipulated.

$$F > \frac{mg}{\mu} SF \quad (3.1.)$$

Where:

F : Allowable gripping force and the sum of push forces [N].

μ : Static friction coefficient between gripping surface and object surface.

m : Object mass [kg].

g : Gravitational acceleration [= 9.81 m/s²].

SF : Safety factor to be used.

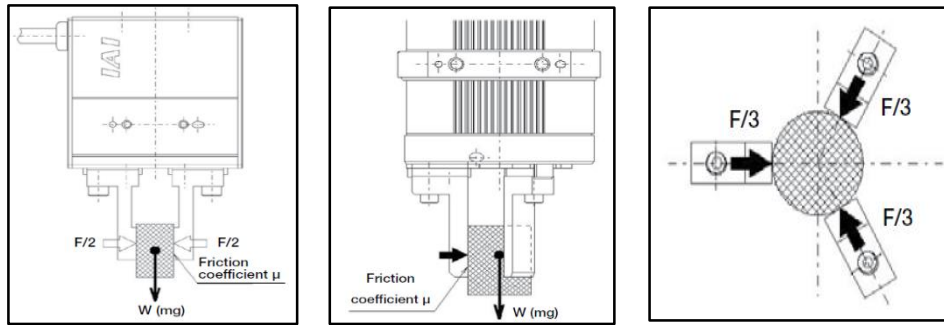


Figure 24: Friction force required for two and 3-fingered gripper [43]

The distance between a gripping point and actuated gripping length should be taken into consideration due to the bending moment applied and may affect the material strength integrity of the manipulator's fingers. The lengths were described as the length from the gripping point L and the overhanging length H as seen in Figure 25 and Figure 26. These lengths should be kept to a minimum to reduce the bending moment.

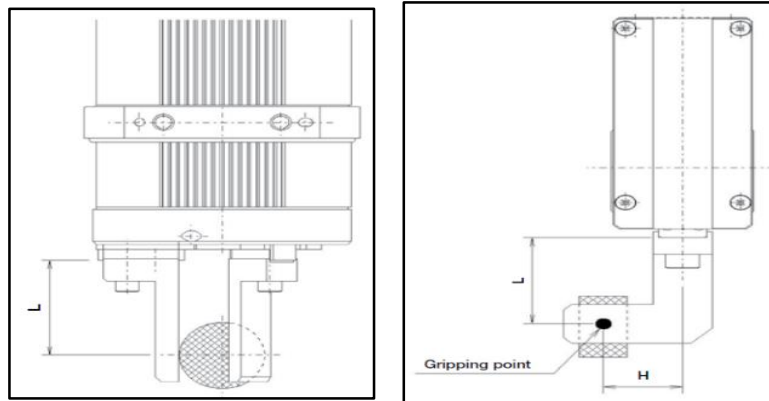


Figure 25: Length shown in gripping geometry [43]

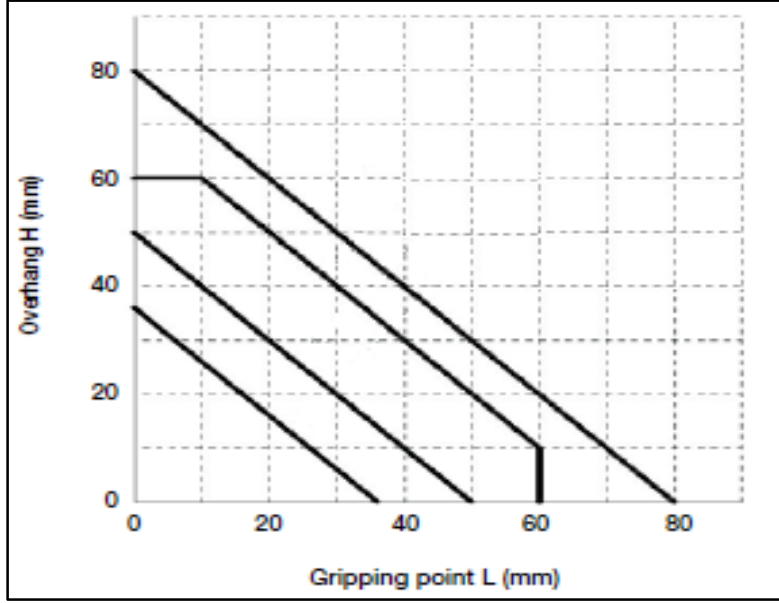


Figure 26: Gripping point L versus overhanging H [43]

Confirm that the maximum vertical load is equal to the allowable load or less to prevent damage to gripper mechanism. This force is related to the force in the upward direction. Allowable load moment should be calculated for all directions of movement and this should correlate with the yield bending stress of the gripping finger material. Moments should be calculated around all directions illustrated in Figure 27. The following equation shows the allowable force required in terms of the moments in the direction of the overhanging length and the length from the gripping point:

$$F > \frac{M}{L} \quad (3.2.)$$

Where:

F : Allowable gripping force and the sum of push forces [N].

M : Moment [N.m.].

L : Length in the chosen direction [M].

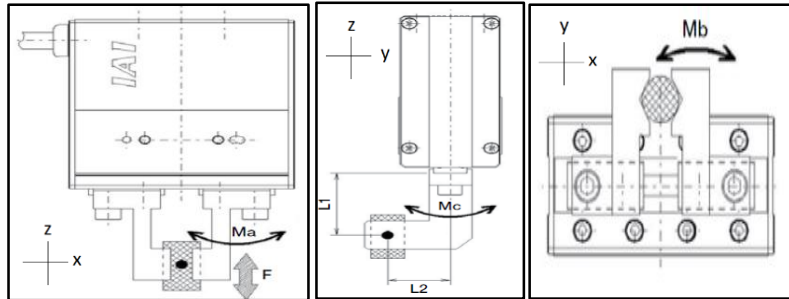


Figure 27: Moments in all direction [43]

Confirm that all the moments of inertia around the z -axis in relation to its fulcrum fall within an allowable range. Moments of inertia are shown in Figure 28. The length taken is the working length of the claw finger.

Moment of inertia around Z_1 -axis.

$$I_{z_1} = \frac{m_1(a_1^2 + b_1^2)}{12} \times 10^{-6} \quad (3.3.)$$

Moment of inertia around Z_2 -axis.

$$I_{z_2} = \frac{m_2(a_1^2 + b_1^2)}{12} \times 10^{-6} \quad (3.4.)$$

All moments of inertia around the Z -axis.

$$I = (I_{z_1} + m_1 R_1^2) + (I_{z_2} + m_2 R_2^2) \quad (3.5.)$$

m_1 : Weight of A [kg] = $a_1 \times b_1 \times c_1 \times \text{specific gravity} \times 10^{-6}$.

a, b, c : Dimensions of section A [mm].

I_{z_1} : Moment of the area around Z_1 [mm⁴].

I_{z_2} : Moment of the area around Z_2 [mm⁴].

R_1 : Distance from the COG of A to finger fulcrum [mm].

R_2 : Distance from the COG of B to finger fulcrum [mm].

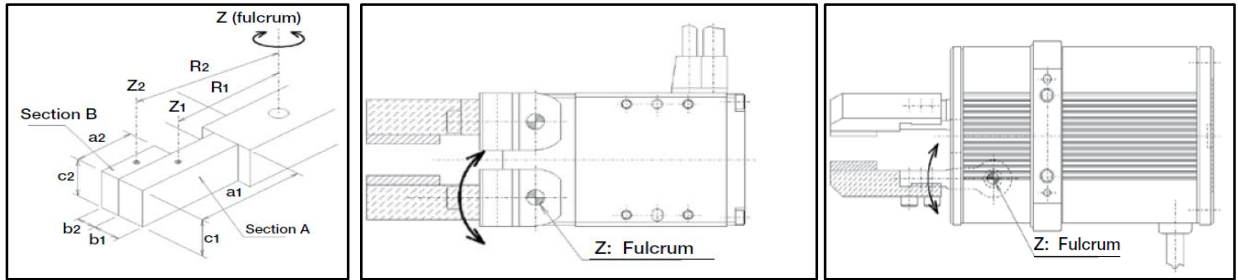


Figure 28: Moment of inertia all z -directions [43]

The load torque applied on to the object being manipulated should be confirmed with the allowable load torque or less as shown in Figure 29. The equation to calculate allowable thrust is given as follows:

$$T = (W_1 \times R_1) + (W_2 \times R_2) + (\text{other load torque}) \quad (3.6.)$$

$$T = (m_1 g \times R_1) + (m_2 \times R_2) = (\text{other load torque}) \quad (3.7.)$$

T : Torque [Nm]

R_1 : Distance from the COG of A to finger fulcrum [mm].

R_2 : Distance from the COG of B to finger fulcrum [mm].

m_1 : Mass of part weight [kg].

m_2 : Mass of clamp/gripper [kg].

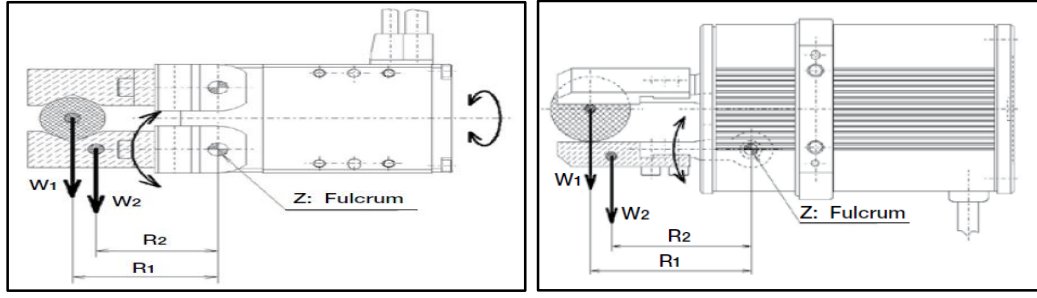


Figure 29: Allowable load torque [43]

Allowable thrust load, which is equivalent to the vertical acceleration of the artefact, should be confirmed according to the allowable load thrust as illustrated in Figure 30. Thrust equation is shown:

$$F = W_1 + W_2 + (\text{other thrust load}) \quad (3.8.)$$

$$F = m_1g + m_2g + (\text{other thrust load}) \quad (3.9.)$$

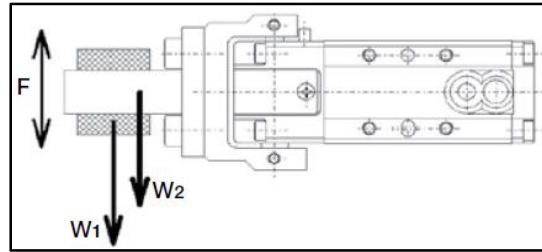


Figure 30: Allowable thrust load [43]

3.3 Precision Placement, Precise Location Control, and Repeatability

In robotic automation, a key emphasis must be placed on repeatability and precision. It is highly favourable for the robot to be repeatable, which affects its task execution. The repeatability is the ability of the robot to achieve repetition of the same task [44]. Accuracy is defined as the difference or error between the task that was obtained and the task that was requested by the operator.

3.3.1 Introduction

To be able to fully define the repeatability and accuracy, it is important to evaluate: path, position, and orientation. These characteristics are included in the equations that are further explained as variable commands. These factors need to be assured of being achieved every time the robot and the end-effector are set in motion. The path accuracy and pose accuracy have variable outcomes that affect the intrinsic movement nature of the end-effector. Methods are discussed in determining models to quantify repeatability and accuracy. The norm used in ISO standards in determining repeatability uses a statistical measurement of experimental results. Another unique method is using fuzzy clustering to determine the repeatability and accuracy of robotic arms.

3.3.2 Statistical Measurement

Precision placement of robotic arms was measured in terms of repeatability. Repeatability as defined by Bouchard et al. [45], is the deviation of position from the average displacement. Accuracy was described as the ability to position precisely at a preferred location within the working area or volume illustrated in Figure 31.

According to the ISO standard 9283: 1998, accuracy and repeatability are measured at pessimistic values, using the largest payload and highest operating speed. A simplified protocol for measuring the repeatability and accuracy of robotic arms is as follows:

- The robot should be warmed up until steady state conditions are reached including thermal stability of motors and gearboxes.
- The robot must be commanded to perform identical movements to 3 different positions in the sequence.
- The positions must be measured by an optical target carried by the robot, two cameras measuring position; or other instruments.

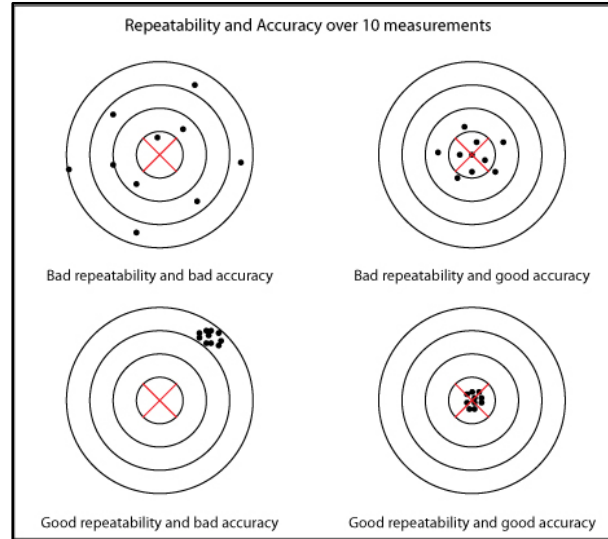


Figure 31: Repeatability and accuracy [45]

The following calculation method determines the repeatability of the data. The experiment is carried out for position command (X_c, Y_c, Z_c) and reaches a position (X_r, Y_r, Z_r):

Average calculation:

$$\bar{X} = \frac{1}{N} \sum_{i=1}^N X_r \quad (3.10.)$$

$$\bar{Y} = \frac{1}{N} \sum_{i=1}^N Y_r \quad (3.11.)$$

$$\bar{Z} = \frac{1}{N} \sum_{i=1}^N Z_r \quad (3.12.)$$

Standard deviation calculation:

$$l_i = \sqrt{(X_r - \bar{X})^2 + (Y_r - \bar{Y})^2 + (Z_r - \bar{Z})^2} \quad (3.13.)$$

$$\bar{l} = \frac{1}{N} \sum_{i=1}^N l_i \quad (3.14.)$$

$$S_l = \sqrt{\frac{\sum_{i=1}^N (l_i - \bar{l})^2}{N - 1}} \quad (3.15.)$$

Repeatability equation:

$$RP_l = \bar{l} + 3S_l \quad (3.16.)$$

Using this formula, statistical theory suggests that the position of the robotic arm used would be in the repeatability range of about 98%. A problem arises when measuring the repeatability of grippers for robots, and therefore the ISO norm does not apply to manipulator fixtures, only to robotic arms. There are two major differences when it comes to robotic arms and robotic grippers, for which the ISO standard is non-compliant:

- Robotic arms have many degrees of freedom, while grippers only have one moving axis. The ISO norm states that there should be at least 10 measurements taken on each axis or degree of freedom.
- Most grippers only have open and closed positions and no intermediate positions, therefore the ISO standard is not advised to be used. The closed position of the jaws of the gripper is used as the fixed datum point. Electric grippers with position control were used in the repeatability ISO standard.

3.4 Kinematics of Robotic Arm

The kinematics of robots is the study the motion of mechanised machines utilised in a repetitive task in assembly procedures. The position, velocity, and acceleration were determined of all the links and segments involved, without considering the forces involved in motion as investigated by [46]. A robot consisting of many parts assigned to the individual frame of references for each component was analysed through a single frame of reference. In the instance of this study, we deal with inverse kinematics by means of solving kinematic equations to determine the relationships between the location of the manipulator and its corresponding links.

3.4.1 Introduction

The transformation matrix for solving the kinematic equations is based on 6 DOF robotic arm. The acceleration is required to compare to force data from force measurements of experimentation. The acceleration can be determined and thus the acceleration can be established through basic kinematic equations. The proficiency of the grasping of the gripper is affected by the forces applied to the object due to the acceleration of robotic arm.

3.4.2

Forward Kinematics: Denavit-Hartenberg (DH) Convention

The Denavit-Hartenberg convention is a widely used algorithm that describes the kinematic model of a robot. Described by Yang, Ma and Fu [47] the links of the serial robotic system can be represented by two parameters, specifically the twist angle α_i and the link length a_i . The twist angle α_i designates the angle of twist of the axis between i and $i-1$. The joints can also be represented by two parameters, namely, link offset d_i and the joint revolute θ_i . The four parameters for DH convention is utilized in a homogeneous transformation matrix as shown in Figure 32.

Each individual homogenous transformation matrix can be represented as the product of four basic transformations:

$$H_i = [Rot_{z,\theta_i}][Trans_{x,d_i}][Trans_{x,a_i}][Rot_{x,\alpha_i}] \quad (3.17.)$$

$$H_i = \begin{bmatrix} c_{\theta_i} & -s_{\theta_i} & 0 & 0 \\ s_{\theta_i} & c_{\theta_i} & 0 & 0 \\ 0 & 0 & 1 & 0 \\ 0 & 0 & 0 & 1 \end{bmatrix} \begin{bmatrix} 1 & 0 & 0 & 0 \\ 0 & 1 & 0 & 0 \\ 0 & 0 & 1 & d_i \\ 0 & 0 & 0 & 1 \end{bmatrix} \begin{bmatrix} 1 & 0 & 0 & a_i \\ 0 & 1 & 0 & 0 \\ 0 & 0 & 1 & 0 \\ 0 & 0 & 0 & 1 \end{bmatrix} \begin{bmatrix} 1 & 0 & 0 & 0 \\ 0 & c_{\alpha_i} & -s_{\alpha_i} & 0 \\ 0 & s_{\alpha_i} & c_{\alpha_i} & 0 \\ 0 & 0 & 0 & 1 \end{bmatrix} \quad (3.18.)$$

$$H_i = \begin{bmatrix} c_{\theta_i} & -s_{\theta_i}c_{\alpha_i} & s_{\theta_i}s_{\alpha_i} & a_i c_{\theta_i} \\ s_{\theta_i} & c_{\theta_i}c_{\alpha_i} & -c_{\theta_i}s_{\alpha_i} & a_i s_{\theta_i} \\ 0 & s_{\alpha_i} & c_{\alpha_i} & d_i \\ 0 & 0 & 0 & 1 \end{bmatrix} \quad (3.19.)$$

a_i : Link length, thus the distance between o_0 and o_1 and is projected along the x_1 axis.

α_i : Link twist, thus the angle between z_0 and z_1 and measured around x_1 axis.

d_i : Link offset, thus the distance between o_0 and o_1 and is projected along the z_0 axis.

θ_i : Joint angle, thus the angle between x_0 and x_1 and is measured around the z_0 axis.

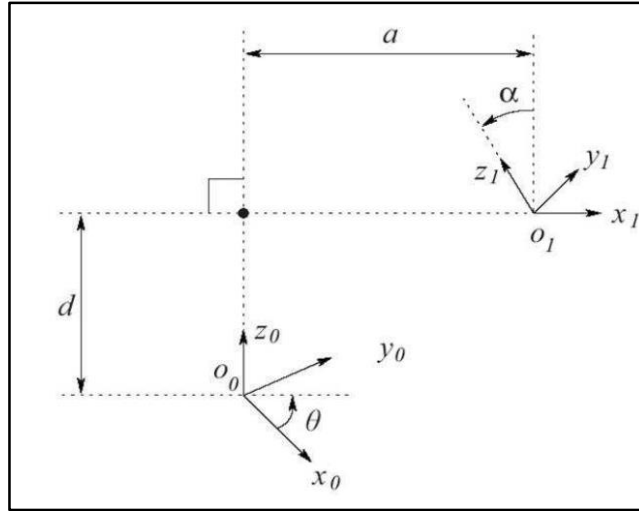


Figure 32: Kinematic link and joint parameters [47]

The values are found by the parameters of the joint that will place the frame of the tool at a desired position and orientation within the workspace area:

$$H = \begin{bmatrix} R & o \\ 0 & 1 \end{bmatrix} \in SE(3) \quad (3.20.)$$

$$c = [q_1, \dots, q_n]^T \in C \quad (3.21.)$$

Such that

$$T_n^0(q_1, \dots, q_n) = H \quad (3.22.)$$

Where

$$T_n^0(q_1, \dots, q_n) = A_1(q_1) \dots A_n(q_n) \quad (3.23.)$$

Noting that

$$H = \begin{bmatrix} h_{11} & h_{12} & h_{13} & h_{14} \\ h_{21} & h_{22} & h_{23} & h_{24} \\ h_{31} & h_{32} & h_{33} & h_{34} \\ h_{41} & h_{42} & h_{43} & h_{44} \end{bmatrix} \quad (3.24.)$$

Where

$$h_{41} = h_{42} = h_{43} = 0 \text{ and } h_{44} = 1 \quad (3.25.)$$

n unknowns in 12 linear equations

The kinematic equations are utilized in built-in kinematic simulation model packages used in demonstrating the robotic arm, as used in RoboDK®. Forward kinematics was of particular interest to determine the end-effector position. Inverse kinematics determines the angular displacement of each joint. The acceleration parameters of the end-effector were of concern. Therefore, further research was not performed on inverse kinematics.

3.5 The Fin Ray Effect®

The Fin Ray Effect®, which is a mechanism naturally occurring in nature, was utilised for efficient gripping. Based on the conforming properties of a fish fin enables the structure to bend around shapes. The biology behind the V-shape appendage allows for a more efficient grasp on objects in gripper systems. The gripper with fin attachments can easily be integrated into any robotic pick and placement procedure.

3.5.1 Introduction

Tharayil, Babu, Cherussery and Joy [48] explained that biologist Kniese of Evologics discovered the Fin Ray Effect® while fishing. The mechanism is based on the deformation of fish fins. The Fin Ray structure is constructed from two V-shaped bones that are connected by means of a muscle tissue. Pushing on a side of the V-shape, the fin shape deforms in a manner of conforming around the force. The mechanism is versatile and scalable for robotic gripper applications.

3.5.2 Fish Ray Effect® Mechanism

The biological mechanism called the Fin Ray Effect® which was an adaption made by Kniese. An A-frame structure incorporating cross-beams which were spaced between the base and the tip of the V, a gripper appendage could be prepared. In the instance where the fins are in contact with an object presented by P, the walls tend to envelop about the object and return provides a secure grasp. The tendency to envelope is shown in Figure 33. The mechanism minimizes the number of joints required

in a gripper system to conform around objects, therefore making it lightweight and adaptable. The self-conforming property reduces the number of moving parts required for the design of complex manipulators. The versatility of the Fin Ray Effect[®] advances new developments in recreating robotic grippers. The appendages can easily be manufactured and incorporated into robotic systems.

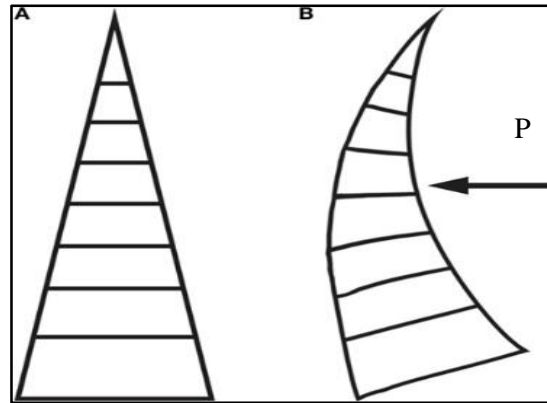


Figure 33: Mechanism of the Fin Ray Effect[®] [48]

3.6 Conclusion

The forces involved in the gripping of the component illustrated the importance in designing a gripper to have full grasping capabilities. In order for the design to be viable, the results from testing will need to correspond with a benchmark and should be repeatable for applications in continuous assembly. Therefore, a mathematical formula is discussed in describing whether the accuracy of the gripper is repeatable. The model was described by using a kinematic model of the system. The kinematic convention of Denavit-Hartenberg would be an appropriate model, as it provides a method for determining variables in the motion of the robotic arm. The acceleration can thus be determined and the occurring forces during movement play a role in the grasping effect of the gripper model. Finally, we looked at the Fin Ray Effect[®] and its unique biological mechanism of gripping. The fin gripper proved to be a viable gripping method for flexible gripping systems.

4 Methodology

4.1 Introduction

This chapter explains the methodology of the project. The research and development section describes the specifications requirements for the research and development of the gripper system in terms of reconfigurable assembly systems. The performance criteria for robotic arms and grippers have to be met with regards to availability and industrial application to increase the efficiency of assembly systems incorporating grippers. The design process defines the procedure of development from first principles and criteria generated from the literature review. The simulation procedure section examines tools used and relevance for the theoretical development of models. Experimental procedure section describes the method attaining actual performance of the system. Finally, the process of data capturing section explains the experimentation to determine the performance of the gripper system.

4.2 Research and Development

4.2.1 *Specifications and Benchmark*

The methodology for research and development summarised important aspects of the project that was looked into when designing the system from the literature review. Several criteria were not necessarily integrated and assumptions were made in rejecting specific criteria. Through the research phase, specifications and benchmarks were generated in order for the design of the gripper to measure up to industry benchmarks. The procedure of the conceptual design would follow the specifications. A benchmark was set up according to criteria indicated throughout the literature. The systems to be investigated must comply with the characteristics of what a reconfigurable assembly system is:

- Customisation: The system's ability to clamp different part families with different geometries.
- Convertibility: The interchangeability of the system to accommodate different part families.
- Scalability: The system's adaption to the influx of component quantities in terms of the production scale.

Requirements for the specific development of reconfigurable fixtures are the following:

- Modularity: The fixture should be composed of standard modules for effortless system combination and assembly.
- Automatic reconfigurability: The fixture should reconfigure automatically according to the change of capabilities and behaviour with regard to change in manufacturing process.

-
- Sensory feedback controllability: Sensory integration and control feedback approach should be included in the system.
 - Programmability: The operating system should be programmable to increase the flexibility of the gripper system concerning process operation.

The following requirements and factors determine the type of gripper and capacity of the task to be accomplished:

- Technological requirements: These include the number of the object acquisitions per gripping cycle, time duration depended on the applied force, gripping path and time capacity.
- Effects of the characteristics of the objects: These include the temperature, strength, material type, surface properties, stability, and centre of gravity, tolerance of determined dimensions, design, and mass.
- Factors related to handling equipment: These include connections specifications, axial accelerations, and positional accuracy.
- Factors related to environmental parameters: these include the vibration, humidity, contaminations, storage conditions, feeding conditions and clamps, and forces.

The gripping procedure was divided into four phases consisting of part prehension and retention:

- Preparation for contact.
- Establishing the contact between the part surface and gripper surface.
- Fixturing and retention of the part during manipulation.
- The release of the component at the destination.

4.2.2 *Robotic Arm Selection*

The proposed robotic system incorporated an articulated arm for part manipulation. Design considerations were important when selecting a robotic manipulation arm and have varying degrees of freedom as seen in Figure 34. The selection criteria were set out for choosing a robotic arm were dependent on the requirements of the arm in a process. The following design considerations were set out for selecting a robotic manipulator arm:

- Maximum payload.
- Degrees of freedom.
- Work envelop.
- Repeatability, accuracy, and precision.
- Speed and cycle time.
- Robot mass.
- Ingress protection rating.

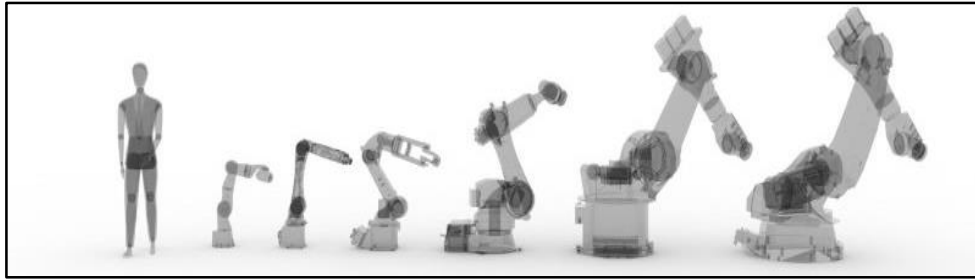


Figure 34: Robotic arm selection

4.2.3 *End effector Selection*

The gripper system required an end effector. Design considerations were important when selecting a robotic end effector and have varied gripping functions as seen in Figure 35. The selection criteria set out for choosing an end-effector was dependent on the requirements of the gripper in a process. The following design considerations were set out for selecting an end effector:

- Effective shape conformity.
- Geometric adaptability.
- Maximum gripping force.
- Sensitivity to the material.
- Sensitivity to surface damage.
- Repeatability, accuracy, and precision.

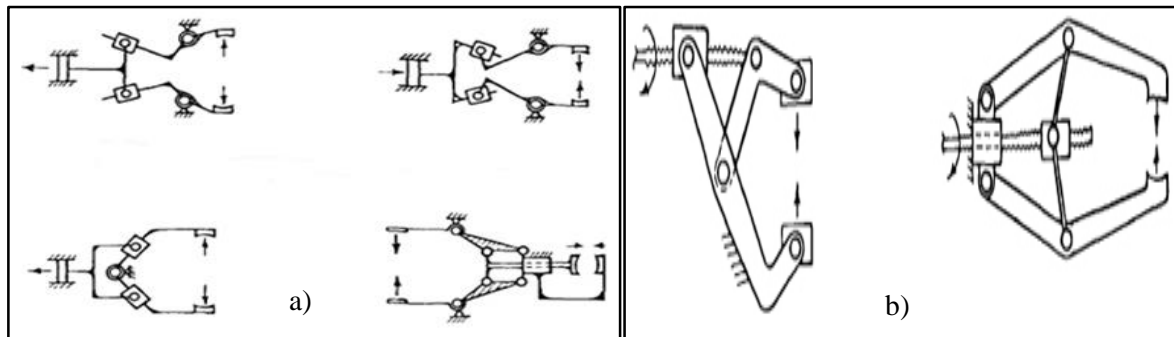


Figure 35: Linkage a) and screw b) driven actuation gripping types

4.2.4 *Design Procedure*

When designing a flexible gripper for the purpose of industrial applications, the gripping of a variety of materials and parts were taken into consideration. Selecting the gripper was important, to avoid interchanging fixtures for different part families. The design solution was critical in the production rate and economy of the assembly process and therefore should be designed for the specific application. In relation to a human hand model, the end effector was inadequate in terms of the mechanical complexity, utilisation of practical movements, and applications for general procedures. The gripper to be designed should have the capabilities of a human hand in terms of material handling, sensory feedback, repeatability, autonomous configuration.

The technical factors of a process and part perspective has to be investigated in selecting a gripper. The following factors contributed to the role the gripper would suit best:

- The task required by the gripper to grasp a component in an assembly procedure.
- Cycle time and speed required for fastening and releasing of the gripper.
- Precision and adaptability required for gripper method.
- The environmental needs and manufacturing industry requirements for part manipulation.
- Part factors include the following: Size, shape, weight and surface type.
- Economic factors and economic restraints present in automation process.

After selecting a gripper for the process, it was required to measure the performance and efficiency of the gripping method. The following specifications were incorporated in the justification of a benchmark for the gripper performance:

- Effective shape conformity, and geometric adaptability.
- Gripping force according to the weight of the object and static force resistant properties.
- Precision gripping and repeatability.
- Sensitivity to material types and surface damage.
- Process integration and adaptability, compared to adjustment with other automation processes.
- Intelligent self-adjusting and flexible properties.

4.2.5 *Simulation Procedure*

Theoretical models were developed in terms of computer simulations using a simulation program called Siemens NX Nastran®, to determine the stress the model experiences during handling of the object, including the strength and failure of the components. A functional mathematical model was set up for path planning, and RoboDK® was used as a software tool.

Theoretical model simulation: Siemens NX Nastran®

- Stress analysis: Determining the stress and deflection criteria of the gripper.

Theoretical path planning model: RoboDK®

- Simulation model: Determining the dynamic behaviour of the gripper system including the robotic arm system.

4.3 Experimental Procedure

4.3.1 *Test Specimen, Test Rig, and Apparatus*

Test specimen/s

The test specimen/s were constructed according to the specifications of the case study with regards to lightweight and complex shaped components. The specimen/s were manipulated and evaluated for semi-autonomous assembly processes.

Test Rig

The test rig was composed of the robotic arm and the end effector. The test was run to practically simulate object conformity, precision and repeatability, and process integration. The results were compared to the efficiency and productivity of the specifications set out in the model.

Testing Apparatus

The testing apparatus was in the form of the following:

- Simulation programs used for simulating theoretical models and acquiring data sorting of the results.
- Sensors that were implanted on the test rig to acquire data from the experimental procedure for result comparison.
- Computer hardware and software used as a communication medium between the data acquisition and data interpretation e.g. laptop, windows operating system etc.

4.3.2 *Configuration for Geometric Adaptability*

The gripper system was tested according to criteria for geometric adaptability. Object conformity would be achieved as a result of the measured force on the surface of the gripper fingers was equal or greater to the gripping force required for that object. In addition, the force should also be smaller than the maximum allowable force before damage can occur to the material structure or surface of the workpiece. The force versus time measurement was represented on a graph as the actual performance of an operational gripper. The following criteria were looked in the experimental procedure:

- Grasping parts securely.
- Deformation of the part during grasping.
- Minimizing of finger length.
- Providing an ample approach clearance.
- Chamfer of approaching surfaces of the gripper fingers.
- Design for proper gripper-part interaction.
- Encompassing of actuator mounting points.

4.3.3 *Configuration for Precision and Repeatability*

Precision can be determined by a statistical model in terms of the standard deviation of the measured force data. The repeatability was related to a 98% effective repeatable movement from ISO 9283:1998 [49]. The statistical method is effective when the initial and final location of the object is known.

4.4 Data Capturing and Recording

4.4.1 *Data Capturing Method*

Data was attained for the various methods of measuring performance by means of placing force sensors on the gripping surface. Sensor configuration has the ability to translate an electrical signal from the tested variable and relayed to a third party program for data recording. The sensory system consisted of

a force feedback sensor loop, and as a result, the data values were retrieved as force values. The magnitude of the force values was related to the grasping strength of the gripper.

4.4.2 *Results Interpretation*

The results of the experimental process were interpreted in terms of performance of the gripper system. The results accumulated from the sensory feedback were processed and compared to the specifications set out in the system. Adaptive changes were made when certain criteria had not been met and experimental procedures were re-evaluated. The force versus time values measured in the dynamic testing correlates to the gripper's performance of the system in a pick and place procedure.

4.5 Conclusion

The specifications were described in terms of the characteristics of a reconfigurable assembly system. The conceptual model was researched and developed concerning the performance requirements of available robotic arms and grippers. The design process was explained relating to mechanical and electronic design. The simulation was discussed using computer software tools. The experimental procedure was examined to generate physical performance criteria for the gripper system. Finally, the method of data capturing and relevance of results was described.

5 System Conceptual Design

5.1 Introduction

This chapter describes the concept design that is generated according to the selection of appropriate models based on studies in the literature study and in the result, a set of specifications is established for the model. A combination of flexible components for the gripper system is required to work in synchronous operation to increase the efficiency and performance of a flexible automated assembly line in terms of pick and place procedures. The gripping system is described as an integral part of an assembly procedure for reconfigurable assembly systems. The system integration section describes the function of the grasping fixture as a part of object manipulation and the role it plays concerning the performance of the system.

5.2 System Specifications

The gripper system was selected and design to mostly match the design criteria according to ISO 14539 standards. The ISO 14539 standard is a highly complex set of requirements and specific design criteria were selected and adjusted accordingly. The gripper must perform according to the following criteria pertaining to ISO 14539 [50].

5.2.1 *Types of States*

The gripper system to be developed, designed and manufactured should follow four (4) grip states accordingly illustrated in Figure 36:

- **State 1 (Gripped):** Constraining occurring by utilizing only the end-effector and excluding aid of the environment.
- **State 2 (Semi-gripped):** Constraining occurring by utilizing the end-effector and the environment.
- **State 3 (Laid):** Constraining occurring by utilizing the environment and not the end-effector.
- **State 4 (Free):** Constraining occurring by neither the end-effector nor the environment.

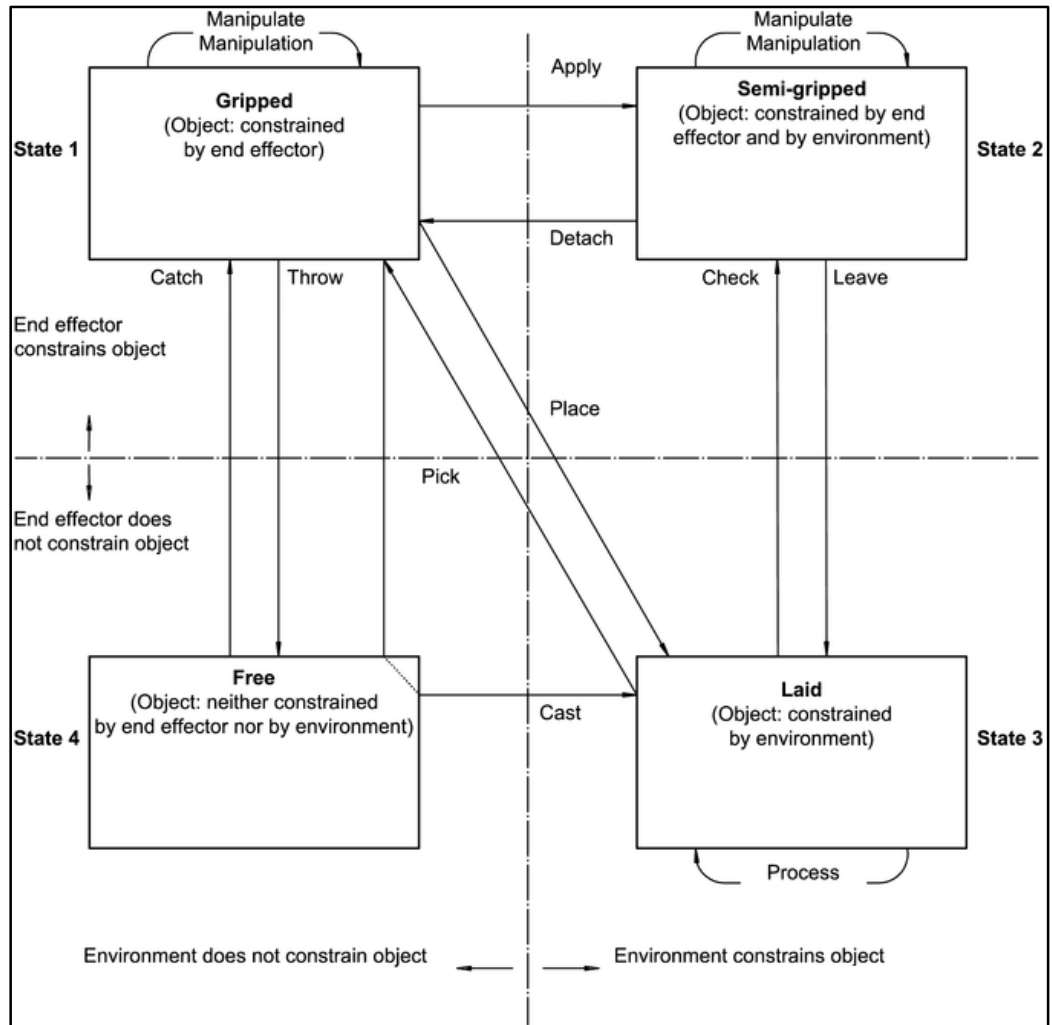


Figure 36: States and actions in object handling [50]

5.2.2 Types of Grasps

The gripper should include object conformity criteria in terms of types of grasps shown in Figure 37:

- **Degrees of freedom of grasped object:** The object's degree of motion in free-space when constrained by appendages including or excluding the friction forces at the point of contact.
- **Form closure grasping:** The degrees of freedom of grasp being zero (0) or less excluding friction force consideration.
- **Force closure grasp:** The degrees of freedom of grasp being one (1) or more excluding friction force consideration.
- **External grasp:** Grasping that influences the objects external surface.
- **Internal grasp:** Grasping that influences the objects internal surface.

The types of grips shown in Figure 37, are illustrated in terms of:

- a), b): One (1) finger type grips;
- c), d), e), f): Two (2) finger type grips;
- g): Multi-finger type grips.

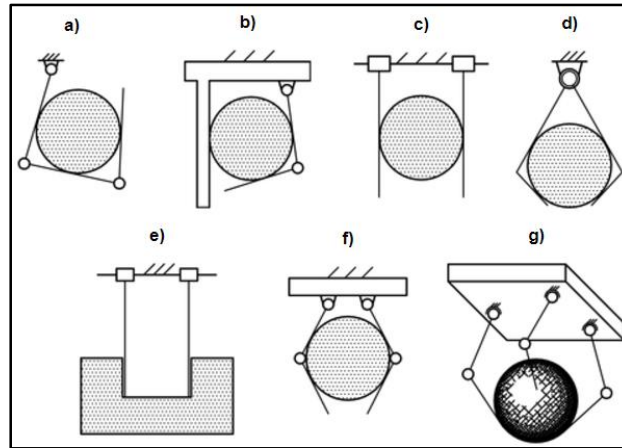


Figure 37: Typical grasps with grasp-type grippers [50]

5.2.3 Forces in Grasps

The gripper should have a gripping strength in terms of minimum gripping loads and forces shown in Figure 38:

- **Contact forces:** The force subjected to the object from the finger through contact, contact plane or contact point should at least be equivalent to 3 N static hold and 1 N dynamic hold. The contact forces are denoted as F_1 or F_2 , shown in a) and b).
- **Manipulating force:** The sum of the vector magnitude of all the forces in contact with the object and fingers should be equivalent to 10 N static hold and 3 N dynamic hold. The manipulating force is denoted as $-F = F_1 + F_2$, shown in a).
- **Gripping force:** The sum of gripping forces should equal to zero (0). The gripping force is denoted as $F_1 = -F_2$, shown in b).

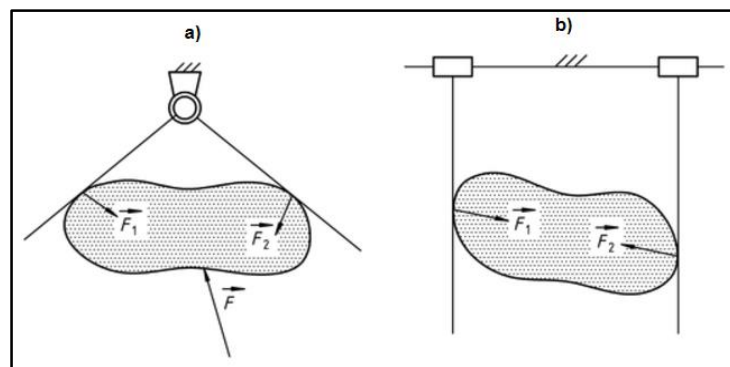


Figure 38: Forces in grasps for gripping [50]

5.2.4 Grasp Stability

The gripping system should be stable in grasping actions according to stable grasp criteria:

- **Grasp stability criteria (1):** The initial state of the gripper pose is restored after an interruption has occurred due to applied disturbance forces.
- **Grasp stability criteria (2):** The contact between the gripper and the object is always kept intact without slippage when the grasp is subjected to applied disturbance forces.

5.2.5 *Sensing in Object Handling*

The system should include sensing capabilities for feedback control of in handling according to the following criteria:

- **Object presence detection:** The following situations are to be used to detect the presence of the object:
 - a) Appropriate gripping of the object should be verified.
 - b) Successful gripping of the object should be confirmed.
 - c) Successful releasing should be ensured.
- **Finger position sensing:** The following situations are to be used to sense the finger position:
 - a) The finger position should be specified for finger control as for example for servo control.
 - b) The gripping process measures the object shape and size.
- **Gripping force sensing:** The following situations are to be used to sense the gripping forces applied to the object:
 - a) Specifications for gripping force in grasping of fragile objects.
 - b) Controlling of finger joints for higher stability of grasps.
- **External force sensing:** The following situations are to be used to sense the torques and the external forces:
 - a) The weight of the object is to be measured.
 - b) Verification of gripping integrity between contact surfaces.
 - c) Information transference to control of object handling for tasks.
- **Slip detection:** The following situations are to be used to sense the slip between the gripped objects and fingers:
 - a) Avoidance of lifting and gripping of heavy objects.
 - b) Avoidance of unstable and loose grasps of objects.
 - c) Use of gripping force higher than the minimum required slipping force.

5.2.6 *Safety in Grasps*

The following safety criteria should be kept in mind:

- **Fail-safe:** Safety functions in place for unforeseen events in terms of the failure of components.
- **Self-holding:** Passive elements are active to restrict the gripper from releasing the grasped object when a power failure occurs.
- **Self-lock:** Mechanical functions are active to restrict the gripper from releasing the grasped object when a power failure occurs.
- **Interlock:** Inhibition or conditional facilitating of release or grasping motion.
- **Grasping safety:** Avoidance function for the avoidance of unstable grips. For example the avoidance of slipping or grasping of heavy objects by means automatic force control.

5.2.7 *Repeatability*

The system should be designed according to maximum repeatability criteria:

- **Repeatability:** The gripping movements of objects should be 98% repeatable.
- **Repetition for accuracy:** At least 10 measurements should be taken for the accuracy.

5.3 System Proposal and System Integration

The proposed system consists of two major subsystems. The system follows design specifications forming part of predefined constraints and design considerations. The first subsystem was the robotic arm and the second subsystem was the gripper system. Figure 39 suggests a conceptual system consisting of BCN3D MOVEO robotic system. The final system integration used a FANUC M-10iA robotic arm and a Fin Ray Effect® gripper system.

The robotic arm concept follows a selection procedure and performs an integral role in the transportation of the gripped object and the design of the arm was not included in the scope. The scope of the project focused on the mechanical and electronic design of the end-effector for the robotic arm system.

The system integration of the gripper system can be described in Figure 40. The closed-loop robotic system consists of a: sensory system, robotic gripper manipulator, controller, robotic arm, communication acquisition between subsystems and computer interface [51]. The end-effector is manipulated by means of motor or pneumatic actuators and are controlled by means of a force feedback control loop. The gripper system is connected to a robotic arm system, which is actuated by means of pneumatic or motor actuators for all degrees of freedom. The robotic arm is controlled by means of a PLC controller. The controllers for the robotic arm and gripper communicate in terms of a controller interface through a human operated computer. The conceptual closed loop was utilized as ground-work for developing a functional manipulation system.

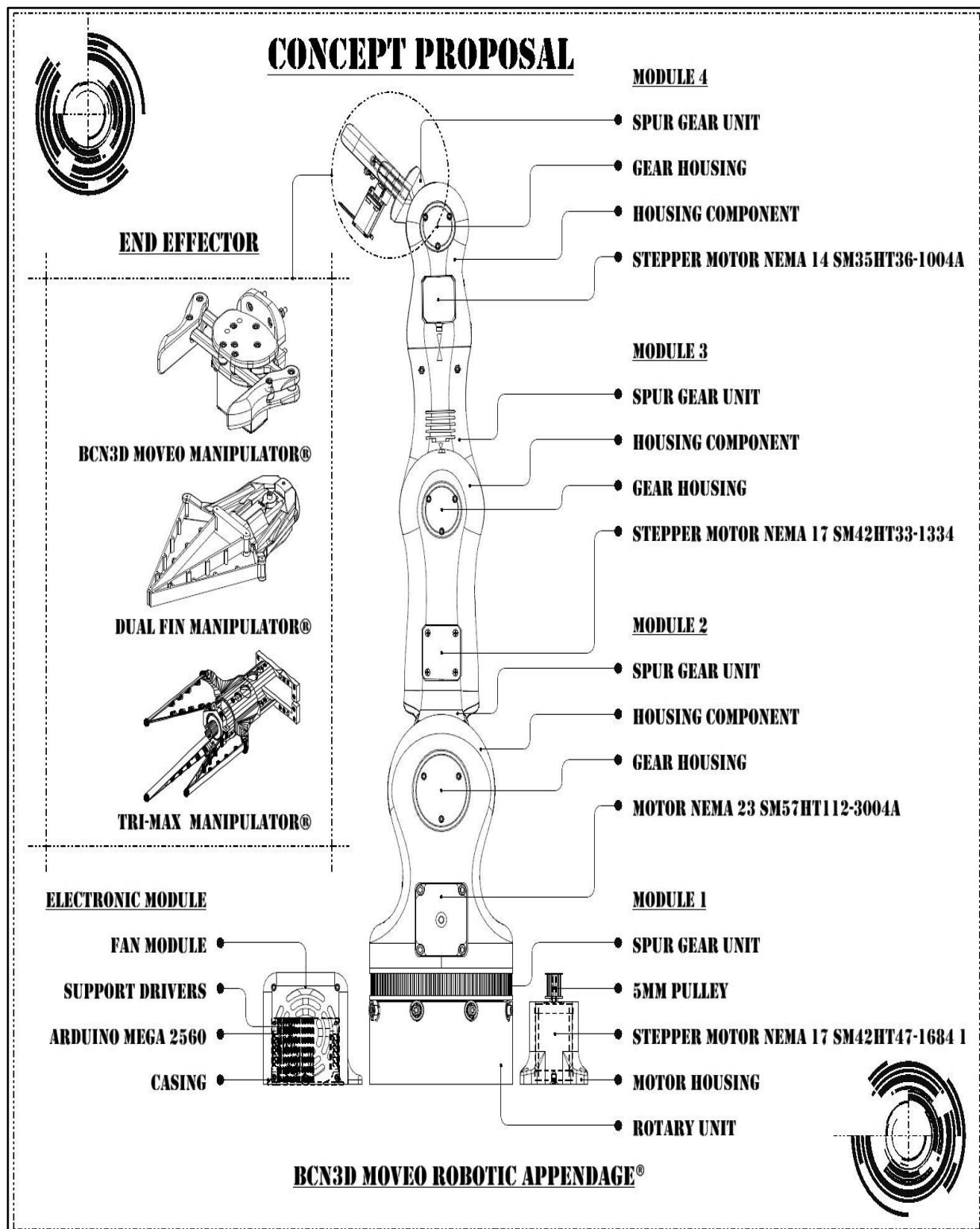


Figure 39: Gripper system conceptual model.

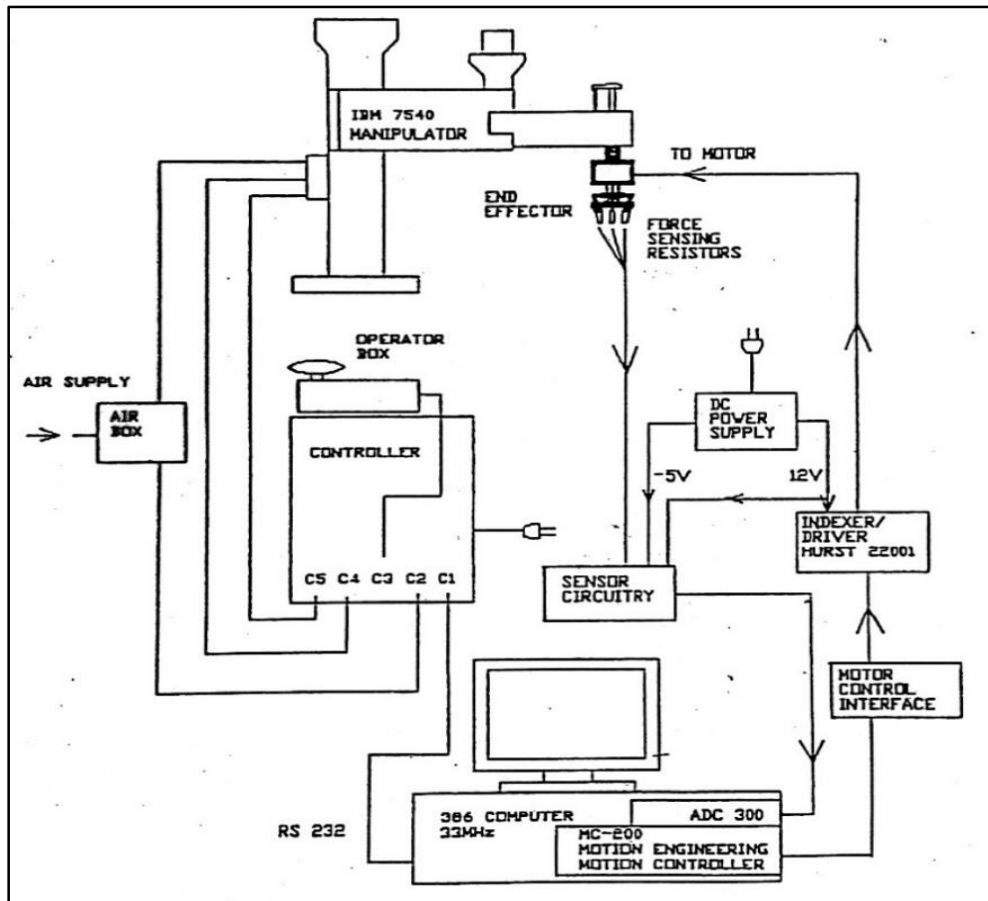


Figure 40: Conceptual closed-loop robotic system setup.

5.4 Robotic Arm Concept Selection

5.4.1 Robotic Arm Selection

Robotic manipulation occurs by using robotic arms. The selection of manipulators has to be considered in terms of payload, robot mass, repeatability, degrees of freedom, material strength, ease of usability and work envelope. The selection criteria affect the flexibility and performance of the operation. Six degrees of freedom robotic arms are commonly used in the production industry [52]. Figure 41 shows the visual representation of a 6-DOF robotic arm. The robotic system arm was selected from 2 proposed robotic systems. The BCN3D MOVEO robotic arm and the FANUC M-10iA robotic arm was considered.

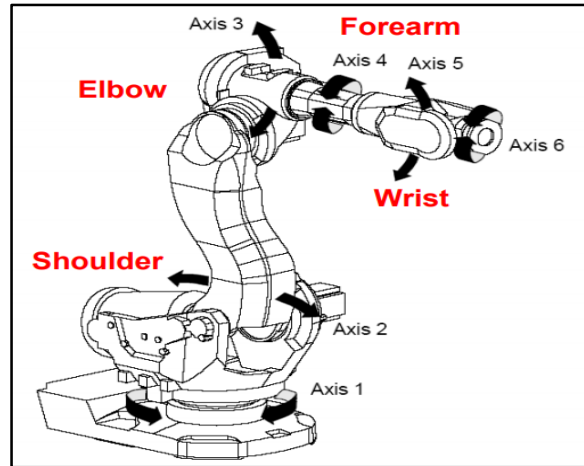


Figure 41: Visual representation of 6-DOF robotic arm [52]

The BCN3D MOVEO robotic arm was selected as a potential manipulating system for possessing adaptability and reproducibility criteria [53]. The system has the possibility to be manufactured by means of 3D printing and the open source systems firmware was available for private and public use. The systems design and setup were simply accessible and were considered to be easily produced for experimental use. The system can be integrated with a gripping system for the operational procedure as shown in Figure 42.

Table 13: BCN3D MOVEO robotic arm technical information

Specifications	Description	Technical Detail
Payload		1 kg
Arm reach		0.8 m
Robot mass		15 kg
Degrees of freedom		6
Robotic body material		ABS or PLA plastic
Robot control		Arduino Mega 2560
Repeatability		± 0.2 mm

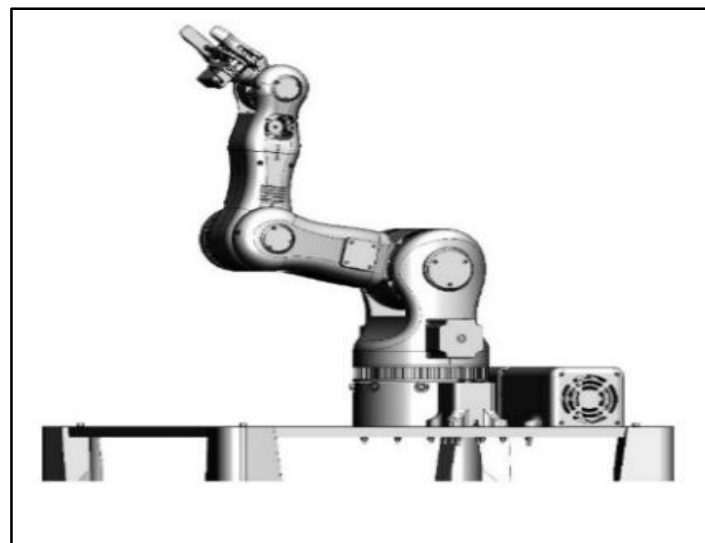


Figure 42: BCN3D MOVEO robotic arm [53]

The FANUC M-10iA robotic arm was considered as a potential manipulation system as result of being an industrial unit used for real-time assembly procedures as shown in Figure 43. The arm was also pre-installed and accessible for the operational procedure and was not required for firmware modification and communication alteration. The FANUC robotic arm was controlled by means of an R30-iA PLC control system previously installed in conjunction with the arm unit. The manipulation system was manipulated manually and automatically by means of programming of the motor actuators [54]. The technical information of the FANUC M-10iA robotic arm is listed in Table 14.

Table 14: FANUC M-10iA robotic arm technical information

Specifications Description	Technical Detail
Payload	10 kg
Arm reach	1.42 m
Robot mass	130 kg
Degrees of freedom	6
Robotic arm body material	Cast iron
Robotic control	PLC
Repeatability	± 0.08 mm



Figure 43: FANUC M-10iA robotic arm [54]

5.4.2 *Path Planning for Operation*

The robotic movement was programmed through RoboDK[®], also known as robot development kit. The operational path was automated for the experimental procedure and for an assembly procedure. The experimental path plan shown in Figure 44, entails a circular sweep in the xy-plane, maximising the acceleration in the tangential and centrifugal direction. The assembly path plan illustrated in Figure 45, describes the initial grasp of the at Target 1, the first movement to Target 2, the release of the object at Target 3 and finally returning to Target 1. Refer to APPENDIX E.1 for the RoboDK code for path planning of robotic arm.

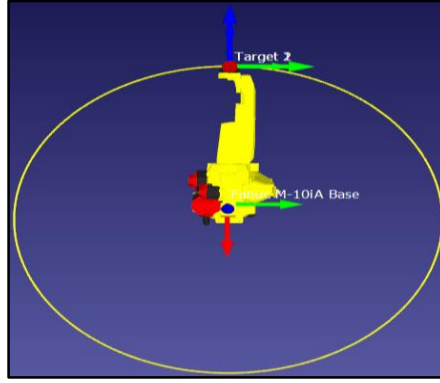


Figure 44: Experimental path plan.

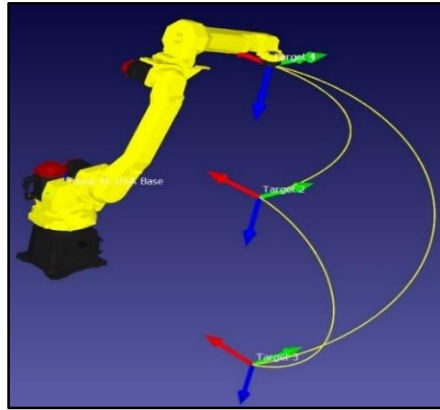


Figure 45: Assembly path plan.

5.4.3 *Kinematic and Dynamic Model Describing Forces Acting on Gripper*

The force of the end-effector attributes to the overall performance of the system. A theoretical load attributes (excluding gravitational effects) was developed by means of mathematically modelling the robotic arm. The Denavit-Hartenberg criteria were used to attain the necessary translational displacement in the x-plane, y-plane and z-plane, in the form of a Jacobian matrix. The Jacobian matrix was differentiated to attain the three velocities in the Cartesian plane and differentiated again to attain the accelerations experienced by the end-effector. The accelerations were model accordingly in terms of an acceleration versus rotational displacement curve. The theoretical force model was established to describe forces experienced by the object being gripped and transported.

The kinematic model required a set of geometrical attributes. The operating dimensions for the FANUC M-10iA robotic arm are described in the FANUC manual [54]. The operational dimensions are shown in Figure 46 as a visual representation. The work envelope can be described as the surface work volume able to be travelled by the end point of the robot arm. The lengths of the joints were applied in the kinematic model. The rotational displacements of the joints were utilised to determine the final translation displacement. The joint rotation of the M-10iA is presented in Figure 47. The rotation of the joints manipulates the position of the end-effector.

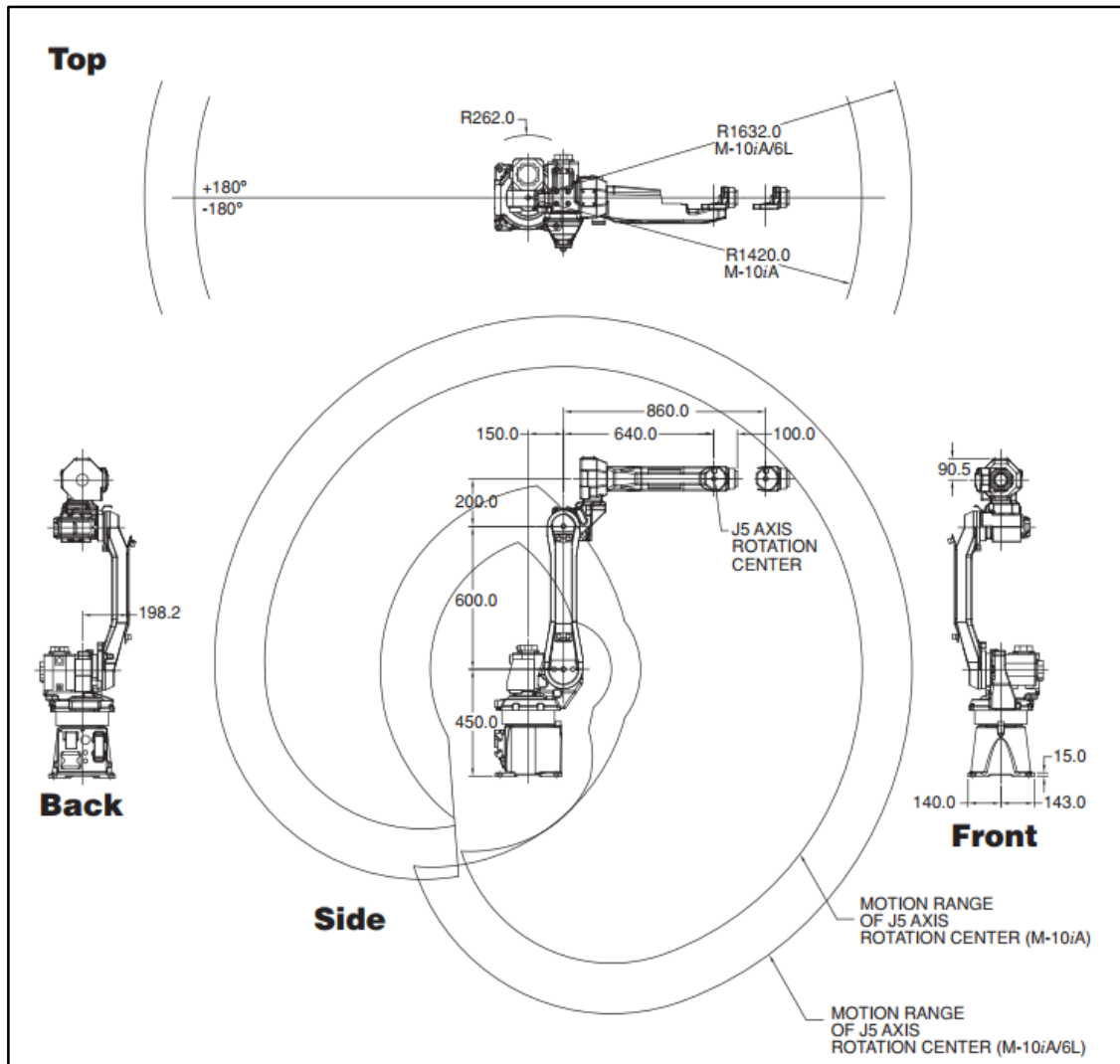


Figure 46: Geometrical dimensions of the M-10iA [54]

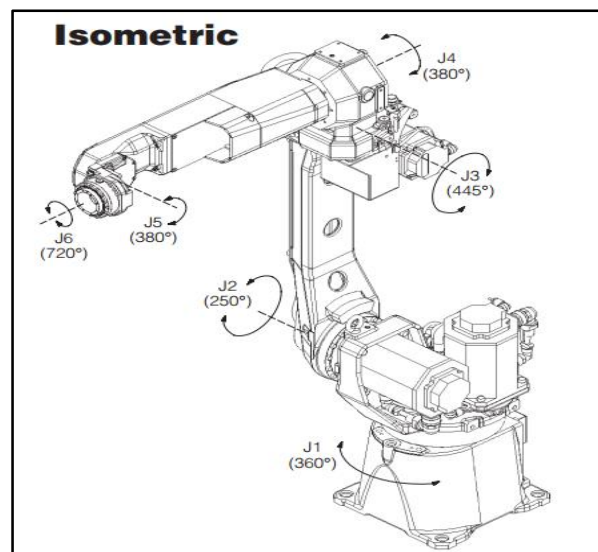


Figure 47: The joint orientation of the M-10iA [54]

The kinematic model can be illustrated in terms of a free body diagram as shown in Figure 48. The free body diagram illustrates rotational elements and geometric dimensions for the DH model. Establishing the diagram requires four rules for each joint orientation [55]. The rules for reference frame was described as follows:

- 1) Z-axis is in the direction of the joint axis.
- 2) X-axis is perpendicular to both Z_n and Z_{n-1} .
- 3) Y-axis follows the right-hand rule.
- 4) The X_n axis must intersect the Z_{n-1} axis.

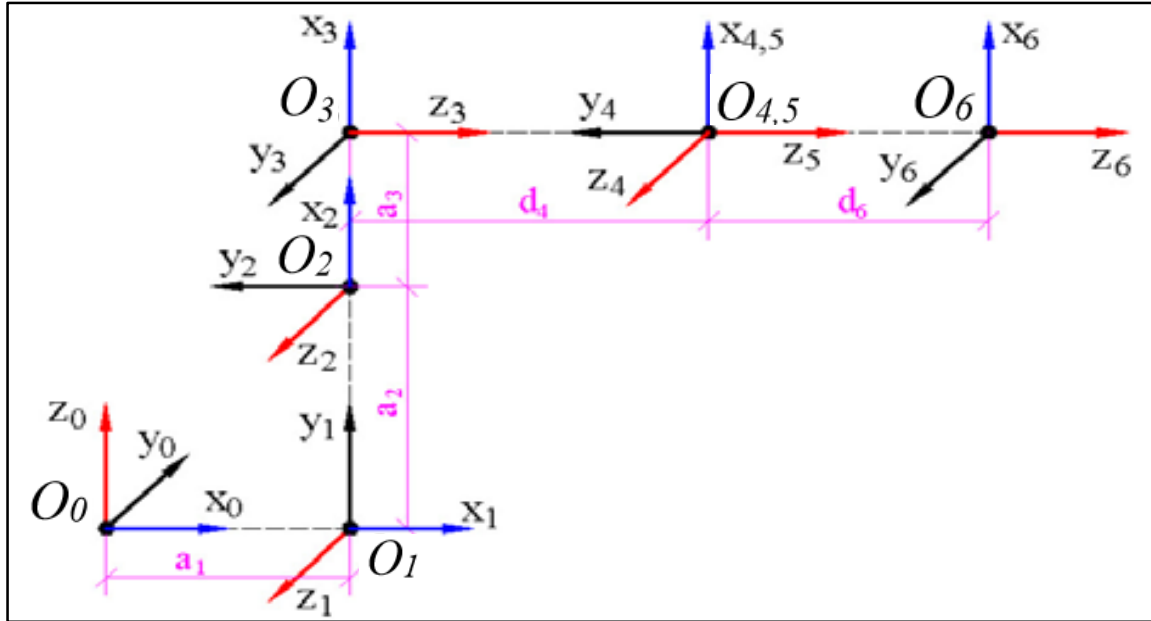


Figure 48: Coordinate reference frames for M-10iA robotic arm [55]

The robotic arm joints links are numbered accordingly 1 to 6 from the base of the arm. The origin of the frame at the base of the robotic arm is represented as O_0 on the reference frame. The axis 4, 5 and 6 present the orientation of the end-effector axis and therefore do not affect the position of the manipulator [56]. Joint 4 has an offset and as a result, the joint is shifted to the position of joint 5 on the reference frame. The offset of joints creates singularities that are difficult to compute through the means of the DH matrix and thus position adjustments are often used. Position adjustments are only performed when the input variables are not affected by the geometric inputs as described in Figure 15.

Table 15: Geometric inputs for the DH model.

T_i	α_i	a_i	θ_i	d_i
1	$\frac{\pi}{2}$	a_1	$\theta_1 + \frac{\pi}{2}$	0
2	0	a_2	θ_2	0
3	$\frac{\pi}{2}$	a_3	θ_3	0
4	$-\frac{\pi}{2}$	0	θ_4	d_4
5	$\frac{\pi}{2}$	0	θ_5	0
6	0	0	θ_6	d_6

Where:

$$a_1 = 150 \text{ mm}$$

$$a_2 = 600 \text{ mm}$$

$$a_3 = 200 \text{ mm}$$

$$d_4 = 640 \text{ mm}$$

$$d_6 = 370 \text{ mm}$$

$$c_i = \cos(\theta_i)$$

$$s_i = \sin(\theta_i)$$

The DH model described in Section 3.3.2 was developed further from the information in Figure 15. The homogeneous transformation matrices shown below describe the characteristics of each joint as T_1 , T_2 , T_3 , T_4 , T_5 and T_6 . The homogeneous transformation matrices are multiplied and can be described as a homogeneous transformation matrix T_n^0 , which describes the translation displacements for x , y and z -axis of the T_6 described by:

$$\begin{aligned} T_1 &= \begin{bmatrix} c_1 & 0 & s_1 & a_1 \cdot c_1 \\ s_1 & 0 & -c_1 & a_1 \cdot s_1 \\ 0 & 1 & 0 & 0 \\ 0 & 0 & 0 & 1 \end{bmatrix} & T_2 &= \begin{bmatrix} c_2 & -s_2 & 0 & a_2 \cdot c_2 \\ s_2 & c_2 & 0 & a_2 \cdot s_2 \\ 0 & 0 & 1 & 0 \\ 0 & 0 & 0 & 1 \end{bmatrix} & T_3 &= \begin{bmatrix} c_3 & 0 & s_3 & a_3 \cdot c_3 \\ s_3 & 0 & -c_3 & a_3 \cdot s_3 \\ 0 & 1 & 0 & 0 \\ 0 & 0 & 0 & 1 \end{bmatrix} \\ T_4 &= \begin{bmatrix} c_4 & 0 & -s_4 & 0 \\ s_4 & 0 & c_4 & 0 \\ 0 & -1 & 0 & d_4 \\ 0 & 0 & 0 & 1 \end{bmatrix} & T_5 &= \begin{bmatrix} c_5 & 0 & s_5 & 0 \\ s_5 & 0 & -c_5 & 0 \\ 0 & 1 & 0 & 0 \\ 0 & 0 & 0 & 1 \end{bmatrix} & T_6 &= \begin{bmatrix} c_6 & -s_6 & 0 & 0 \\ s_6 & c_6 & 0 & 0 \\ 0 & 0 & 1 & d_6 \\ 0 & 0 & 0 & 1 \end{bmatrix} \end{aligned} \quad (5.1)$$

$$T_n^0 = T \cdot T_2^1 \cdot T_3^2 \cdot T_4^3 \cdot T_5^4 \cdot T_6^5 \quad (5.2)$$

The translation displacements are expressed as P_x , P_y , and P_z described by:

$$T_n^0 = \begin{bmatrix} s_x & n_x & a_x & P_x \\ s_y & n_y & a_y & P_y \\ s_z & n_z & a_z & P_z \\ 0 & 0 & 0 & 1 \end{bmatrix} \quad (5.3)$$

The Jacobian matrix describes the velocity vectors for the x , y and z -axis of Joint 6. The partial differential of the combined Jacobian matrix defines the acceleration matrix. The Jacobian matrix can be described by the following equation:

$$J(s, n, a, P) = \begin{bmatrix} \frac{\partial T_x^0}{\partial s} & \frac{\partial T_x^0}{\partial n} & \frac{\partial T_x^0}{\partial a} & \frac{\partial T_x^0}{\partial P} \\ \frac{\partial T_y^0}{\partial s} & \frac{\partial T_y^0}{\partial n} & \frac{\partial T_y^0}{\partial a} & \frac{\partial T_y^0}{\partial P} \\ \frac{\partial T_z^0}{\partial s} & \frac{\partial T_z^0}{\partial n} & \frac{\partial T_z^0}{\partial a} & \frac{\partial T_z^0}{\partial P} \\ \frac{\partial 0}{\partial s} & \frac{\partial 0}{\partial n} & \frac{\partial 0}{\partial a} & \frac{\partial 1}{\partial P} \end{bmatrix} \quad (5.4)$$

The forward acceleration kinematics equation can be expressed as follows:

$$\ddot{\mathbf{X}} = \mathbf{J}\ddot{\mathbf{q}} + \dot{\mathbf{J}}\dot{\mathbf{q}} \quad (5.5)$$

Where:

$\ddot{\mathbf{X}}$: Acceleration vector matrix.

\mathbf{J} : Jacobean matrix.

$\dot{\mathbf{J}}$: Differential of the Jacobean matrix.

\mathbf{q} : Joint displacement vector.

$\dot{\mathbf{q}}$: Joint velocity vector.

$\ddot{\mathbf{q}}$: Joint acceleration vector.

The acceleration and velocity parameters have been utilized to explain the applicable forces applied to the grasped object in a movement as shown in Figure 49. The force components are described by inertia forces a , the Coriolis c and centripetal forces b and the gravitational forces g [57]. The force vector can be described by the following equation:

$$a(\mathbf{q})[\ddot{\mathbf{q}}] + b(\mathbf{q})[\dot{\mathbf{q}}\dot{\mathbf{q}}] + c(\mathbf{q})[\ddot{\mathbf{q}}] + g(\mathbf{q}) = \boldsymbol{\tau} \quad (5.6)$$

Where:

\mathbf{q} : Vector of joint angles.

$a(\mathbf{q})$: Symmetric, bounded, positive definite inertia matrix.

$c(\mathbf{q})$: Coriolis forces.

$b(\mathbf{q})$: Centripetal forces.

$g(\mathbf{q})$: Gravitational force

$\boldsymbol{\tau}$: Vector of actuator torques.

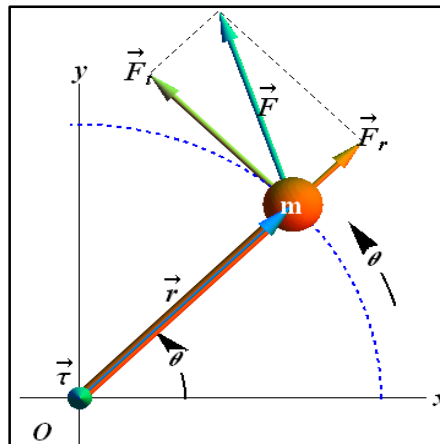


Figure 49: Force attributes of a moving object [58]

5.5 End Effector Concept Development

5.5.1 *Gripper Selection*

The selection of conceptual grippers for flexible operation is determined by the following factors: effective shape conformity, geometric adaptability, maximum gripping force, and sensitivity to material, sensitivity to surface damage, repeatability, accuracy and precision. The selection criteria affect the flexibility and performance of the gripping operation according to ISO 14539. The robotic gripping system was selected from 3 proposed robotic systems. The BCN3D MOVEO gripper, the Dual Fin gripper and the Tri-max gripper were considered.

The BCN3D MOVEO gripper consists of a 2-Finger approach to gripping objects, illustrated in Figure 50. The appendages are designed from solid appendages and are actuated by means of a centralized motor. The force is transferred from the motors to the fingers, by means of 4 hinged joints connected to the rods controlling the motion [53]. The appendages are solid and therefore conformity around a gripped object is restricted.

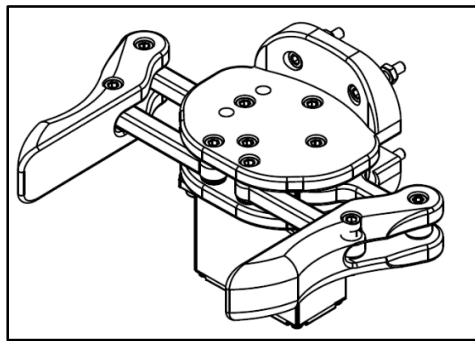


Figure 50: BCN3D MOVEO gripper [53]

The Dual Fin gripper consists of a 2-Finger approach to gripping objects, shown in Figure 51. The appendages are designed from the Fin Ray Effect[®] appendages and are actuated by means of a centralized pneumatic piston. The force is transferred from the piston to the fingers, by means of gears from the piston to a centralized unit [59]. The appendages are connected to the body by means of a hinge on one end and on the other is connected to the centralized unit. The gripper is flexible due to the Fin Ray Effect[®], but the gripping force is sensitive to change due to pneumatic pressure loss through leakage.

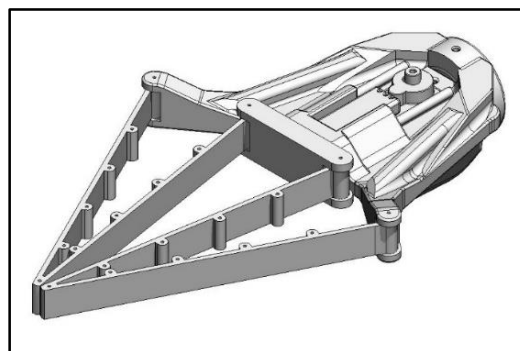


Figure 51: Dual fin gripper [59]

The Tri-Max gripper consists of a 3-Finger approach to gripping objects, illustrated in Figure 52. The appendages are designed from the Fin Ray Effect® appendages and are actuated by means of a centralized stepper motor [60]. The force is transferred from the motor to the fingers, by means of a threaded bar. The appendages are connected to the body by means of a hinge on one end and on the other, is connected to the centralized unit. The gripper is flexible due to the Fin Ray Effect®. The particular gripper has full load holding capabilities. Additionally, the number of appendages were manipulated according to the design allowance.

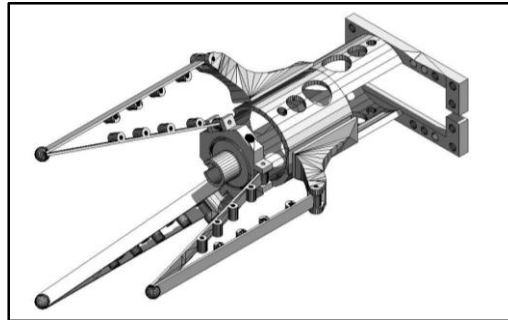


Figure 52: Tri-max gripper [60]

5.5.2 Material Selection

The material selected was ABS plastic and PLA plastic. The components used in the gripper assembly was manufactured through 3D printing. The designated material and manufacturing method proved to be manageable and adaptable according to design changes. High complexity and accuracy of the part were produced through 3D printing. Table 16, shows the material properties of ABS plastic, Nylon, PLA plastic and TPE rubber, and are all useable in rapid prototyping operations. The common materials used in the conceptual design was ABS plastic and PLA plastic. The exotic material used in the conceptual design was TPE rubber. The accuracy of the hole, shrinkage factor and melting point were considered when designing components from 3D printing materials [61].

Table 16: Mechanical properties of the 3D-printing material.

Material	ABS Plastic	Nylon	PLA Plastic	TPE Rubber
Elastic Modulus [GPa]	2	1	2.62	0.03
Poisson's Ratio [-]	0.4	0.3	0.34	0.5
Yield Stress [MPa]	45	60	61	30
Print temperature [°C]	220-260	235-260	190-220	200-230

5.5.3 Finger Gripper Concept Model

The appendages designed for the gripper system are based on geometric requirements in terms of the rib structure (refer to Figure 53). The figure shows four sets of geometry selected according to rib design based on natural occurring shapes in fins. Geometry 1 shows the traditional rib structure of the Fin Ray Effect®. Geometry 2 has been adapted for higher deflection by shifting the ribs into a slanted direction. Geometry 4 used the parallel configuration of Geometry 1, and additionally, the ribs were curved. Geometry 4 combined Geometry 2 and Geometry 3, and the ribs were slanted and curved.

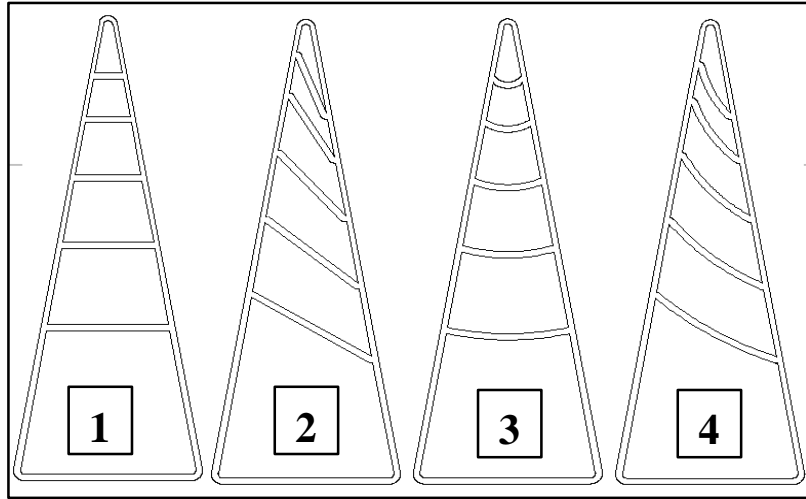


Figure 53: Rib structure design for appendages.

A gripper was designed around the fin-ray appendages for adaptable grasping. Figure 54 shows a conceptual model for a 4-finger and a 3-finger gripper based on the Tri-Max gripper. The gripper was intended to be easily attached to the robotic arm. The design features employed in the design improves the strength of the original Tri-Max gripper concept and incorporates actuator housing inside the gripper itself. The gripper finger design allows for attaching of sensors on the contact surface. The gripper body and fingers are 3D printed and made from plastic, designed for lightweight and compact handling.

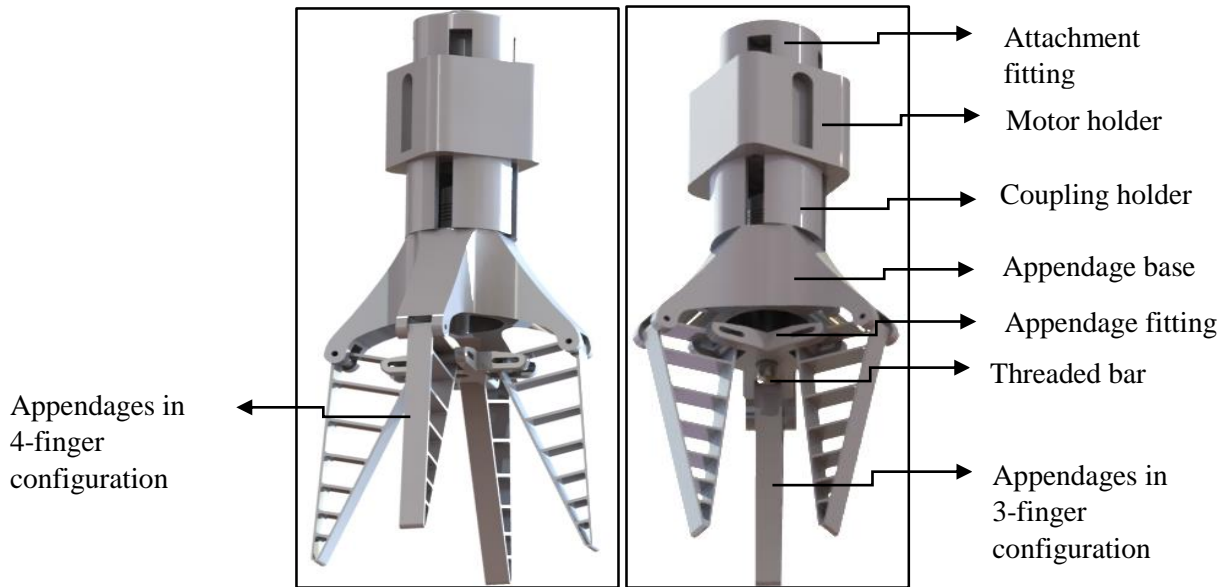


Figure 54: 4-Finger gripper and 3-finger gripper design

5.5.4 *Gripping Modes*

The designed gripper is aimed for specific gripping operations where internal and external gripping is required on components. The fingers are actuated in a two-way direction namely, opening and closing. The finger surface was utilised on both sides for internal and external gripping shown in Figure 55 and describes the operation each gripping mode [33]. The flexibility and function of gripper were increased by the incorporation of this capability.

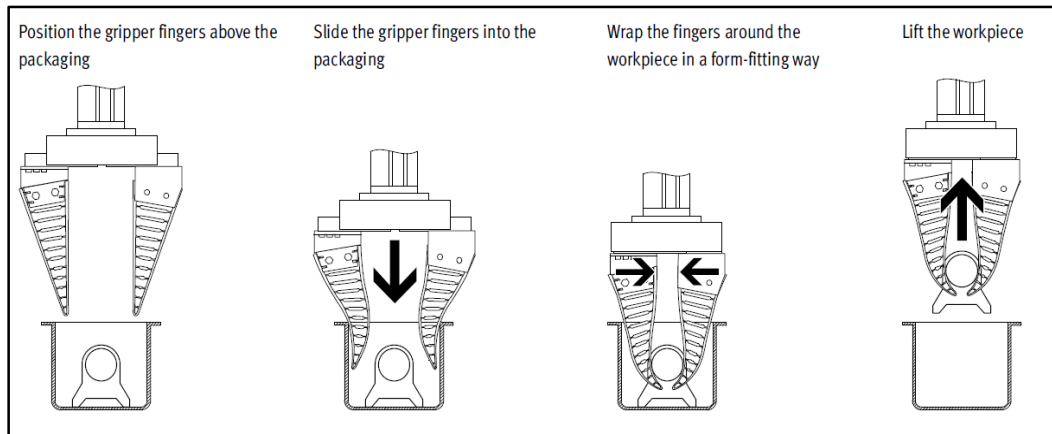


Figure 55: Gripping modes for gripper system [33]

5.6 Specimen Design

5.6.1 Specimen Geometry

The testing procedure for effective gripping required varying shape and weighted specimens. The specimens varied geometries including cubes, cylinders and spheres. Design specifications had to be considered when designing the specimens. The specimens were designed to be lightweight, different geometries had to be included yet concentric gripping also had to be tested and the ease of gripping and manufacturing was considered. Specimen 1 was designed to provide a surface geometry matching shape change of different grasped components shown in Figure 56. Specimen 2 was designed to provide both concentric gripping surface area and holding space for measured weights as illustrated in Figure 57. Only two (2) of the five (5) specimens have been illustrated. Refer to Section 9.9.1.

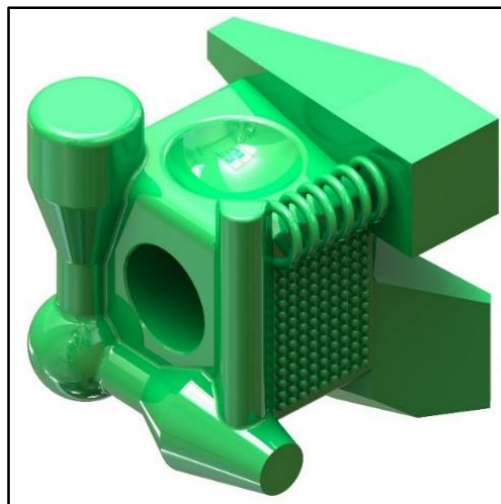


Figure 56: Specimen 1 – Design cube



Figure 57: Specimen 2 – Mass holder

5.7 Electronic Control

5.7.1 Pseudocode

Object manipulation requires the consideration of the object and mechanics behind the gripping strength. The force regulation for gripping intensity and grasp control was described by the pseudocode in Figure 58. The flow diagram describes the gripper system control procedure within a pick-up and place procedure. The system identifies locations by means of a written code which was preselected depending on the operation required. The object contact location is found. The micro-controller identifies the correct force intensity required for gripping in the gripping phase. The component is located in a new position and released. The cycle starts again with a new component.

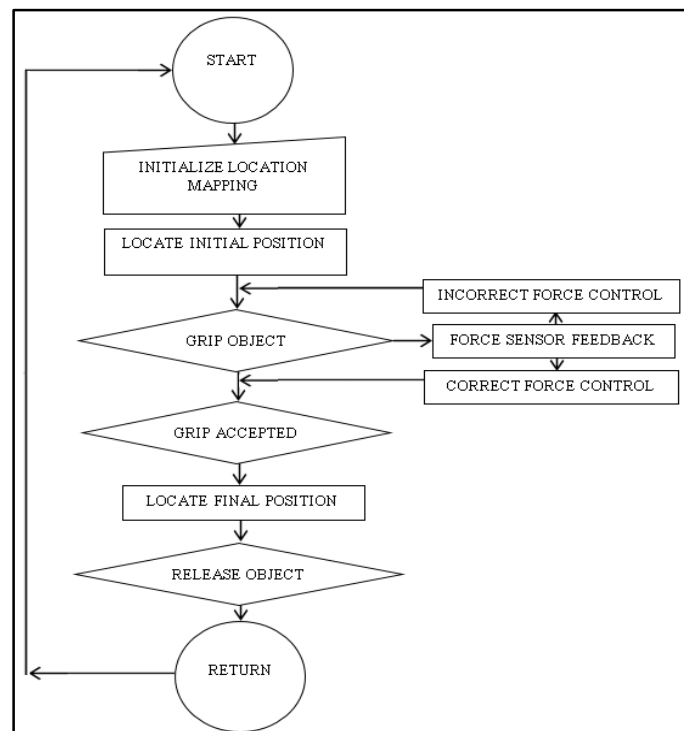


Figure 58: Pseudocode for gripper system

5.7.2 Force Feedback Control

Sensors are attached to each appendage and therefore require a feedback control loop to determine the correct gripping force required. The desired force signal is compared to the actual force applied by means of a force sensor feedback loop illustrated in Figure 59. The signal is converted from a voltage signal retrieved from the force sensor. The data signal is updated with the condition that the signal is incorrect in comparison to the required force signal, and thus the corrected force signal is applied to the motor torque for grasping.

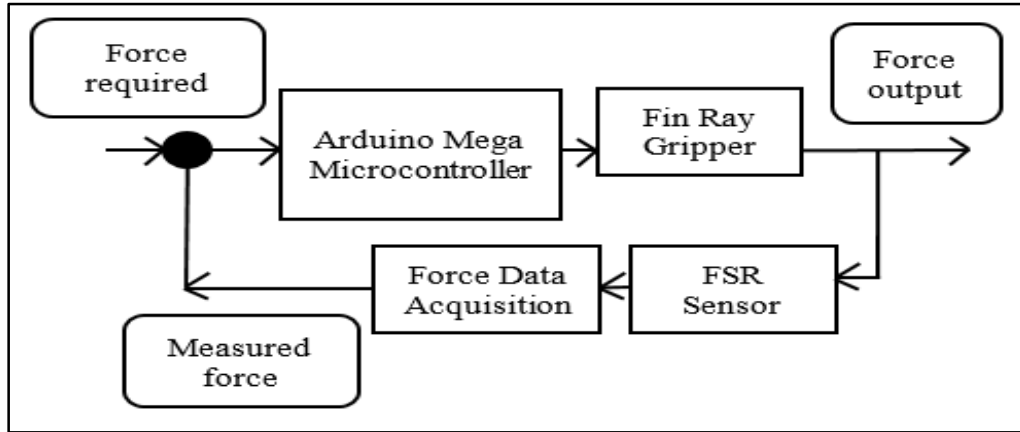


Figure 59: Force sensor feedback loop

5.7.3 System Circuit Diagram Layout

The Arduino® Mega 2560 was selected due to possessing good processing capabilities and pin numbers. The Mega 2560 was used to process and calculate the data signals attained from the sensor system. Additionally, the microcontroller sent signal outputs to the motor by means of motor controllers. The Mega 2560 was highly rated and was easily obtainable by a retail seller. The support information and software Arduino® operating system were accessible. Refer to APPENDIX B.6 for technical specifications.

The circuit diagram of the TB6560-V2 motor controller is shown in Figure 60. The TB-6560-V2 was selected due to having good processing capabilities. The TB-6560-V2 was used to process and compute the data signals attained from the microcontroller to the stepper motors [62]. The TB-6560-V2 was highly rated and was easily obtainable by a retail seller. The TB-6560-V2 possesses good accuracy for signal output to motors. Refer to APPENDIX B.6 for technical specifications.

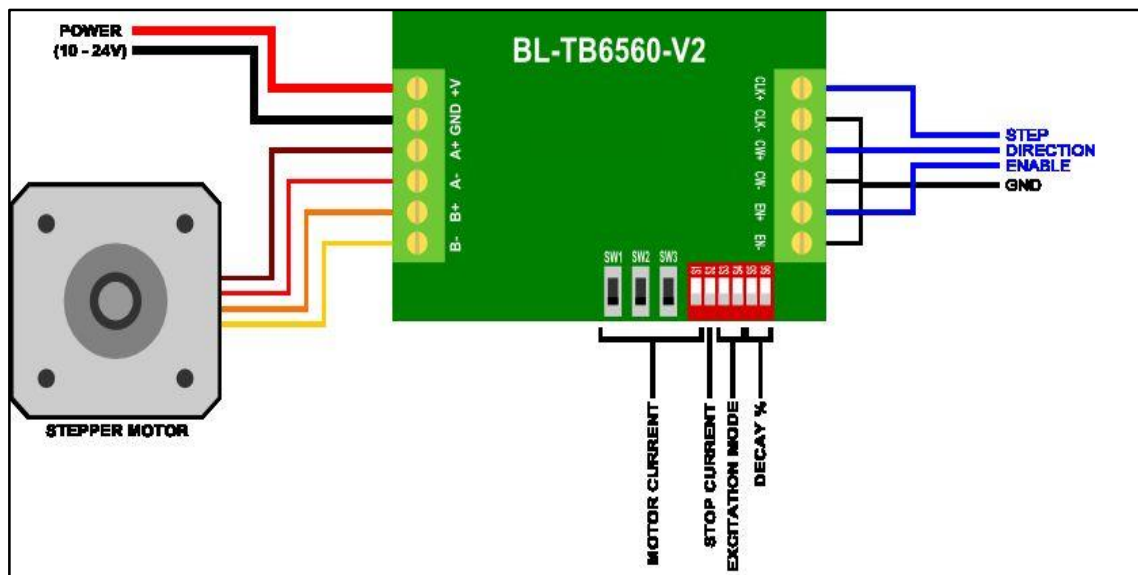


Figure 60: TB-6560 motor controller circuit diagram [62]

5.7.4 Motor Selection

Electric motors were selected as the principal source of actuation. Motors provide rotational displacement for actuation. Three primary motors were considered in the actuator selection namely: Stepper motors, direct current motors and servo motors are compared in Table 19.

Stepper motors are modified DC motors that rotate in distinct steps. The coils of the motor are organized in phases, when energized the motor rotates in discrete steps, hence it is called a stepper motor [63]. The positioning of these steps was controlled by means of a motor controller for precise motion control application. The specific motor model to be selected from NEMA 17 range. The technical specifications are tabularized in Table 17. Refer to APPENDIX B.6 for technical specifications.

Table 17: NEMA 17 technical specifications

Specification	Operation Range
Phase current (A)	1.5 – 1.8
Voltage (V)	1 - 4
Inductance per phase (mH)	3 - 8
Holding torque (N.cm)	44
Degrees per step	1.8 – 0.9

DC motors are used in conjunction with encoders or potentiometers to measure the angular motion. DC motors have a high speed at a range of 5000 to 10000 rpm range but have low torque ranges [64]. The DC motor uses direct current power sources and requires an inverter when power is to be supplied from an AC power source. Servo motors include a DC motor, rotary potentiometer and gearing. The servo motors rotate to a precise angular position [64]. The technical specifications are generally the equivalent to DC motor requirements and are described in Table 18.

Table 18: 12V DC motor technical specifications

Specification	Operation Range
Operating current (A)	0.053 – 1.5
Operating voltage (V)	4.5 - 18
Gear ratio	3 - 8
Startup torque (kg.cm)	3.6
Degrees per step	1.8 – 0.9
No-load speed	200 RPM

Table 19: Comparison of motor types

Motor Type	Advantages	Disadvantages
Continuous DC	<ul style="list-style-type: none"> - A wide selection is available. - Easy to control. - Larger DC motors can power a 90 kg robot with a gearbox. 	<ul style="list-style-type: none"> - Requires gear reduction to provide torques needed for most robotic applications. - Poor standards in sizing and mounting arrangements.
Stepper	<ul style="list-style-type: none"> - Does not require gear reduction to power at low speeds. - Low cost when purchased on the surplus market. - The dynamic braking effect achieved by leaving coils of stepper motor energized. 	<ul style="list-style-type: none"> - Poor performance under varying loads. - Consumes high current. - Needs special driving circuit to provide stepping rotation.
R/C servo	<ul style="list-style-type: none"> - Least expensive non-surplus source for gear motors. - Can be used for precise angular control, or for continuous rotation. - Available in several standard sizes, with standard mounting holes. 	<ul style="list-style-type: none"> - Requires modification for continuous rotation. - Requires special driving circuit. - More powerful servos are available, the practical weight limit for powering a robot is about 4.5 kilogram.

5.7.5 Motion Transmission Selection

Motion transmission was selected by transferring a rotational motion into a translational motion [65]. Motion can be transmitted through this method by means of a threaded rod or leadscrews [66]. The considerations to be kept in mind when selecting the type of transmission are machining effort, operational consideration, production costing and torque requirements.

5.7.6 Sensor Selection

The selection of sensors for force feedback is considered in terms of signal type, accuracy, surface application and robustness of sensor. The sensors that were considered were strain gauges, piezoelectric force sensors, force sensing resistors and flexi-force pressure sensors. Force sensing sensors are incorporated into the system to monitor the applied force conditions on the surface of the gripper and object being grasped.

Strain gauges function by means of electrical conductance. The change in electrical resistance signal is due to the displacement in compression and expansion of the gauge and is measured as strain [67]. The resistance signal corresponds to the stress applied to the surface and thus can be calculated in terms of force. Strain gauges are used in high precision stress feedback for static testing. Strain gauges are permanent when installed onto the surface of the specimen to be tested for stress (refer to Figure 61).

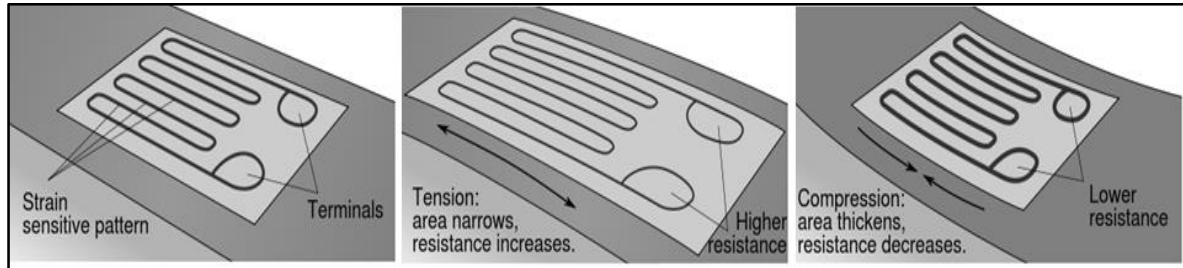


Figure 61: Operation of the strain gauge.

Piezoelectric force sensors operate on the electrostatic charge generated by means of a quartz crystal expansion and contraction [68]. The signal is generated by means of the piezoelectric effect and output signal is collected by means of electrodes that are crammed around the crystals shown in Figure 62. The charge can be amplified and converted to provide a signal proportional to the input force.

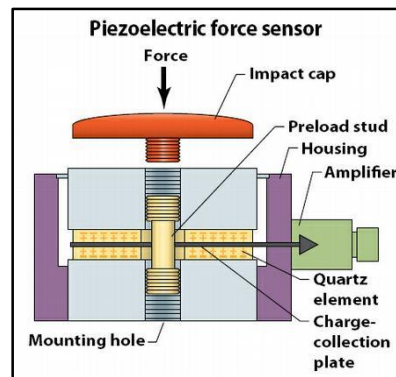


Figure 62: Piezoelectric force sensor

The sensor selected was a force sensitive resistor as shown in Figure 63. The FSR has the ability to measure a distributed force over an area. The mean force determined can be used as accurate data measured for experimental data acquisition [69]. The FSR is easily installed and incorporated into the system. A drawback of FSR's is that they are not capable of high precision measurements, but are economical and removable when being used for multiple applications. The FSR can be used for both static and dynamic force purposes. The force is inversely proportional to applied force load.

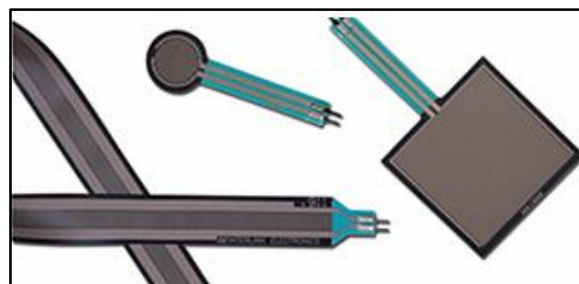


Figure 63: Force sensitive resistor

FlexiForce pressure sensors can be used in both dynamic and static force applications [69]. The FlexiForce sensors can be applied in non-intrusive applications. The FlexiForce sensor operates on the same principle as the FSR. Figure 64 illustrates a FlexiForce sensor.



Figure 64: FlexiForce pressure sensors

5.8 Conclusion

The conceptualization of the design was established from the Fin Ray Effect[®]. The gripper was designed according to a 3-finger and 4-finger configuration and appendages were set up according to the four described geometries. A NEMA 17 stepper motor in conjunction with a microcontroller and motor controller was designed. The motion actuation was designed by utilizing a threaded bar due to financial and operational viability. The FSR sensor was used in the concept design in the force feedback design.

6 System Embodiment Design

6.1 Introduction

This chapter discusses the mechanical and electronic design of the gripper system. The mechanical design section demonstrates a 3-finger and 4-finger gripper design developed from the generated specifications. The mechanical assembly section explains the part composition of the gripper system. The gripper system requires incorporating actuation mechanisms. The electronic design section describes the development of control for gripper actuation. Additionally, the sensory system section describes the sensor feedback system to be implemented for testing and data acquisition. The budget and energy audit section designates the initial cost for components and the annual running costs required for the system.

6.2 Mechanical Design

The mechanical design describes the detail design of the assembled components. The modelling of components and assembly illustrate the gripper system that was manufactured. Material and geometric considerations were taken into account for the gripper to be installed on the robotic arm. The gripper appendages were installed and tested according to the 4-geometries designed for the gripper fingers. Additionally, a high friction coefficient material called CrocGrip® was added to reduce slippage in grasp. The component design can be seen in the APPENDIX B.1 – B.5.

6.2.1 3-Finger Gripper

The gripper system was designed for a 3-finger configuration grasp. The bottom view, front view and isometric views of the 3-finger gripper system design assembly are shown in Figure 65. Refer to APPENDIX B.1 for detail drawings.

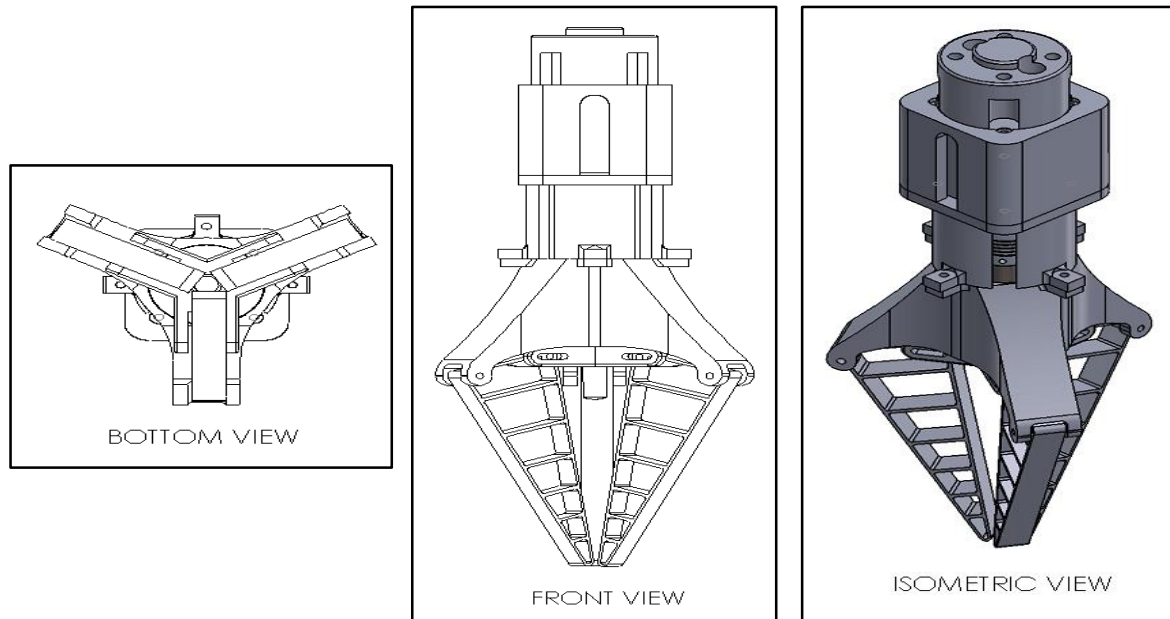


Figure 65: Assembly of 3-Finger gripper design

The exploded view of the 3-finger gripper system assembly is shown in Figure 66. Refer to APPENDIX B.2 for the design sheet drawing of the exploded view and bill of materials. The assembly consists of the following components:

- A motor holder: To provide the housing for the NEMA 17 motor.
- A NEMA 17 motor: To provide actuation motion from electrical power.
- A shaft housing: To provide protected covering for the threaded bar.
- A fastening base: To provide a method of attachment to the robotic arm.
- A 3-finger holder: To provide a method of attaching the appendages by means of hinges.
- A solid coupler: To provide flexible transmission and attachment to the motor shaft.
- An M8 threaded bar: To provide movement motion from rotational displacement to translational motion.
- An appendage fitting: To provide a method of attaching the appendages by means of adjustable hinge movement and housing for an M8 nut used for motion transmission.
- 3 X Appendages: To provide a method of gripping of components.

Auxiliary components:

- 11 x M3x25 bolts
- 20 x M3 nuts
- 4 x M3 x 65 mm threaded bar

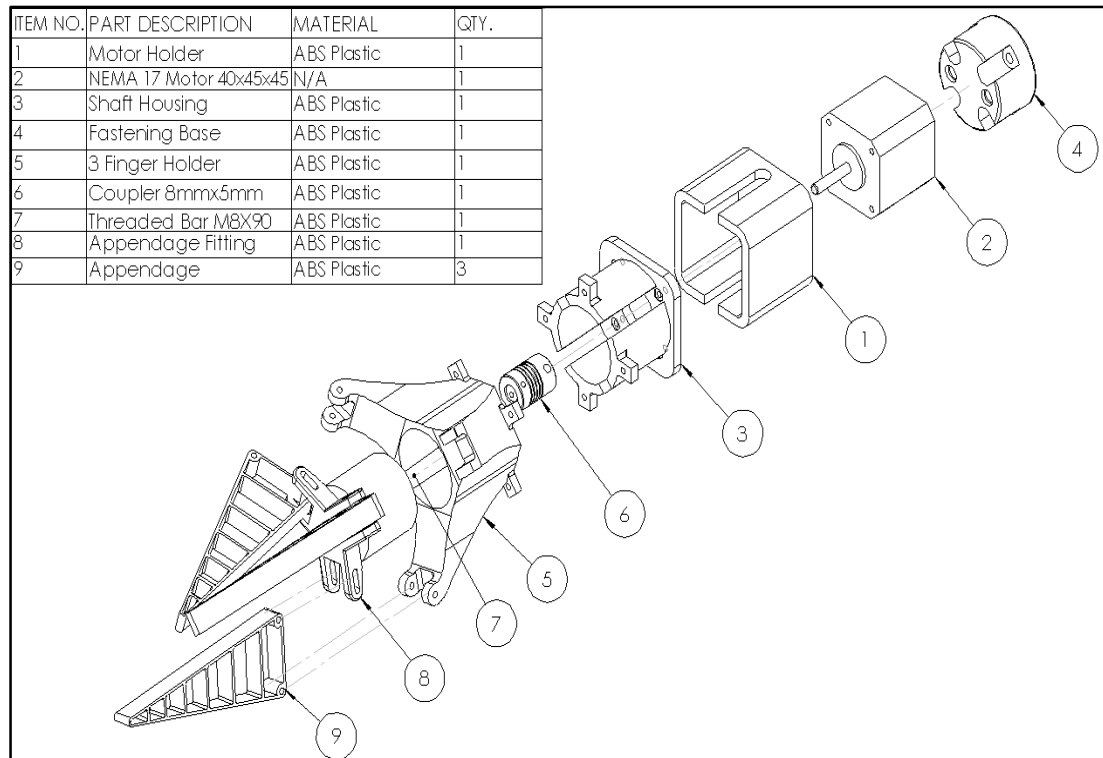


Figure 66: Exploded view and BOM of 3-finger gripper system

6.2.2 4-Finger Gripper

The gripper system was designed for a 4-finger configuration grasp. The bottom view, front view and isometric views of the 4-finger gripper system design assembly are shown in Figure 67. Refer to APPENDIX B.3 for design sheet drawing of drawing views.

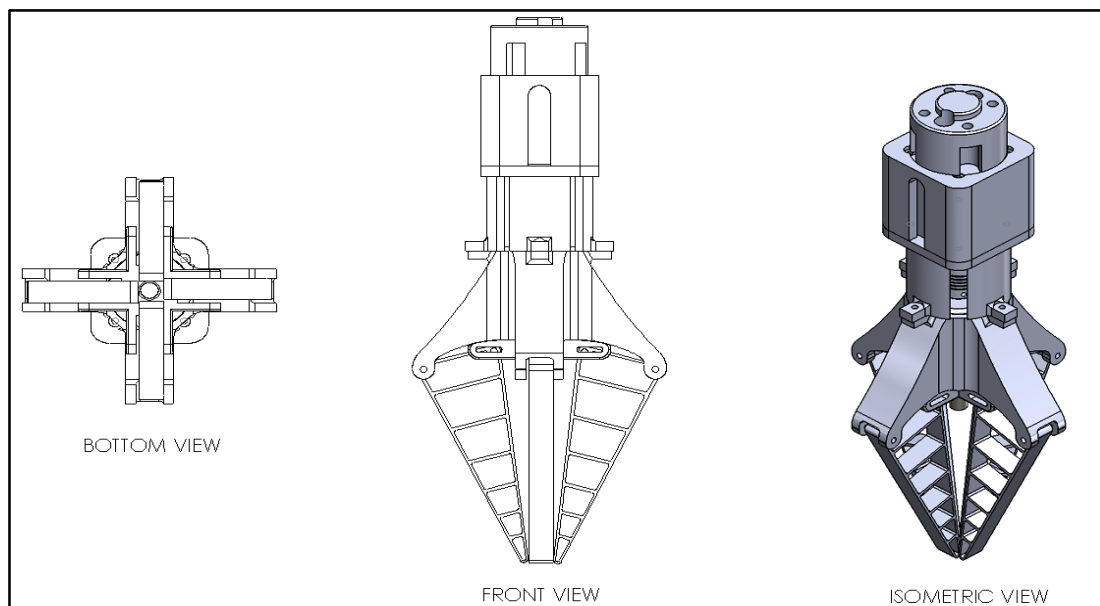


Figure 67: Assembly of 4-Finger gripper design

The exploded view of the 4-finger gripper system assembly is shown in Figure 68. Refer to APPENDIX B.4 for design sheet drawing of exploded view and bill of materials. The assembly consists of the following components:

- A motor holder: To provide the housing for the NEMA 17 motor.
- A NEMA 17 motor: To provide actuation motion from electrical power.
- A shaft housing: To provide protected covering for the threaded bar.
- A fastening base: To provide a method of attachment to the robotic arm.
- A 3-finger holder: To provide a method of attaching the appendages by means of hinges.
- A solid coupler: To provide flexible transmission and attachment to the motor shaft.
- An M8 threaded bar: To provide movement motion from rotational displacement to translational motion.
- An appendage fitting: To provide a method of attaching the appendages by means of adjustable hinge movement and housing for an M8 nut used for motion transmission.
- 4 X Appendages: To provide a method of gripping of components.

Auxiliary components:

- 12 x M3x25 bolts
- 20 x M3 nuts
- 4 x M3 x 65 mm threaded bar

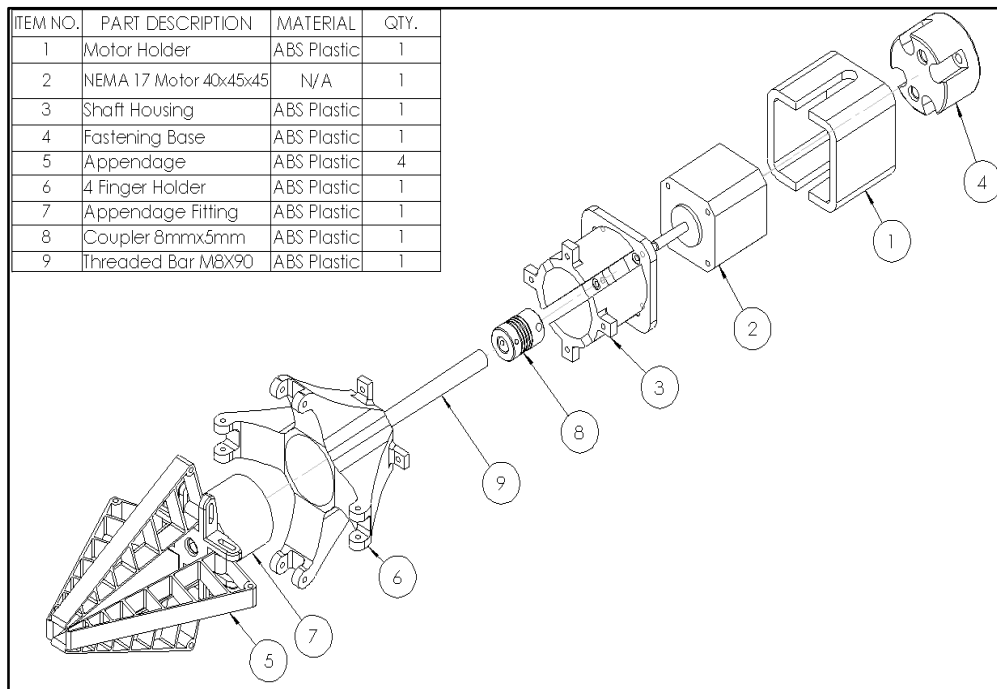


Figure 68: Exploded view and BOM of 3-finger gripper system

The parts are specifically designed to handle force loads of the gripping procedure and to house all necessary components. The motor housing was designed according to the NEMA 17 motor dimensions as shown in Figure 69. The design was manufactured to be compact and assembled for straightforward attachment to the robotic arm [70]. Detail design of all parts is referred to APPENDIX B.5.

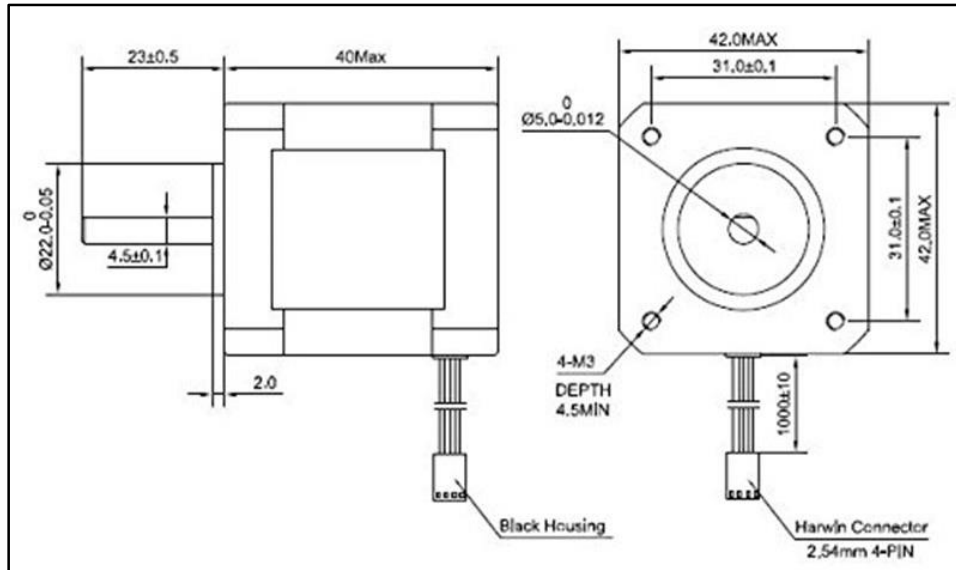


Figure 69: Design dimensions for NEMA 17 motor housing [70]

6.3 Electronic Design

6.3.1 Microcontroller Board Layout

The pin layout for the ARDUINO MEGA 2560 microcontroller is shown in Figure 70. The pin numbering 1 - 53 represents the digital pin input signals and the pin numbering A0 - A15 represents the analogue data input signals. The symbol GND denotes the attachment to the ground and all pins with the symbol V denotes the voltage input signal with the option of 3.3 V and 5 V [71].

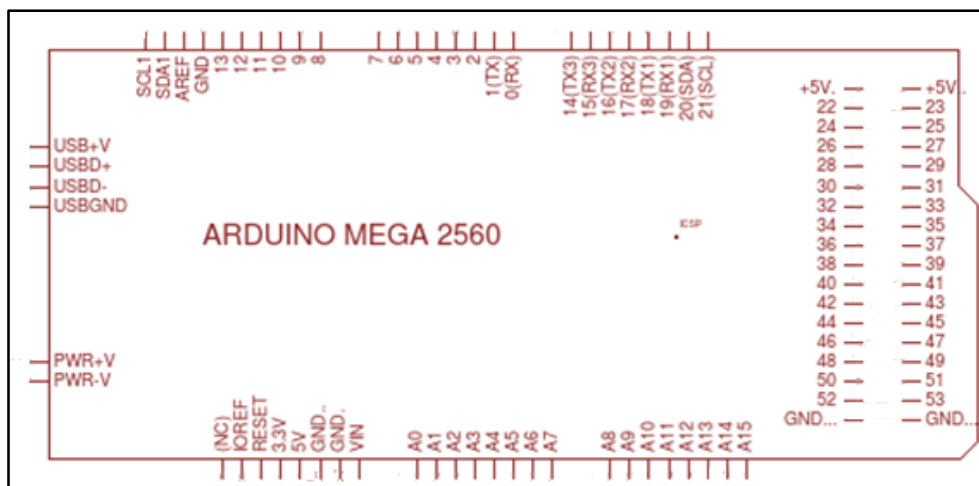


Figure 70: ARDUINO MEGA 2560 board layout [71]

6.3.2 Sensory System Schematic

The schematic shown in Figure 71, presents the force sensory system installed on the gripper system. The FSR sensors (VR) are composed of a variable resistor fluctuating between 1 M Ω and 100 k Ω , depending on the amount of pressure applied to the FSR surface. The FSR is wired in a parallel connection with a 10 k Ω resistor (R) to prevent noise feedback. The pins A0, A1, A2, A3 and A4 are connected to the corresponding variable resistors VR1, VR2, VR3 and VR4. The force signals are transmitted to the computer output through the USB jack. Refer to APPENDIX E.2 for the Arduino® code for the sensory system and APPENDIX B.7 for the schematic design.

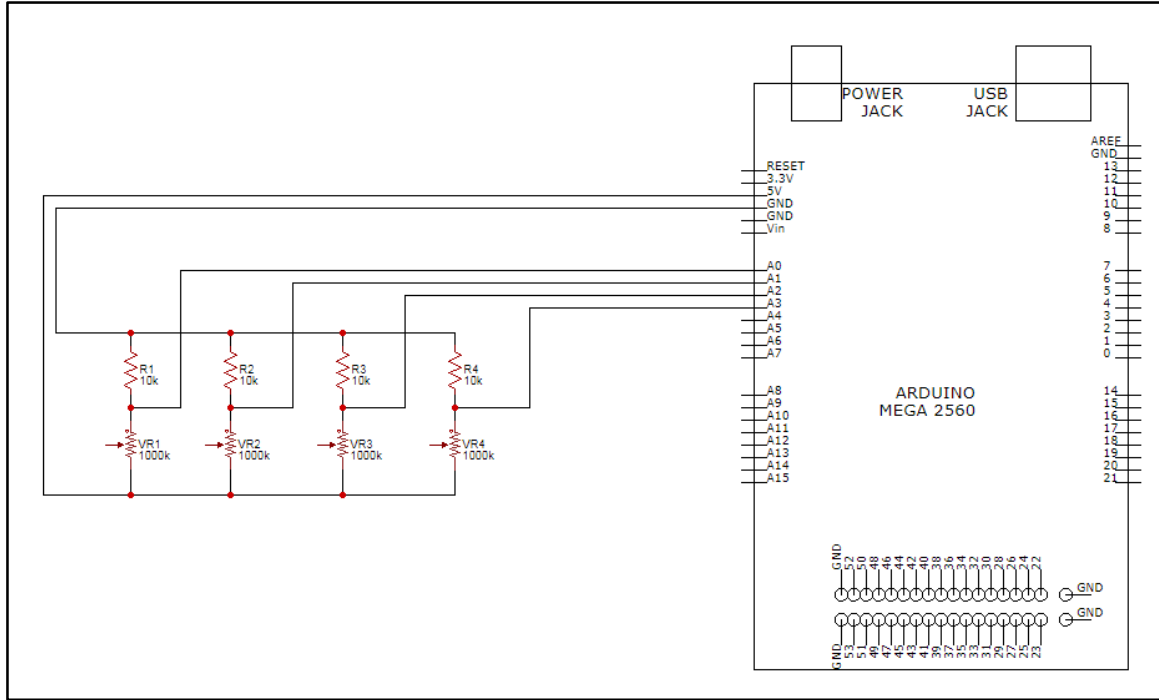


Figure 71: Sensory system schematic

6.3.3 Motor Push-Button Control Schematic

The schematic shown in Figure 72, presented the motor control for the actuators of the gripper. The stepper motor is controlled by a stepper driver, which was supplied by a 24 V AC/DC power supply. The stepper received control signals from the microcontroller by means of push-buttons. The gripper force was variably controlled in terms of switch buttons for opening and closing of the gripper appendages. The clockwise and anti-clockwise rotation of the stepper motor represented the opening and closing of the gripper fingers. The motor rotated clockwise when a low voltage signal on pin 8 was received and a high signal on pin 9 was received. The opposite occurs to the motor rotating anti-clockwise when pin 8 received a high voltage signal and pin 9 received a high voltage signal. Refer to APPENDIX E.3 for the Arduino® code for the push-button control and APPENDIX B.7 for the schematic design.

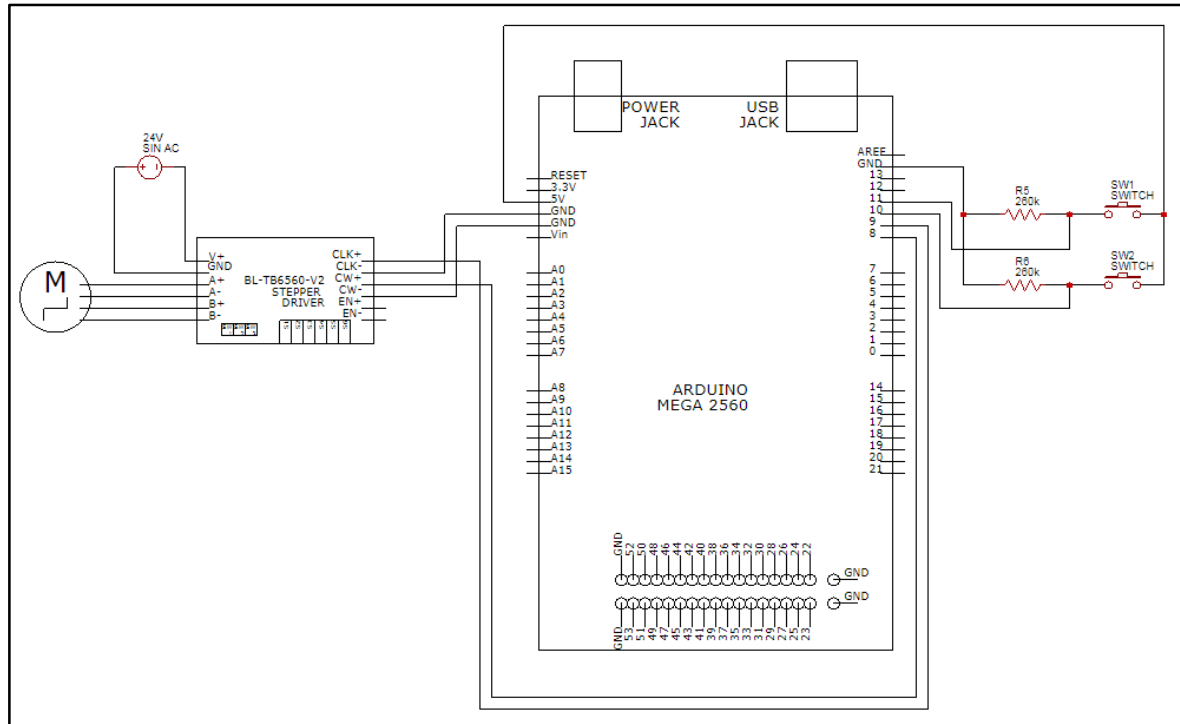


Figure 72: Motor push-button control schematic

6.4 System Proposed Budget and Energy Audit

A budget was generated for the total cost of the gripper assembly. The budget for components and assembly was R 6361.50. An energy audit was generated to demonstrate the annual running cost of the system. The annual running cost of the system during daytime was estimated to be R 7108.69 per year. Refer APPENDIX A.3 and A.4 for system proposed budget and energy audit.

6.5 Conclusion

A 3-finger and 4-finger gripper configuration were designed for the conceptual investigation. The gripper system incorporated a NEMA 17 stepper motor for actuation. The motion was transferred from the motor from rotational to transitional displacement by means of threaded bar. The appendages of the gripper were designed using the Fin Ray Effect[®] mechanism. The electronic design consisted of a motor controls schematic and a sensory layout design. The closing and opening modes for the gripper were controlled by means of push-buttons programmed for gripping connected to a motor driver. The sensory system was designed by using FSR sensors and 10 k Ω resistors. A microcontroller was attached to both the motor control and the sensory system. The microcontroller communicated with the computer for data processing of voltage signal outputs.

7 System Computer Aided Simulation

7.1 Introduction

This chapter describes the Finite Element Analysis, (FEA) simulation that is performed on the gripper appendages. The analysis determines the stress and deflection throughout an object. FEA's are used to establish static failure conditions for design structures. The simulation package uses an FEA algorithm and is called Siemens NX® and is employed for stress analysis in industrial applications. This chapter discusses the simulation preparation and procedure of simulating the stress and deflection criteria of the design fin ray appendages for the 3-finger and 4-finger systems. The simulation is performed on the materials specifically used in 3-D printing. The results from the simulation are discussed in terms of applicability for conformity characteristics.

7.2 Simulation Procedure

The design approach of the appendage was to confirm the displacement of the designed geometries by means of a stress simulation. The shapes and sizes of products in a pick-up and placements procedure influence the adaptability and conformity of the gripper. Improving the shape of the appendages could possibly reduce lead time and effort in gripping considerations and path planning.

The simulation software package used to simulate the deflection and stress characteristics of the fingers was Siemens NX®. The geometry was imported into software and a Finite Element Analysis (FEA) was simulated. A force resembling the part handling contact was applied to the surface area of the gripper finger. The following model procedure describes the adequate preparation of the simulation model:

- The solid model was imported as a Parasolid file.
- The model's geometry was prepared by dividing the surface geometry into different regions.
- Boundary constraints and loading conditions were specified.
- The material properties, nylon and ABS plastic, was selected for the model. The material selection included the mechanical properties (Poisson's ratio, elastic modulus etc.) of each material.
- The solid model was meshed according to tetrahedron (10) division.
- An "Element Shape Check" was performed on the selected mesh.
- The model has simulated using linear statics.
- The model has simulated using non-linear statics.
- An "Iterative Solver Convergence" was generated to prove convergence of solved equations.

A surface area was created on the contact area 25 mm from the edge and 15 mm in length. A distributed force is applied to the 15 mm area and resembles the load from the object being grasped. The model meshes with 1 mm grid and the material was selected as ABS plastic and nylon for both stress simulations. The mesh element properties were selected as a tetrahedron (10). A tetrahedron (10) consists of 10 nodal points per element and increases the number of required equations to be performed for that element. An increase in equations per element increases the accuracy of results of variables to be solved. The performed “Element Shape Check” verified 41648 total elements. The check showed zero (0) failed elements and 98 element warnings. The warning elements represent a minimum element size smaller than 1 mm and a maximum element size larger than 50 mm. The failed or error elements represent a minimum element size smaller than 0.1 mm and a maximum element size larger than 100 mm. A distributed loading P of 10 N was applied as the loading magnitude. Fixed boundary conditions C were applied to the hinged areas as shown in Figure 73.

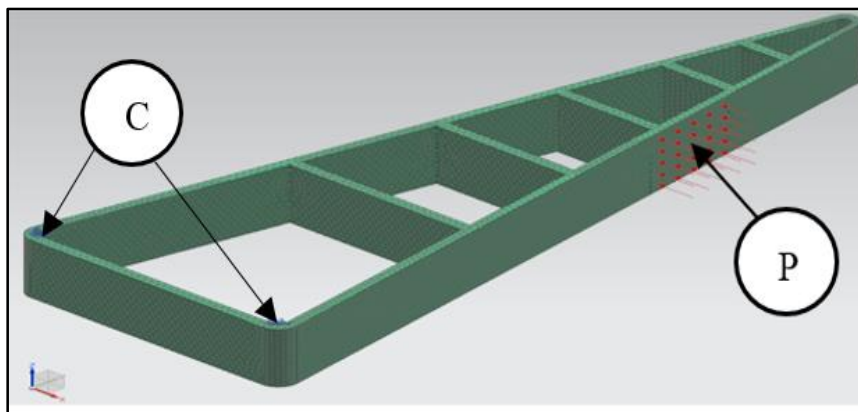


Figure 73: Constraints and loads applied to the first Geometry structure.

The model was simulated using linear statics and non-linear statics simulation option. A convergence was found after the simulation was performed on the model. A convergence graph is important to illustrate that the equation solver has calculated all variables and values. The convergence proved that the equation matrix converged the computed finite values. The appendages are set up according to design considerations for rib structures. The ribs adjoining the wall, must all attach with the same thickness by means of using fillets in the model design. The geometrical considerations, if not considered, affect the outcome of the results and the deflection and stress values will be inconsistent. The convergence for linear statics simulation is shown in Figure 74. The convergence of non-linear statics simulation is shown in Figure 75 and Figure 76.

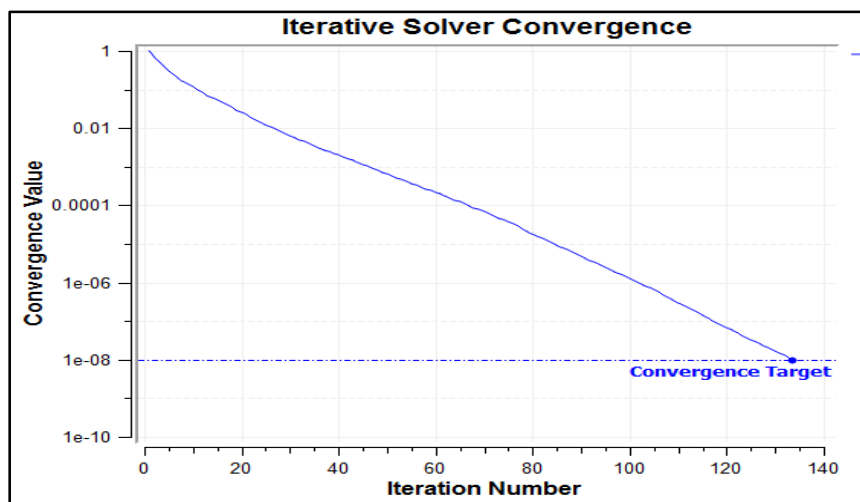


Figure 74: Convergence of iterative equation solver for linear statics

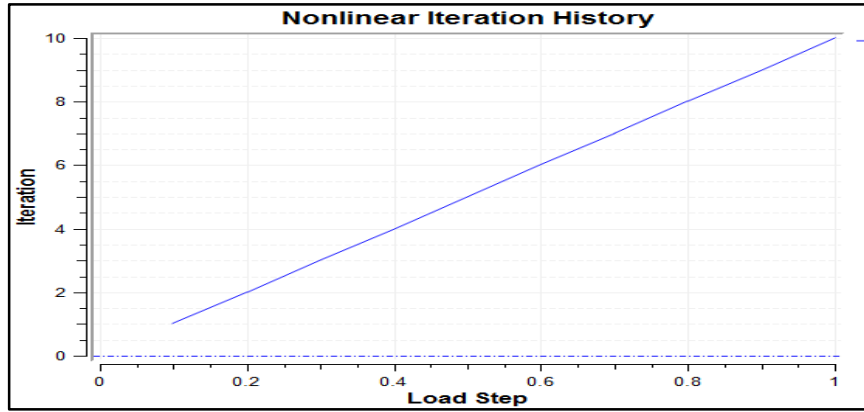


Figure 75: Non-linear iteration history for non-linear statics

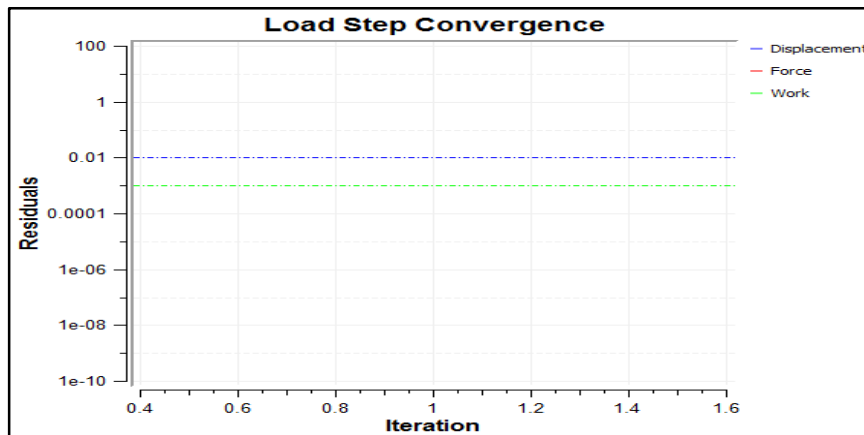


Figure 76: Load step convergence solver for non-linear statics

7.3 Simulation Results

The effect of wall deformation on the adjacent walls of the appendage was clearly demonstrated. The force distribution moves across the rib network and deforms the wall accordingly. A deformation occurs on the wall of the appendage in the circumstance of geometric change. The force vector changed according to the rib structure modification and as a result deformity difference was seen. The simulation is applied to both ABS plastic and Nylon materials.

Geometry 1 was used as a reference for comparison, as it illustrated the traditional Fin Ray structure as shown in Figure 77. Geometry 2 included a slanted rib structure, therefore the force vector changed direction accordingly as illustrated in Figure 78. The deformation increased in Geometry 2 as a result of the stiffness property decreasing in the finger structure. Geometry 3 incorporated a curved parallel rib structure and slightly decreased the stiffness of the structure, therefore lesser deformation occurred as compared to Geometry 2, shown in Figure 79. Geometry 4 incorporated slanted and curved ribs accordingly and deflection magnitudes were observed to be in the same range as Geometry 2, portrayed by Figure 80. The linear static analysis for the different geometries are shown in Figure 77 - 80. The non-linear static analysis is shown in Figure 81 – 84. The simulation summarized results was discussed in Section 10.2.1.

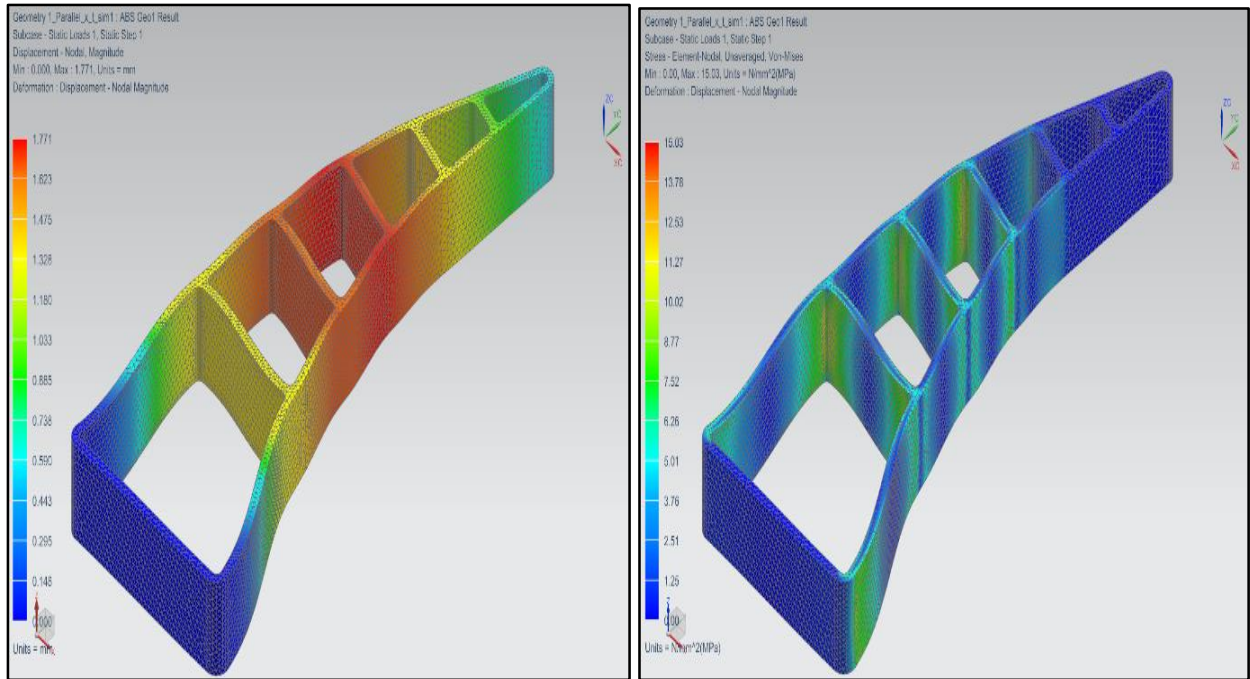


Figure 77: Geometry 1 deflection and Von Mises stress result visual illustration for linear statics

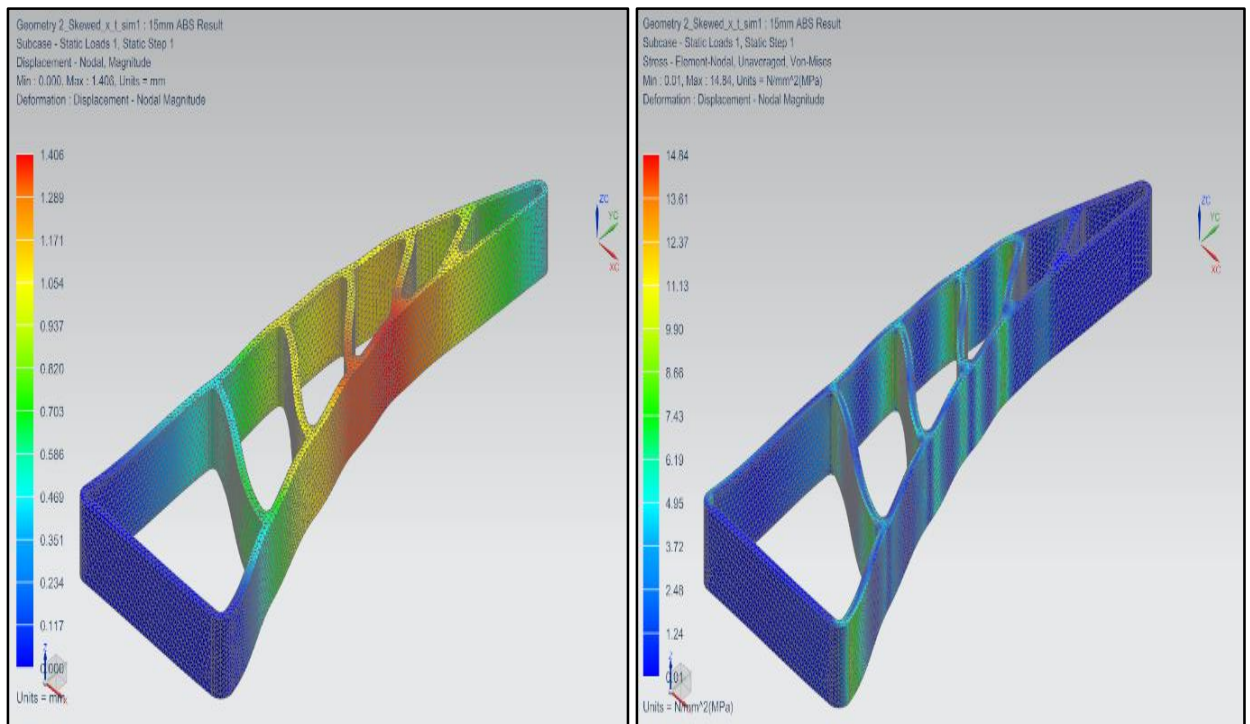


Figure 78: Geometry 2 deflection and Von Mises stress result visual illustration for linear statics

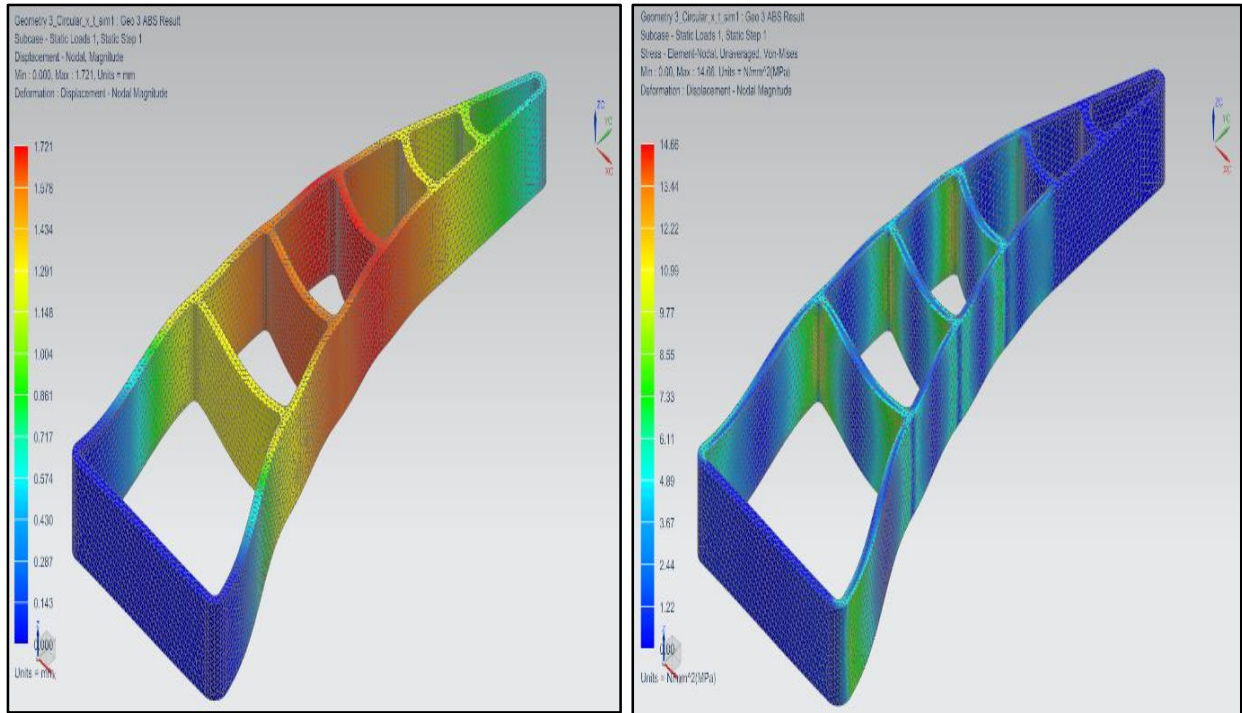


Figure 79: Geometry 3 deflection and Von Mises stress result visual illustration for linear statics

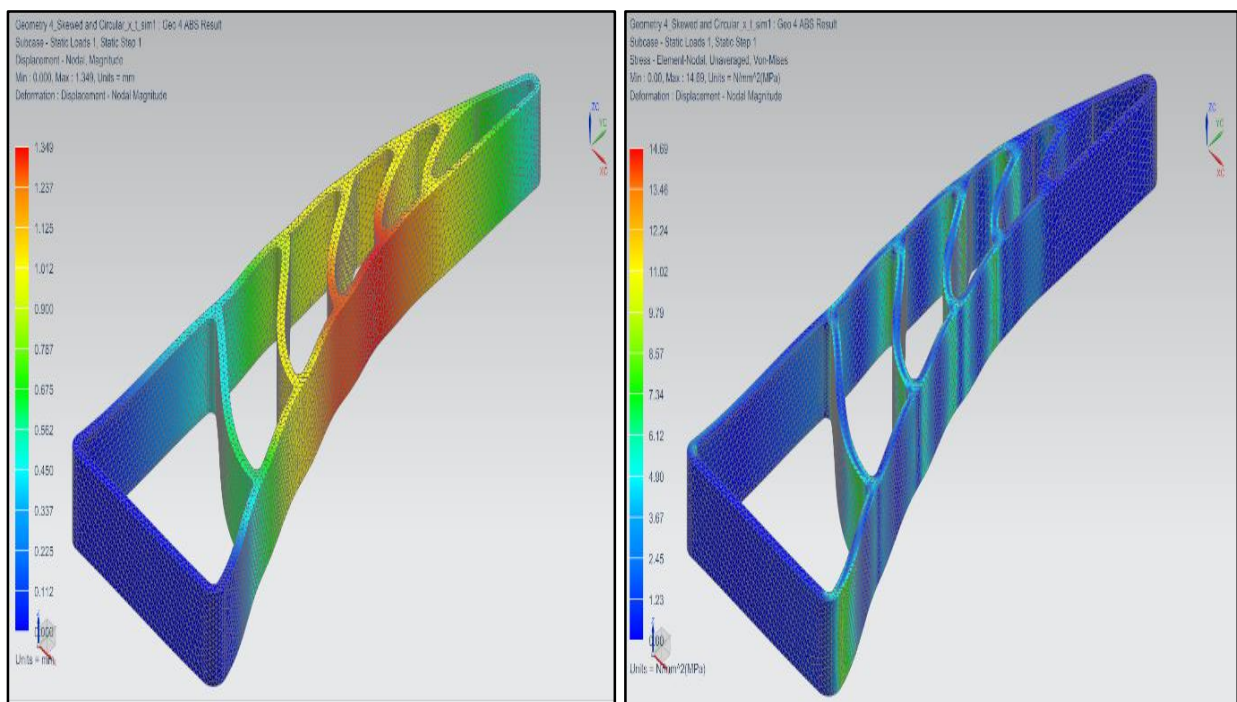


Figure 80: Geometry 4 deflection and Von Mises stress result visual illustration for linear statics

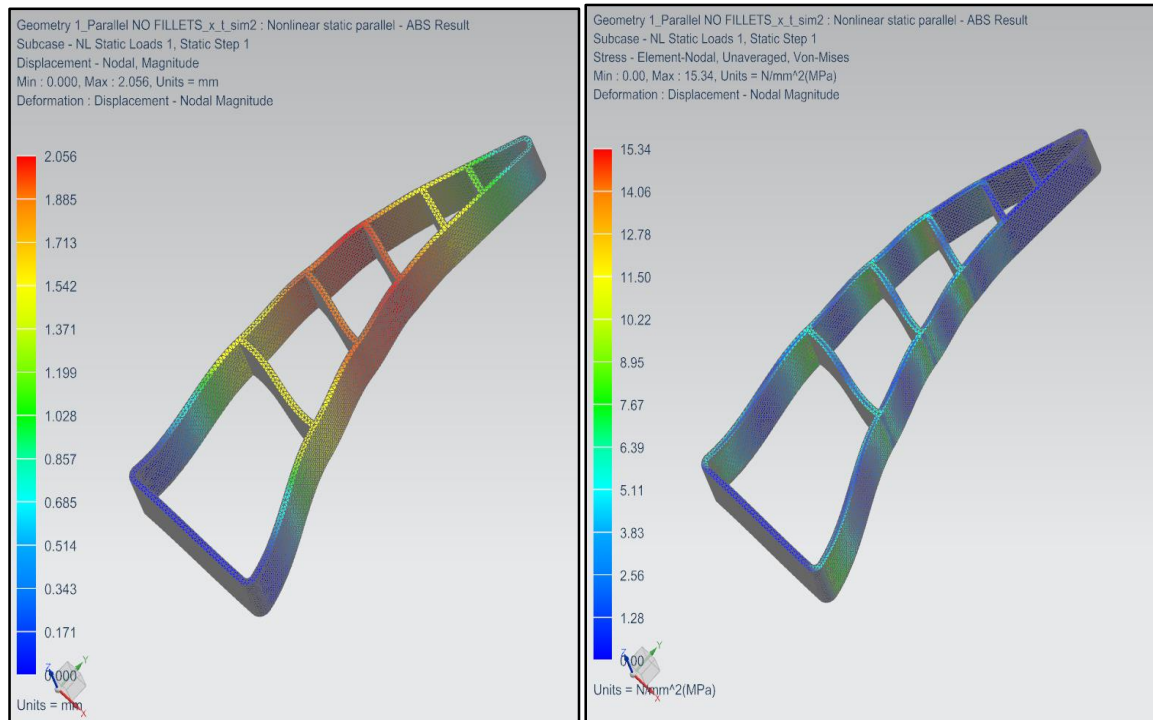


Figure 81: Geometry 1 deflection and Von Mises stress result visual illustration for non-linear statics

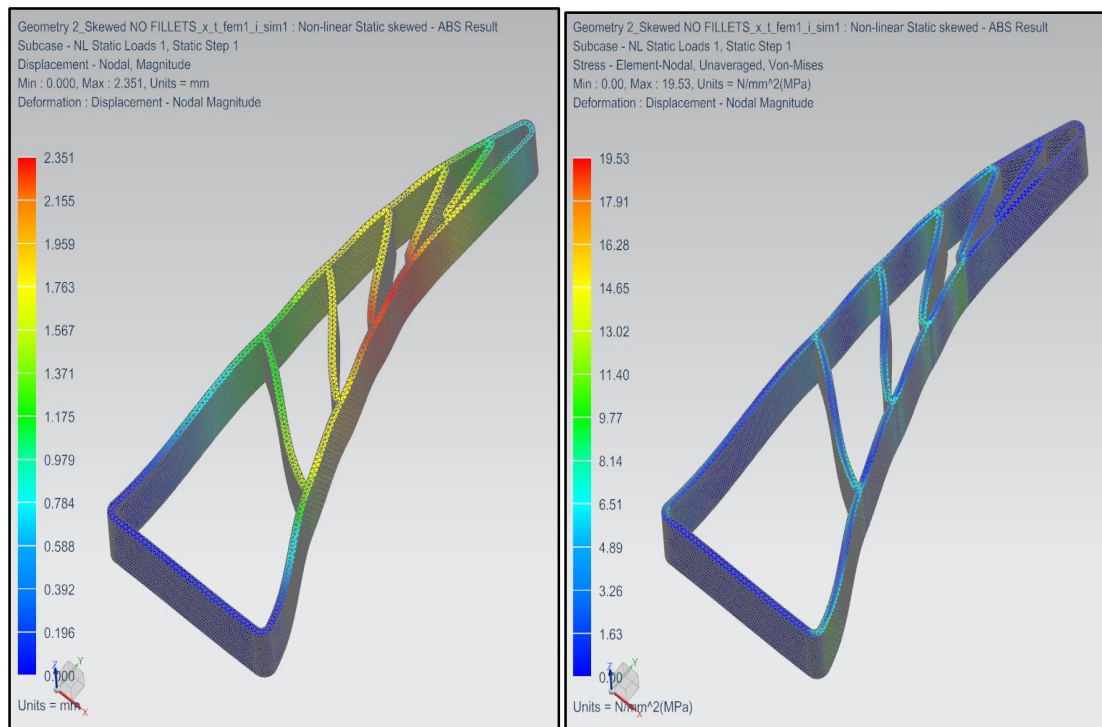


Figure 82: Geometry 2 deflection and Von Mises stress result visual illustration for non-linear statics

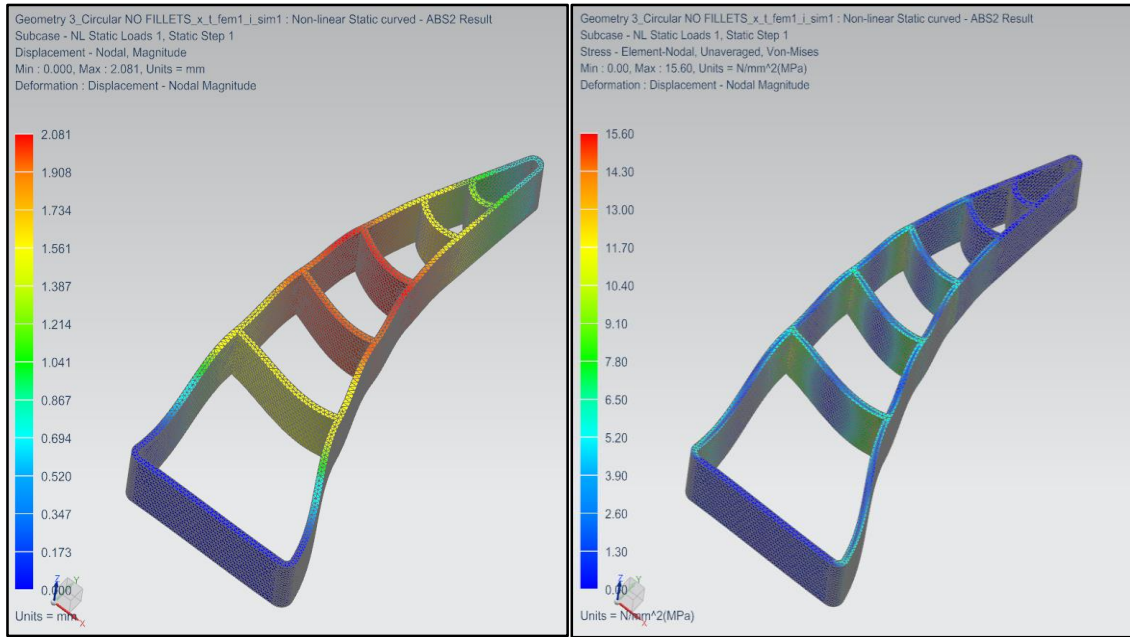


Figure 83: Geometry 3 deflection and Von Mises stress result visual illustration for non-linear statics

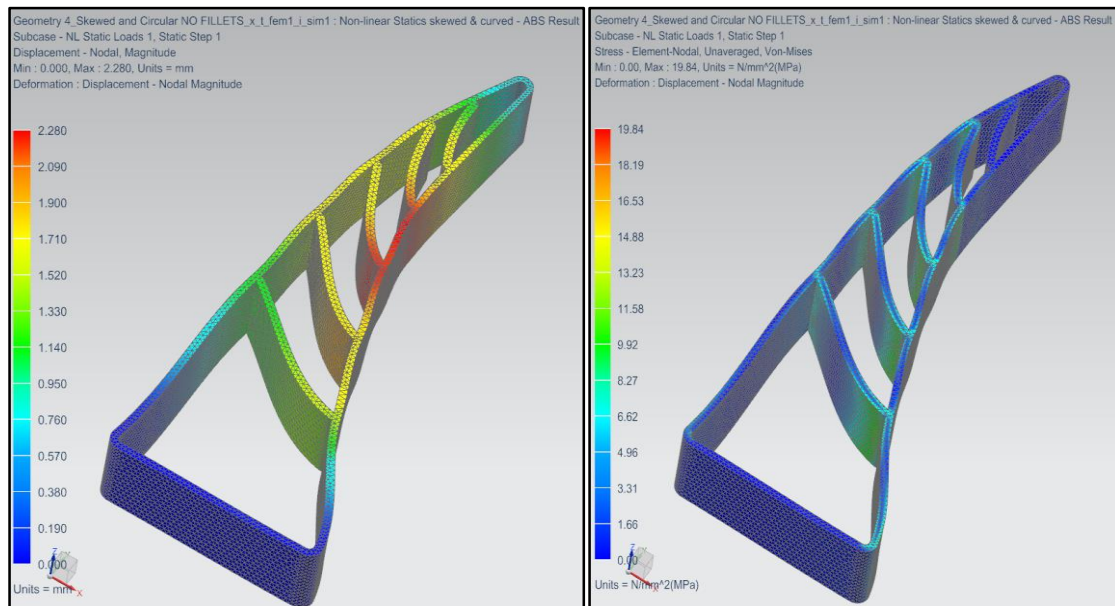


Figure 84: Geometry 4 deflection and Von Mises stress result visual illustration for non-linear statics

7.4 Conclusion

The simulation demonstrated a directly proportional relationship between the deflection and high Von Mises stress distribution. The change in rib structure changed the object conformity properties of the gripper. Therefore, the increase in deflection illustrates holding conformity and reduced slippage of components from appendage contact. The improvement of the design has the potential to increase the performance of the gripper system and was integrated into the gripper design.

8 Manufacturing and Assembly

8.1 Introduction

This chapter discusses the manufacturing and assembly process of the gripper system. The 3-D printing procedure is discussed for producing the system components and housing. The assembly and instalment procedure of components is explained. The assemblage is illustrated for the electronic components and system integration to a robotic arm. The attachment of gripper system prepared for experimentation is described.

8.2 3D Printing

Rapid prototyping by means of plastic deposition was selected as the manufacturing process for producing the required components. The parts were produced using a UP 3D-printing system and a modified Prusa-I3 3D-printing system. Plastic is deposited layer by layer to build up the part from the base plate as shown in Figure 85. Level calibration has to be done to the printing bed in order for the 3D print to be perfectly aligned for each layer. The layer thickness used was 0.3 mm and a density of 100 % was chosen for appendages and 60 % for gripper components. Preheat was required on bed according to a temperature range of 200 °C - 250 °C, depending on the print material chosen. A nearly completed part is illustrated in Figure 86.

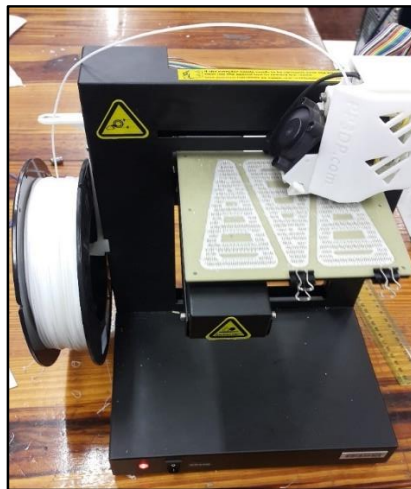


Figure 85: Foundation scaffolding of the printed appendages.

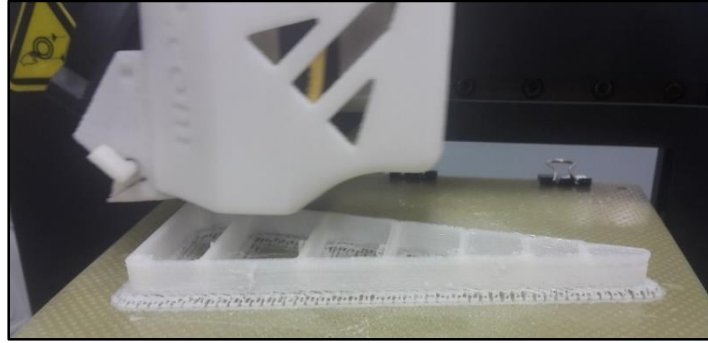


Figure 86: Layer build-up of the appendage.

8.3 3-D Printing of Appendages

The gripper fingers were manufactured through 3-D printing. The fingers were used throughout the experimental procedure and were tested for conformity performance. The final printed gripper appendages are shown in Figure 87.

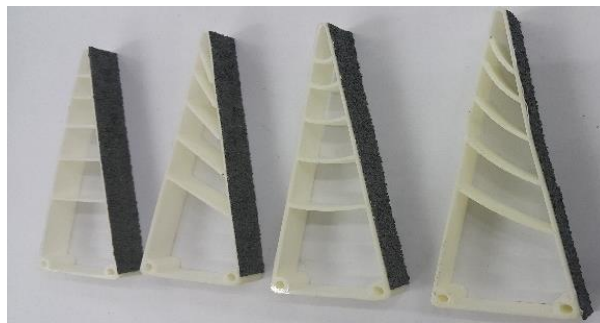


Figure 87: Final manufactured appendages.

Potential gripper appendages incorporating hinge movements were manufactured through 3-D printing. The fingers were intended for larger flexibility and conformity on the object. The hinged type appendages were not tested. The disadvantage of hinges was the uncontrolled deflection factors during force application and may cause a variable degree of repeatability. The hinged type fingers are shown in Figure 88.



Figure 88: Hinged type appendages.

Flexible filament material for 3D-printing was available and strength properties were adjusted using hardening resin. The specific material was thermoplastic ester elastomer and proved to have the elastic properties required for flexible gripping. The appendages were printed using the flexible filament, however, was not tested. The 3D printer that was used lacked the necessary printing resolution and components were produced with inconsistent layering. The flexible filament fingers are shown in Figure 89.

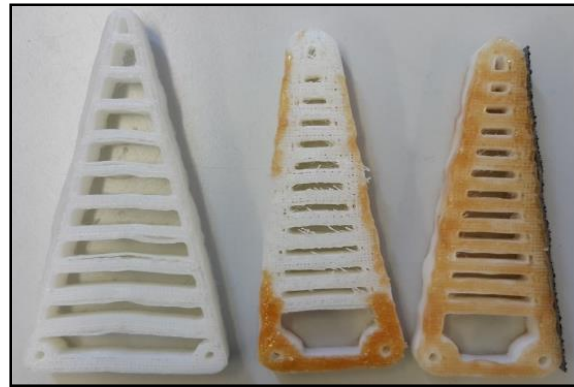


Figure 89: Flexible filament appendages.

8.4 Part Assembly

All components were printed for the 3-finger and 4-finger gripper system and ready for assembly as shown in Figure 90. The assembly procedure follows the exploded view drawing, explained in Section 6.1. The hinge attachments are connected by means of M3 bolts and nuts. The shaft housing and finger holder are fastened by means of four (4) M3 bolts and nuts. The motor was held in place by means of four (4) M3 threaded bars and M3 nuts. The final assembly prototype, illustrated in Figure 91, was prepared for testing.



Figure 90: Unassembled components for gripper system



Figure 91: Assembled prototype of gripper system.

8.5 Electronic Assembly

The sensory system assembly is shown in Figure 92. The sensory system consisted of 4 FSR sensors used in the 3-finger or 4-finger configuration. The sensors were attached to the contact surface area of the gripper appendages to measure force characteristics of the gripper movement. The sensors were connected to the microcontroller and received a power signal from the USB jack attached to a computer. The raw signal was transferred to CoolTermWin®, a software program that converted the raw data signal into voltage magnitudes that were extracted for plotting of results. The motor push-button control assembly is shown in Figure 93. The motor forward and reverse directions were controlled by means of pushbuttons. The push-buttons represent the required force input for grasping. The stepper driver was powered by means of a 24V AC/DC power supply. The gripper is shown to be attached to the wire harness leading from the stepper driver to the stepper motor.

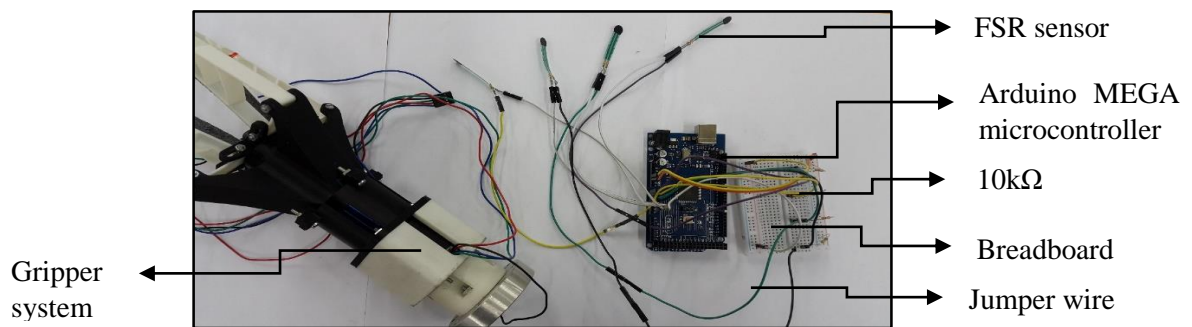


Figure 92: Sensory system assembly

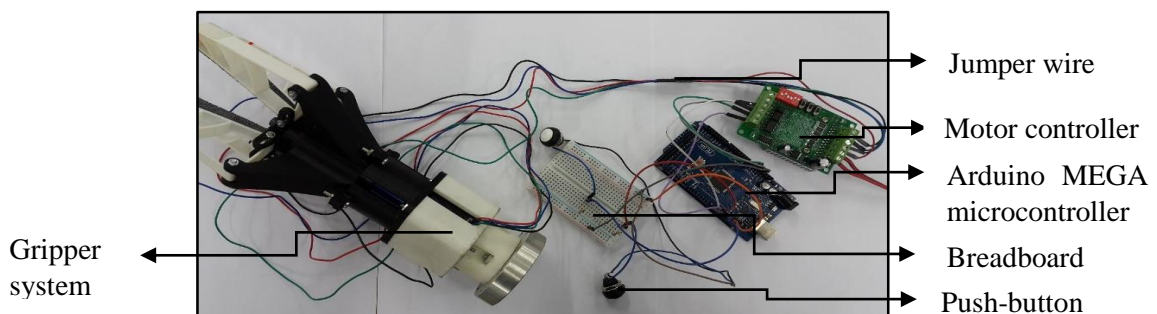


Figure 93: Motor push-button control assembly

8.6 Final Assembly onto Robotic Arm

A control board was installed for the gripper system to be operated, shown in Figure 94. The gripper system was activated from the control board before the robotic arm was operated. The sensor placement on the gripper system is shown in Figure 95. The FSR sensor is placed at the most common gripping position for the gripper to grasp objects.

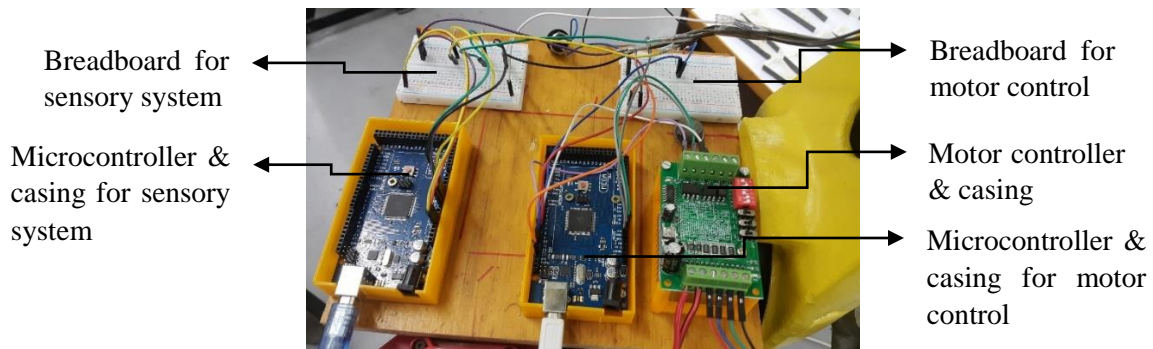


Figure 94: Electronic control board

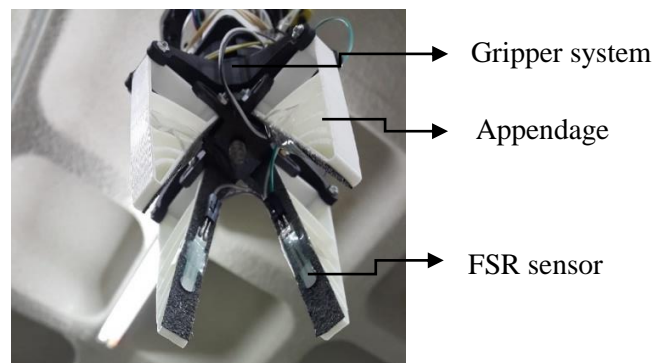


Figure 95: Sensor installation

A power supply was used possessing 5V DC from a laptop and a 24V DC power supply using alternating current from the wall socket, shown in Figure 96: Power supply. The power supply is placed close to the control system and sensory system for correct wiring to electronic components. The power supplied was continuously monitored for correct voltage magnitude supplied to the electronic sub-systems.



Figure 96: Power supply

The side and front view of the assembled robotic arm and gripper system are shown in Figure 97 and Figure 98. The sensor and motor wiring harness followed the robotic arm to the control board. The harness is laid out with enough length for the robotic arm to move comfortably without entanglement.

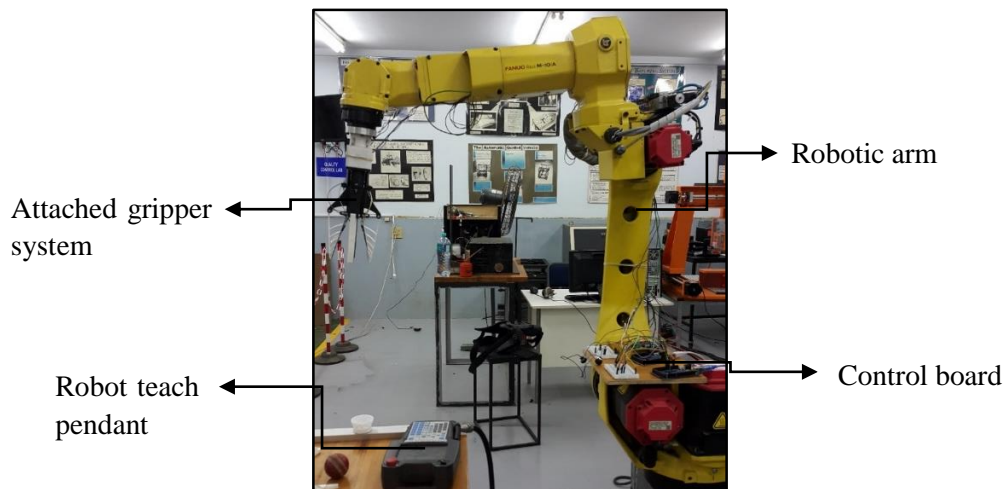


Figure 97: Side view of robot arm and gripper system

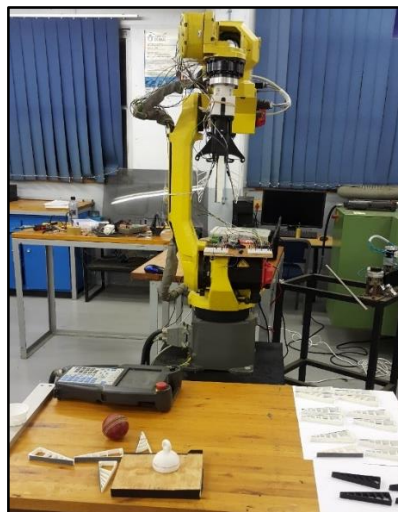


Figure 98: Front view of robot arm and gripper system

8.7 Conclusion

The gripper system was assembled and installed for both 3-finger and 4-finger configuration. The components were manufactured from ABS plastic due to the materials high strength properties. The electronic system was connected and programmed for gripping operation. The 12V power supply was distributed from the laptop to the microcontrollers. The 24V power supply was distributed from the AC/DC inverter to the motor controller. The system was installed onto the FANUC robotic arm and was prepared for experimentation.

9 Testing and Validation

9.1 Introduction

This chapter discusses the testing and evaluation of the gripping system. The safety required for experimentation and the robotic operation is reviewed. The calibration for the FSR sensors is illustrated since the sensors have manufacturing inaccuracies and compression errors. The path plan used for experimentation is illustrated. The data interpretation from sensory output signals is shown and discussed. The testing is performed in 3 phases. Phase 1 tests the repeatability of the gripper system a static holding mass test. Phase 2 establishes the dynamic performance of the gripper system by means of a dynamic holding test. The final testing phase determines the flexibility of conformity of the gripper by means of grasping a variety of part shapes and sizes.

9.2 Safety Preparation for Experimentation

The safety of the system and the operator should always be kept in mind. All the safety precautions should be followed when operating the robotic arm and all its peripheral devices [72]. The operator's safety is the priority and then the safety of the machine to be operated. Additionally, it is dangerous for any person to enter the operational environment when the robot is in motion. The following precautions should be kept in mind when operating the robot:

- Even in a stationary position, the robot is still able to receive a signal and robot is regarded as still in motion. The operator should be alert and place a warning that the robot is in motion.
- The robot should be operated in a safe environment where no damaged should occur to other machinery. The robot should always be attached to emergency stop buttons located on the teach pendant and on the PLC control panel.
- All peripheral devices should be grounded, in case of electrical shortage or surges.
- The range of robot motion should be kept in mind and operator should stay clear of work envelope.
- Unless specifically necessary to enter the robot envelope, all tasks required should be carried out outside of robot work area.
- All peripheral devices of the robot must be ensured to be in working condition before teaching robot through the pendant.
- Before entering workspace of the robot, the location and condition of all safety devices must be checked.
- Careful attention should be paid that no other person enters the work area.
- The robot must not be operated in automatic mode when someone is in work area.

-
- When replacing or reinstalling components and parts, it must be confirmed that foreign matter has not entered the system.
 - Delicate components should be considered when operating or maintaining robot as components may break under excessive force when installing.

9.3 Test Preparation

The test procedure was followed according to Section 5.8. The sample mass for experimentation was measured before experimentation as shown Figure 99. The gripper was unloaded by means of a push button control as illustrated in Figure 100. The mass holder or specimen is then loaded in Figure 101. The mass holder was loaded by means of a sample mass. The test preparation was executed for both the 3-finger gripper and the 4-finger gripper.



Figure 99: Mass measurement of sample weights



Figure 100: Unloaded 3-finger gripper



Figure 101: Loaded 4-finger gripper with mass holder

9.4 Sensor Calibration

The relationship between the force applied to the FSR sensor and the voltage output signal was not linear [73]. The relation graph showing voltage versus force characteristics of the FSR sensors are shown in Figure 102. An exponential relation describing the estimation to force ranges for FSR readings is shown in Figure 103. The FSR sensor is inexpensive and is widely used for a range of dynamic measurements. The FSR has an underlying error in compression of 5% to 10% due to prolonged shear [74]. The sensors used for experiments were calibrated after the readings were taken.

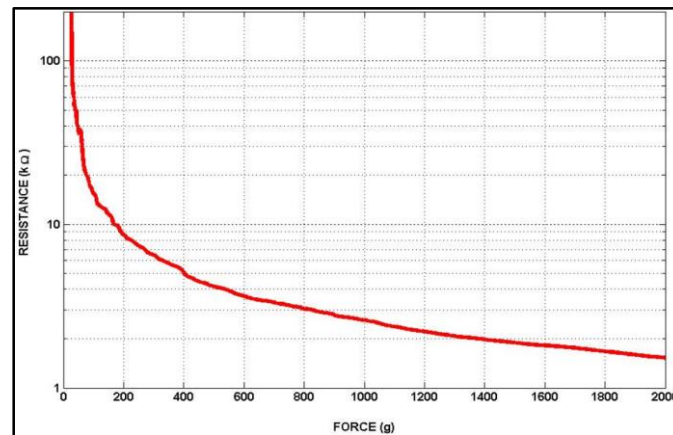


Figure 102: Resistance versus force graph for FSR sensor calibration [73]

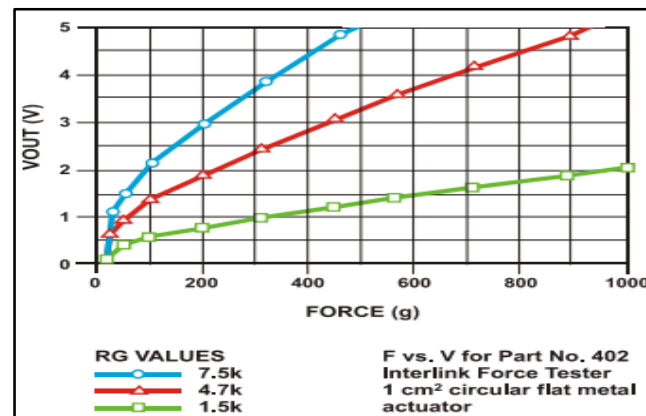


Figure 103: Voltage versus force graph of different resistors for FSR sensor calibration [73]

The calibration changes for the sensors used was between 1 V and 4 V. The loss of 1 V from the maximum input voltage of 5 V can be explained due to stray capacitance within the breadboard. The calibration estimation curves are shown in Figure 104, Figure 105, Figure 106 and Figure 107 for Sensor 1, 2, 3 and 4 consecutively. Refer to APPENDIX D.1 for calibration result tables of the four sensors. The data from the result output tables were converted to a voltage using the following formula:

$$V_{out} = \frac{val * V_{in}}{1024} * 1000 \quad 9.1$$

V_{out} : Output voltage (mV)

val : Value reading output (-)

V_{in} : Input voltage (5V)

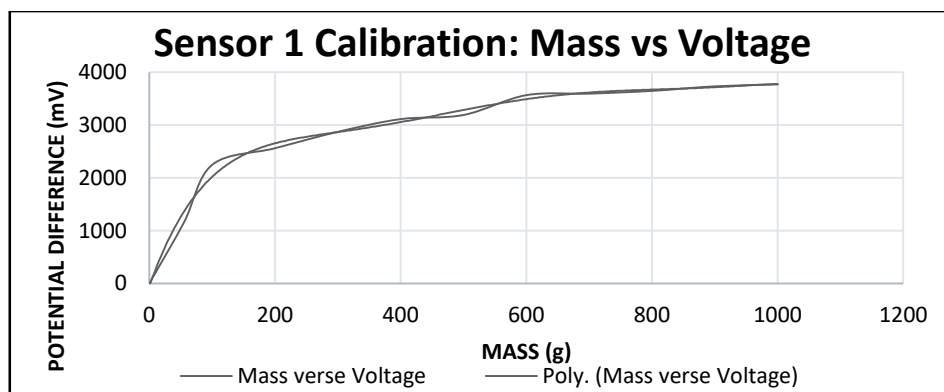


Figure 104: Mass vs voltage calibration graph for Sensor 1.

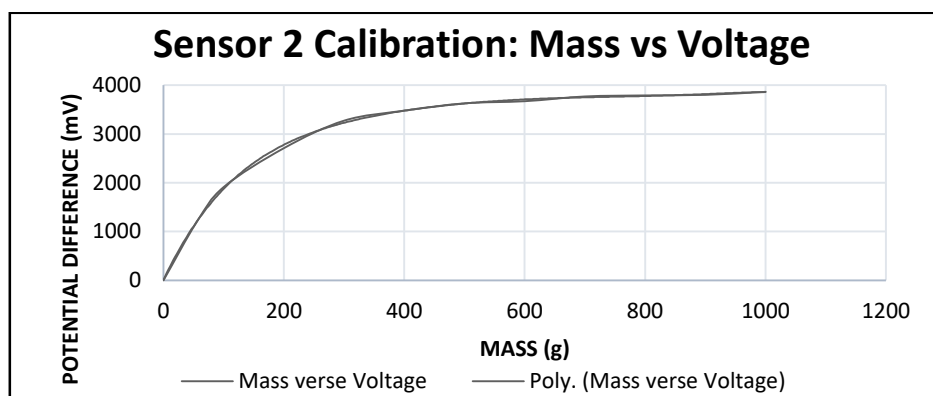


Figure 105: Mass vs voltage calibration graph for Sensor 2.

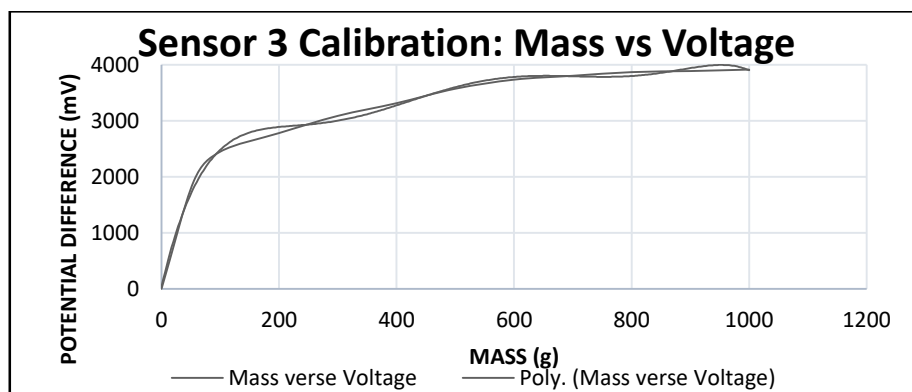


Figure 106: Mass vs voltage calibration graph for Sensor 3.

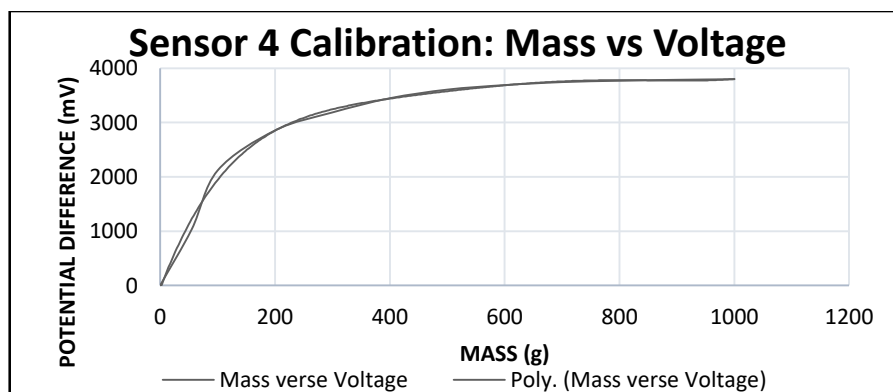


Figure 107: Mass vs voltage calibration graph for Sensor 4.

9.5 Path Plan for Robotic Arm

The robotic arm path plan for experimentation consisted of three periods illustrated in Figure 108. The first period of the movement consisted of time segments of approximately 10 seconds long in a stationary position. The second period of the movement was performed to illustrate the dynamic movement of a pick and place undertaking. The dynamic movement was applied between a high reach grip zone and a low reach release zone.

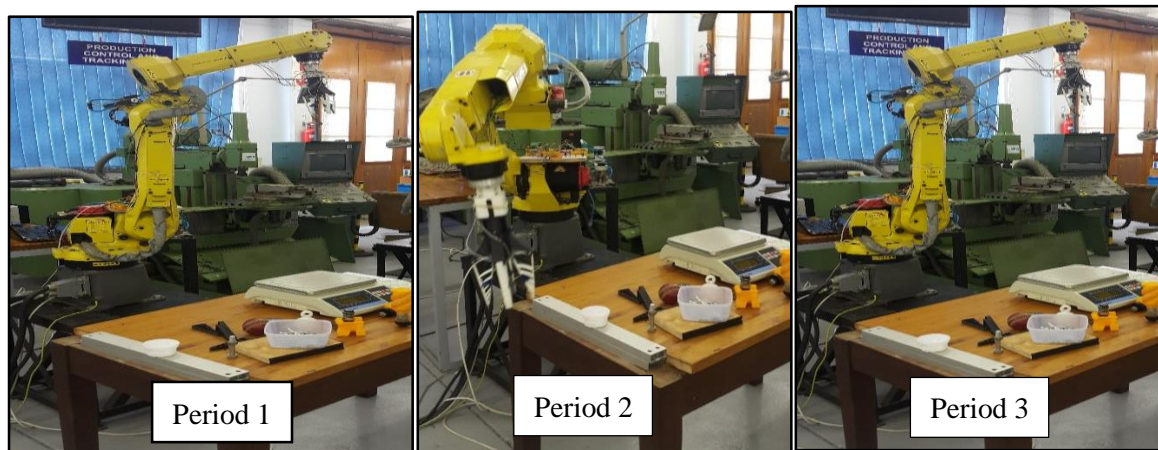


Figure 108: Pick and place path plan for gripper testing.

9.6 Dynamic Data Interpretation

The data received from the dynamic holding force test can be interpreted as the performance of the gripper system in operation. The data is represented as a force versus time graph that shows the time on the x-axis and force on the y-axis shown in Figure 109. High impulse values can result due to slippage or high loading events within the motion of the experiment. Dynamic motion attributes attained through experimentation describes the range of actual measured dynamic force.

Grippers can be compared to the gripping motion of human hands. Grip strength measurements are demonstrated in medical diagnosis of muscle fatigue [75]. Force measurements are taken over time to determine the grip strength deterioration of muscle tissue due to muscle fibre weaknesses caused by sepsis, malnutrition, etc. A comparison between grip performance of a robotic gripper and human hand grasping was determined to be a viable model.

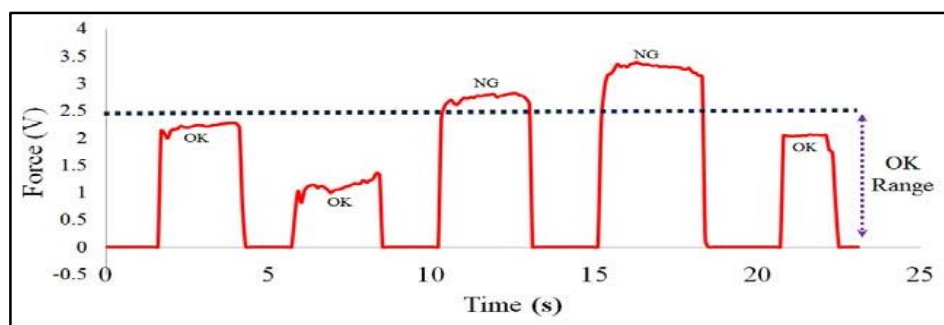


Figure 109: Gripping performance in terms of a force verse time graph [75]

9.7 Test Phase 1: Static Holding Mass Test Procedure

The static holding mass test is set up to determine the holding strength of the gripper by means of holding a set mass and slowly increasing the increments of the mass until failure occurs. The holding force was determined by multiplying the mass by the gravitational acceleration constant. The repeatability of the experiment is determined by repeating the experiment multiple times. The repeatability is expressed as a percentage and represents the probability of the gripper being able to perfectly grasp the sample weight.

AIM:

- The aim was to investigate the static gripping behaviour of a 3- finger and 4-finger gripper system design in gripping a sample mass.

OBJECTIVES:

- Determine the maximum static handling mass range for 4 geometric design considerations.
- Determine the repeatability of 4 geometric rib design considerations.

APPARATUS:

- Calibrated weight scale.
- Brass weights with 100 g increments.
- Symmetric holding unit.
- Gripping system.

METHOD:

- Step 1: The holding unit is gripped to the maximum holding torque of the motor (4.2 kg.cm²) at 35 mm from the fingertips of the appendages.
- Step 2: An initial mass of 1630 g is placed on holding unit.
- Step 3: Mass of 100g increments is added until the mass capacity of 2435 g is achieved.
- Step 4: Mass reading is taken when mass slips out of gripper with 100 g sensitivity.
- Step 5: Slipped mass is measured on calibrated scale and reading is logged.
- Step 6: Experiment is repeated 15 times per testing configuration.
- Step 7: Repeatability is calculated in terms of standard deviation of average holding mass.

PREDICTION:

- Maximum holding mass would be 2000 g.
- Repeatability would be above 90 %.

Loading sequence 1 in Figure 110: 3-Finger gripper loading sequence 1-3 for mass holding test shows the starting load mass of 1630 g stacked and increased by 100 g increments until maximum mass capacity is reached. Loading sequence, 2-9 shown in Figure 110, Figure 111 and Figure 112, illustrates the incremental loading of 100 g until a maximum mass load of 2435 g is reached. The experiment was repeated 15 times to determine the repeatability of the system. The experiment was also executed on the 4-finger gripper system. All combinations of geometries of the 3-finger gripper and 4-finger gripper were proved to hold the maximum weight load in some instance throughout the experiment as shown in Figure 113 and Figure 114. The static holding test and summarized results for the 3-finger and 4-finger gripper were discussed in Section 10.2.1.

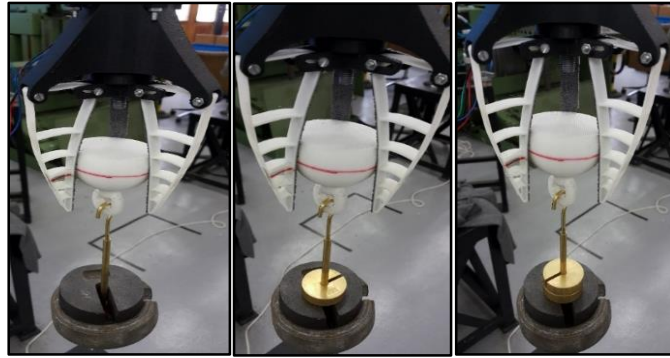


Figure 110: 3-Finger gripper loading sequence 1-3 for mass holding test

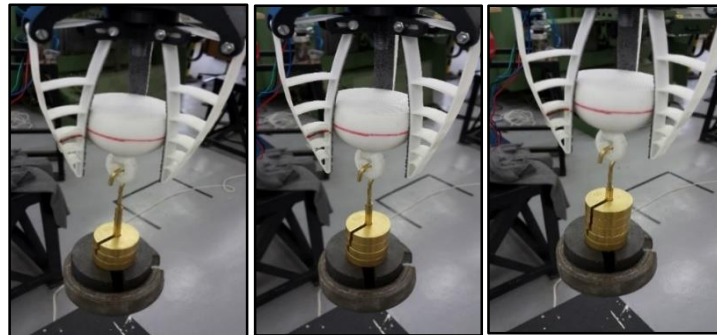


Figure 111: 3-Finger gripper loading sequence 4-6 for mass holding test

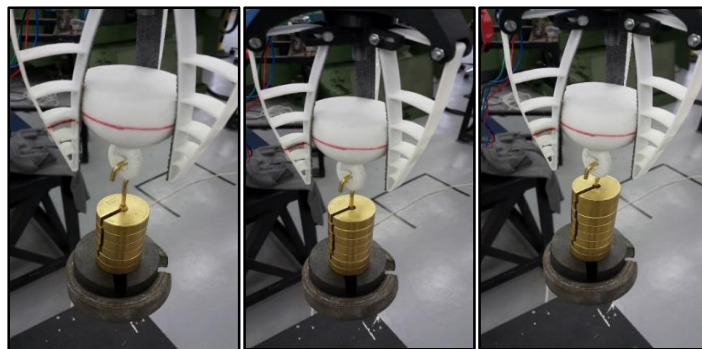


Figure 112: 3-Finger gripper loading sequence 7-9 for mass holding test



Figure 113: Maximum mass hold for all four geometries for 3-finger gripper

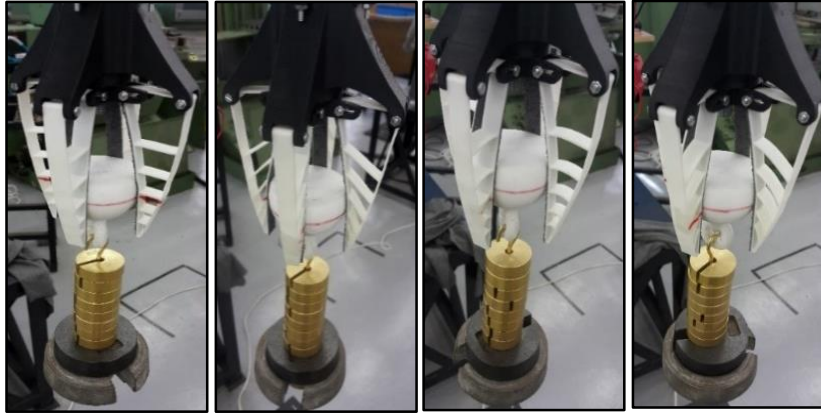


Figure 114: Maximum mass hold for all four geometries for 4-finger gripper

9.8 Test Phase 2: Dynamic Holding Force Test Procedure

The dynamic holding force test was set up to determine the holding strength of the gripper by means of holding a set mass and driving the gripper into a predetermined motion. The holding force was determined by means of a received force magnitude in terms of voltage signals. The resulting output was given as the force versus time graphs and can be related to the force model described in Section 5.4.3.

AIM:

- The aim was to investigate the dynamic gripping behaviour of a 3- finger and 4-finger gripper system design of the forced behaviour of gripping a sample mass.

OBJECTIVES:

- To determine the maximum static handling force range for 4 geometric design considerations.

APPARATUS:

- Calibrated weight scale.
- Symmetric holding test specimen.
- Gripping system.
- Force feedback control using forces sensitive resistors.

METHOD:

- Step 1: The holding unit is gripped to maximum torque load of gripper on the sensors at 15 mm from the fingertips of the appendages.
- Step 2: A mass of 329 g is grasped and force measurements in terms of voltage units are taken.
- Step 3: The robotic gripper follows a pick and place sweep motion.
- Step 4: Mass and force reading is taken.
- Step 5: Force versus time graph is computed and reading is logged.
- Step 6: Experiment is repeated 5 times per testing configuration.

PREDICTION:

- Maximum dynamic holding mass would be above 329 g.

9.8.1 *Dynamic Test Run – Specimen: Cricket Ball*

An initial dynamic test was performed to determine sensor sensitivity and calibration required. The test was repeated 5 times for Geometry 4 and a cricket ball was grasped by the 4-finger gripper system. The ball was weighed and was determined to be 119 g shown in Figure 115. The cricket ball was gripped between the gripper fingers and the arm was deployed into the dynamic movement described in Section 9.1. Contact made between the ball and all the sensors produces a potential difference signal. The signal was recorded according to 10 Hz data transferral rate as shown in Figure 116. The voltage output signal can be converted into a force output signal according to the calibration curves in Section 9.3. The signal shows a stable grip and a slight increase in signal. The slight increase in converted force signal proved that self-conformity takes place throughout a dynamic movement. The 5 experiment runs in terms voltage versus time signals are shown in APPENDIX D.12 – D.15.



Figure 115: Initial dynamic experimental operational test on cricket.

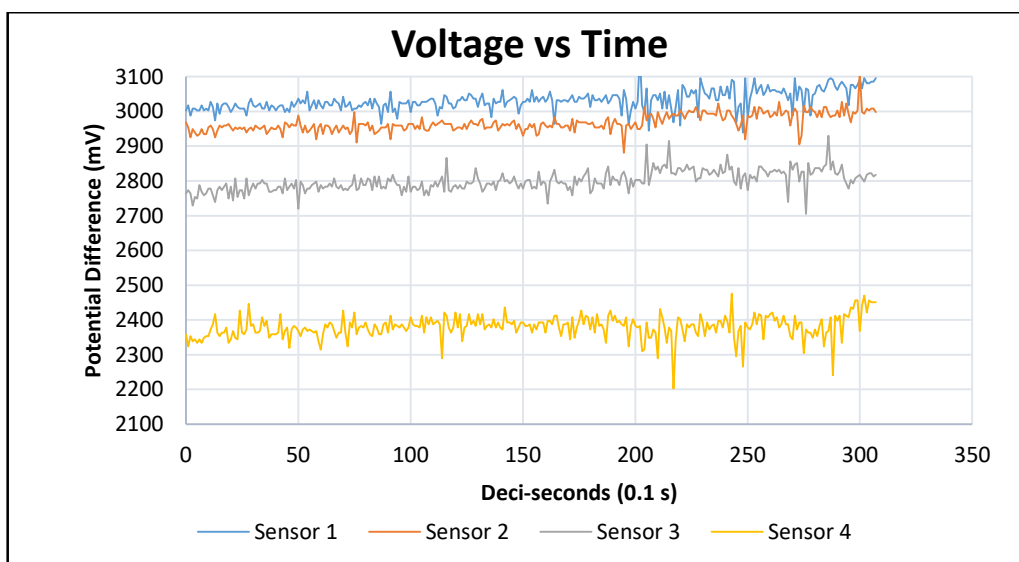


Figure 116: Voltage verse time graph for 4-finger gripper- Cricket ball: Geometry 4.

9.8.2 *Dynamic Test Run for 3-Finger Gripper – Specimen: Sphere*

The dynamic experimental procedure was performed on the 3-finger gripper system. The procedure was executed on all 4 geometry configurations. The spherical test sample was grasped by the gripper with the sensors in contact with the part surface shown in Figure 117. The spherical specimen was gripped between the gripper fingers and the arm was deployed into the dynamic movement described in Section 9.1. The voltage output signal can be converted into a force output signal according to the calibration curves in Section 9.3. The dynamic test and summarized results for the 3-finger gripper was discussed in Section 10.2.3.

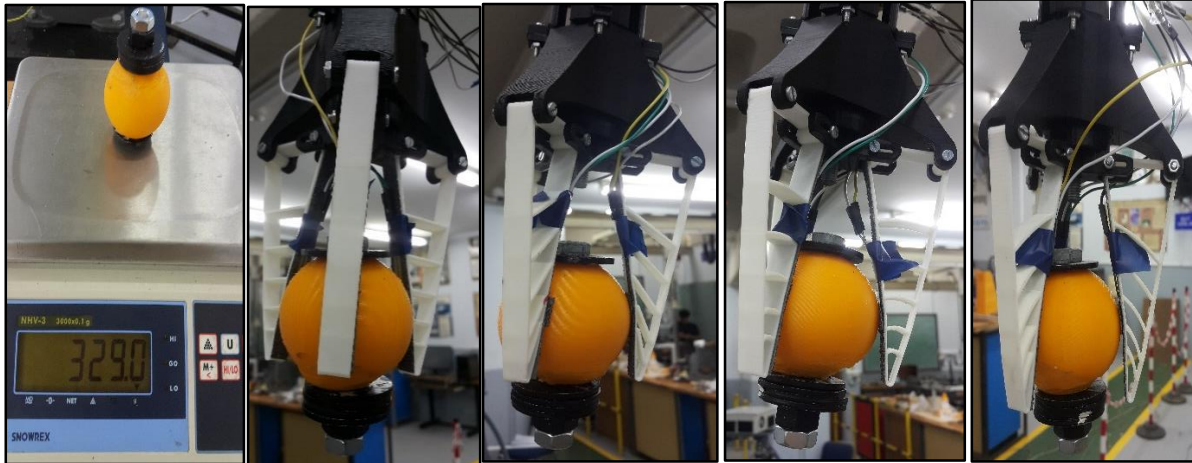


Figure 117: Dynamic test for 3-finger gripper: Geometry 1, 2, 3 and 4.

9.8.3 *Dynamic Test Run for 4-Finger Gripper – Specimen: Sphere*

The dynamic experimental procedure was performed on the 4-finger gripper system. The procedure was executed on all 4 geometry configurations. The spherical test sample was grasped by the gripper with the sensors in contact with the part surface shown in Figure 118. The spherical specimen was gripped between the gripper fingers and the arm was deployed into the dynamic movement described in Section 9.1. The dynamic test and summarized results for the 4-finger gripper was discussed in Section 10.2.3.

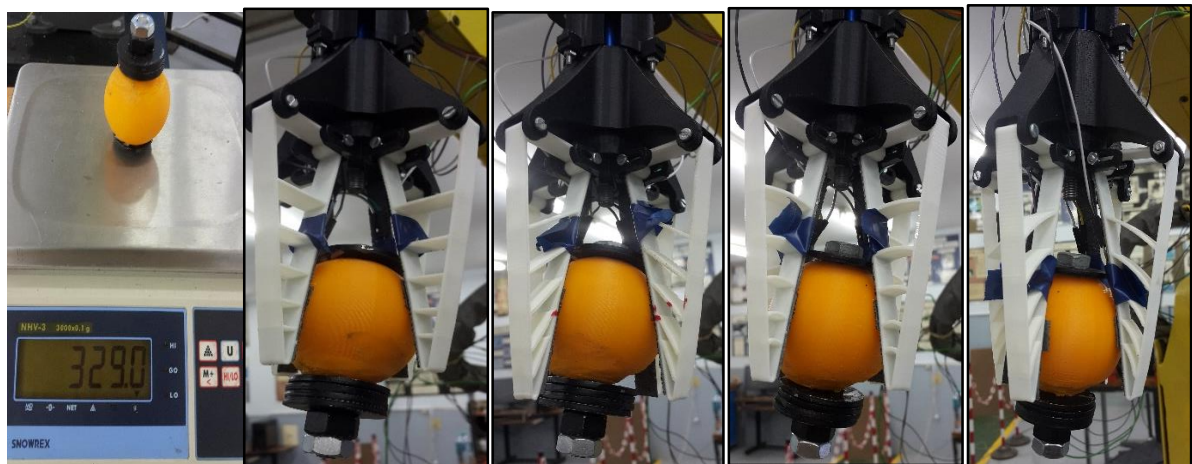


Figure 118: Dynamic test for 4-finger gripper: Geometry 1, 2, 3 and 4.

9.9 Test Phase 3: Dynamic and Static Visual Testing Procedure for Miscellaneous Parts

Dynamic and static visual testing procedure for miscellaneous parts was set up to determine the holding strength of the gripper by means of holding different size and weighted components and driving the gripper into a predetermined motion. Effective holding was visually confirmed. The resulting output was relayed as “yes” for grip confirmation and “no” for grip denied.

AIM:

- The aim was to investigate the dynamic and static gripping behaviour of a 3- finger and 4-finger gripper system design for gripping different part mass and geometry.

OBJECTIVES:

- To determine successful gripping and failed gripping for different part components.

APPARATUS:

- Calibrated weight scale.
- Different parts with varying weights and geometries.
- Symmetric holding unit.
- Gripping system.

METHOD:

- Step 1: The specimen is gripped to maximum gripper torque.
- Step 2: Static grip is confirmed for successful grasping.
- Step 3: The robotic gripper follows a pick and place sweep motion.
- Step 4: Dynamic grip is confirmed for successful grasping
- Step 5: Results are logged as “yes” or “no”.
- Step 6: Experiment is repeated 5 times per testing configuration.
-

PREDICTION:

- All part geometries should be successfully handled.

9.9.1 Test Specimen Weights

The specimens were weighed to determine their mass for the gripping procedure. The specimens are shown in Figure 119. The specimen shapes consisted of a spherical mass, a cube mass, a triangular prism, a power screw and a crazy cube tester. The specimens represented the different part families utilized in assembly. The specimens were gripped and deployed through a dynamic path plan. The maximum gripped weight was in the range of 320 g.



Figure 119: Test specimen weights

9.9.2 3-Finger Dynamic and Static Visual Testing Procedure

The dynamic experiment for the 3-finger gripper system followed the same dynamic movement described in Section 9.1. The gripped specimens are shown for a spherical mass, a cube mass, a triangular prism, a power screw and a crazy cube for Geometry 1, 2, 3 and 4 shown in Figure 120, Figure 121, Figure 122 and Figure 123 accordingly. The dynamic test and summarized results for the 3-finger gripper was discussed in Section 10.2.4.

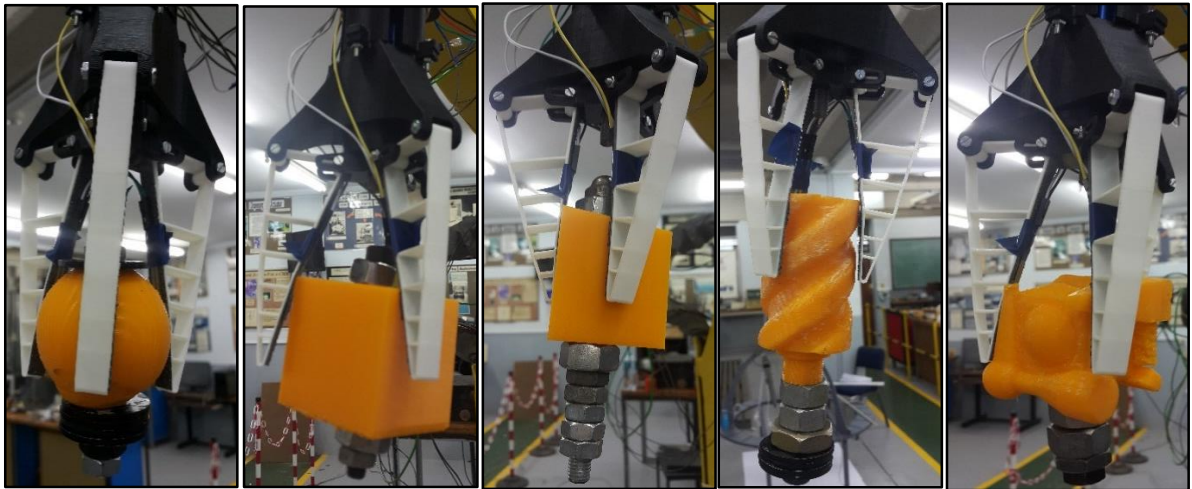


Figure 120: Visual dynamic and static testing of the 3-finger gripper for Geometry 1.

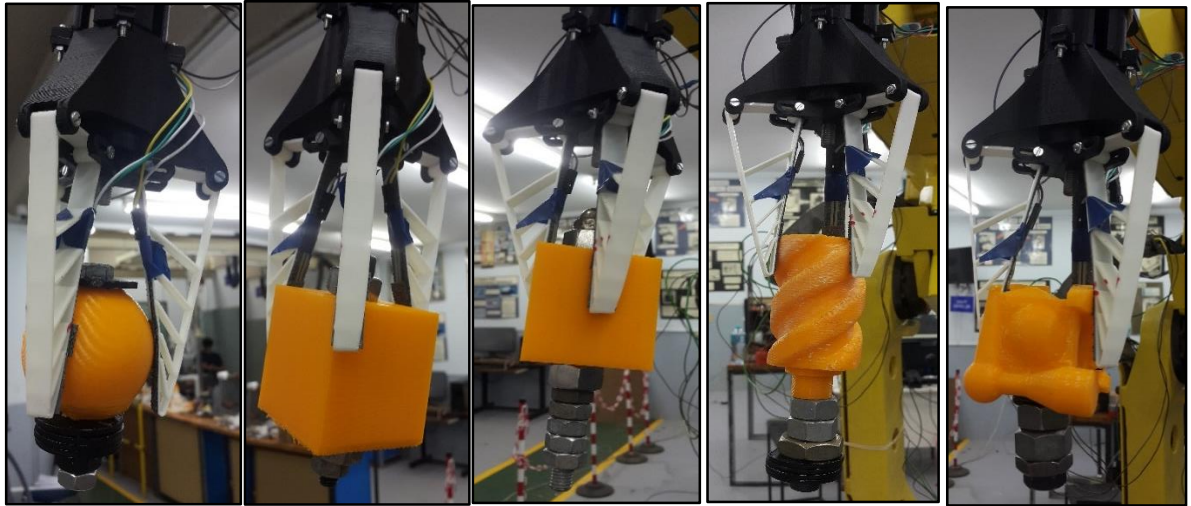


Figure 121: Visual dynamic and static testing of the 3-finger gripper for Geometry 2.



Figure 122: Visual dynamic and static testing of the 3-finger gripper for Geometry 3.



Figure 123: Visual dynamic and static testing of the 3-finger gripper for Geometry 4.

9.9.3

4-Finger Dynamic and Static Visual Testing Procedure

The dynamic experiment for the 4-finger gripper system followed the same dynamic movement described in Section 9.1. The gripped specimens are shown for a spherical mass, a cube mass, a triangular prism, a power screw and a crazy cube for Geometry 1, 2, 3 and 4 shown in Figure 124, Figure 125, Figure 126 and Figure 127 accordingly. The dynamic test and summarized results for the 4-finger gripper was discussed in Section 10.2.4.

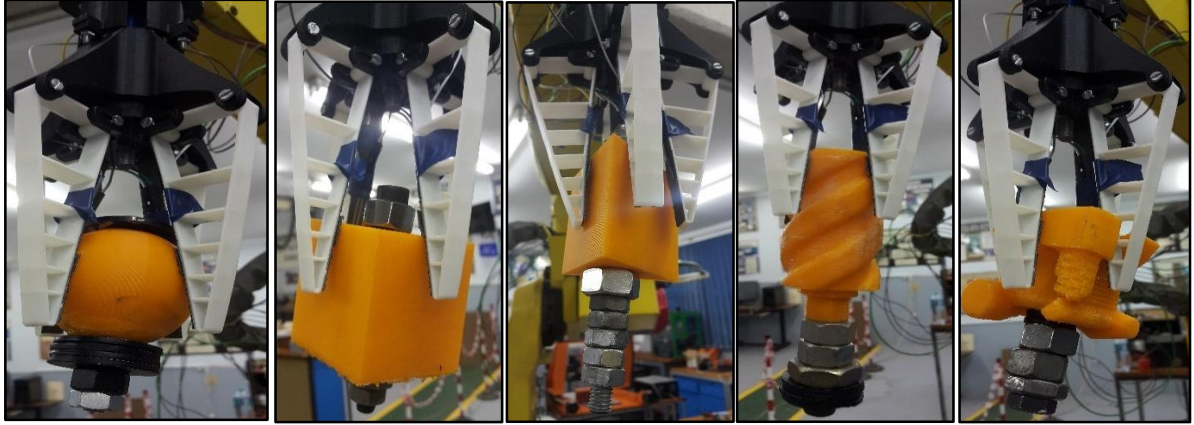


Figure 124: Visual dynamic and static testing of the 4-finger gripper for Geometry 1.



Figure 125: Visual dynamic and static testing of the 3-finger gripper for Geometry 2.

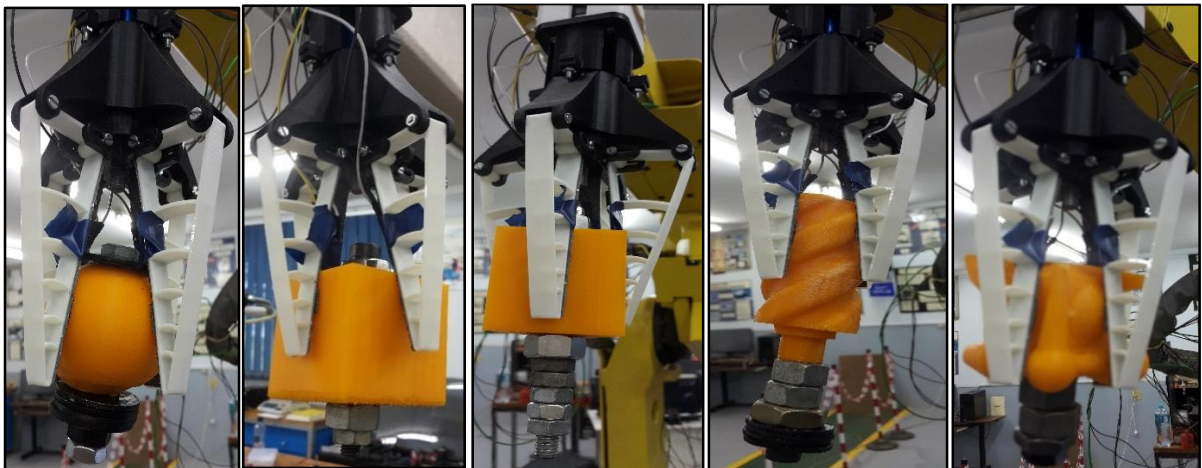


Figure 126: Visual dynamic and static testing of the 3-finger gripper for Geometry 3.

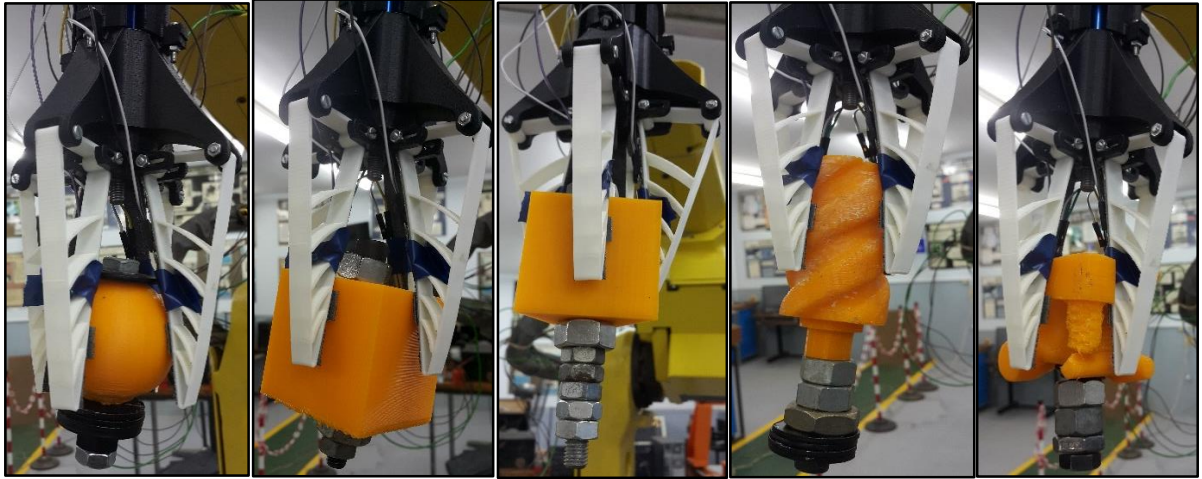


Figure 127: Visual dynamic and static testing of the 3-finger gripper for Geometry 4

9.10 Conclusion

The experimental procedure followed safety measures described by the FANUC robotics operation manual. Post-calibration was done on the sensors according to the FSR sensor manual. The force-time graphs generated were interpreted according to grip performance. The robotic arm was programmed according to the path plan described for testing.

The experimental results were attained for phase 1 and showed evidence of repeatability performance for the appendage geometries and gripper configuration. The 4-finger gripper system performs the best in the static holding mass test integrated with Geometry 4. Similar performance results were seen in dynamic testing where the 4-finger gripper system with appendage Geometry 4 outperformed the other configurations. The final testing phase showed gripping conformity adaption for all configurations in grasping components of different sizes and shapes that present various part families in assembly procedures. The detailed results are discussed in Chapter 10.

10 Results and Discussion

10.1 Introduction

This chapter discusses the significance of the project investigation and findings concerning flexibility of gripper systems in reconfigurable assembly systems. The literature provides insight on possible gripping systems applicable in object manipulation and geometric conformity. The design generates a compatible gripper system for incorporation in pick and place operational procedures. The system is analysed and examined through simulation and testing according to performance for gripping systems in industrial application. Results are generated through static and dynamic testing to confirm flexible criteria for the biologically inspired gripper system.

10.2 Result Discussion

10.2.1 Appendage Conformity FEA Simulation

The deflection and Von Mises stress values for linear statics are shown in Table 20 for ABS plastic and in Table 21 for Nylon. The deflection and Von Mises stress values for non-linear statics are shown in Table 22Table 20 for ABS plastic and in Table 23 for Nylon. The tables show the percentage of the increased values from the reference values from Geometry 1, which were obtained from the simulation. The exaggerated deflection shapes of the Geometry 1, 2, 3 and 4 are illustrated in Figure 128.

Table 20: Tabulated results for ABS plastic for linear statics

Geometry	Deflection	Stress	Deflection $\Delta\%$	Stress $\Delta\%$
1	2.027 mm	14.90 MPa	Reference	Reference
2	2.317 mm	19.27 MPa	14.3	29.3
3	2.052 mm	15.28 MPa	1.2	2.6
4	2.248 mm	19.68 MPa	10.9	32.1

Table 21: Tabulated results for Nylon for linear statics

Geometry	Deflection	Stress	Deflection $\Delta\%$	Stress $\Delta\%$
1	1.013 mm	14.90 MPa	Reference	Reference
2	1.159 mm	19.27 MPa	14.4	29.3
3	1.026 mm	15.28 MPa	1.3	2.6
4	1.124 mm	19.68 MPa	11.0	32.1

Table 22: Tabulated results for ABS plastic for non-linear statics

Geometry	Deflection	Stress	Deflection $\Delta\%$	Stress $\Delta\%$
1	2.056 mm	15.34 MPa	Reference	Reference
2	2.351 mm	19.53 MPa	14.3	27.3
3	2.081 mm	15.60 MPa	1.2	1.7
4	2.280 mm	19.84 MPa	10.9	29.3

Table 23: Tabulated results for Nylon for non-linear statics

Geometry	Deflection	Stress	Deflection $\Delta\%$	Stress $\Delta\%$
1	1.028 mm	15.34 MPa	Reference	Reference
2	1.175 mm	19.53 MPa	14.3	27.3
3	1.041 mm	15.60 MPa	1.3	1.7
4	1.140 mm	19.84 MPa	10.9	29.3

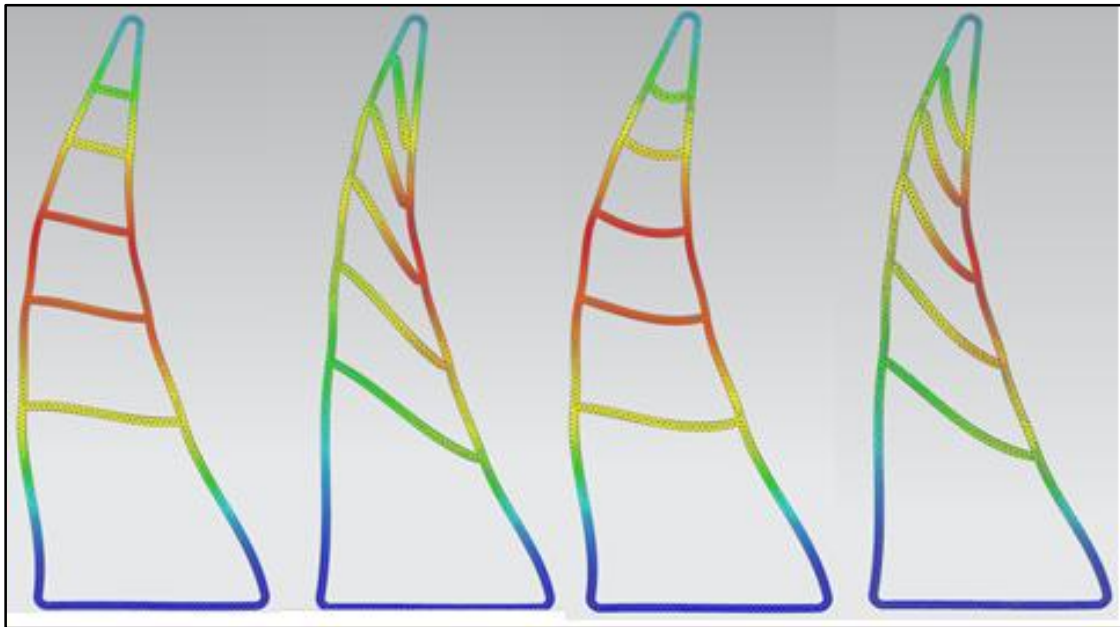


Figure 128: Deflection of shape of Geometry 1,2,3 and 4

10.2.2 Test Phase 1: Static Holding Mass Test Procedure Results

The repeatability demonstrated the ability of the gripper to hold a perfect grasp. The average mass was calculated for all 15 repetitions. Table 24 shows the summarized results for the 3-finger holding mass test. Table 25 shows the summarized results for the 4-finger holding mass test. The variation in repeatability was a result of the gripper not being able to grasp the maximum sample mass throughout all repetitions. The repeatability the was smaller than a 100 % is due to the following factors: surface characteristics changes, variation in grip force, slippage, static coefficient irregularities, eccentric grip factors, etc. The ideal grip repeatability was proven to be 98 % through benchmark specifications, however, an appropriate magnitude for a real result was 90 %. Refer to APPENDIX D.1 and APPENDIX D.2 for complete testing results for holding mass experiment.

Table 24: Summarized results for repeatability and average mass hold of 3-finger gripper

Geometry	Average Mass	Repeatability
1	2177.05 g	89.2 %
2	2297.99 g	93.7 %
3	2338.34 g	92.4 %
4	2418.87 g	97.3 %

Table 25: Summarized results for repeatability and average mass hold of 4-finger gripper

Geometry	Average Mass	Repeatability
1	2344.80 g	93.4 %
2	2418.89 g	96.9 %
3	2398.64 g	95.9 %
4	2459.15 g	98.6 %

10.2.3 Test Phase 2: Dynamic Holding Force Test Results

The results are tabulated in terms of estimated force (g) for each geometry for the 3-finger gripper system in Table 26. The results showed that the total normal force gripped by Geometry 1 was 1660 g, Geometry 2 was 1607 g, Geometry 3 was 1686 g and Geometry 4 was 1257 g. The summarised result showed that Geometry 4 has the best performance.

Table 26: 3-Finger dynamic grip performance.

Configuration	Voltage value (mV)				Estimated force value (g)			
	Sensor1	Sensor2	Sensor3	Sensor4	Sensor1	Sensor2	Sensor3	Sensor4
Geometry 1	3373	3952	3892	0	550	1145	1069	0
Geometry 2	3890	3458	3876	0	1068	581	1051	0
Geometry 3	3860	3971	3515	0	1062	1163	602	0
Geometry 4	3243	3847	3374	0	502	1013	551	0

The signal shows a stable grip and a slight increase in signal. The slight increase in converted force signal proved that self-conformity takes place throughout a dynamic movement. The 5 experiment runs in terms voltage versus time signals are shown in APPENDIX D.12 – D.15. The voltage versus time graphs for Geometry 1, 2, 3 and 4 are shown in Figure 129, Figure 130, Figure 131 and Figure 132 accordingly. The results generated from the dynamic test for each geometric configuration showed self-conformity with regards to the Fin Ray Effect®. The voltage versus time graph for a dynamic simulation shows estimated grasping properties due to the sensor error as previously described. Therefore, an estimated force value was determined for the gripper performance in dynamic motion.

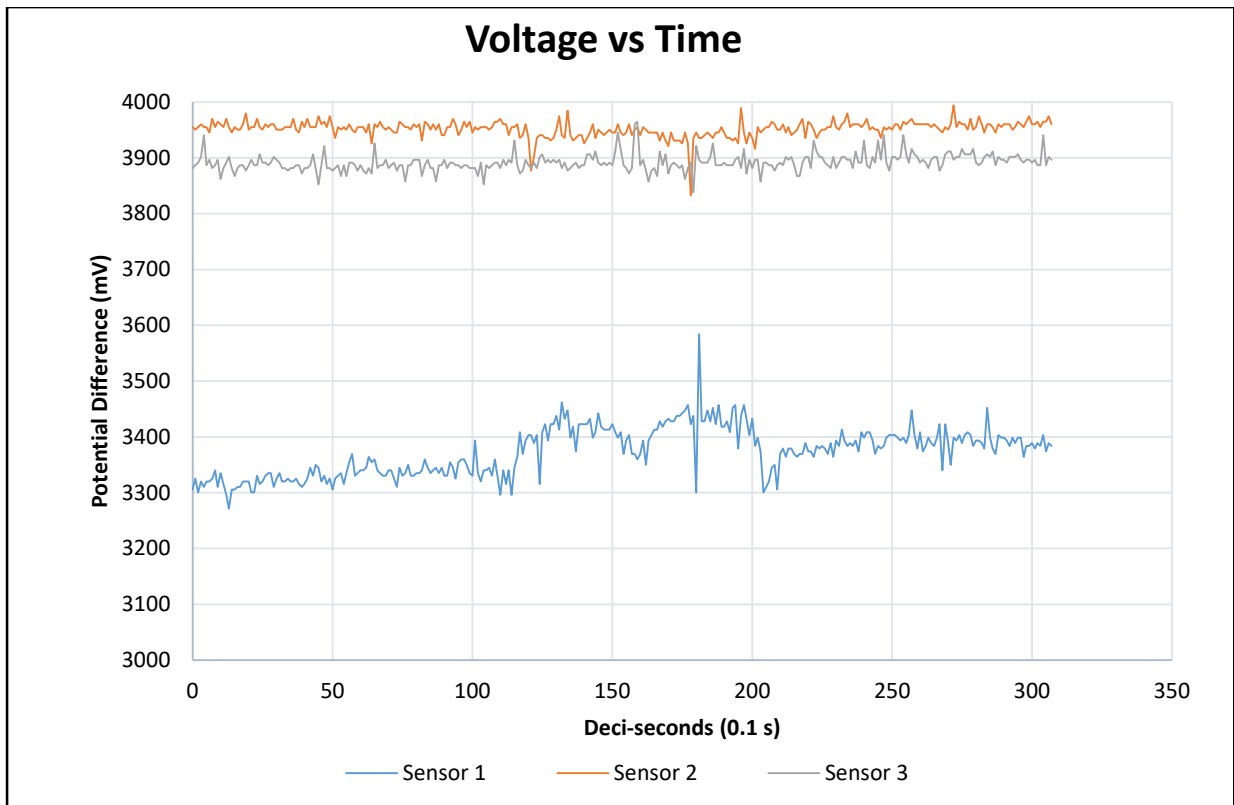


Figure 129: Voltage verse time graph for 3-finger gripper: Geometry 1.

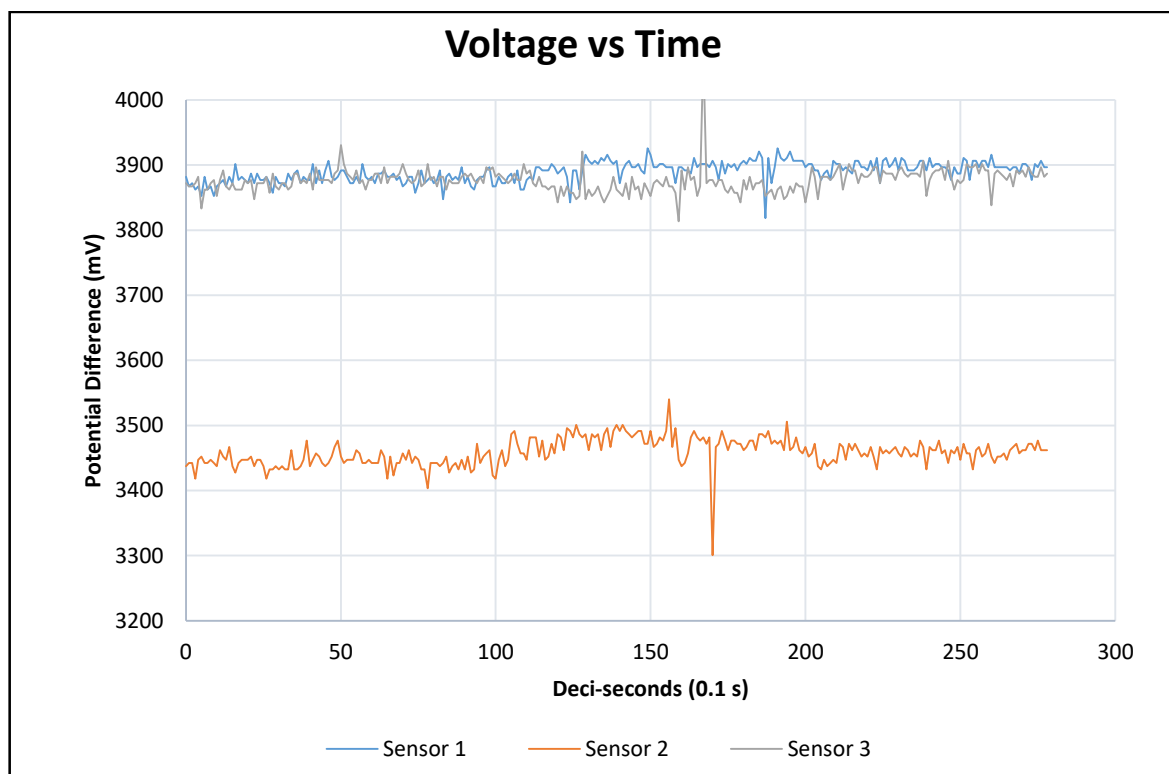


Figure 130: Voltage verse time graph for 3-finger gripper: Geometry 2.

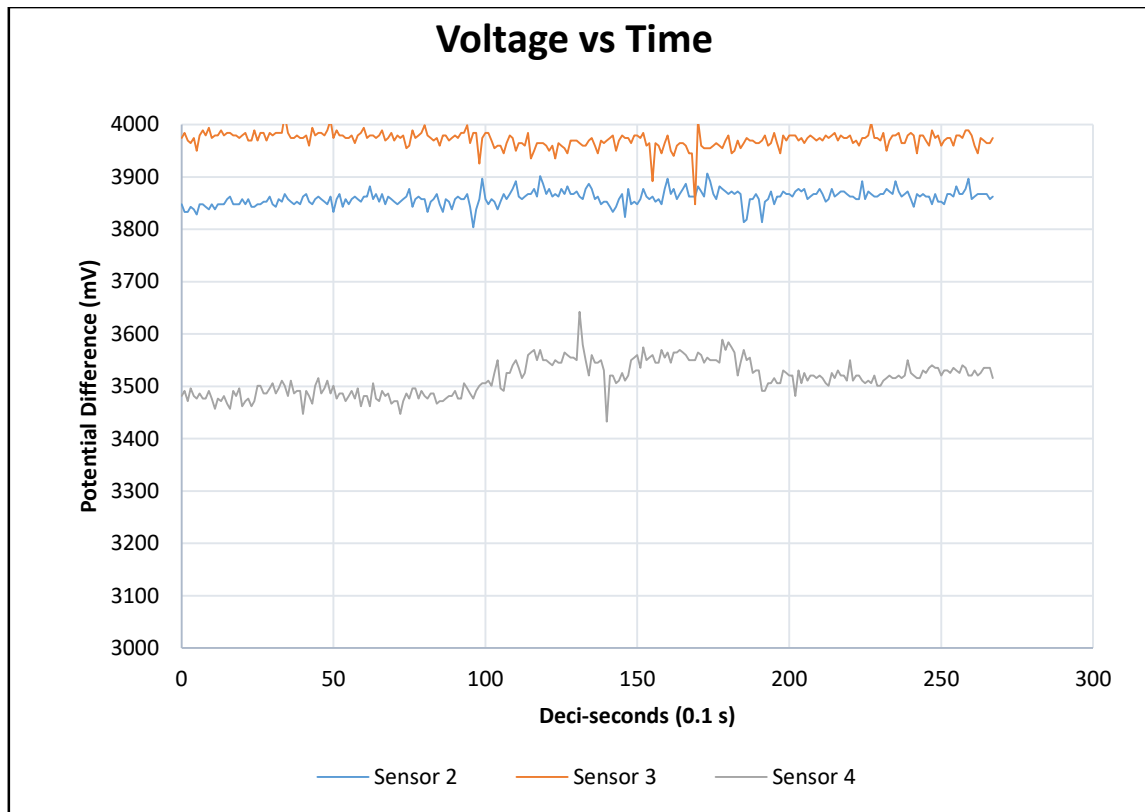


Figure 131: Voltage verse time graph for 3-finger gripper: Geometry 3.

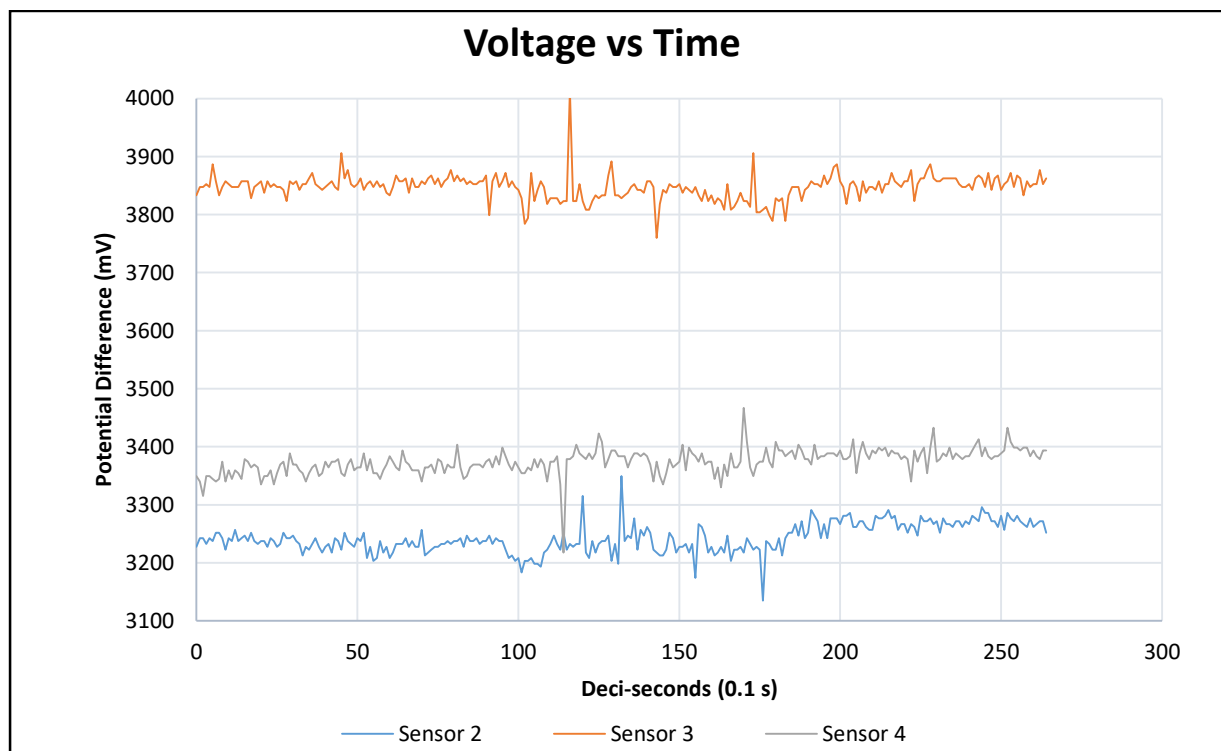


Figure 132: Voltage verse time graph for 3-finger gripper: Geometry 4.

The results are tabulated in terms of estimated force (g) for each geometry for 4-finger gripper system in Table 27. The results showed that the total normal force gripped by Geometry 1 was 1504 g, Geometry 2 was 1420 g, Geometry 3 was 1479 g and Geometry 4 was 1146 g. The summarised result showed that Geometry 4 has the best performance.

Table 27: 4-Finger dynamic grip performance.

Configuration	Voltage value (mV)				Estimated force value (g)			
	Sensor1	Sensor2	Sensor3	Sensor4	Sensor1	Sensor2	Sensor3	Sensor4
Geometry 1	3625	3940	3060	3251	750	1127	424	500
Geometry 2	3340	3801	3564	3430	536	971	677	572
Geometry 3	3397	3816	3641	3440	558	977	767	578
Geometry 4	3441	3604	3530	2565	576	717	636	250

The voltage output signal was converted into a force output signal according to the calibration curves in Section 9.3. The signal shows a stable grip and a slight increase in signal. The slight increase in converted force signal proved that self-conformity takes place throughout a dynamic movement. The 5 experiment runs in terms voltage versus time signals are shown in APPENDIX D.12 – D.15. The voltage versus time graphs for Geometry 1, 2, 3 and 4 are shown in Figure 133, Figure 134, Figure 135 and Figure 136 respectively.

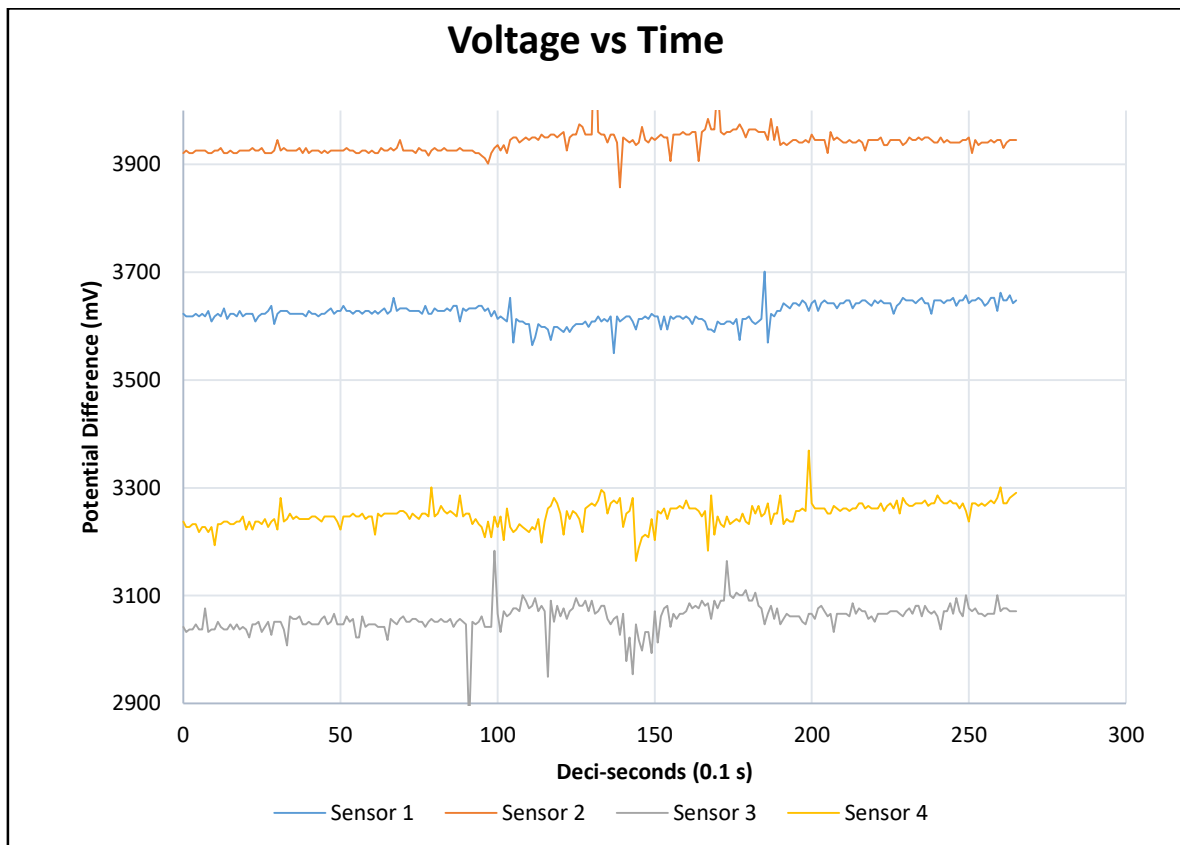


Figure 133: Voltage verse time graph for 4-finger gripper: Geometry 1.

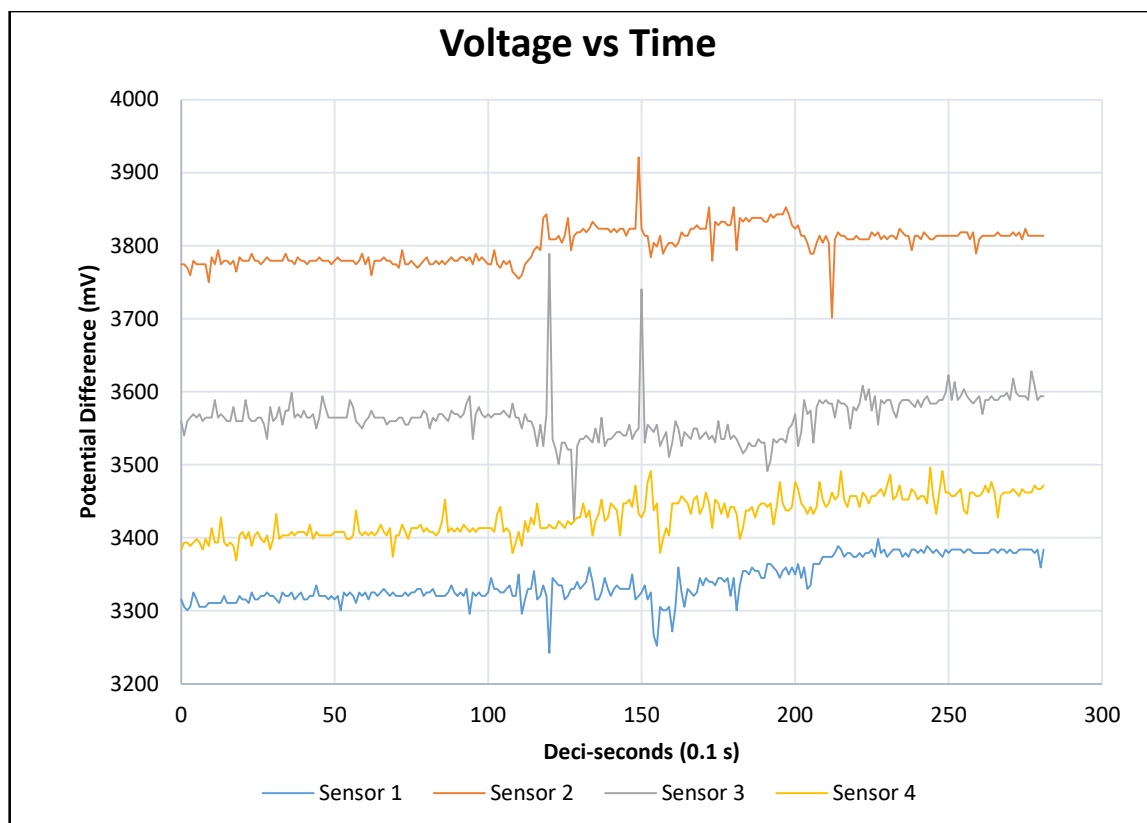


Figure 134: Voltage verse time graph for 4-finger gripper: Geometry 2.

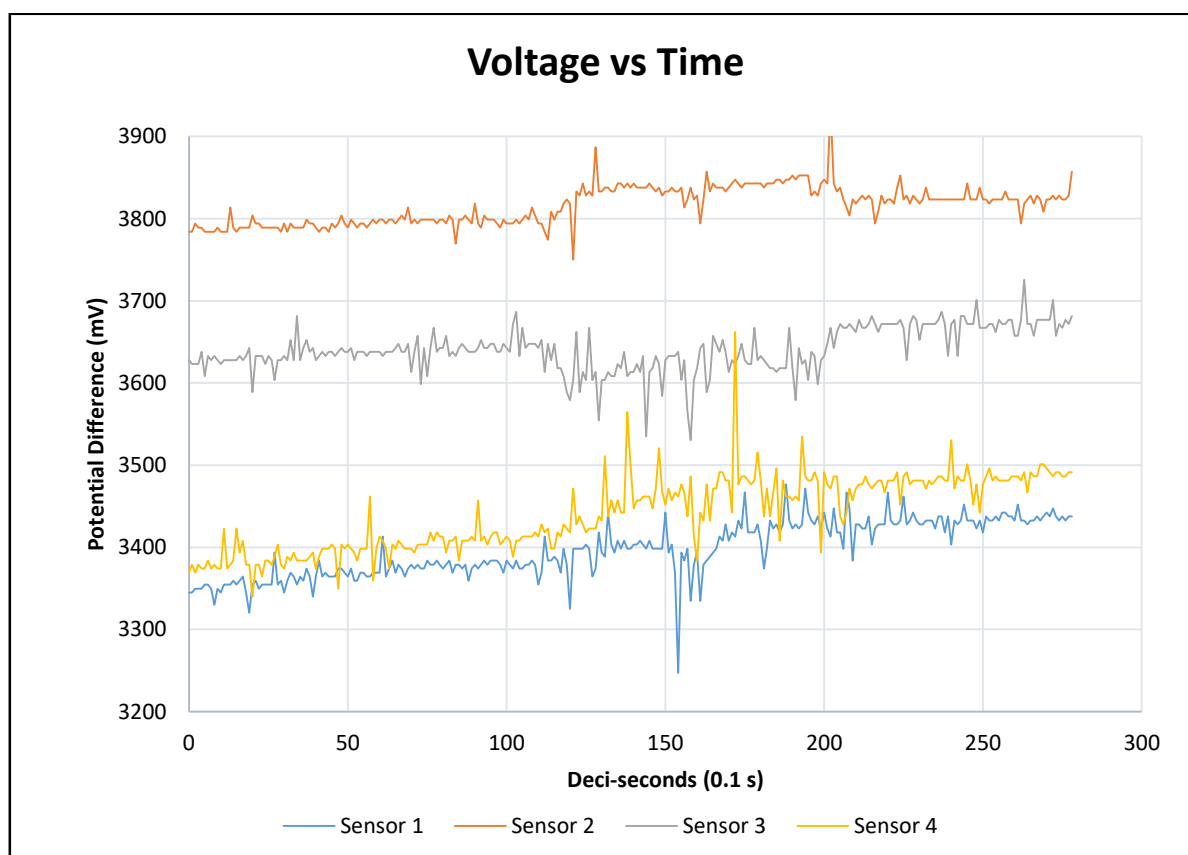


Figure 135: Voltage verse time graph for 4-finger gripper: Geometry 3.

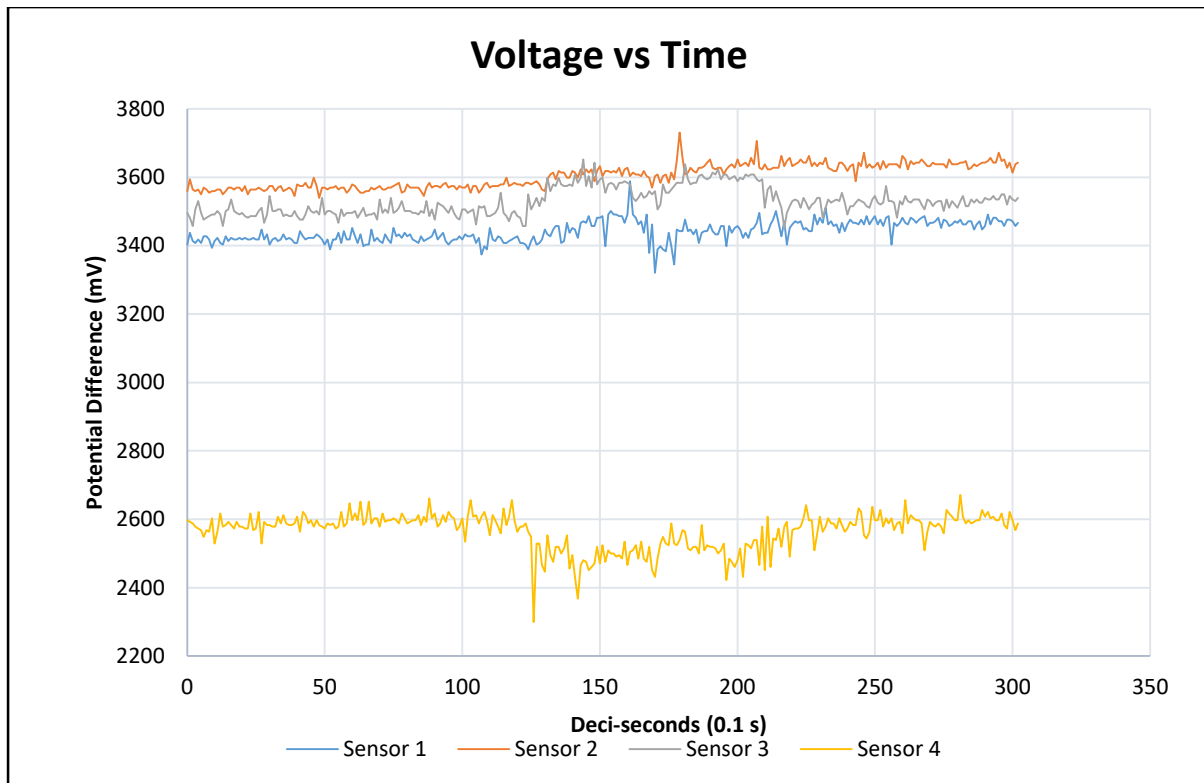


Figure 136: Voltage verse time graph for 4-finger gripper: Geometry 4.

10.2.4 Test Phase 3: Dynamic and Static Visual Test Results

The results showed that the 4-finger gripper system performed better by a fraction due to higher gripping surfaces. The results for dynamic and static visual testing for the 3-finger and 4-finger gripper system are shown in Table 28 and Table 29 for all specimen loading. The experiment was repeated 5 times and results were expressed as successful grips or failed grips per experimental run. Isolated grip failure occurred when gripping four (4) sided objects with a 3-finger grip. Grip stability was compromised when gripping surfaces were in contact with edges.

Table 28: Visual dynamic and static testing results of the 3-finger gripper for Geometry 1, 2, 3 and 4.

3-Finger Gripper										
	Spherical		Cube		Triangle prism		Extrusion screw		Crazy Cube	
	Static and dynamic		Static and dynamic		Static and dynamic		Static and dynamic		Static and dynamic	
	Success	Fail	Success	Fail	Success	Fail	Success	Fail	Success	Fail
Geometry 1	5	0	5	0	5	0	5	0	5	0
Geometry 2	5	0	5	0	5	0	5	0	5	0
Geometry 3	5	0	4	1	5	0	5	0	4	1
Geometry 4	5	0	5	0	5	0	5	0	5	0

Table 29: Visual dynamic and static testing results of the 4-finger gripper for Geometry 1, 2, 3 and 4.

4-Finger Gripper										
	Spherical		Cube		Triangle prism		Extrusion screw		Crazy Cube	
	Static and dynamic		Static and dynamic		Static and dynamic		Static and dynamic		Static and dynamic	
	Success	Fail	Success	Fail	Success	Fail	Success	Fail	Success	Fail
Geometry 1	5	0	5	0	5	0	5	0	5	0
Geometry 2	5	0	5	0	5	0	5	0	5	0
Geometry 3	5	0	5	0	5	0	5	0	5	0
Geometry 4	5	0	5	0	5	0	5	0	5	0

10.2.5 Summary of Gripper Test Performance

The 3-finger and 4-finger gripper system were evaluated, tested and compared to each other. The results for performance output of the gripper is shown in Table 30 and Table 31 for the 3-finger gripper system and the 4-finger gripper system, respectively. The testing was carried out across a mass load test to determine the repeatability for loading of different masses. Dynamic testing was performed on the selected specimen to determine the dynamic gripping force required. The testing was carried out to determine the applicability of varying object geometry handling. The 4-finger gripper performed marginally better than the 3-finger gripper due having more gripping surfaces. The testing proved that Geometry 2 and Geometry 4 were potential rib structure for static loading. Geometry 4 was proven to be the superior configuration for dynamic loading.

Table 30: 3-Finger gripper performance

Configuration	Repeatability	Max static loading (g)	Dynamic loading (g)	Estimated grip force required (g)
Geometry 1	89.2 %	2177.05	320	1660
Geometry 2	93.7 %	2297.99	320	1607
Geometry 3	92.4 %	2338.34	320	1687
Geometry 4	97.3 %	2418.87	320	1257

Table 31: 4-Finger gripper performance

Configuration	Repeatability	Max static loading (g)	Dynamic loading (g)	Estimated grip force required (g)
Geometry 1	93.4 %	2344.80	320	1504
Geometry 2	96.9 %	2418.89	320	1420
Geometry 3	95.9 %	2398.64	320	1479
Geometry 4	98.6 %	2459.15	320	1146

10.3 Industrial Application of Research

Flexible grippers used in pick and place procedures have the potential to increase production rates. The gripper possesses self-conformity without requiring a transition between applicable grippers for specific tasks operations. The procedure time is reduced in terms of software and hardware changes for various end-effectors. Flexibility increased the handling of non-uniform production items, referring to a variety of part families and mixed assembly procedures. The flexible gripper system has the potential of handling various shapes, geometries and masses. In summary, the flexible gripper system grasps a variety of dissimilar items in assembly procedures.

The integration with any robotic arm system is simple. The housing components are printed in a matter of hours and require minimal adaption of mounting components. The flexible gripper holds the ability to function adequately with the instalment onto industrial robotic arms. The flexible fixtures have the capability to be mounted onto a wide range of robotic manipulators for effective gripping.

10.4 Scientific Contribution

Robotic manipulators are required to hold and grip objects appropriately for prerequisite tasks. The research and development of the gripper studied the characteristics of shape conformity. The design process demonstrated a gripping model of possible techniques of improving object handling throughout assembly processes, by reducing slippage and increasing effective gripping. The study established optimization on self-adjustment of grippers.

Previous research has proven that biological influences into robotic manipulation processes have proven to be valuable. The concept design of a robotic gripper in the design process was based on the natural phenomenon of self-adjustment in the fins of fish. The displacement response from applied force to the mechanism was investigated. The results proved that using the biologically based technique can improve the self-adjustment properties in geometric conformity in gripping procedures.

A stress study of the appendages showed conformity properties and gripping behaviour of the self-adjustable gripper. The technique, specifically the Fin-Ray Effect[®], was analysed in terms of deformation and force application properties while grasping an object in a pick-up and place process. The holding properties were investigated through static and dynamic testing, simulating stationary and motion actions of the robotic manipulator to be used in a procedure.

The fluctuating forces were thoroughly studied within a movement to develop a theoretical model to understand the required retention forces. The required force retention should ideally be symmetrical along the three-dimensional surface of the object to enclose a stable grip. The forces involved in the procedure was evaluated according to a time period in relation to a dynamic procedure and results were interpreted according to maximum forces experienced by object throughout a movement phase.

In summary, the scientific knowledge contributed in the dissertation, was to investigate the characteristics of intelligent gripping systems based on biological processes. Subsequently promoting research in developing intelligent grasping mechanisms for robotic processes. The impact of the study was to create a concept whereby a complicated high degree of freedom gripping mechanism, including numerous moving components, could be simplified for ease of manufacturing and application.

10.5 Conclusion

The flexible gripper system developed was verified through testing to be a potential addition to reconfigurable assembly systems. Testing provided performance criteria concerning fixture adaptability and part sensitivity in assembly procedures. The gripper was discussed with regards to industrial application and was proved to be potentially implemented in manufacturing systems. The project provided a scientific contribution to understanding biologically inspired mechanisms, namely the Fish Ray Effect[®], in terms of self-adjustment properties for object handling.

11 Conclusion and Recommendations

11.1 Conclusion

The project researched a gripper that incorporated the Fin Ray[®] effect. The conceptual design was integrated with a sensor feedback loop to provide a gripping system. The construct was evaluated according to four geometric considerations for the gripper appendage. The conceptual design discussed the gripper system utilizing a force feedback control system. Consequently, the forces taking part in the gripping mechanism was described by the Lagrangian Dynamic Model.

Siemens NX[®] incorporated an FEA, predicted the conformity of the Fin Ray-based gripper. The displacement obtained from the FEA depicts the degree of deflection. Geometry 1 was set as a baseline design for result comparison. The force applied to the surface of the gripper attachment resembles the grasping action of the gripper around an object. The results from the simulation indicated that Geometry 2 attained the largest deflection of 14.3% increased displacement as compared to Geometry 1. However, Geometry 2 experienced a 29.33% increase in Von Mises stress. The simulation demonstrated a directly proportional relationship between high Von Mises stress points and deflection of the geometric designs. The phenomenon could be explained by the Fin Ray[®] effect.

The conformity around an object being manipulated was influenced by the changing rib structures of the appendages. Experimental testing validated the results in the static mass load test as compared with the simulation. Geometry 2 and Geometry 4 handled a greater average mass and repeatability as with regards to Geometry 1. Object conformity could be manipulated through rib orientation in the gripper geometric design. The design changes reduced slippage of the object while grasping as proven by higher deflection. The improvement in design could potentially be integrated into a functional gripper system.

The conformity was tested through dynamic force experiments. The data readings from the sensors on the dynamic test demonstrated that Geometry 4 experienced less force due to grasping. The object was gripped with a higher geometric conformity. The gripper system was tested by gripping different part geometries and weight ranges between 160 g and 330 g. The specimens presented the range of part families used in assembly. The 4-finger gripper performed marginally better than the 3-finger gripper. Nevertheless, the testing concluded that both the 3-finger and 4-finger gripper systems were proven to be potential flexible systems for RAS.

The project requirements were produced for adaptable, flexible and sensitive properties to increase the performance of a gripper system. The research required an overview of potential gripping criteria for integrated flexible end-effectors in reconfigurable assembly systems. The postulated research question was: Is it possible for flexible fixtures to incorporate self-adjustment characteristics with regards to flexible, adaptable and sensitive clamping related to reconfigurable assembly systems? The final solution proved to incorporate self-adjustment characteristics through gripping of various objects in

dynamic operational environments. The gripper system developed was tested and effectively grasped objects representing various part families. The grasping mechanism was incorporated into an industrial robotic arm and was evaluated in operational procedure representing a pick and place process. The system represented an assembly process in a reconfigurable manufacturing system.

The research question was satisfied by meeting the objectives set out for the project. Objective 1 was reached through research in terms of flexible fixtures to attain performance criteria for conformity, object handling, maximum gripper loading and flexibility. The literature review generated suitable solutions. The possible solutions were compared through a selection matrix and the Fin Ray Effect® in terms of a 3-finger and 4-finger gripper was selected. Requirements for the specific development of reconfigurable fixture was generated for the selected system. The gripper system was required to consist of an input, process and output elements. The design was required to consist of subsystems consisting of the following: a mechanical skeletal structure, a sensory system, actuation, a robotic arm and a control system. The control system was required to possess force feedback characteristics to determine dynamic force properties.

Objective 2 was attained through literature by determining performance criteria to be tested and evaluated with regards to repeatability, maximum static loading, dynamic grip force, material sensitivity and geometric conformity. Objective 3 and objective 6 were achieved by developing, designing and manufacturing a gripping system that followed industrial ISO standards described in the conceptual design. The final detail design described the output gripper system to be manufactured. The gripper system was manufactured, assembled and prepared for testing in an operational environment.

The concept design developed 4 geometric considerations for the gripper appendages from traditional ray mechanism. Objective 5 was accomplished by means of simulation through a finite element method software package. The stress proved geometric conformity properties in all the geometric constructs. Geometry 2 and Geometry 4 possessed the most effective in deflection with regards to object conformity.

The performance was tested through experimental procedures to achieve objective 4 and objective 7. Testing was done on the gripper to determine empirical data in terms of the static holding load, dynamic holding load and force control properties. The testing proved that the gripper held slight self-conformity through dynamic movement. The system efficiency was validated through overall system performance of the system and discussed the results of the experimental testing. Objective 8 was achieved through validating gripping proficiency in testing and multiple runs were done to attain accuracy.

11.2 Recommendations

The recommendations describe the part assemblies and methods that have the possibility to improve the efficiency of the project. The results from the project show conclusive evidence of design and testing results for conformity. Improvements are available to enhance design and performance criteria.

The motor selected performed well in testing in accordance with the design and experimentation. Although, a motor with higher torque output would be necessary for loading and manipulating of heavier objects. Higher torques loads may also increase holding forces and loading control. Motors that comprise of higher holding torques are necessary in case of power failure so that the object would still be gripped. Stepper motors are an appropriate actuation method for gripping.

The motion transmission was performed by means of rotation movement to translation displacement in the form of threaded bars. Threaded bars have the disadvantage of small tooth heights, which reduces allowable stress on helical teeth applied by the motor. The small pitch of the helical teeth reduces the maximum speed of gripping motion. Preferable motor transmission would be lead screws and ACME profiles and have the advantages of high translational speeds and high strength.

The original force feedback loop required a human interface to determine the force required by visual inspection. A closed force feedback loop would require the motor to be controlled by means of sensory data feedback. The force input would require a maximum limit to reduce the surface damage of the object and a minimum limit to overcome the friction force needed.

References

- [1] F. S. D. Dymond, "Conceptual Design of Fixtureless Reconfigurable Automated Assembly System," Stellenbosch University, Stellenbosch, 2009.
- [2] T. Savu and A. Vlase, "Next-generation Manufacturing Project: A Framework for Academic Curricula and Research Strategy," University Politehnica of Bucharest, Bucharest, 2006.
- [3] M. Rundle, "Building Tesla: inside Elon Musk's car factory of the future," *Wired*, 12 January 2017. [Online]. Available: <http://www.wired.co.uk/article/tesla-factory-interview>. [Accessed 15 November 2017].
- [4] O. Grenier-Lafond, "Robotic Material Handling Case Study - Robotiq Adaptive Gripper," *RobotIQ*, 26 August 2014. [Online]. Available: <http://blog.robotiq.com/bid/72187/Robotic-Material-Handling-Case-Study-Robotiq-Adaptive-Gripper>. [Accessed 01 November 2016].
- [5] J. C. Trappey, "A literature survey of fixture design automation," *The international journal of advanced manufacturing technology*, vol. 5, no. 3, pp. 240-255, 1990.
- [6] J. L. Sancho-Bru, A. Perez-Gonzalez, M. C. Mora, E. B. Leon, M. Vergara, J. L. Iserte, P. J. Rodriguez-Cervantes and A. Morales, *Theoretical Biomechanics*, London: InTech, 2011.
- [7] J. Padayachee and G. Bright, "The Design of Reconfigurable Assembly Stations for High Variety and Mass Customisation Manufacturing," *South African Journal of Industrial Engineering*, vol. 24, no. 3, pp. 43-57, 2013.
- [8] Robotiq, "Adaptive Gripper," Robotiq, Quebec City, 2016.
- [9] W. Crooks, G. Vukasin, M. O'Sullivan, W. Messner and C. Rogers, "Fin Ray Effect Inspired Soft Robotic Gripper: From the RoboSoft Grand Challenge Toward Optimization," *Frontiers in Robotics and AI*, vol. 3, no. 70, 2016.
- [10] K. C. Chan, B. Benhabib and M. Q. Dai, "A Reconfigurable Fixturing System for Robotic Assembly," *Journal of manufacturing systems*, vol. 9, no. 3, pp. 206-221, 1990.
- [11] M. Belanger-Barrette, "What does Flexibility in Automated Manufacturing Means?," *RobotIQ*, Saint-Nicolas, 2014.
- [12] Z. M. Bi, L. Wang and S. Y. T. Lang, "Current Status of Reconfigurable Assembly Systems," *International Journal of Manufacturing Research*, vol. 2, no. 3, pp. 303-328, 2007.
- [13] R. Bostelman and J. Falco, "Survey of Industrial Manipulation Technologies for Autonomous Assembly Applications," National Institute of Standards and Technology, Gaithersburg, Maryland, 2012.
- [14] Schunk, "SCHUNK Grippers: Product Overview," Schunk, Lauffen am Neckar, 2015.

-
- [15] A. Naidoo, R. B. Pillay and T. Ramnath, "Reconfigureable Robotic Assembly Station," University of KwaZulu-Natal, Durban, 2011.
 - [16] N. Kärcher, M. M. Moerdijk and S. Schrof, "FlexShapeGripper," FESTO AG & Co. KG, Esslingen, 2015.
 - [17] Goudsmit Magnetic Systems, "Magnet Grippers," Goudsmit, Waalre, 2014.
 - [18] R. S. Wadhwa, T. Lien and M. Monkman, "Study on the Holding Characteristics of a Magnetic Gripper," in *COMSOL*, Boston, 2011.
 - [19] Empire Robotics, "Versball Gripper: Research Kit Model CV2-1 - Product Manual," Empire Robotics, Boston, 2015.
 - [20] J. R. Amend, E. Brown, N. Rodenberg, H. M. Jaeger and H. Lipson, "A Positive Pressure Universal Gripper Based on the Jamming of Granular Material," *IEEE Transactions on Robotics*, vol. 28, no. 2, pp. 341-350, 2012.
 - [21] Y. Jiang, J. R. Amend, H. Lipson and A. Saxena, "Learning Hardware Agnostic Grasps for a Universal Jamming Gripper," in *IEEE*, New York, 2012.
 - [22] R. E. Preis, "MATRIX Clamping Systems," Matrix-Innovations, 2014/2015. [Online]. Available: <http://www.matrix-innovations.com>. [Accessed 01 May 2016].
 - [23] J. Keijia, "Design and Fabrication of Polymer Based Dry Adhesives Inspired by the Gecko Adhesive," Tulane University, New Orleans, 2013.
 - [24] nanoGriptech, "Gecko Inspired Adhesive," nanoGriptech, 2015. [Online]. Available: <http://nanogriptech.com/>. [Accessed 11 September 2016].
 - [25] M. P. Murphy, B. Aksak and M. Sitti, "Gecko Inspired Directional and Controllable Adhesion," Carnegie Mellon University, Pittsburgh, 2009.
 - [26] J. Yu, S. Chary, S. Das, J. Tamelier and N. S. Pesika, "Gecko-Inspired Dry Adhesive for Robotic Applications," WILEY, Weinheim, 2011.
 - [27] J. Shintake, S. Rosset, B. Schubert, D. Floreano and H. Shea, "Versatile Soft Grippers with Intrinsic Electro-adhesion Based on Multi-functional Polymer Actuators," *Advanced Materials*, vol. 28, no. 2, pp. 231-238, 2015.
 - [28] SRI International, "Electroadhesion for Industrial, Biomedical, Military and Consumer Applications," SRI International, Washington, 2010.
 - [29] J. A. Falco, J. A. Marvel and E. R. Messina, "Dexterous Manipulation for Manufacturing Applications Workshop," NIST, Gaithersburg, Maryland, 2013.
 - [30] V. Tincani, M. G. Catalano, E. Farnioli, M. Garabini, G. Grioli, G. Fantoni and A. Bicchi, "Velvet Fingers: A Dexterous Gripper with Active Surfaces," in *IEEE*, Vilamoura-Algarv, 2012.
 - [31] M. Horák and F. Novotný, "The Study of Mechanics of Deformation Behaviour of Service Robots Gripping Systems," in *ENGINEERING MECHANICS*, Svratka, 2012.
 - [32] J. Schmalz GmbH, "Vacuum Technology from Schmalz," Schmalz, 2008. [Online]. Available: <https://www.schmalz.com/en/>. [Accessed 30 September 2016].
 - [33] FESTO, "MultiChoiceGripper," FESTO, Esslingen, 2014.
 - [34] D. Lang, "A Study on Micro-gripping Technologies," Univeristy of Southern Denmark, Odense, 2008.

-
- [35] B. López-Walle, M. Gauthier and N. Chaillet, "Dynamic Modelling For a Submerged Freeze Micro-Gripper Using Thermal Networks," *Journal of Micromechanics and Microengineering*, vol. 20, no. 2, 2009.
- [36] A. M. El-Sayed, A. Abo-Ismael, M. T. El-Melegy, N. A. Hamzaid and N. A. Osman, "Development of a Micro-Gripper Using Piezoelectric Bimorphs," *Sensors*, vol. 13, no. 5, pp. 5826-5839, 2013.
- [37] S. Bouchard, "How to Choose the Right Robotic Gripper for Your Application," Robotiq, 25 May 2014. [Online]. Available: <http://blog.robotiq.com/bid/33127/How-To-Choose-The-Right-Robotic-Gripper-For-Your-Application>. [Accessed 13 September 2016].
- [38] L. Lipot, "Mechanical Systems," Multimedia Design and Technology Education, September 2016. [Online]. Available: http://www.notesandsketches.co.uk/Mechanical_systems.html. [Accessed 26 06 2017].
- [39] J. Prešeren, D. Avguštin and T. Mravlje, "Guidelines for the Design of Robotic Gripping Systems," University of Ljubljana, Ljubljana, 2005.
- [40] chiprobot, "TriMaxGripper & Linear Servo Actuator (GM)," Hackaday, 2017. [Online]. Available: <https://hackaday.io/project/1011-trimaxgripper-linear-servo-actuator-gm>. [Accessed 2017 January 15].
- [41] "Top 4 Reasons to Use 3D Printing Services," stratsys, 21 10 2015. [Online]. Available: <https://www.stratasysdirect.com/blog/four-reasons-to-use-3d-printing-services/>. [Accessed 24 06 2017].
- [42] M. Bélanger-Barrette, "Robotic End Effectors - Payload vs Grip Force," ROBOTIQ, 29 January 2014. [Online]. Available: <http://blog.robotiq.com/bid/69524/Robotic-End-Effectors-Payload-vs-Grip-Force>. [Accessed 13 October 2016].
- [43] Intelligent Actuator, "Selection Guide (Gripping Force)," Intelligent Actuator, Atlanta, 2016.
- [44] A. Joubair, "What are Accuracy and Repeatability in Industrial Robots?," ROBOTIQ, 7 October 2014. [Online]. Available: <http://blog.robotiq.com/bid/72766/What-are-Accuracy-and-Repeatability-in-Industrial-Robots>. [Accessed 13 October 2016].
- [45] S. Bouchard, "Robotic Gripper Repeatability Definition and Measurement," RobotIQ, Saint-Nicolas, 2014.
- [46] C. Yetim, "Kinematic Analysis for Robot Arm," Yildiz Technical University, Istanbul, 2009.
- [47] C. Yang, H. Ma and M. Fu, Robot Kinematics and Dynamics Modeling, Singapore: Springer publishing, 2016, pp. 27-48.
- [48] V. Tharayil, E. Babu, A. A. Cherussery and J. P. Joy, "Design, Fabrication and Analysis of Three Fingered Fin Gripper for KUKA KR[^]R900 Robot," *SSRG International Journal of Mechanical Engineering*, no. Special, pp. 42-44, 2017.
- [49] International Organization of Standards, "ISO 9283:1998 Manipulating industrial robots - Performance criteria and related test methods," ISO, Geneva, 1998.
- [50] Technical Committee ISO/TC 184, "International Standard ISO 14539," International Standard, Geneva, 2012.
- [51] F. Petruzella, Industrial Electronics, Singapore: Mc-Graw Hill, 1996.
- [52] M. Tyson, "Robotics 101," ABB Robotics, Zurich, 2013.
- [53] BCN3D, "BCN3D MOVEO: User Manual," CIM UPC, Barcelona, 2017.

-
- [54] FANUC Robotics, “M-10iA SERIES,” FANUC Robotics America, Lutho, 2008.
 - [55] D. Constantin, M. Lupoae, C. Baciuc and D.-I. Buliga, “Forward kinematics of an industrial robot,” Institute for Natural Sciences and Engineering, Vienna, 2015.
 - [56] K. Bouzgou and Z. Ahmed-Foitih, “Geometric Modeling and Singularity of 6 DOF Fanuc 200IC Robot,” in *Innovative Computing Technology (INTECH)*, Luton, 2014.
 - [57] C. Yang, H. Ma and M. Fu, *Advanced Technologies in Modern Robotic Applications*, Singapore: Springer, 2016.
 - [58] D. A. Wiley, “Velocity, acceleration and force,” Lumen, Brigham, 2017.
 - [59] Alexis67, “Adaptive Claw / Gripper,” Thingiverse, 6 March 2016. [Online]. Available: <https://www.thingiverse.com/thing:1395188>. [Accessed 2016 November 16].
 - [60] Chiprobot, “Tri_Max_Gripper (Conforming Robotic gripper),” Thingiverse, 01 December 23. [Online]. Available: <https://www.thingiverse.com/thing:193851>. [Accessed 2016 November 16].
 - [61] S. Brischetto, C. G. Ferro, P. Maggiore and R. Torre, “Compression tests of ABS specimens for UAV components produced via the FDM technique,” *Technologies*, vol. 5, no. 20, pp. 1-25, 2017.
 - [62] A. L. Saravanan, “Saravana Electronics,” alselectro, 2015.
 - [63] B. Earl, “What is a stepper motor?,” adafruit, New York, 2015.
 - [64] GlobalSpec, “DC Servomotors Information,” GlobalSpec, New York City, 2017.
 - [65] V. R. Chennu, “Screw Threads Terminology,” ME Mechanical, 2016.
 - [66] V. B. Bhandari, *Design of Machine Elements*, New Delhi: Tata McGraw-Hill, 2007.
 - [67] L. C. Shull, R. L. Hannah and S. E. Reed, *Basic Circuits*, Society for Experimental Methods, 1992.
 - [68] PCB Piezotronics, PCB Piezotronics MTS Systems Corporation, 2017. [Online]. Available: http://www.pcb.com/Resources/Technical-Information/Tech_Force. [Accessed 28 06 2017].
 - [69] Images SI, “Force Sensing Resistors,” IMAGES SCIENTIFIC INSTRUMENTS, 2007. [Online]. Available: <http://www.imagesco.com/sensors/force-sensors.html>. [Accessed 28 06 2017].
 - [70] NEMA, “NEMA 17 Stepper Motor,” NEMA, 7 November 2017. [Online]. Available: http://reprap.org/wiki/NEMA_17_Stepper_motor. [Accessed 15 November 2017].
 - [71] PapukGroup, “arduino mega 2560 eagle schematic,” Vesselyn, 2017.
 - [72] FANUC, “FANUC Robot ARC Mate 100iC: Mechanical Unit Operator's Manual,” FANUC, Oshino, 2008.
 - [73] VersaPoint Technology, “FSR Force Sensing Resistor Integration Guide and Evaluation Parts Catalog,” Interlink Electronics, Camarillo, 2015.
 - [74] R. S. Hall, G. T. Desmoulin and T. E. Milner, “A technique for conditioning and calibrating force-sensing resistors for repeatable and reliable measurement of compressive force,” *Journal of Biomechanics*, vol. 41, no. 16, pp. 3492-3495, 2008.
 - [75] L. L. Chan, M. F. Tracy, J. Guttormson and K. Savik, “Description of Peripheral Muscle Strength Measurement and Correlates of Muscle Weakness in Patients Receiving Prolonged Mechanical Ventilatory Support,” *Am J Crit Care*, vol. 24, no. 6, pp. e91-e98, 2016.

APPENDIX A: Selection Criteria

APPENDIX A.1: Flexible Gripping Technologies: Selection Matrix

	Effective Shape Conformity	Gripping Strength	Repeatability	Material Sensitivity and Limitation	Process Integration	Self-adjustment	<u>TOTAL</u>
FESTO'S FlexShapeGripper®	5	2	1	5	1	5	<u>19</u>
GOUDSMIT Magnetic Gripper®	1	3	5	1	5	1	<u>16</u>
Empire Robotics Versa ball®	5	2	1	5	1	5	<u>19</u>
MATRIX® Form Adapting Clamp System	3	5	3	5	5	4	<u>25</u>
Dry Adhesive Gripping	3	2	3	2	1	5	<u>16</u>
Electro-Adhesive Gripping	2	1	3	2	1	4	<u>13</u>
Velvet Fingers®	3	4	3	4	4	4	<u>22</u>
Robotiq® Adaptive Gripper	3	5	4	5	4	4	<u>25</u>
SCHMALZ® Vacuum Gripper	2	3	4	5	5	2	<u>21</u>
TIHRA® Gripper	3	3	2	5	1	4	<u>18</u>
FESTO® Multi-Choice Gripper	3	4	3	5	4	4	<u>23</u>

Key: 1 = Worst 5 = Best

APPENDIX A.2: Flexible Gripping Technologies: Quality Function Deployment

		Engineering Metrics												Customer Perception					
Customer Requirements	Customer Weights	Force on appendages	Torque from actuator	Number of components	Mass of system	Force response to dynamics	Flexibility of material	Accuracy	Ease of manufacturing	Manufacturing costs	Safety	Efficiency	Aesthetic appeal		1 Worse	2	3	4	5 Better
Effective shape conformity	5	4	4	4	2	5	5	1	1	1	1	5	1						
Gripping strength	3	5	5	2	1	4	1	1	1	1	1	5	1						
Repeatability	4	2	4	2	1	5	2	5	1	1	2	5	1						
Material sensitivity and limitation	2	4	2	2	2	4	5	1	1	1	3	5	1						
Process integration	4	3	4	4	4	4	3	5	3	4	5	4	3						
Self-adjustment	3	4	4	4	2	4	3	1	1	1	1	5	1						
Technical Benchmarking	Better 5 4 3 2 Worse 1																		
	Raw score	75	83	66	43	93	67	53	29	33	45	101	29						
	Relative Weight	10%	12%	9%	6%	13%	9%	7%	4%	5%	6%	14%	4%						

APPENDIX A.3: Proposed Budget for Gripper System

The budget was compiled for the design and manufacturing of the 3-finger and 4-finger gripper system and is tabulated in Table 24. The budget summary was estimated to be R6361.50 for both the 3-finger and 4-finger gripper design.

Components	Price / Unit	QTY	Cost
M3 Drill Bit	R 50.00	1	R 50.00
M5 Drill Bit	R 50.00	1	R 50.00
M6 Drill Bit	R 50.00	1	R 50.00
M3x25mm Screw + Nut	R 1.50	40	R 60.00
M3x60mm Screw + Nut	R 1.50	12	R 18.00
M3x20mm Screw + Nut	R 1.50	126	R 189.00
M8 Nut	R 5.00	6	R 30.00
Rubber Grip	R 130.00	1	R 130.00
Verbatim Primalloy Flex Filament - 1.75mm - 0.5kg	R 799.95	1	R 799.95
Arduino Mega 2560	R 244.95	2	R 489.90
Nema 17 Stepper Motor (0.45Nm , 40mm)	R 219.95	2	R 439.90
TB6560 Stepper Motor Driver	R 149.95	2	R 299.90
Flexible Aluminium Coupling (5mm/8mm)	R 39.95	2	R 79.90
Tactile switch	R 99.95	1	R 99.95
LCD Display 16x2 - LCD Arduino Shield / Keypad	R 84.95	2	R 169.90
BATTERY 9V NiMH EIE	R 128.80	6	R 772.80
UNIVERSAL BATTERY CHARGER AA/AAA/C/D /9V	R 210.00	1	R 210.00
Solderless Breadboard 400TP	R 29.95	3	R 89.85
Breadboard Jumpers	R 37.95	1	R 37.95
Rigid Aluminium Coupling (5mm/8mm) - Anodised	R 39.95	2	R 79.90
3D Printed Components and Materials	R 1200.00	1	R 800.00
Interlink Electronics 0.2" Circular 20N FSR 5 mm	R 101.46	10	R 1 014.60
	TOTAL		R 6361.50

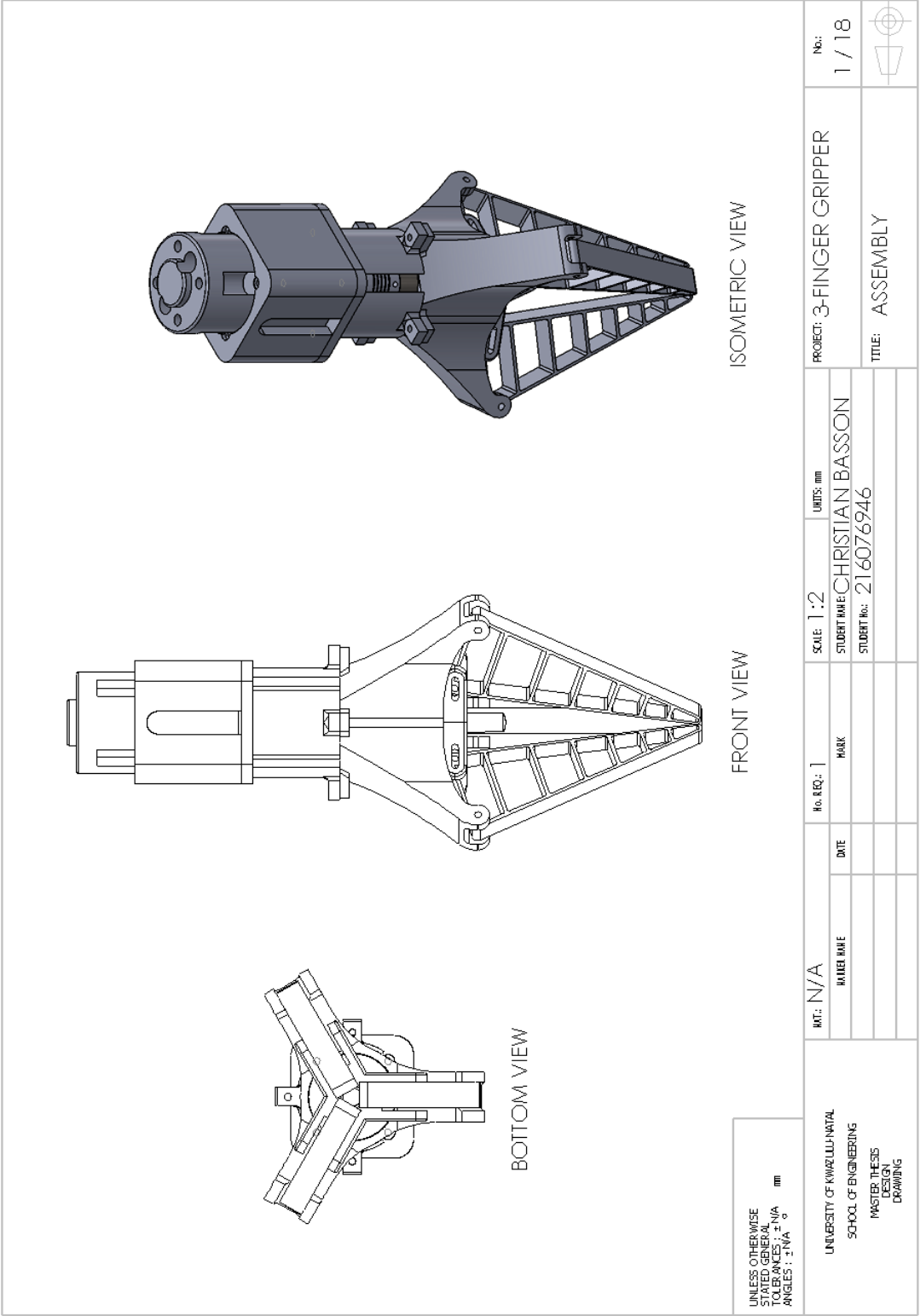
APPENDIX A.4: Energy Audit

Energy amortisation table shows the electrical energy consumption for the assembly system over a year of operation. Assuming operation runs 8 hours a day, 5 days a week and 12 months a year (excluding public holidays). Assuming the energy payment rate is R1.96 per kWh the energy cost per year is calculated.

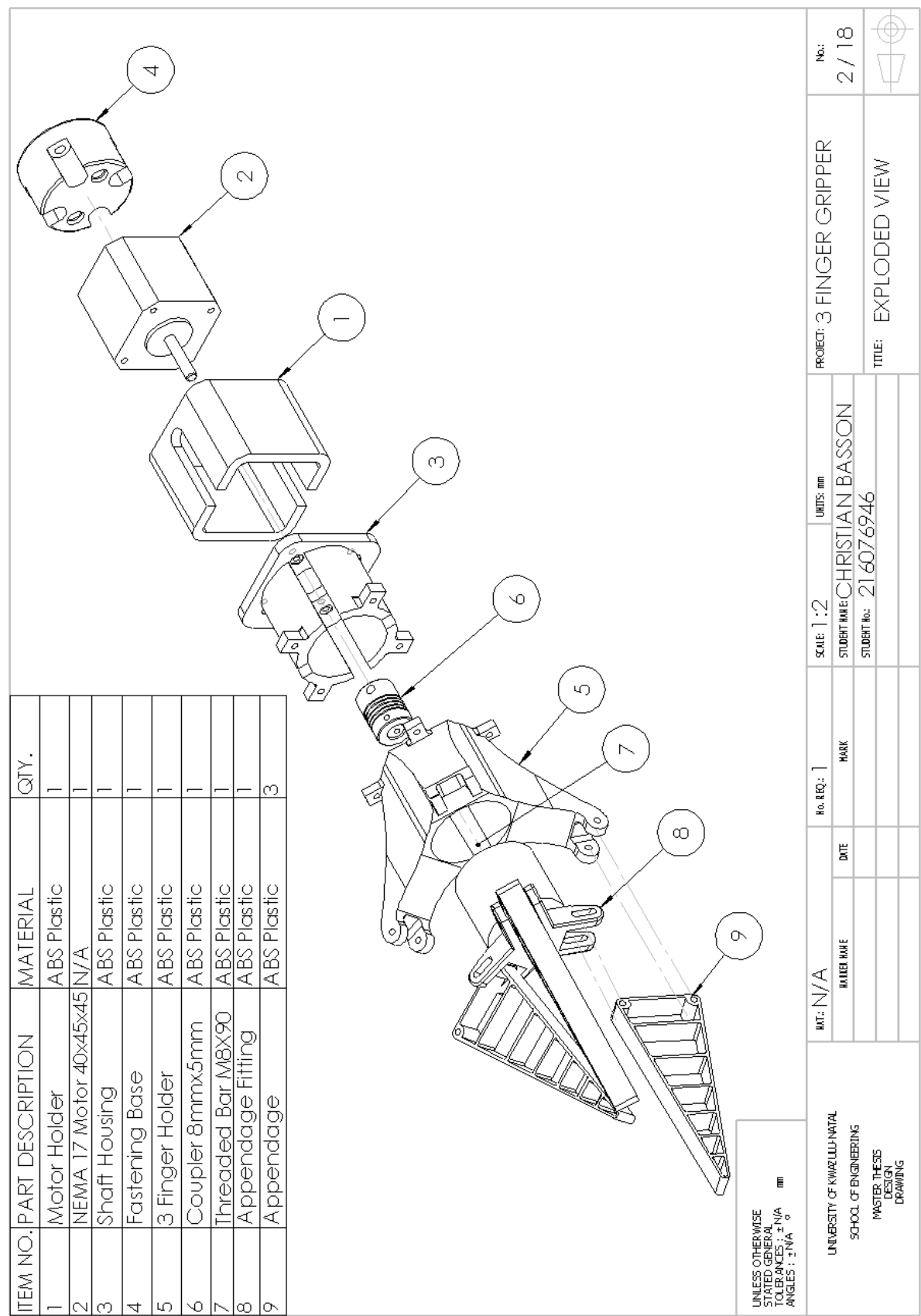
Component	Power Consumption (kWh)	Monthly Cost	Yearly Cost
Gripper motor	0.144	R 45.16	R 541.90
FANUC M10ia Robotic Arm	1	R 313.60	R 3763.20
PLC control system	0.5	R 156.80	R 1881.60
Laptop computer	0.175	R 54.88	R 658.56
24V power supply	0.07	R 21.95	R 263.42
TOTAL	1.889	R 592.39	R 7108.69

APPENDIX B: Design

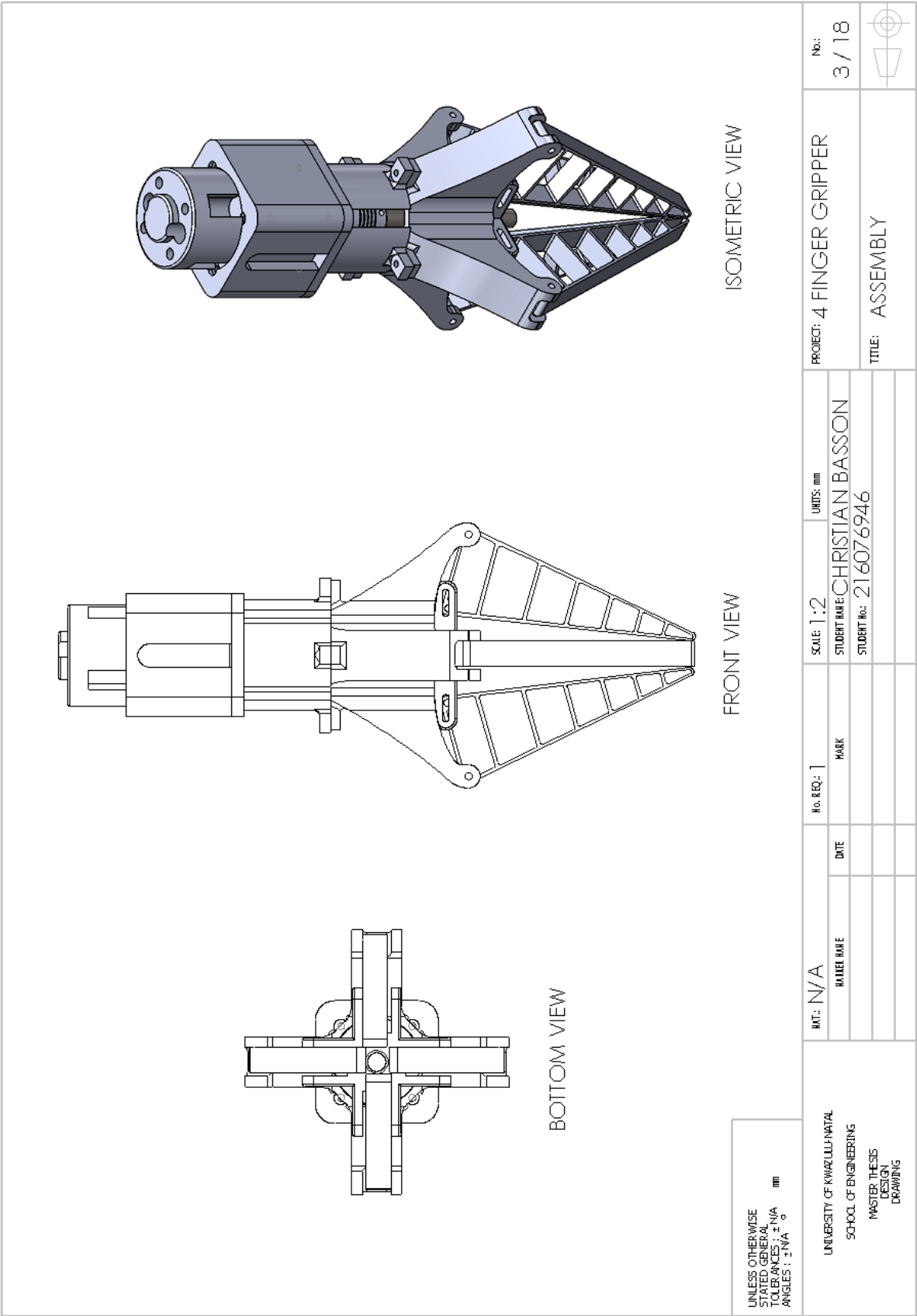
APPENDIX B.1: 3-Finger Gripper Assembly



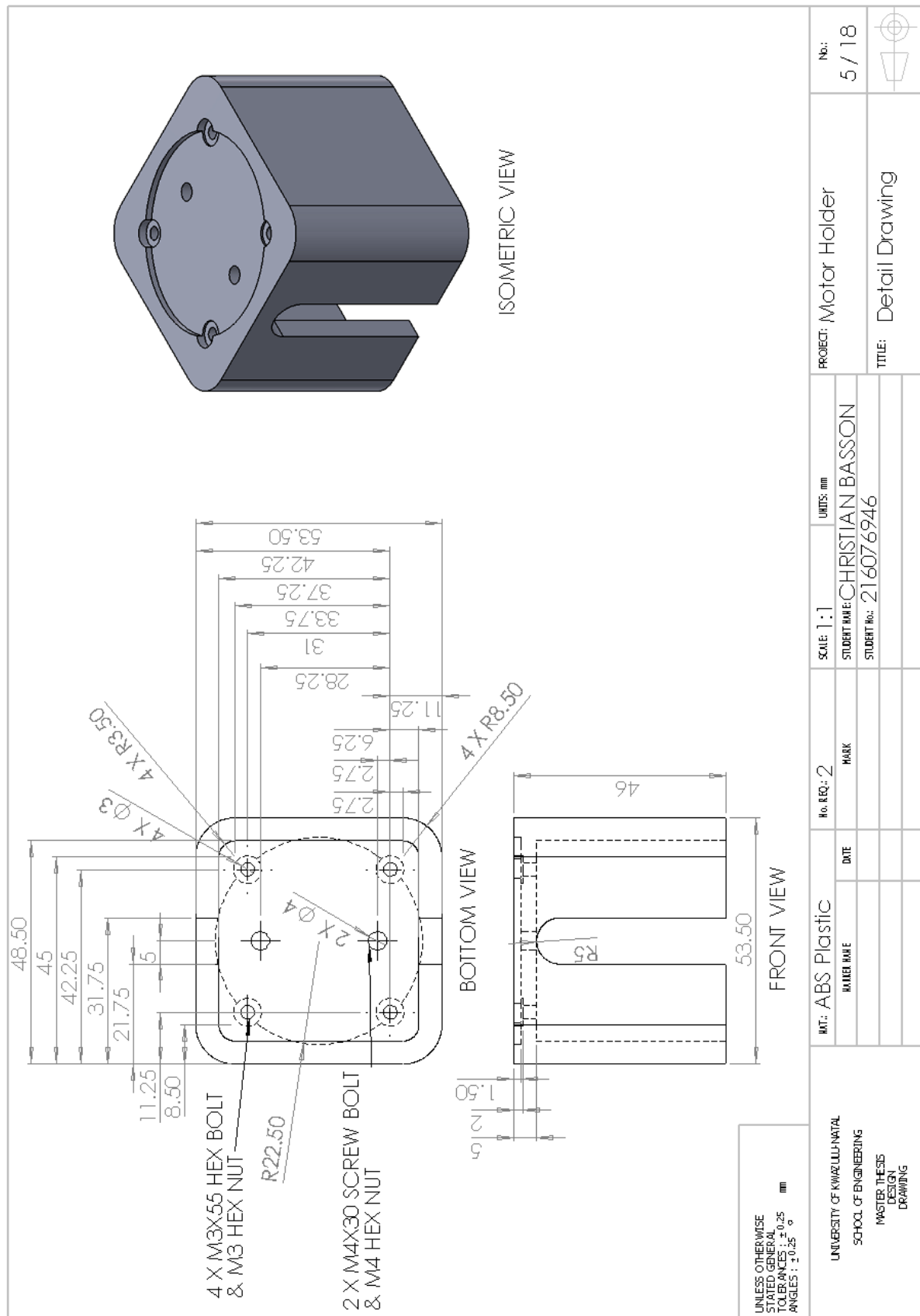
APPENDIX B.2: 3-Finger Gripper Exploded View

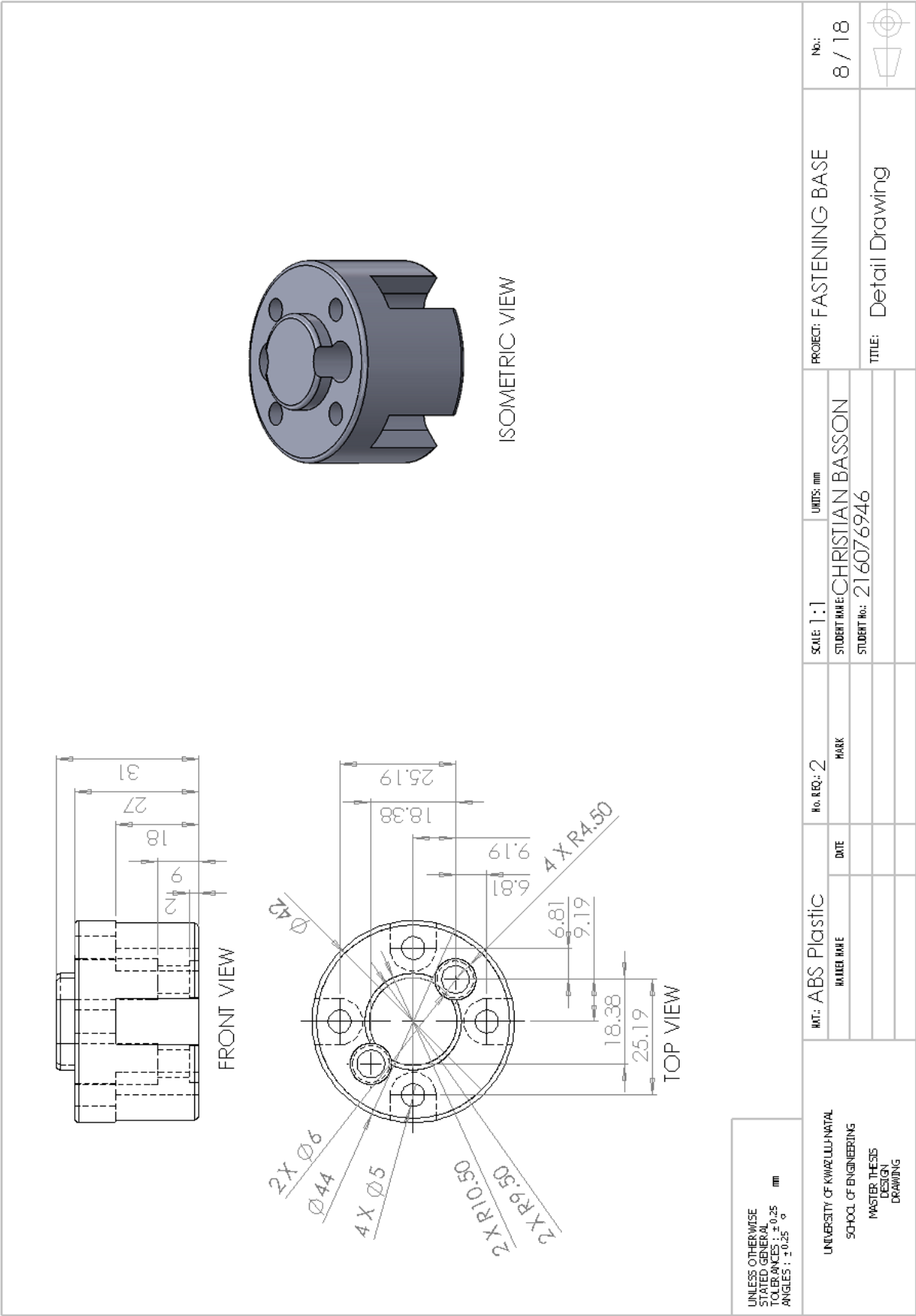


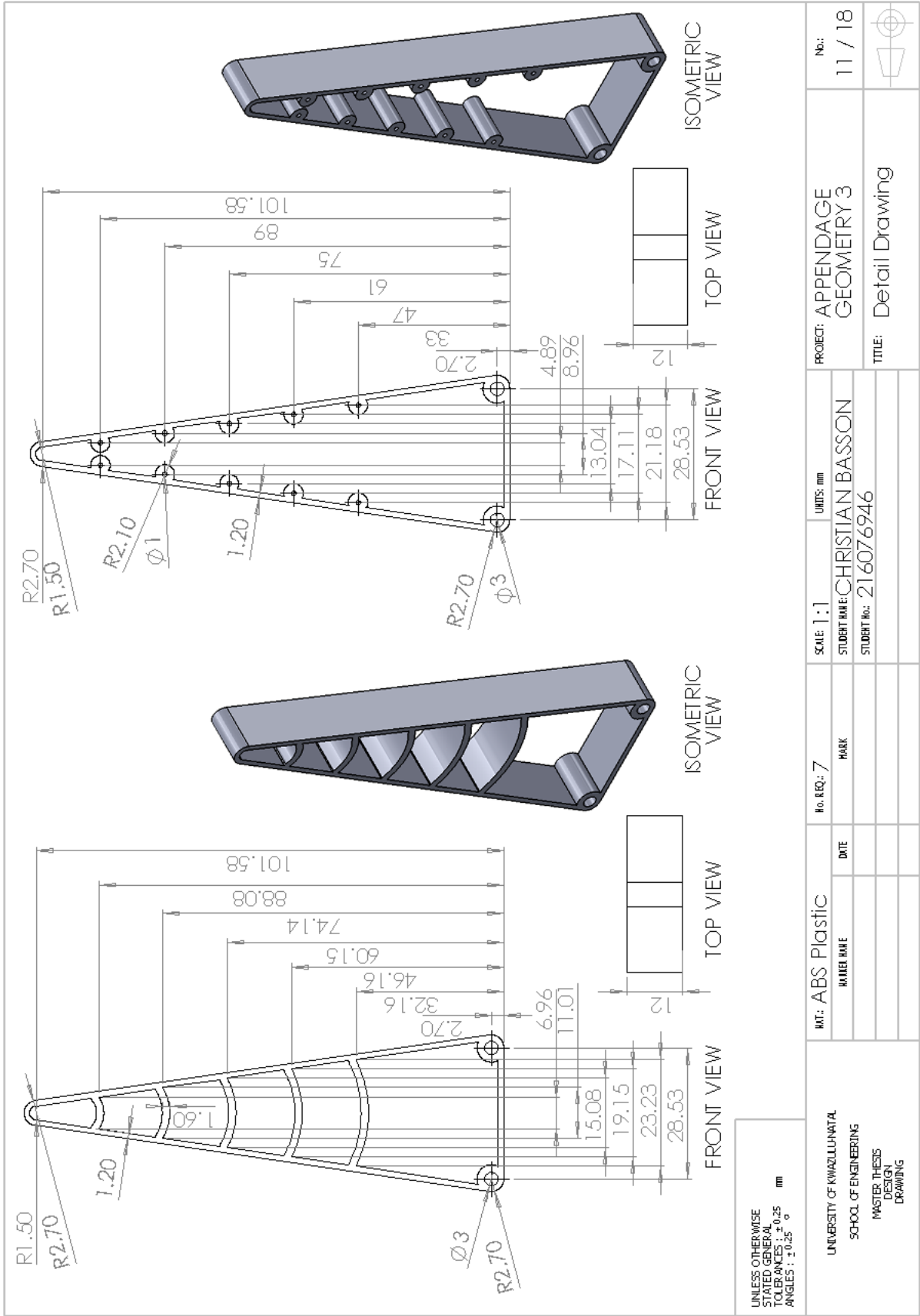
APPENDIX B.3: 4-Finger Gripper

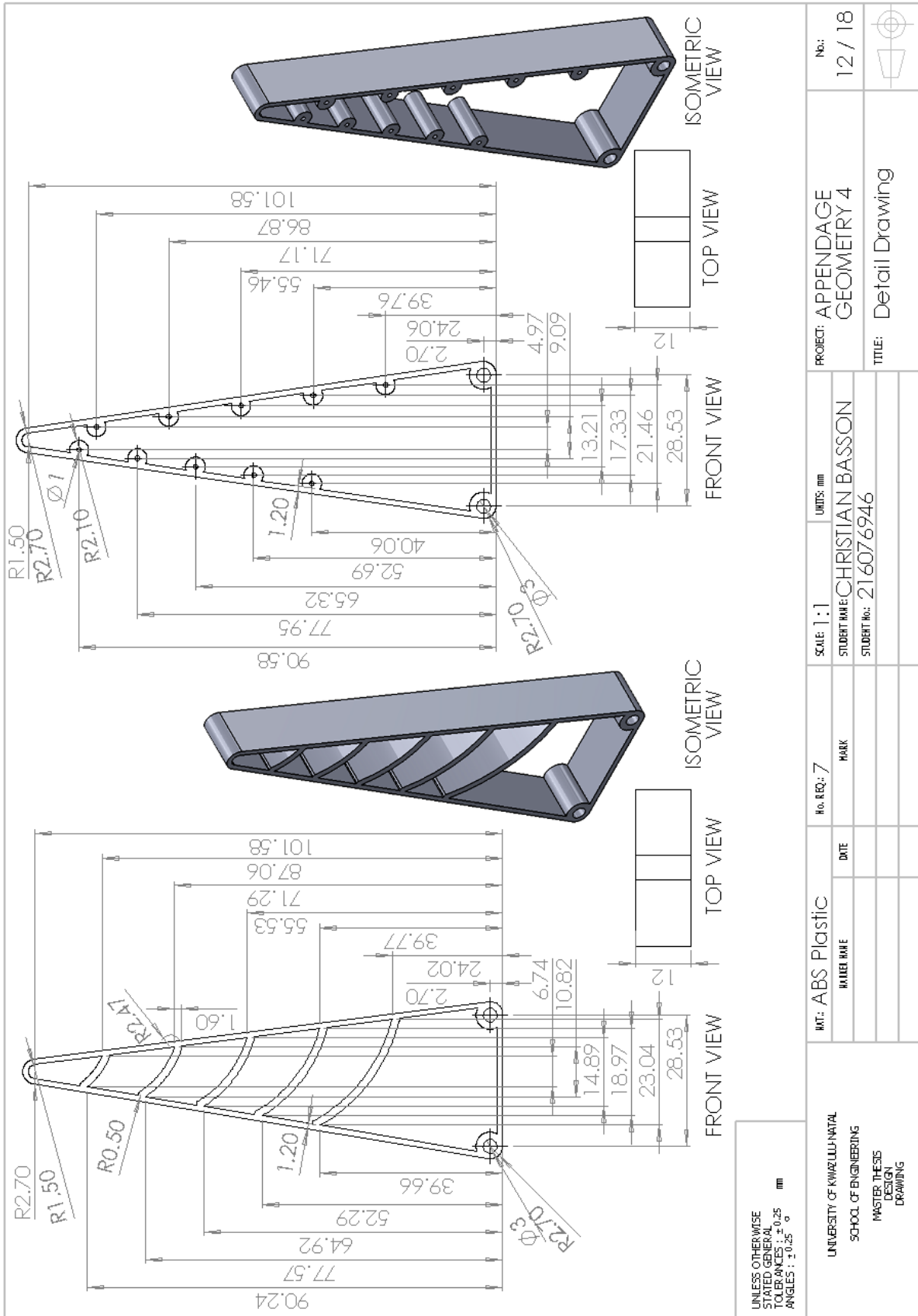


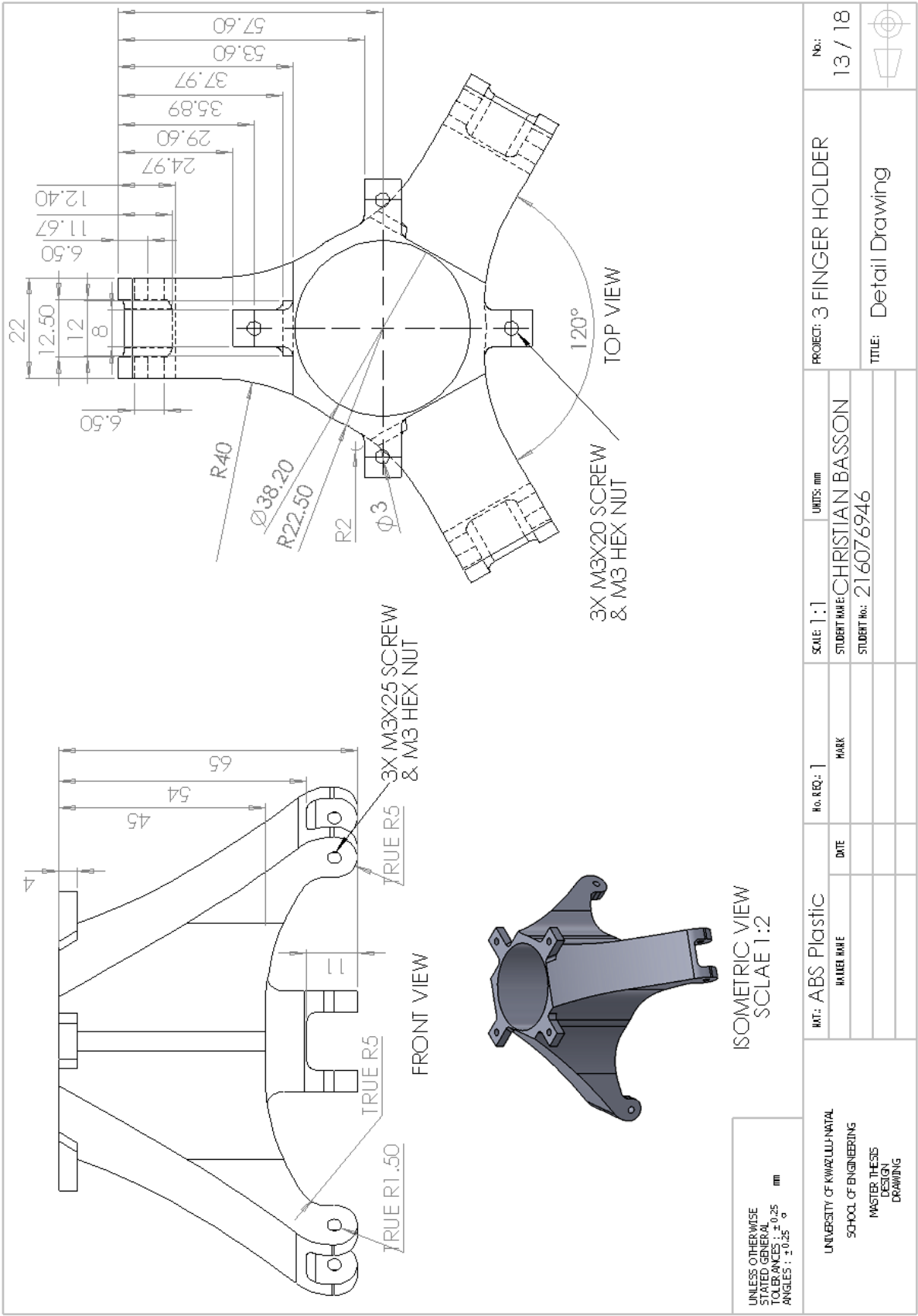
APPENDIX B.5: Gripper Parts and Components

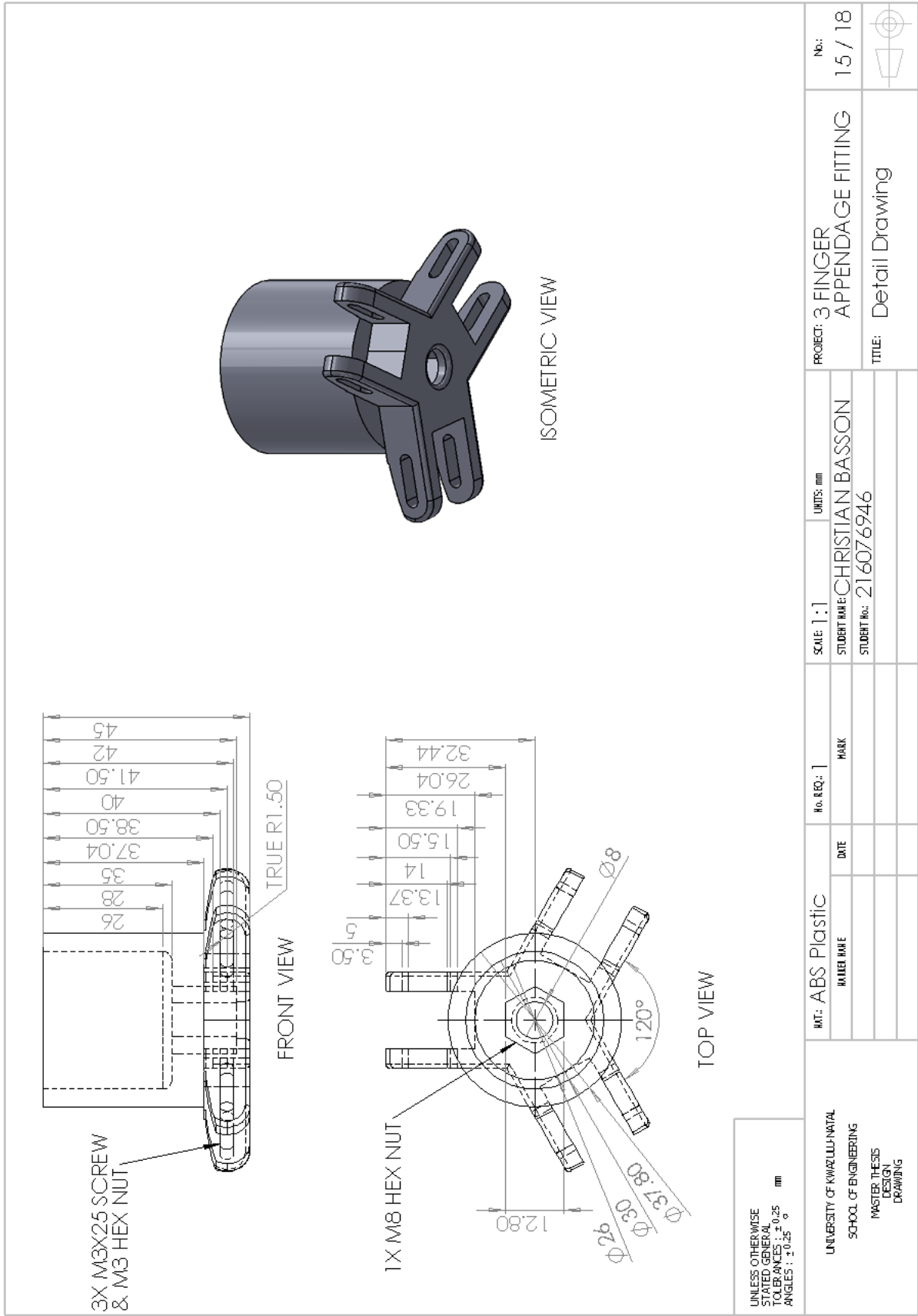


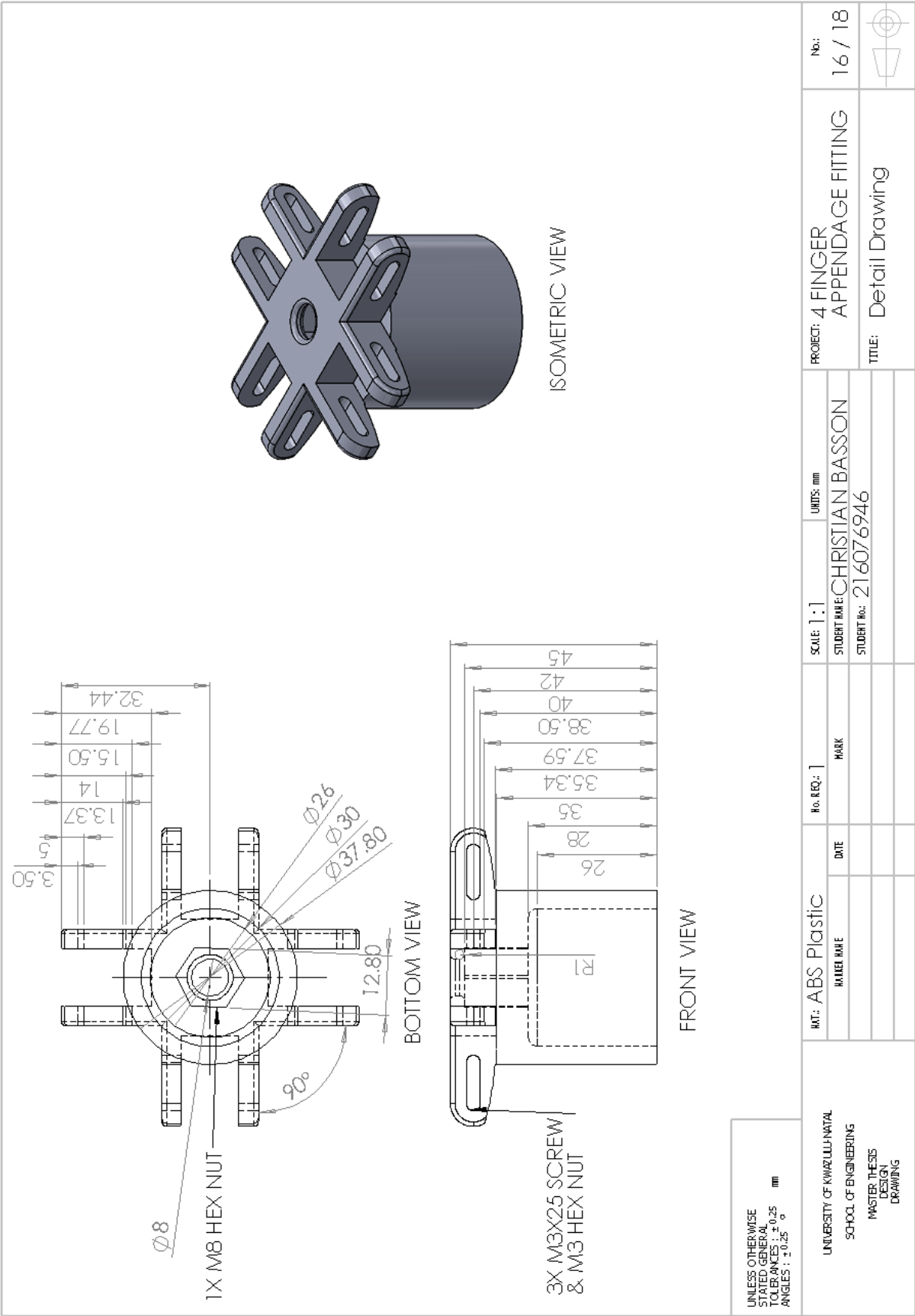


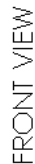








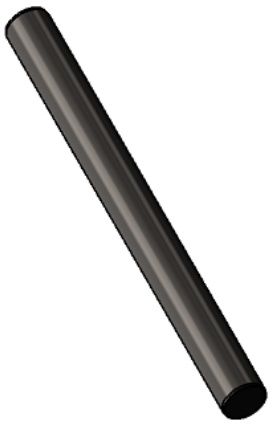
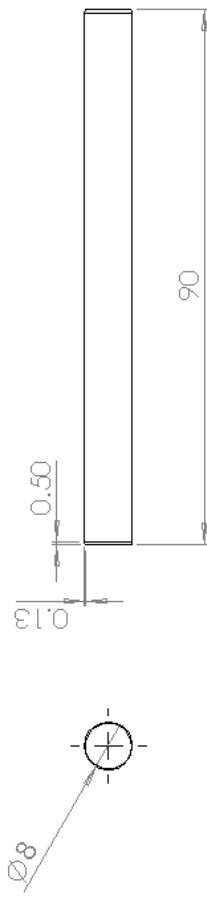





ISOMETRIC
VIEW

UNLESS OTHERWISE
STATED GENERAL
TOLERANCES : ± 0.25
ANGLES : $\pm 0.25^\circ$

UNIVERSITY OF KWAZULU-NATAL SCHOOL OF ENGINEERING MASTER THESIS DESIGN DRAWING	MAT: Steel		No. REQ: 2	SCALE: 2:1	UNITS: mm	PROJECT: COUPLER	No.: 17 / 18
	NAME NAME	DATE					
		MARK					
						TITLE: Detail Drawing	



<div>UNLESS OTHERWISE STATED GENERAL TOLERANCES : ± 0.25 mm ANGLES : $\pm 0.25^\circ$</div>	UNIVERSITY OF KWAZULU-NATAL			SCHOOL OF ENGINEERING			MASTER THESIS DESIGN DRAWING			PROJECT: THREADED BAR	No.: 18 / 18	
	MAT: ABS Plastic		No. REQ: 2	MARK	DATE		SCALE 1:1					
	UNIVERSITY NAME				STUDENT NAME: CHRISTIAN BASSON							
	DATE				STUDENT No.: 216076946							

APPENDIX B.6: Electronic Parts Catalogue Details

Arduino ATmega2560 Microcontroller

Technical Specification

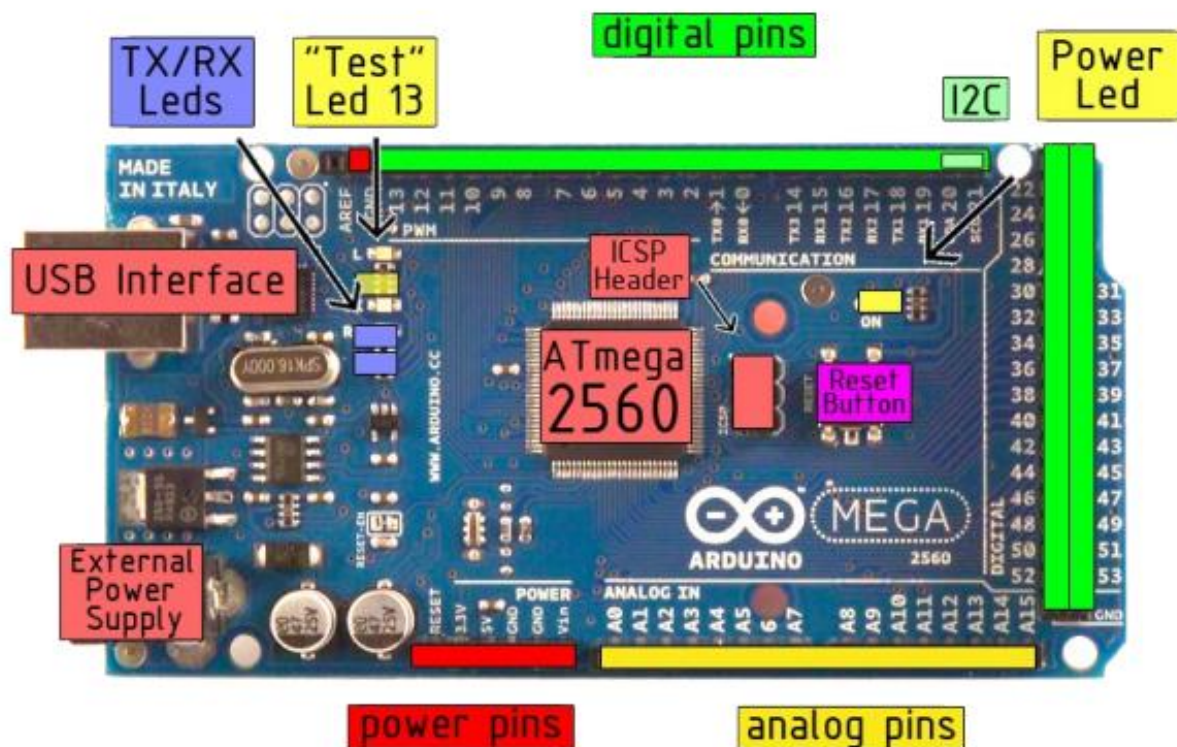


EAGLE files: [_arduino-mega2560-reference-design.zip](#) Schematic: [arduino-mega2560-schematic.pdf](#)

Summary

Microcontroller	ATmega2560
Operating Voltage	5V
Input Voltage (recommended)	7-12V
Input Voltage (limits)	6-20V
Digital I/O Pins	54 (of which 14 provide PWM output)
Analog Input Pins	16
DC Current per I/O Pin	40 mA
DC Current for 3.3V Pin	50 mA
Flash Memory	256 KB of which 8 KB used by bootloader
SRAM	8 KB
EEPROM	4 KB
Clock Speed	16 MHz

the board



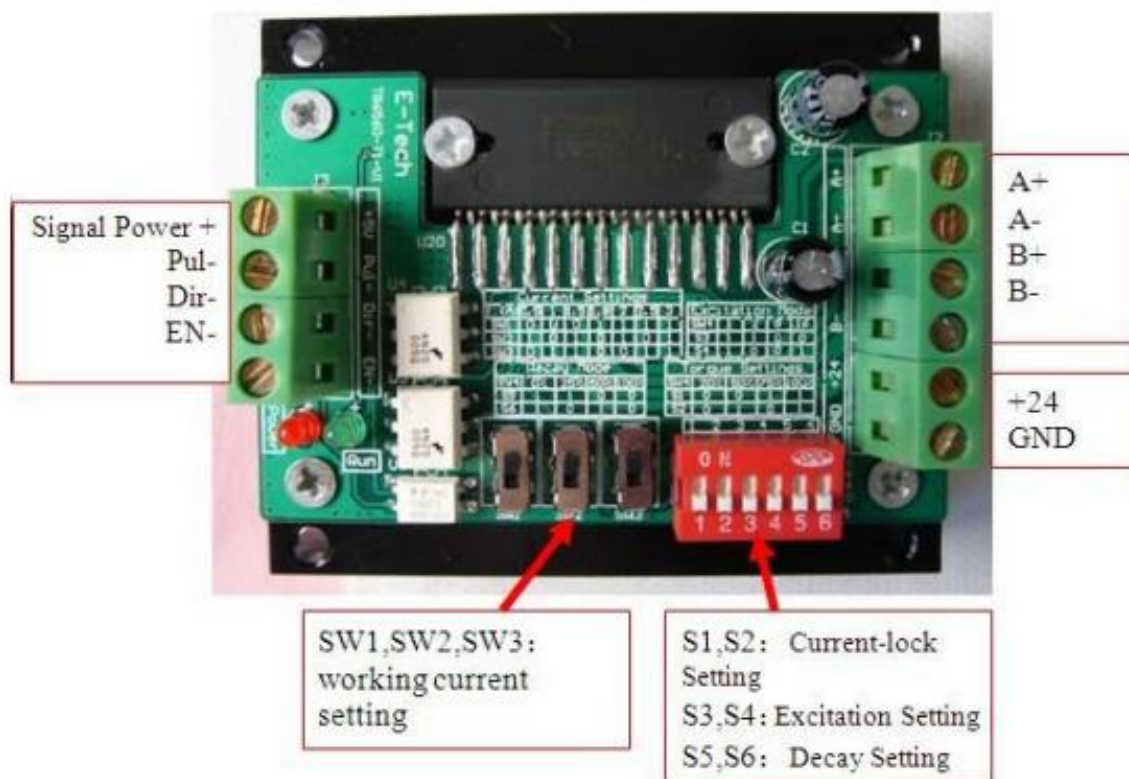
TB6560 Stepper Motor Controller

Specifications and Operating Environment

Electrical Specifications (T_j=25°C)

Parameters	TB6560-3AXIS			
	Min	Typical	Max	Unit
Output current	0.6	-	3	A
Input voltage	7	24	32	VDC
Inner Frequency	640		20000	Hz
Outer input frequency	0	-	16000	Hz
Connector Voltage	H	4.5	5	VDC
	L	0	0	VDC

TB6560-3Axis Interface Definition

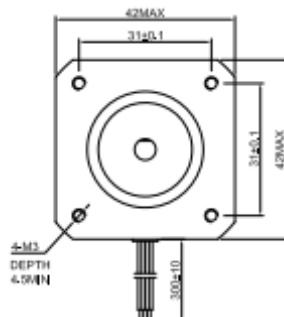
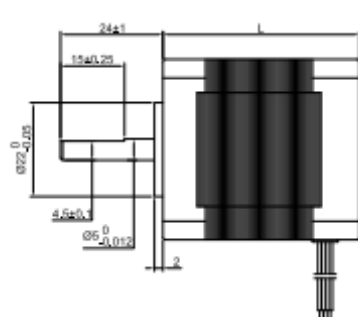


NEMA 17 Bipolar Stepper Motor

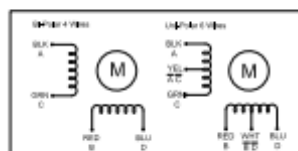
□42.3mm(□1.67in.)

Step Angle 1.8° 17HS High-Torque Type

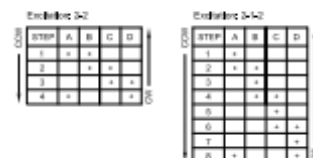
■ Dimension Unit = mm(in.)



■ Wiring Diagram



■ Excitation Sequence



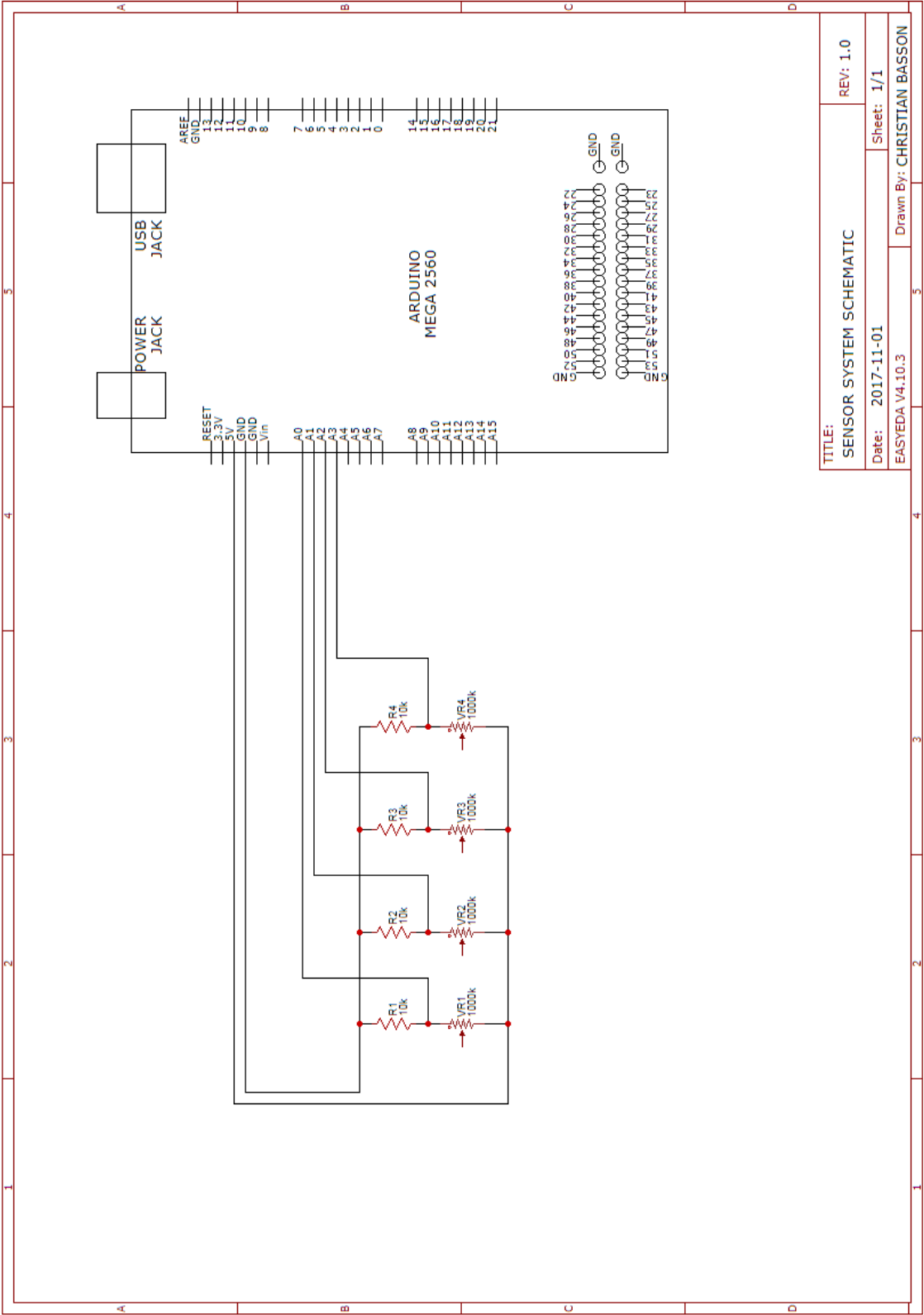
■ Specifications

Model	Torque		Voltage	Current	Resistance	Inductance	Inertia	Bi/Unipolar	Weight	Length "L"	
	Ncm	oz.in	V/Phase	A/Phase	Ohm/Phase	mH/Phase	g.cm ²	# of Leads	Kg	mm	in
17HS08-1004S	13	18.4	3.5	1	3.5	4.5	15	Bi (4)	0.15	20	0.79
17HS13-0316S	16	22.7	12	0.31	38.5	21	35	Uni (6)	0.22	33	1.30
17HS13-0406S	16	22.7	9.6	0.4	24	15	35	Uni (6)	0.22	33	1.30
17HS13-0956S	16	22.7	4	0.95	4.2	2.5	35	Uni (6)	0.22	33	1.30
17HS13-1334S	22	31.2	2.8	1.33	2.1	2.5	35	Bi (4)	0.22	33	1.30
17HS13-1504S	23	32.6	1.65	1.5	1.1	1.6	35	Bi (4)	0.22	33	1.30
17HS13-0404S	26	36.8	12	0.4	30	37	35	Bi (4)	0.22	33	1.30
17HS13-0844S	28	39.7	4.83	0.84	5.75	9.3	35	Bi (4)	0.22	33	1.30
17HS15-0406S	26	36.8	12	0.4	30	30	54	Uni (6)	0.28	39	1.54
17HS15-0806S	26	36.8	6	0.8	7.5	6.7	54	Uni (6)	0.28	39	1.54
17HS15-1206S	26	36.8	4	1.2	3.3	3.2	54	Uni (6)	0.28	39	1.54
17HS15-0854S	36	51.0	5.4	0.85	6.3	10	54	Bi (4)	0.28	39	1.54
17HS15-1684S	36	51.0	2.8	1.68	1.65	3.2	54	Bi (4)	0.28	39	1.54
17HS15-0404S	40	56.6	12	0.4	30	58	54	Bi (4)	0.24	39	1.54
17HS16-2004S	45	63.7	2.2	2	1.1	2.6	54	Bi (4)	0.24	40	1.57
17HS19-0406S	32	45.3	12	0.4	30	25	68	Uni (6)	0.35	47	1.85
17HS19-0806S	32	45.3	6	0.8	7.5	6.3	68	Uni (6)	0.35	47	1.85
17HS19-1206S	32	45.3	4	1.2	3.3	2.8	68	Uni (6)	0.35	47	1.85
17HS19-1684S	44	62.3	2.8	1.68	1.65	2.8	68	Bi (4)	0.35	47	1.85
17HS19-0854S	44	62.3	5.3	0.85	6.2	11	68	Bi (4)	0.35	47	1.85
17HS19-2004S	59	83.6	2.8	2	1.4	3	68	Bi (4)	0.4	48	1.89
17HS20-0854S	55	77.9	8	0.85	9.3	20	72	Bi (4)	0.42	52	2.05
17HS24-0644S	60	85.0	10	0.64	15	13.2	82	Bi (4)	0.45	60	2.36
17HS24-1206S	65	92.0	7.2	1.2	6	7	82	Uni (6)	0.45	60	2.36
17HS24-2104S	65	92.0	3.4	2.1	1.6	3	82	Bi (4)	0.45	60	2.36

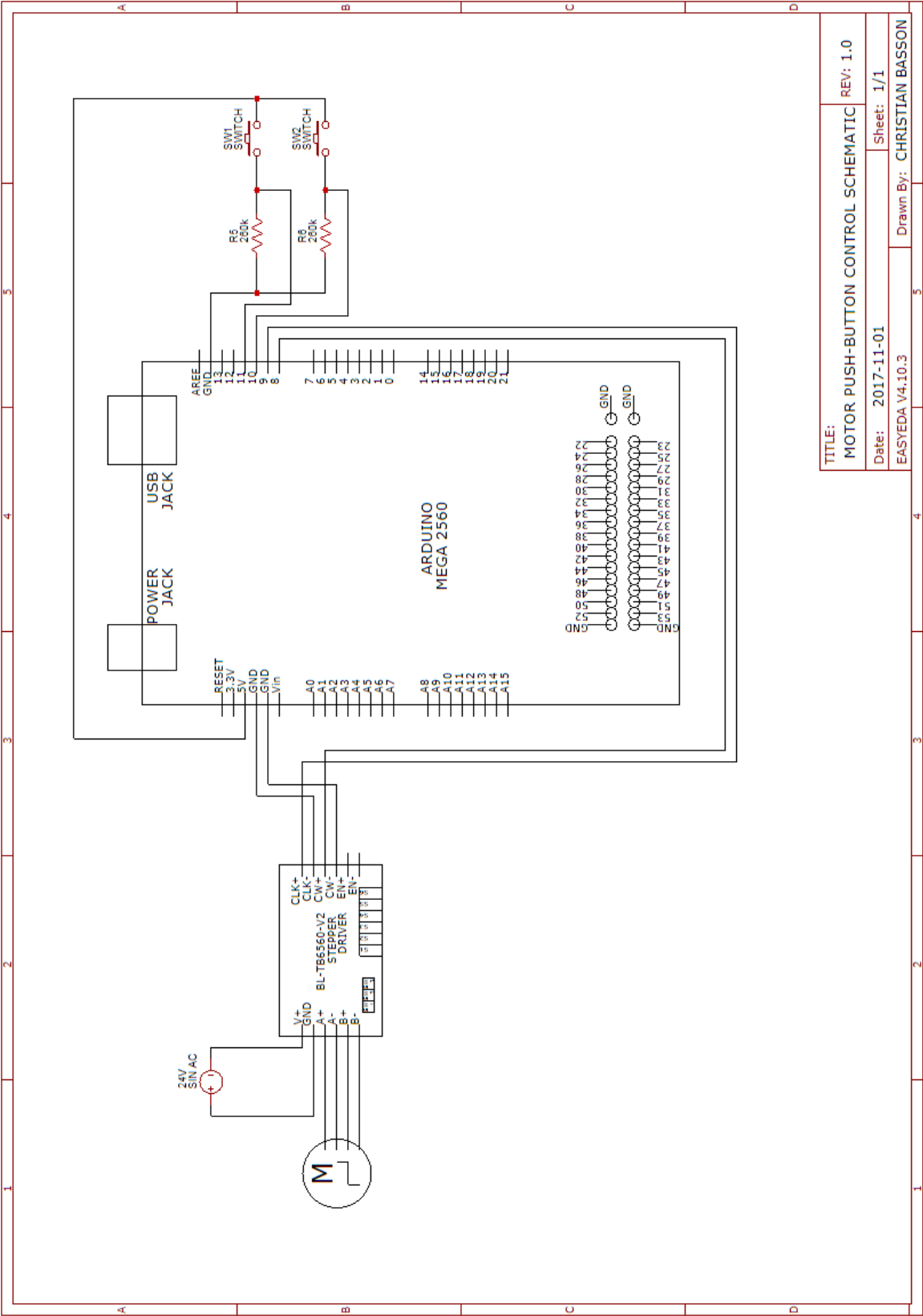
* Specify -S for Single Shaft; -D for Double Shaft * All motor's specifications are based on full-step constant current operation

APPENDIX B.7: Electronic Design

Sensor System Schematic



Motor Push-Button Control Schematic

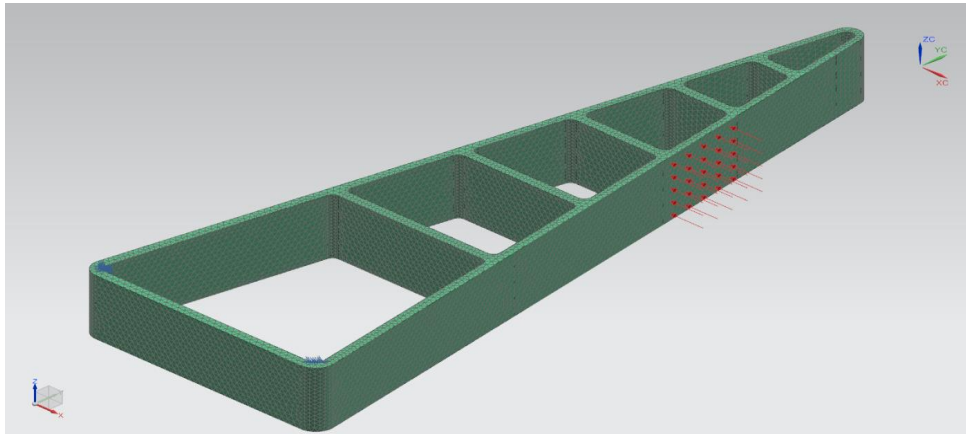


TITLE:		MOTOR PUSH-BUTTON CONTROL SCHEMATIC		REV: 1.0	
Date:		2017-11-01		Sheet: 1/1	
EASYEDA V4.10.3		Drawn By:		CHRISTIAN BASSON	

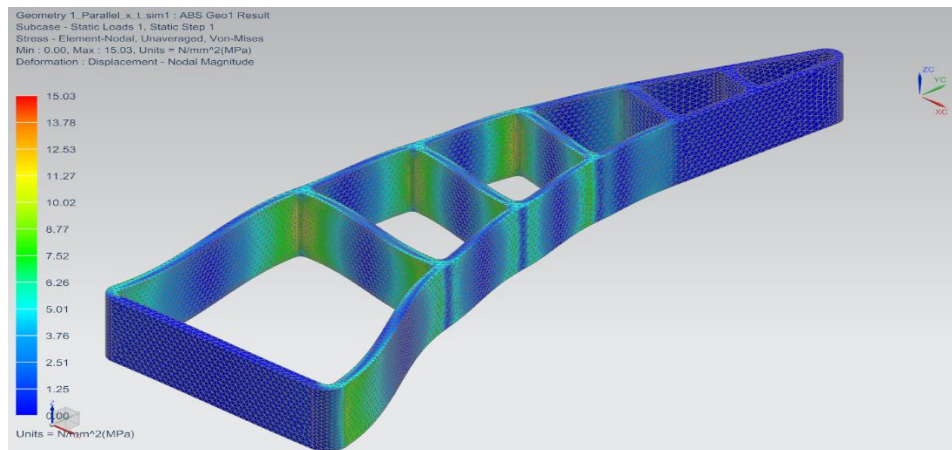
APPENDIX C: Simulation

APPENDIX C.1: Concept Design Simulation: Geometry 1 ABS Plastic

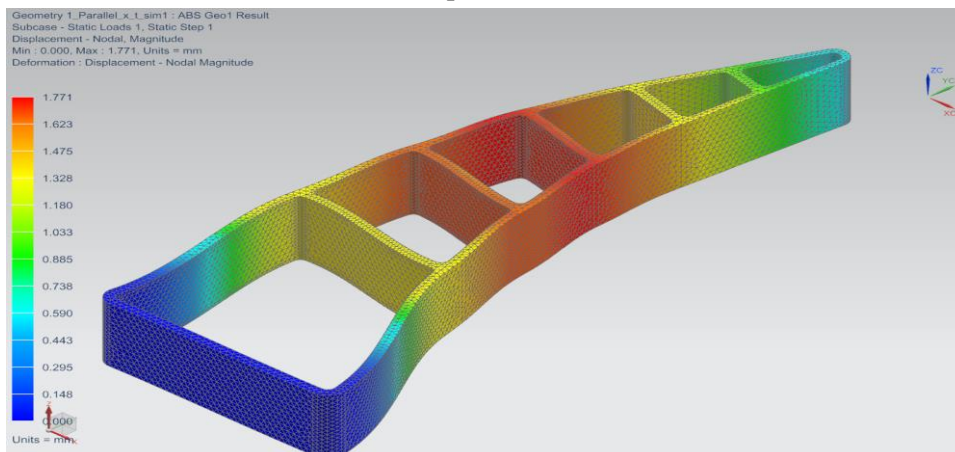
Constraint and load



Von Mises Stress Criteria

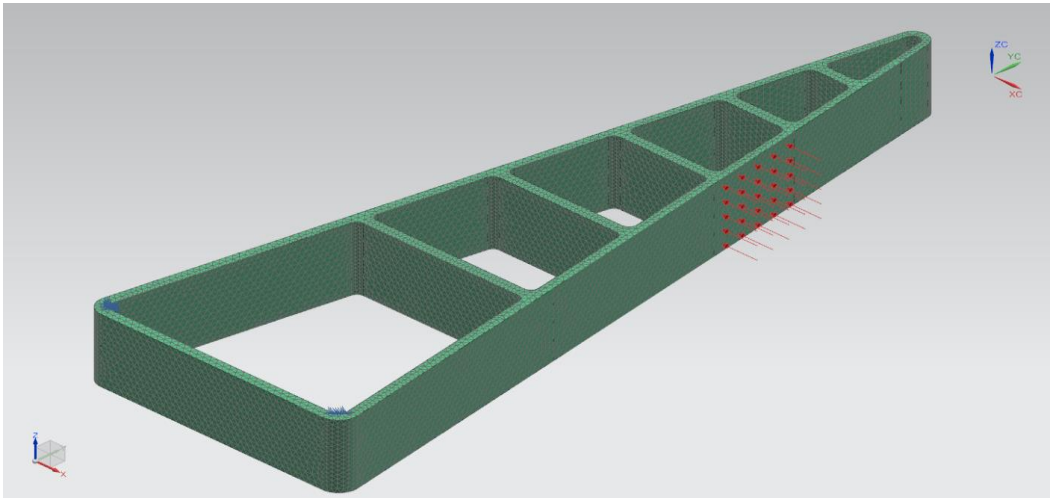


Displacement

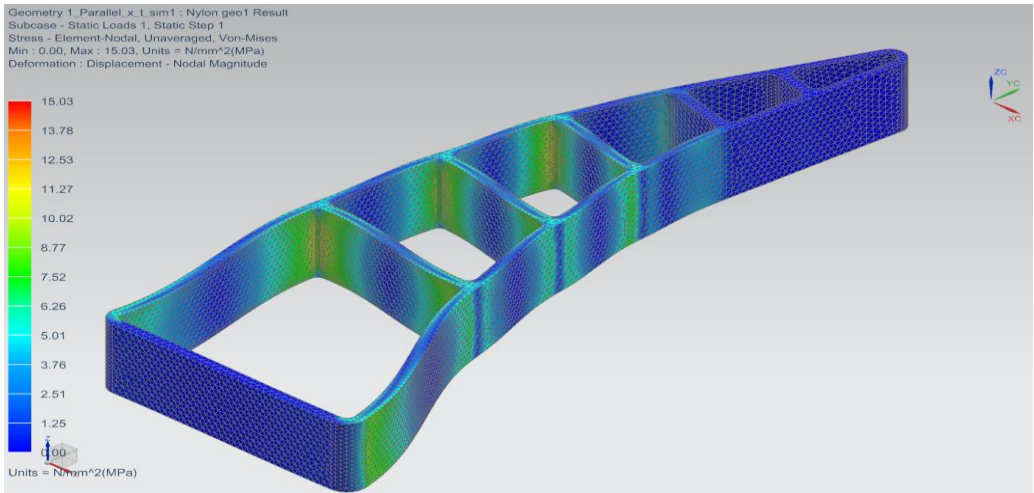


APPENDIX C.2: Concept Design Simulation: Geometry 1 NYLON

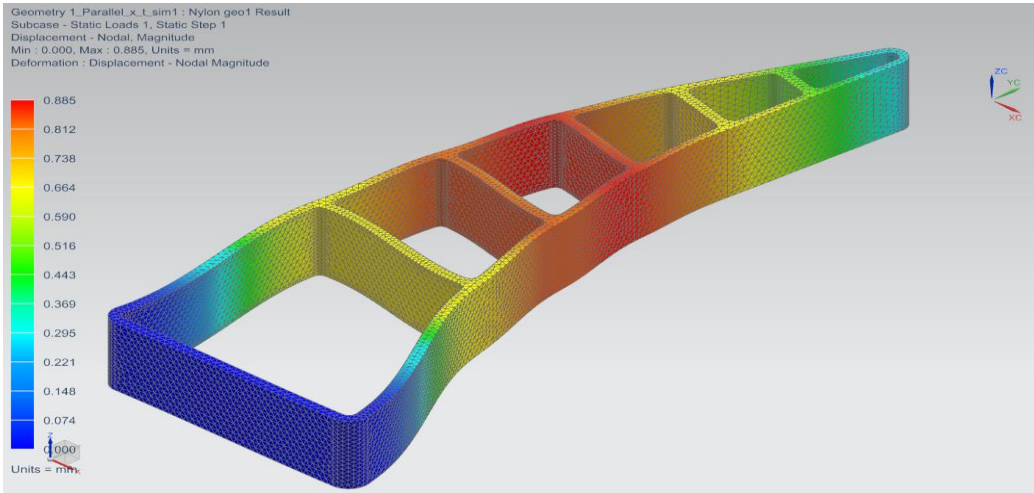
Constraint and load



Von Mises Stress Criteria

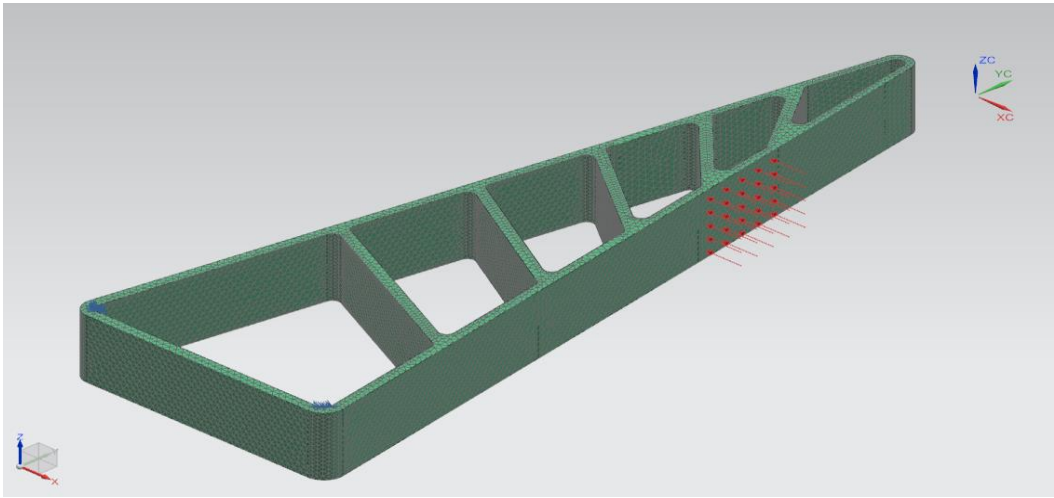


Displacement

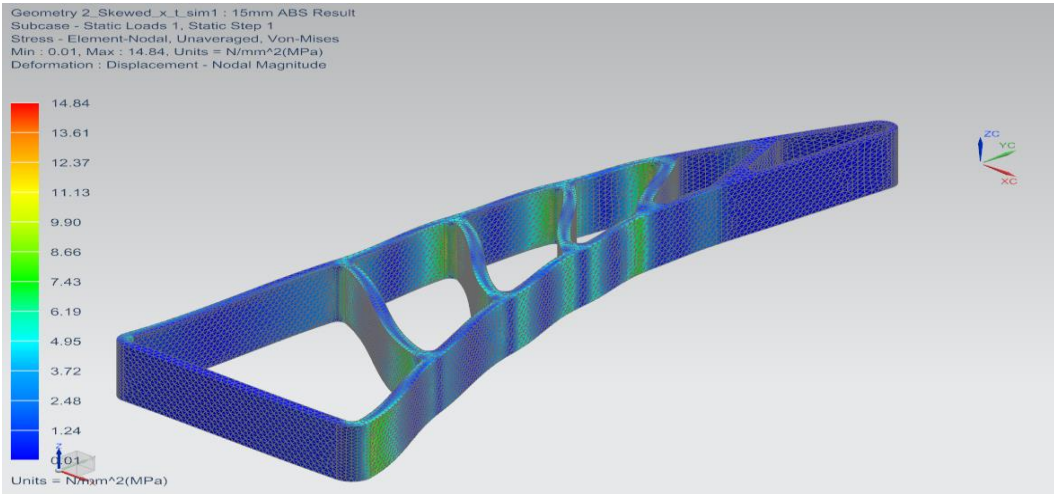


APPENDIX C.3: Concept Design Simulation: Geometry 2 ABS Plastic

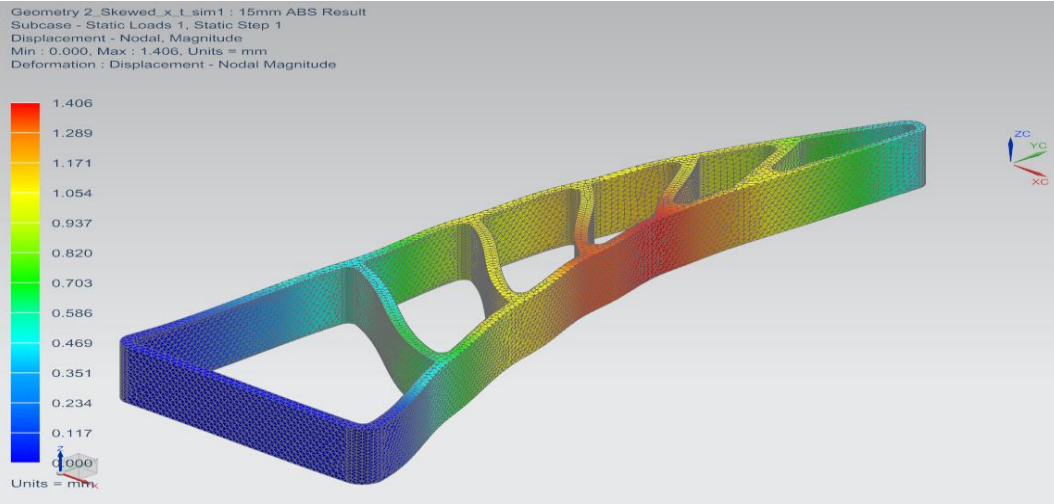
Constraint and load



Von Mises Stress Criteria

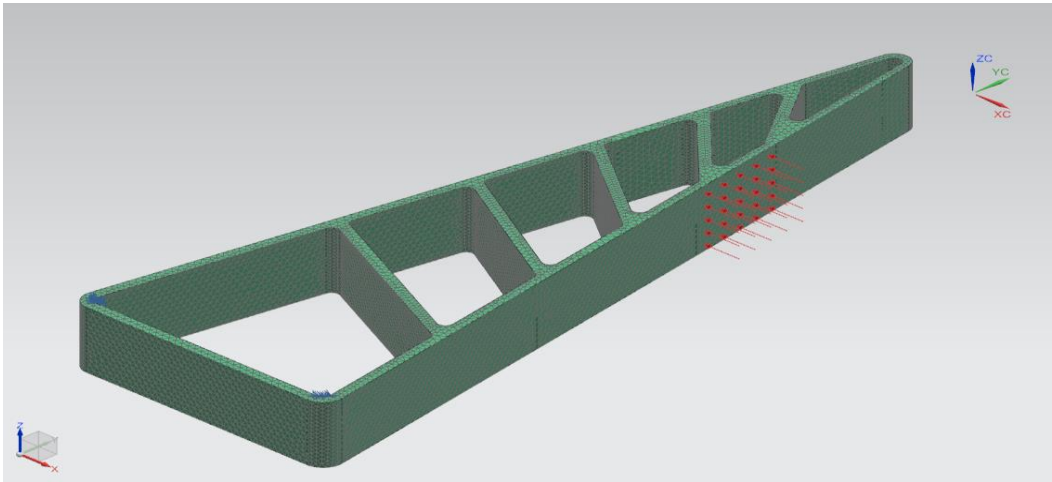


Displacement

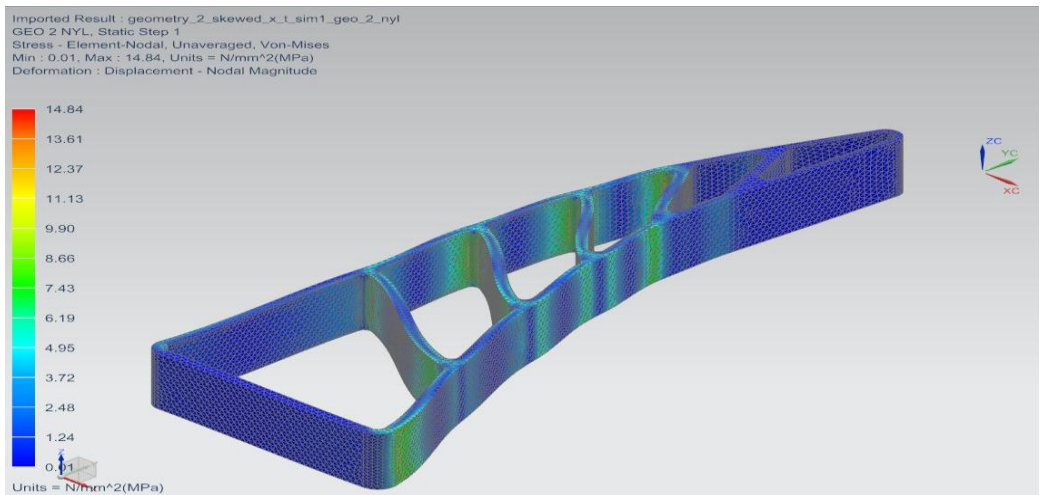


APPENDIX C.4: Concept Design Simulation: Geometry 2 NYLON

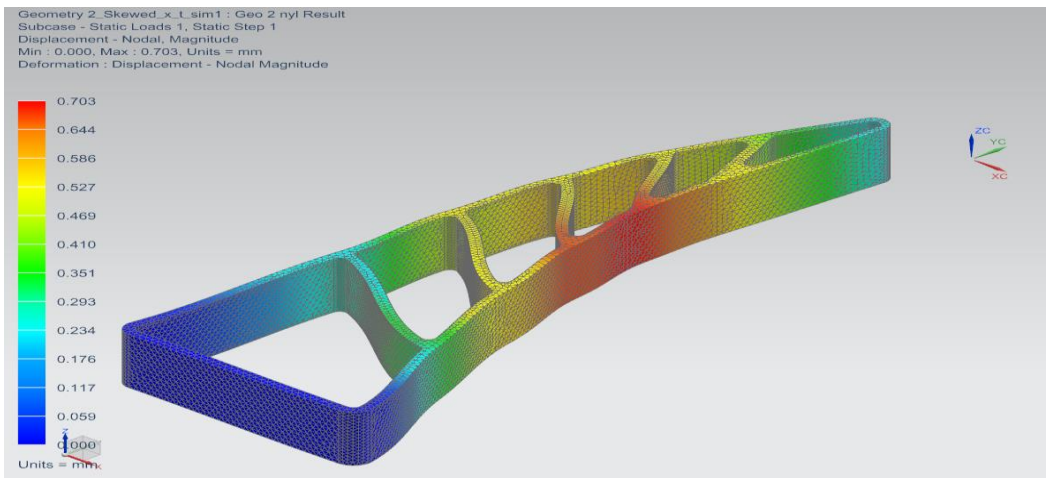
Constraint and load



Von Mises Stress Criteria

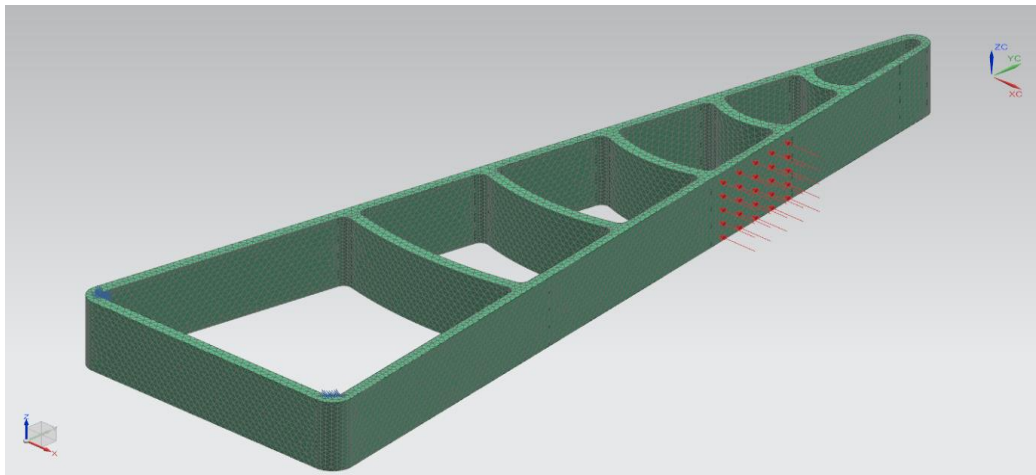


Displacement

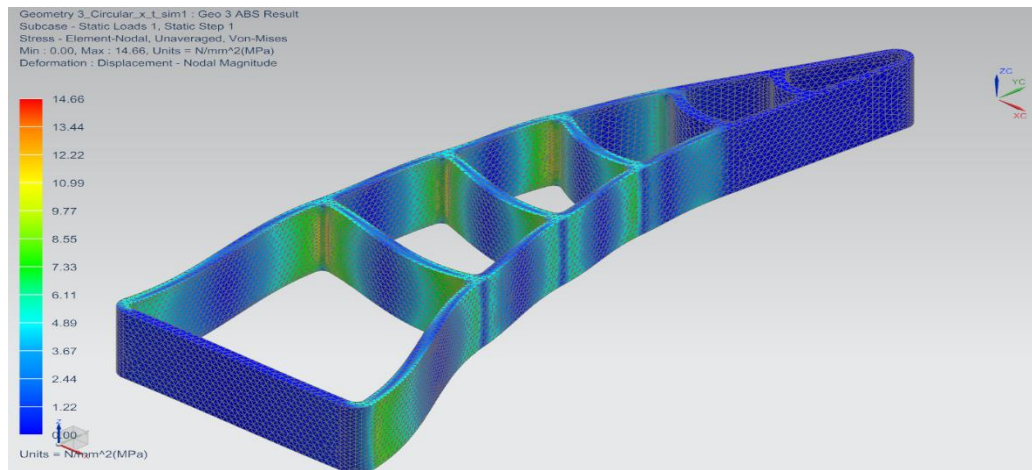


APPENDIX C.5: Concept Design Simulation: Geometry 3 ABS Plastic

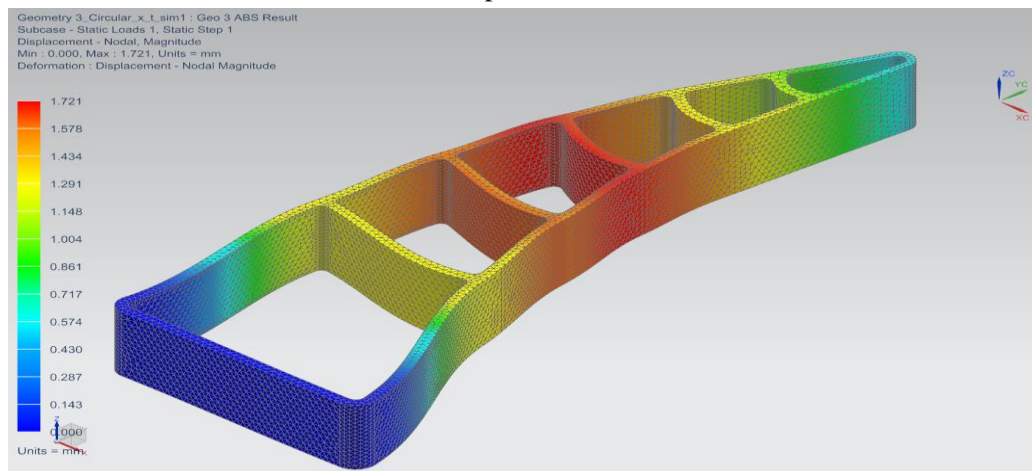
Constraint and load



Von Mises Stress Criteria

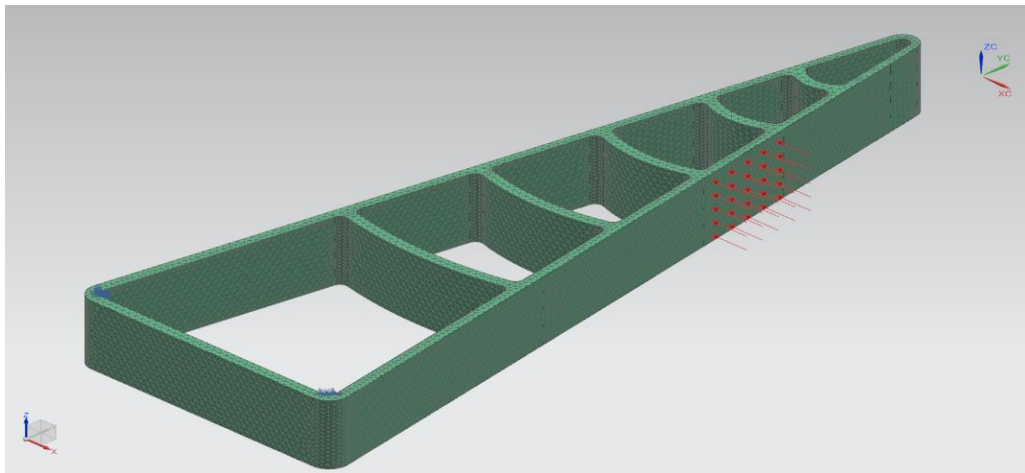


Displacement

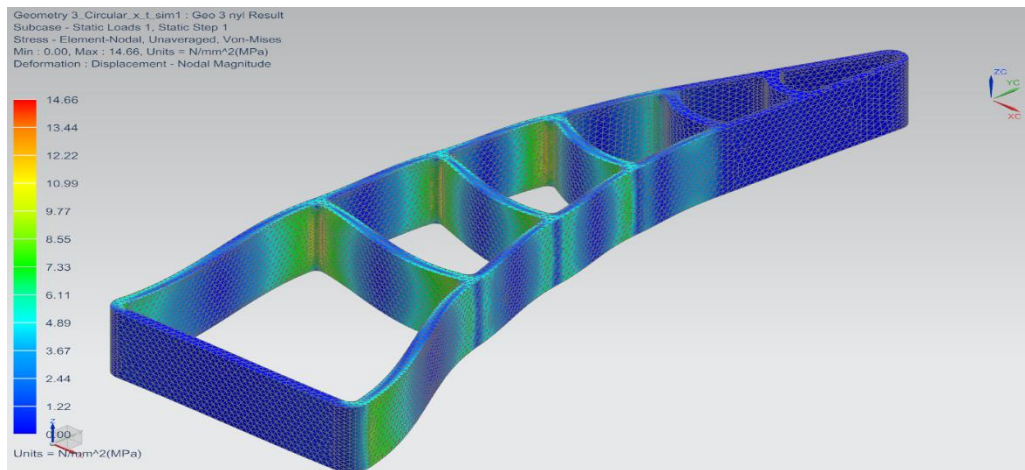


APPENDIX C.6: Concept Design Simulation: Geometry 3 NYLON

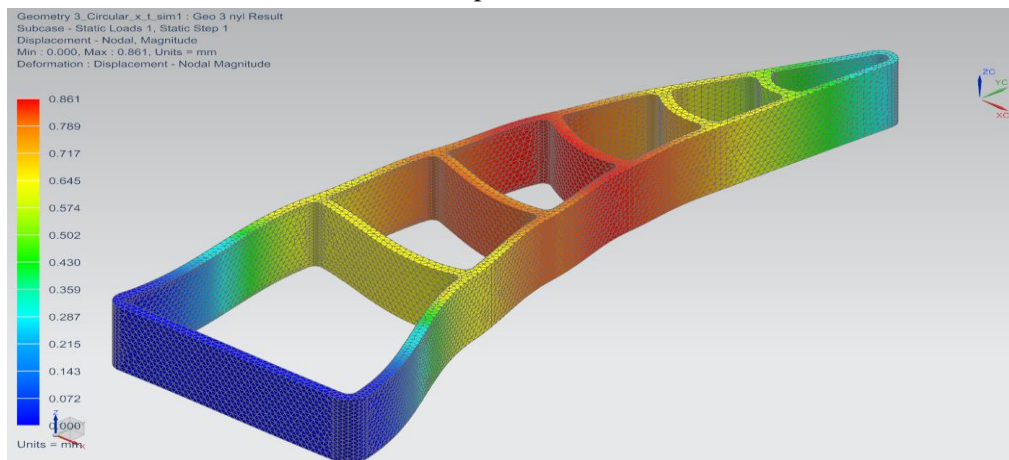
Constraint and load



Von Mises Stress Criteria

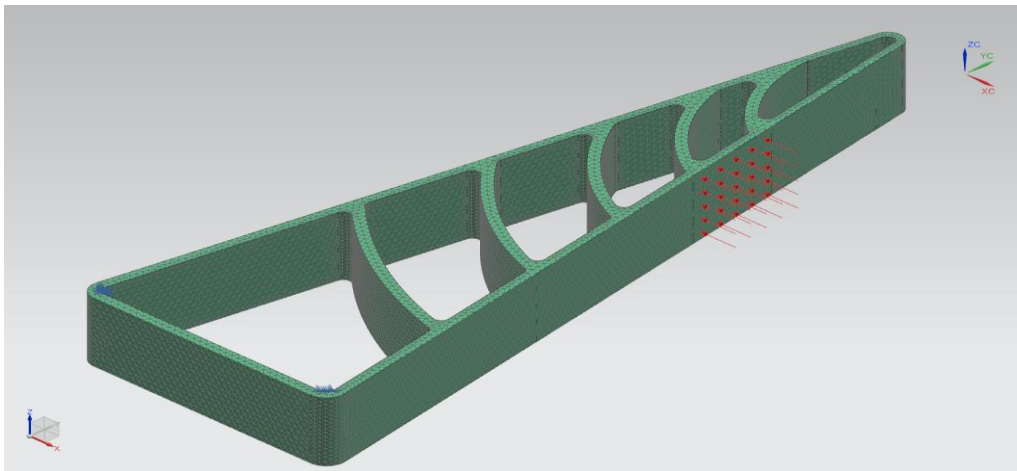


Displacement

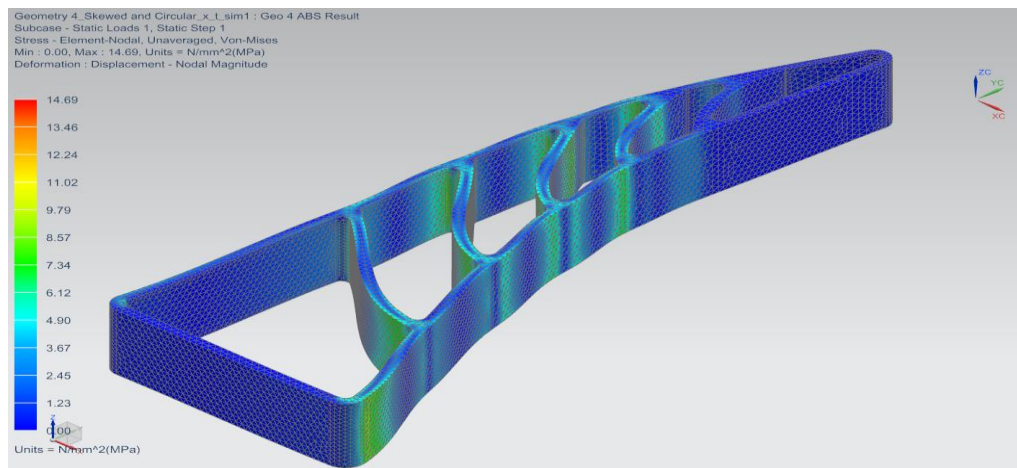


APPENDIX C.7: Concept Design Simulation: Geometry 4 ABS Plastic

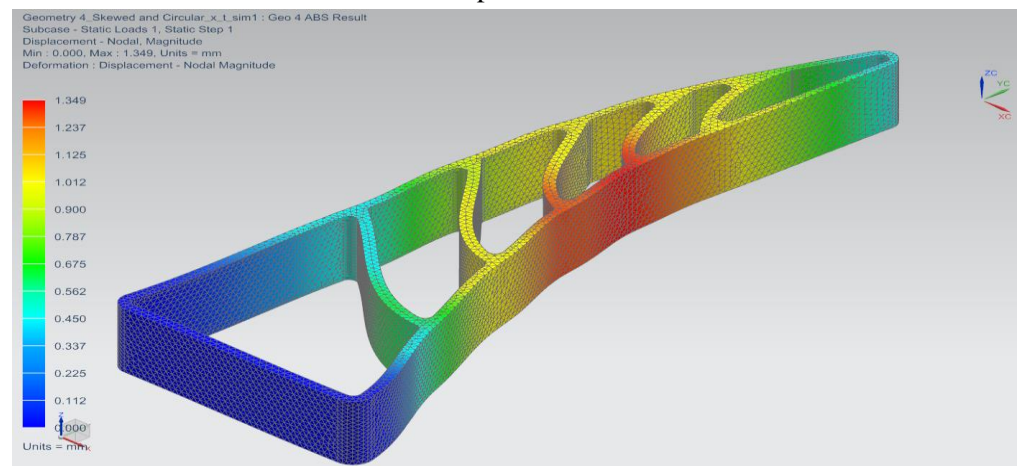
Constraint and load



Von Mises Stress Criteria

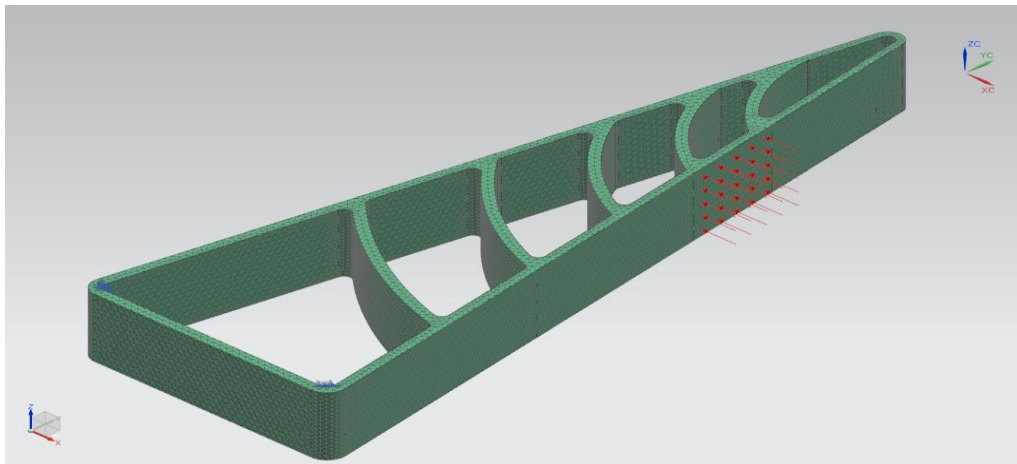


Displacement

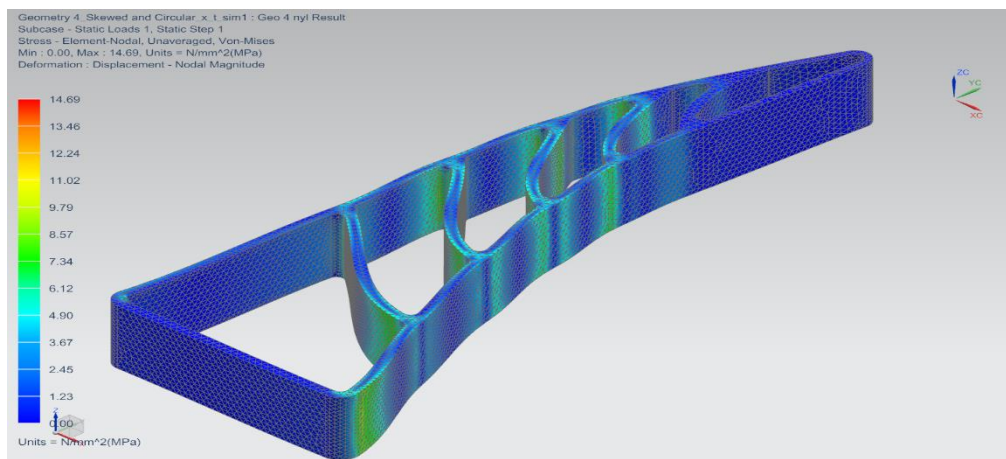


APPENDIX C.8: Concept Design Simulation: Geometry 4 NYLON

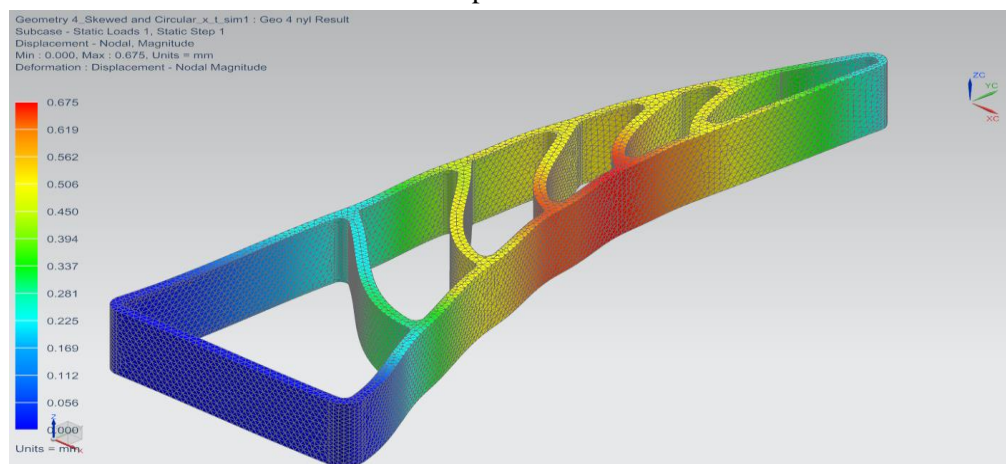
Constraint and load



Von Mises Stress Criteria



Displacement



APPENDIX D: Testing

APPENDIX D.1: Sensor Calibration Data

SENSOR 1

Mass value (g)	Voltage (mV)
0	0
55	1155
100	2249
200	2563
300	2873
400	3115
500	3193
600	3569
700	3597
800	3649
900	3735
1000	3773

SENSOR 2

Mass value (g)	Voltage (mV)
0	0
55	1191
100	1913
200	2709
300	3274
400	3479
500	3628
600	3672
700	3770
800	3791
900	3803
1000	3864

SENSOR 3

Mass value (g)	Voltage (mV)
0	0
55	1924
100	2448
200	2779
300	3086
400	3312
500	3571
600	3732
700	3801
800	3867
900	3886
1000	3912

SENSOR 4

Mass value (g)	Voltage (mV)
0	0
55	1033
100	2116
200	2854
300	3186
400	3447
500	3606
600	3689
700	3744
800	3770
900	3787
1000	3797

APPENDIX D.2: Test Phase 1: Test Mass

Description	Value
Sample Test Weight (g)	2435.00
Plastic Test Holder (g)	37.80
Starting Mass (g)	1629.20
Incremental Mass Sensitivity (g)	100.00

APPENDIX D.3: Test Phase 1: 3-Finger - Geometry 1

Test run number	Mass value (g)
1	2472.50
2	1868.50
3	2472.50
4	2170.20
5	2069.50
6	2170.30
7	2170.40
8	2069.70
9	2472.40
10	1666.80
11	2371.70
12	2069.60
13	2371.50
14	1969.10
15	2271.10
Average	2177.05
Standard deviation (Repeatability)	236.03
Repeatability Percentage	89.16%

APPENDIX D.4: Test Phase 1: 3- Finger - Geometry 2

Test run number	Mass value (g)
1	2271.20
2	2170.40
3	2371.80
4	2170.50
5	2069.50
6	2371.70
7	2472.60
8	2472.50
9	2069.60
10	2170.50
11	2271.20
12	2472.70
13	2371.90
14	2472.60
15	2271.20
Average	2297.99
Standard deviation (Repeatability)	144.82
Repeatability Percentage	93.70%

APPENDIX D.5: Test Phase 1: 3-Finger - Geometry 3

Test run number	Mass value (g)
1	2472.60
2	2472.70
3	2472.70
4	2170.60
5	2472.60
6	2372.00
7	2472.60
8	2472.70
9	1969.00
10	2472.70
11	2472.70
12	2170.50
13	2069.50
14	2170.40
15	2371.80
Average	2338.34
Standard deviation (Repeatability)	177.24
Repeatability Percentage	92.42%

APPENDIX D.6: Test Phase 1: 3-Finger - Geometry 4

Test run number	Mass value (g)
1	2472.60
2	2472.60
3	2371.90
4	2371.80
5	2472.60
6	2472.60
7	2472.60
8	2371.80
9	2472.70
10	2371.80
11	2472.70
12	2472.50
13	2371.90
14	2271.10
15	2371.80
Average	2418.87
Standard deviation (Repeatability)	64.49
Repeatability Percentage	97.33%

APPENDIX D.7: Test Phase 1: 4-Finger - Geometry 1

Test run number	Mass value (g)
1	2472.50
2	2472.20
3	2472.40
4	2472.50
5	2170.30
6	2472.40
7	2371.70
8	2472.50
9	2170.30
10	2270.70
11	2472.30
12	2170.00
13	2069.50
14	2472.40
15	2170.30
Average	2344.80
Standard deviation (Repeatability)	154.50
Repeatability Percentage	93.41%

APPENDIX D.8: Test Phase 1: 4-Finger - Geometry 2

Test run number	Mass value (g)
1	2472.60
2	2472.40
3	2472.70
4	2371.80
5	2472.60
6	2271.60
7	2472.60
8	2371.70
9	2472.60
10	2472.60
11	2371.90
12	2472.40
13	2271.30
14	2472.60
15	2371.90
Average	2418.89
Standard deviation (Repeatability)	74.77
Repeatability Percentage	96.91%

APPENDIX D.9: Test Phase 1: 4-Finger - Geometry 3

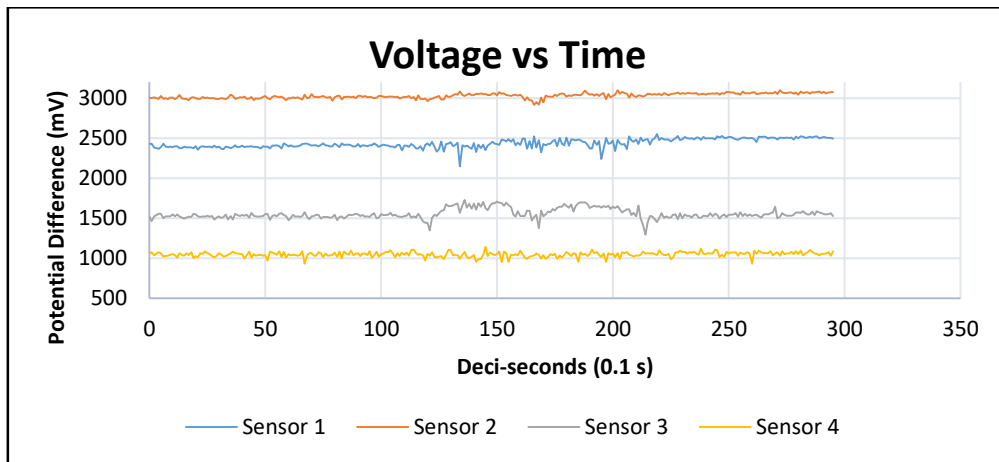
Test run number	Mass value (g)
1	2472.50
2	2371.80
3	2170.30
4	2472.50
5	2472.50
6	2472.50
7	2472.60
8	2371.70
9	2271.10
10	2371.80
11	2472.50
12	2270.90
13	2472.50
14	2371.90
15	2472.50
Average	2398.64
Standard deviation (Repeatability)	96.83
Repeatability Percentage	95.96%

APPENDIX D.10: Test Phase 1: 4-Finger - Geometry 4

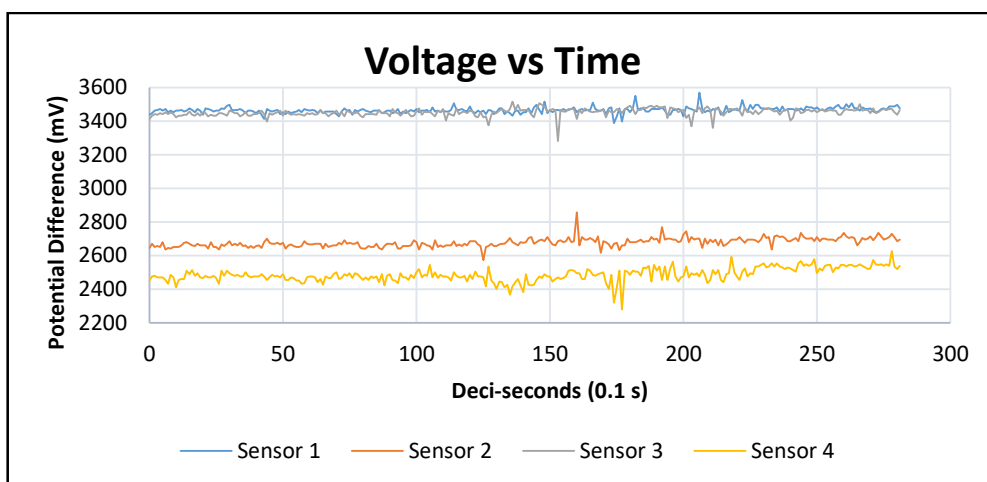
Test run number	Mass value (g)
1	2472.60
2	2472.70
3	2472.60
4	2472.40
5	2472.60
6	2472.60
7	2371.90
8	2472.70
9	2472.40
10	2472.60
11	2472.60
12	2371.90
13	2472.60
14	2472.60
15	2472.40
Average	2459.15
Standard deviation (Repeatability)	35.42
Repeatability Percentage	98.56%

APPENDIX D.11: Test Phase 2: 4-Finger –Geometry 4 Initial Test Cricket Ball

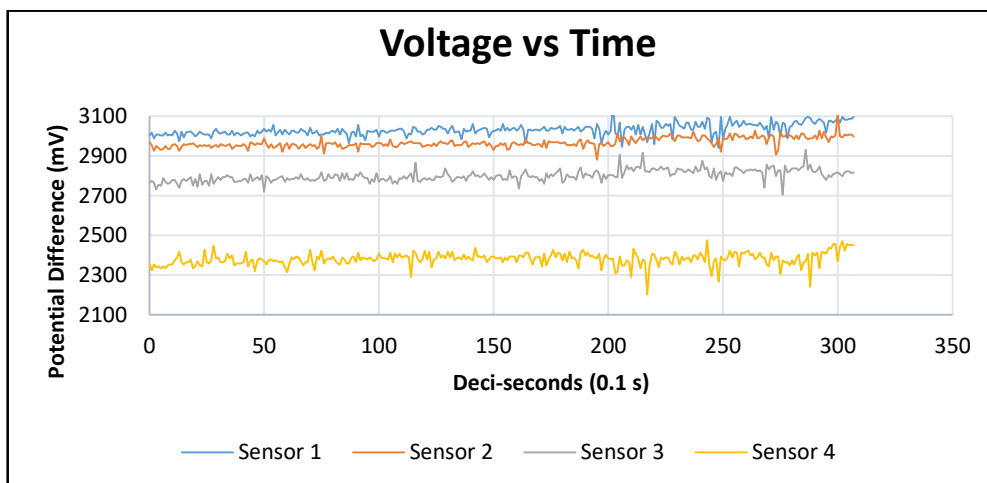
RUN 1



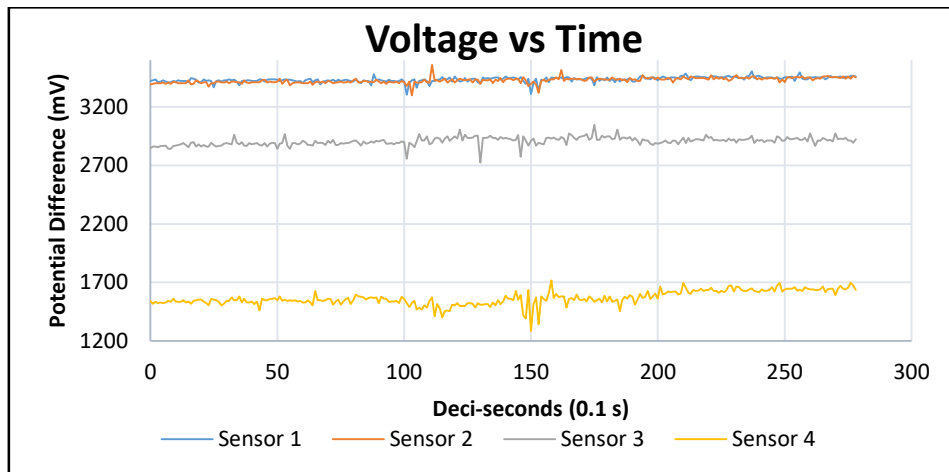
RUN 2



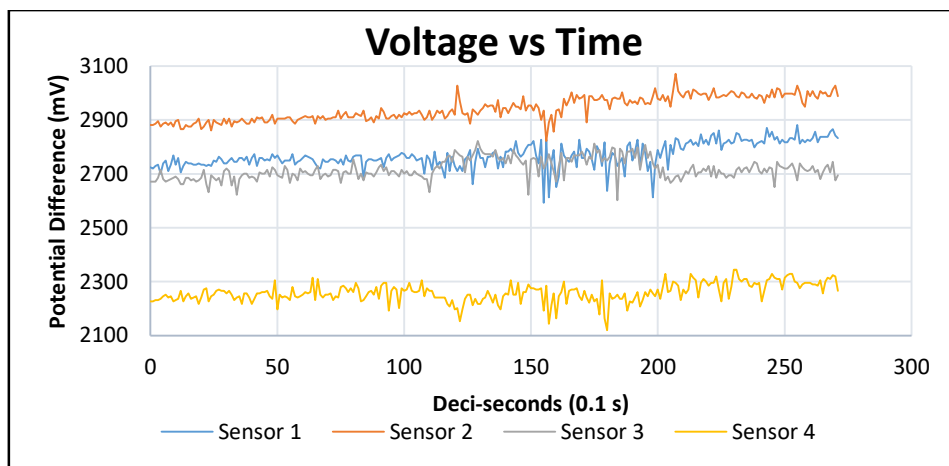
RUN 3



RUN 4

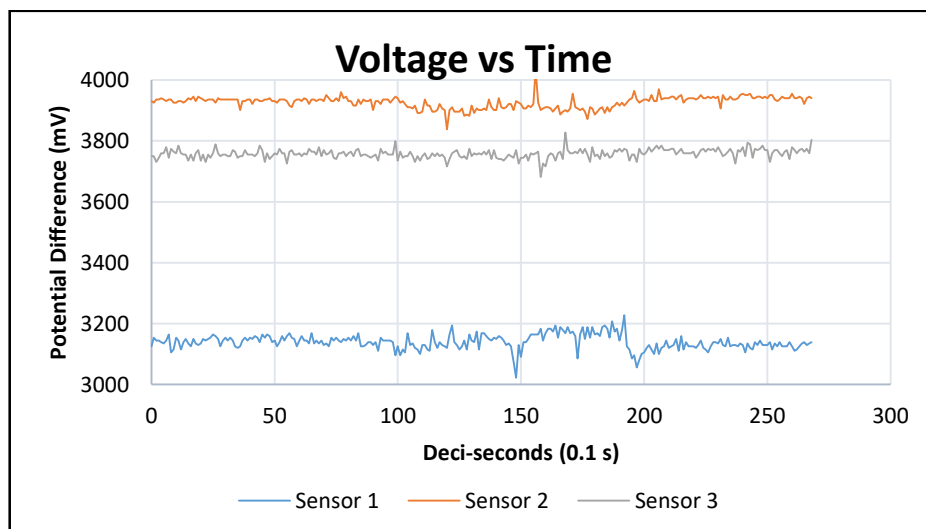


RUN 5

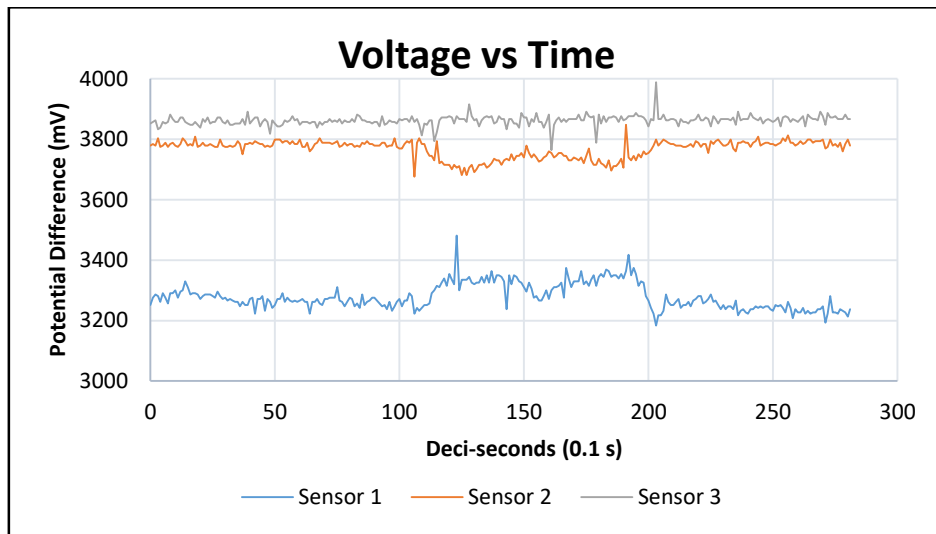


APPENDIX D.12: Test Phase 2: 3-Finger - Geometry 1

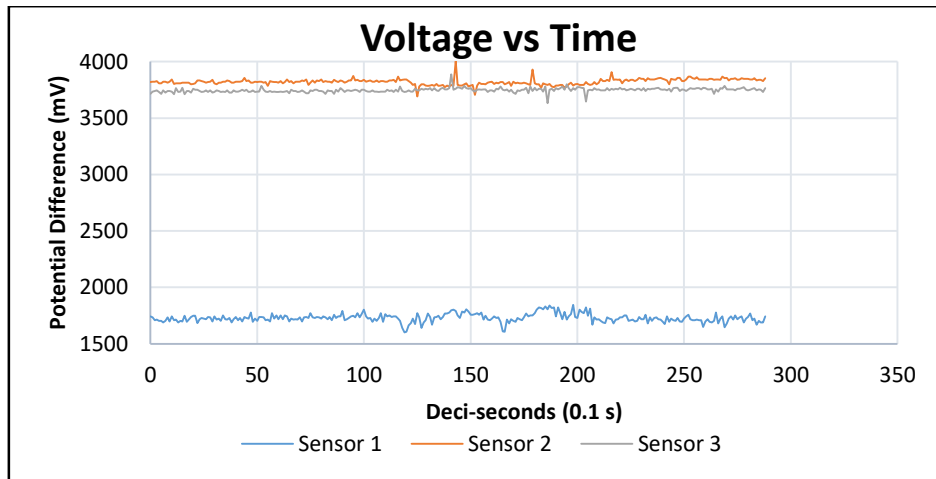
RUN 1



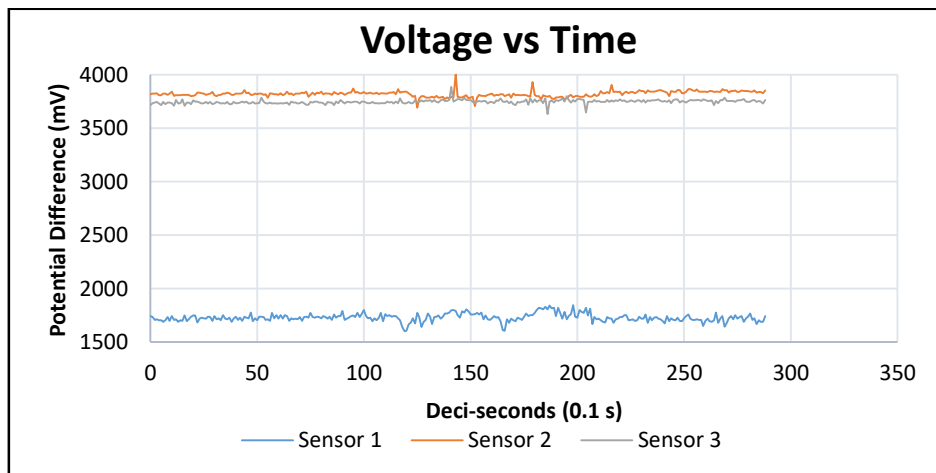
RUN 2



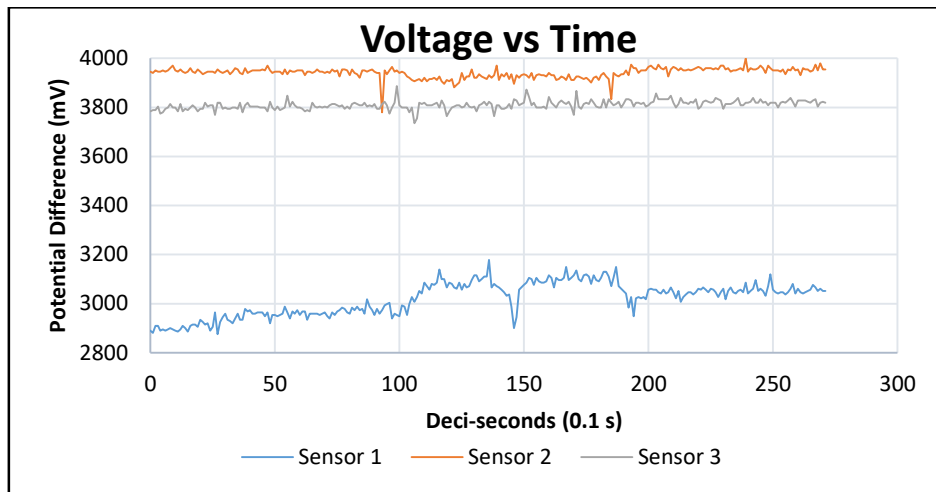
RUN 3



RUN 4

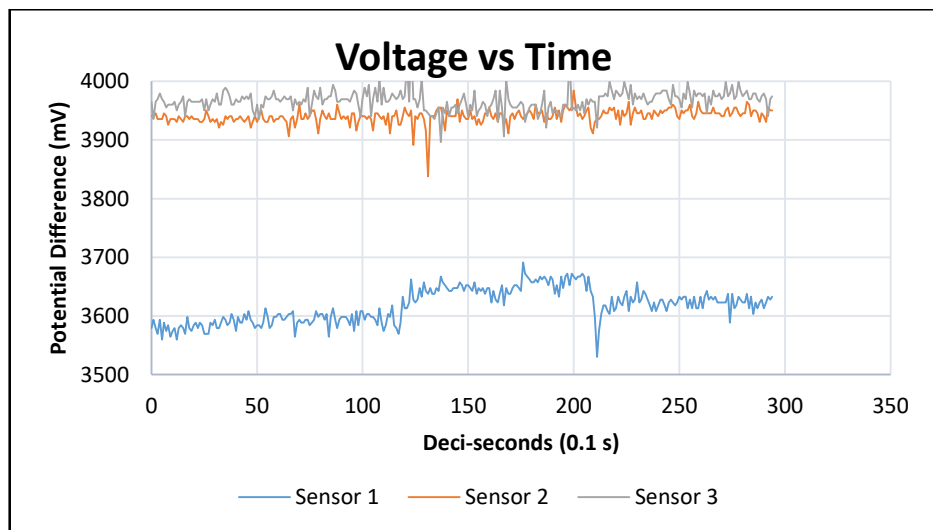


RUN 5

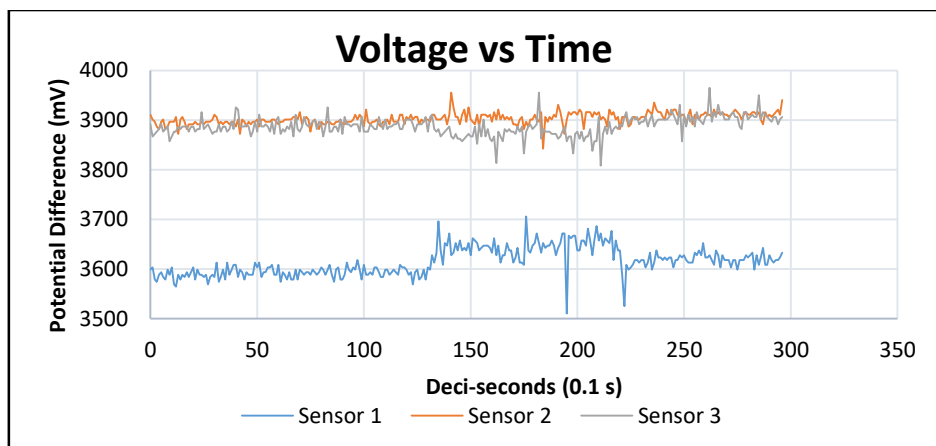


APPENDIX D.13: Test Phase 2: 3-Finger - Geometry 2

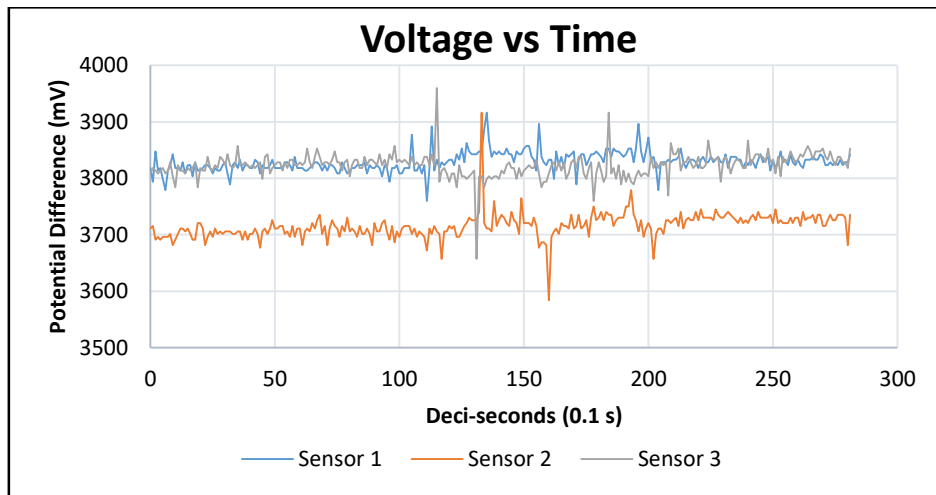
RUN 1



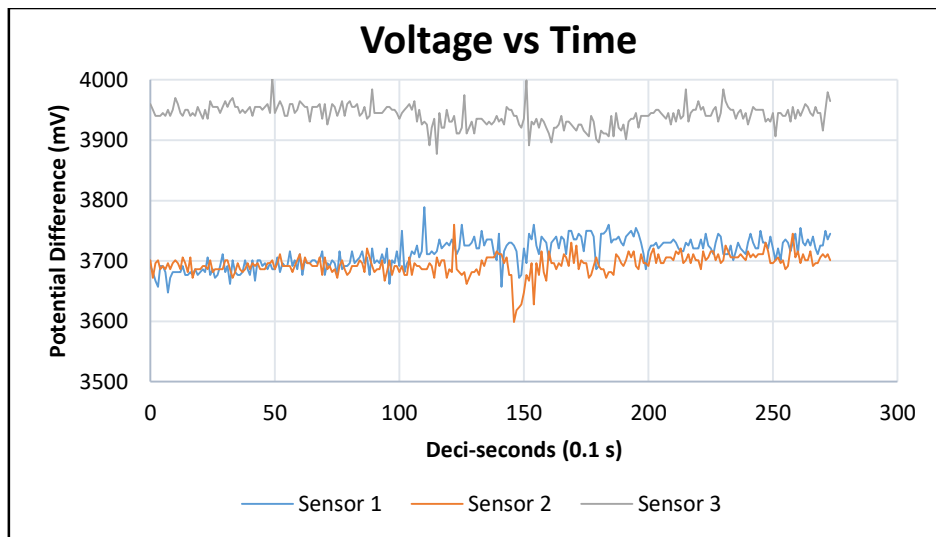
RUN 2



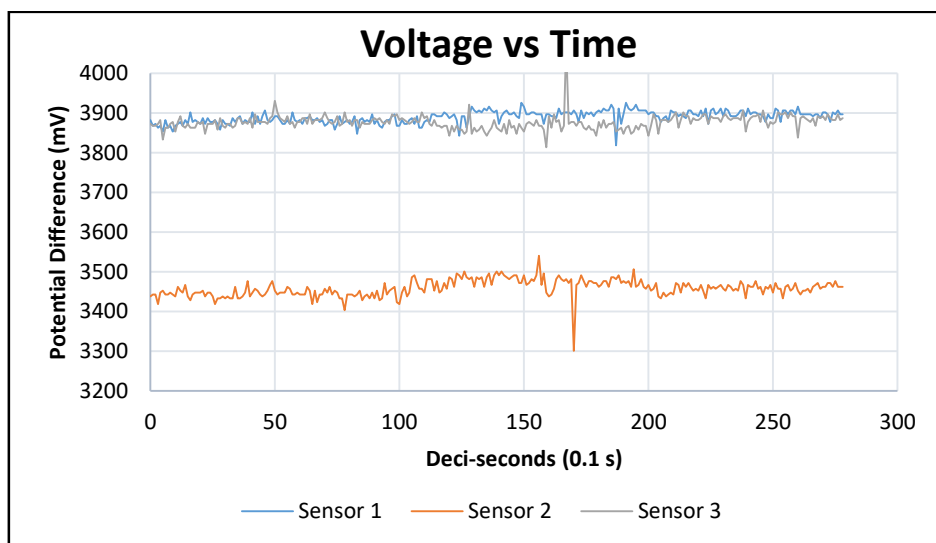
RUN 3



RUN 4

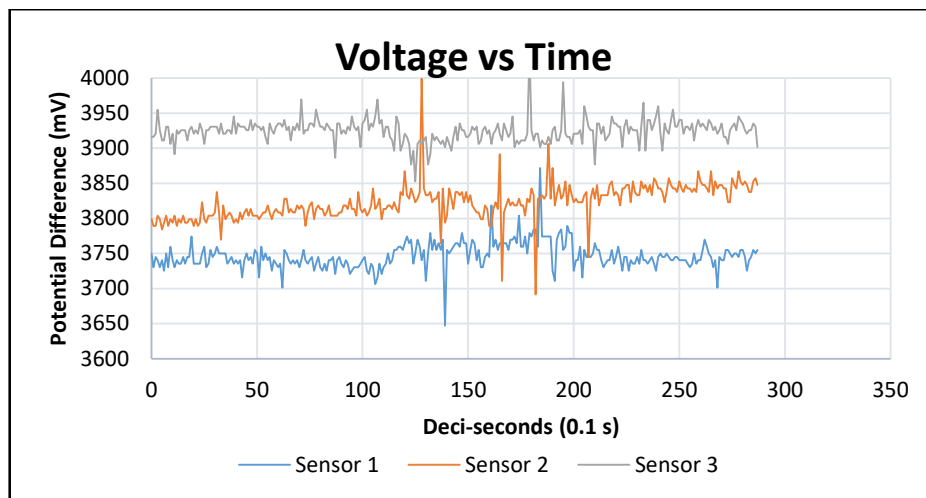


RUN 5

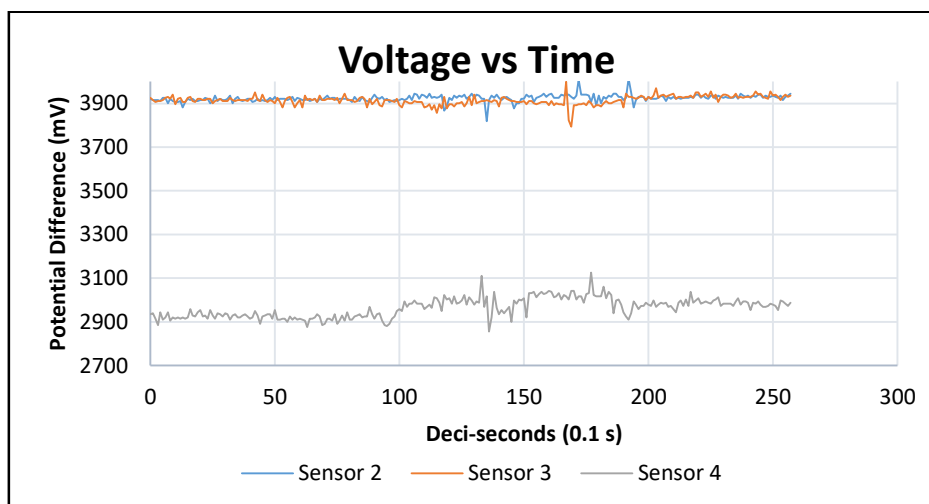


APPENDIX D.14: Test Phase 2: 3-Finger - Geometry 3

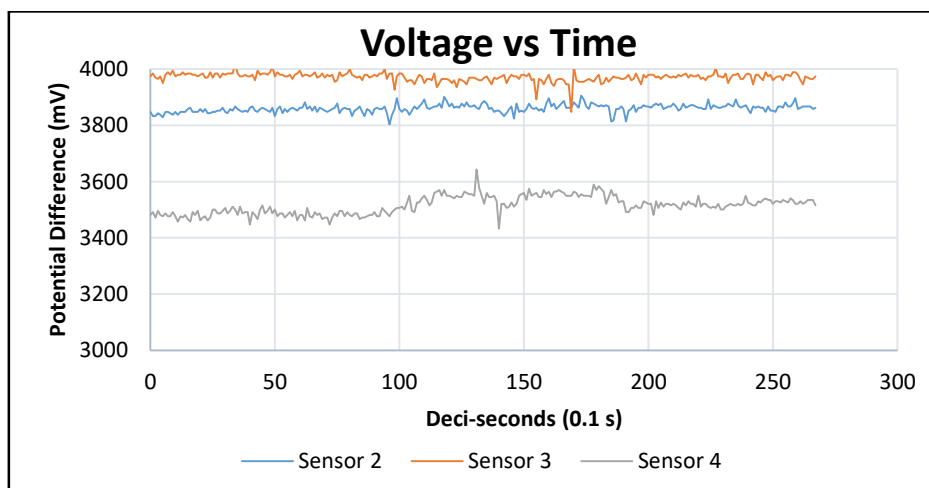
RUN 1



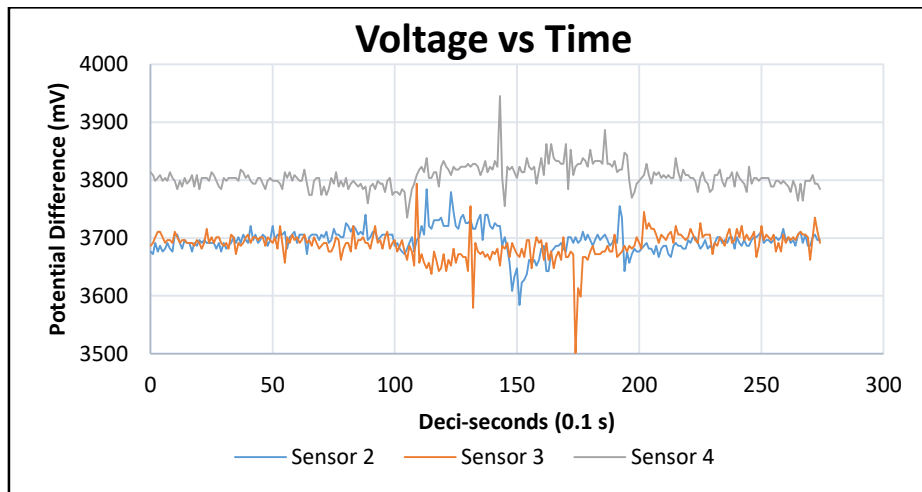
RUN 2



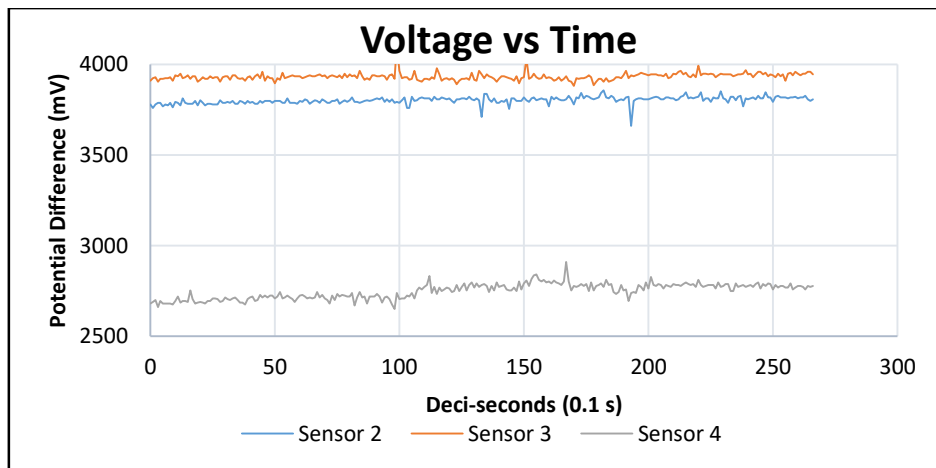
RUN 3



RUN 4

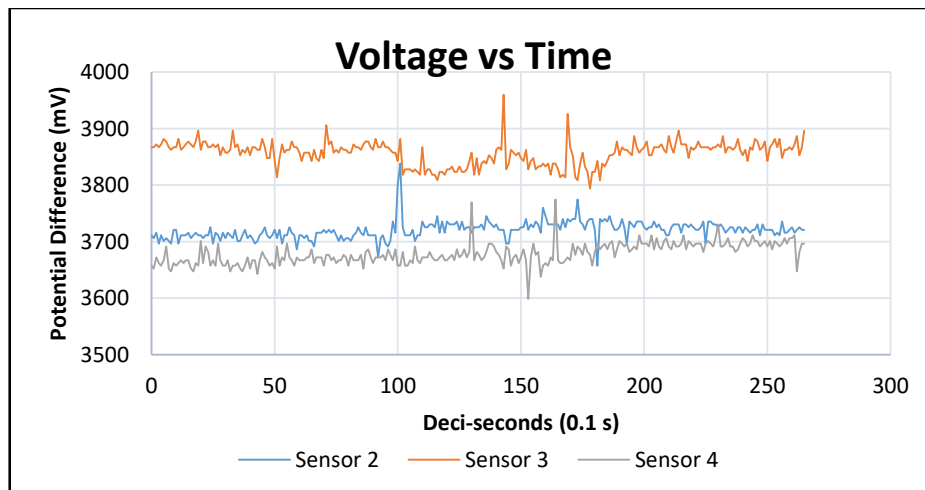


RUN 5

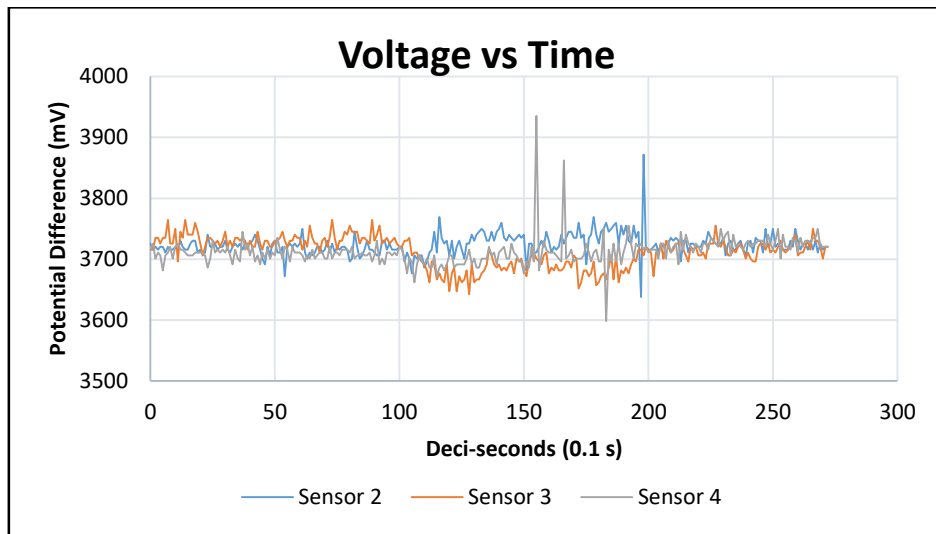


APPENDIX D.15: Test Phase 2: 3-Finger - Geometry 4

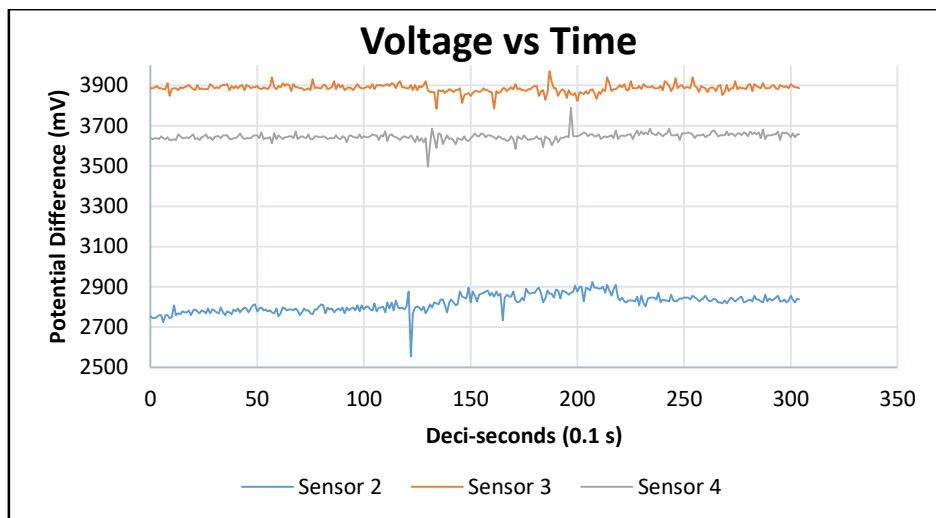
RUN 1



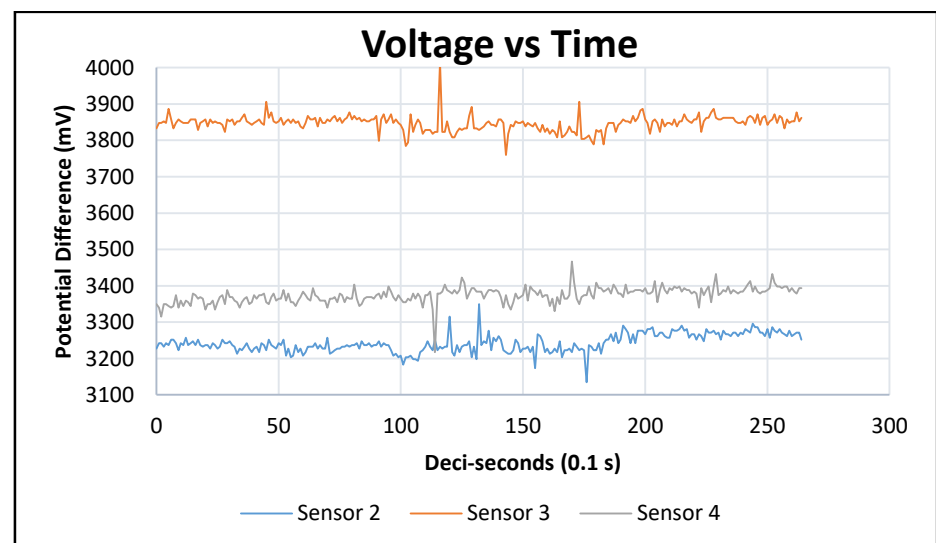
RUN 2



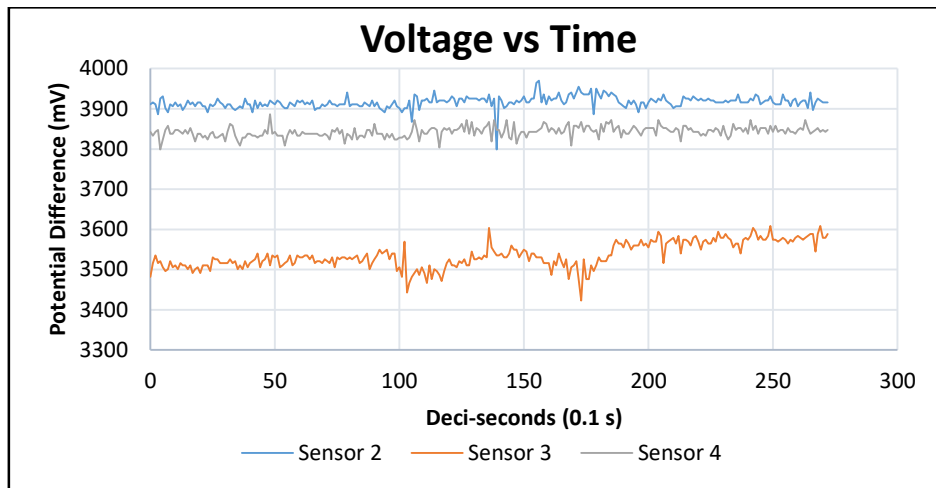
RUN 3



RUN 4

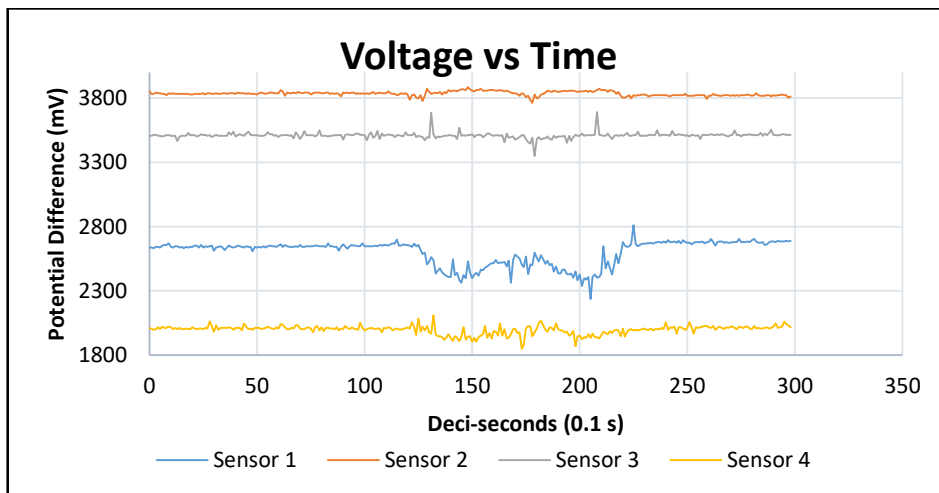


RUN 5

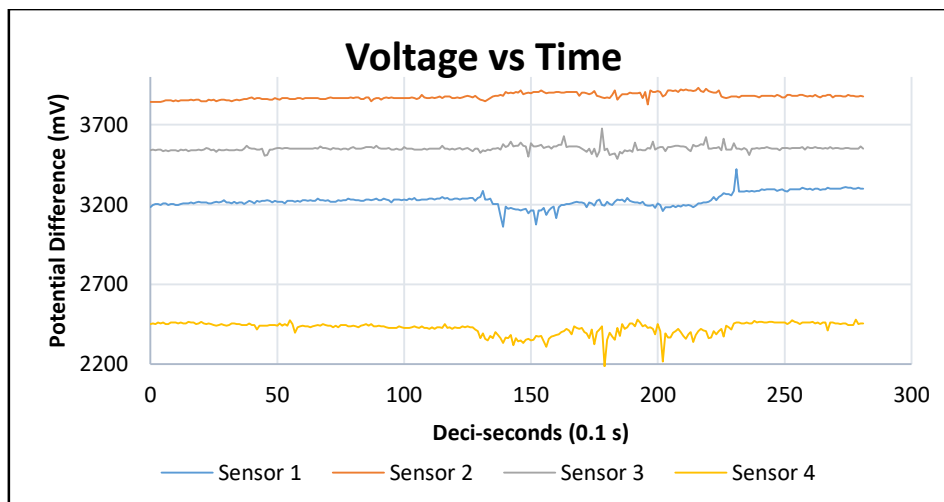


APPENDIX D.16: Test Phase 2: 4-Finger - Geometry 1

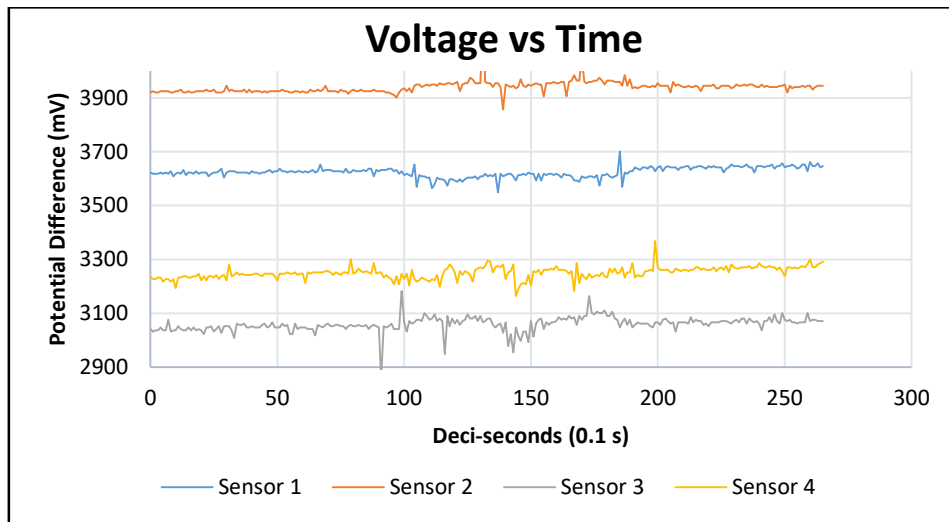
RUN 1



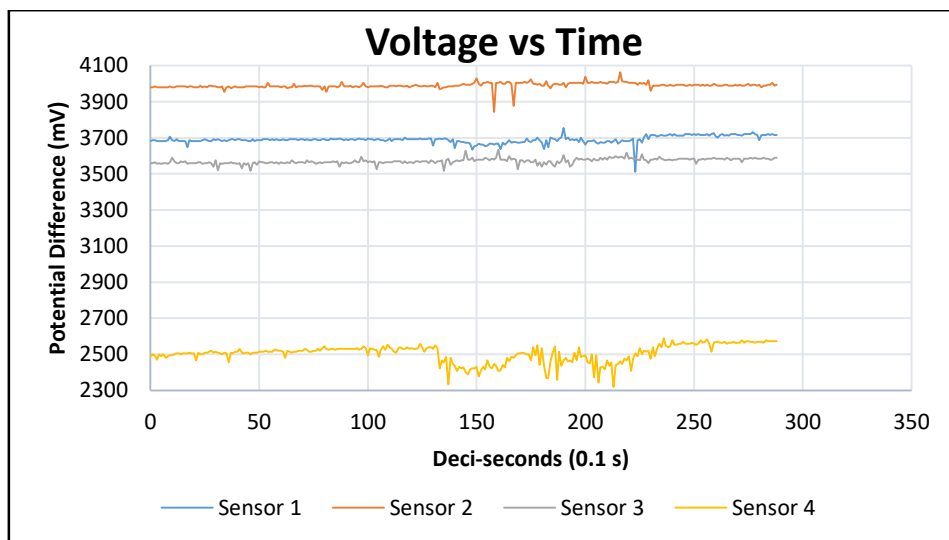
RUN 2



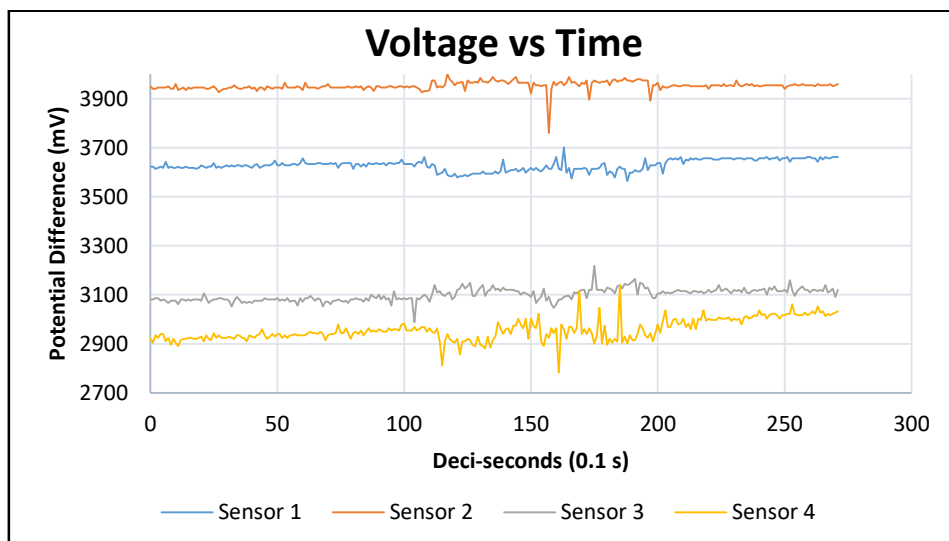
RUN 3



RUN 4

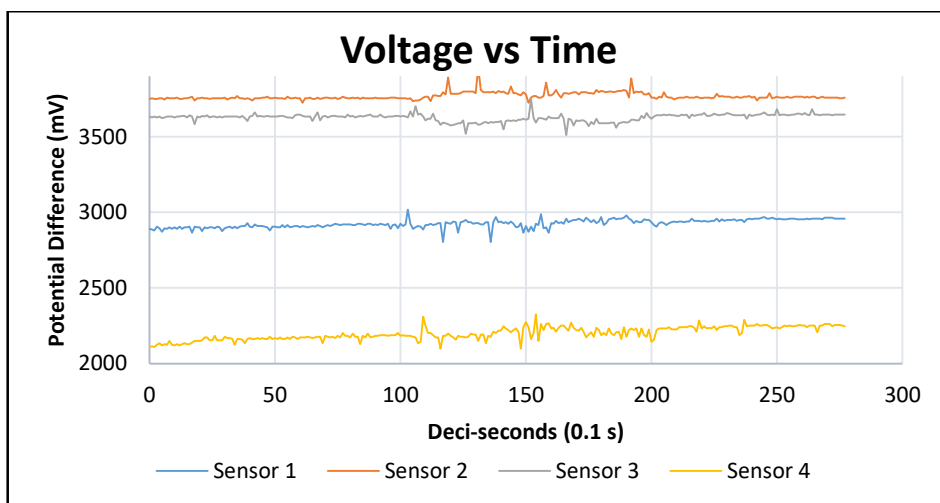


RUN 5

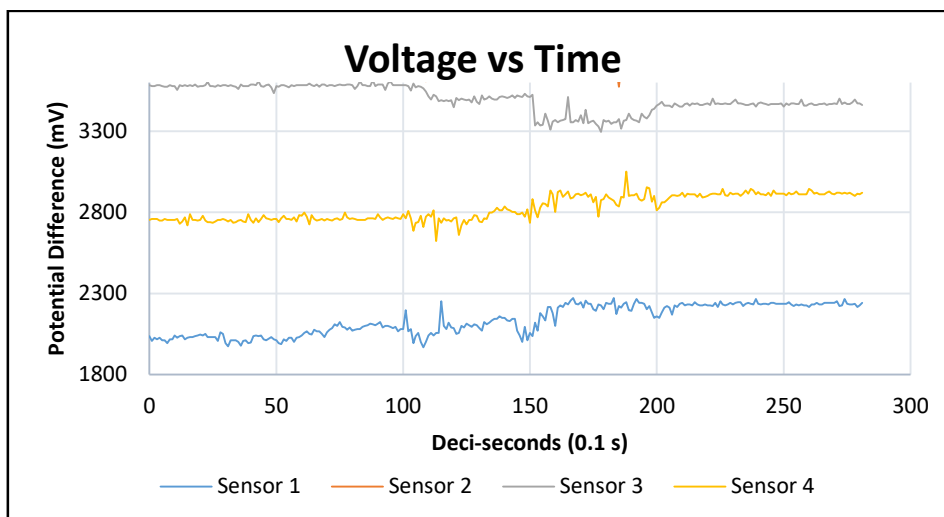


APPENDIX D.17: Test Phase 2: 4-Finger - Geometry 2

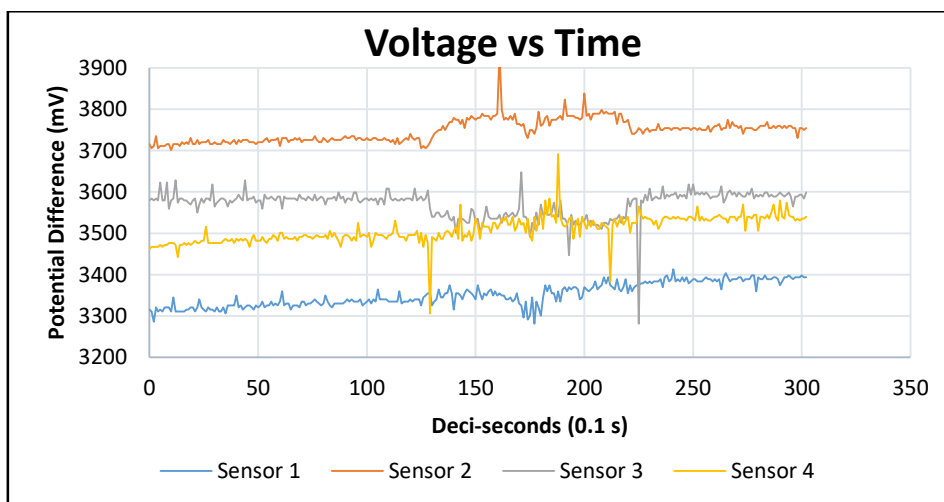
RUN 1



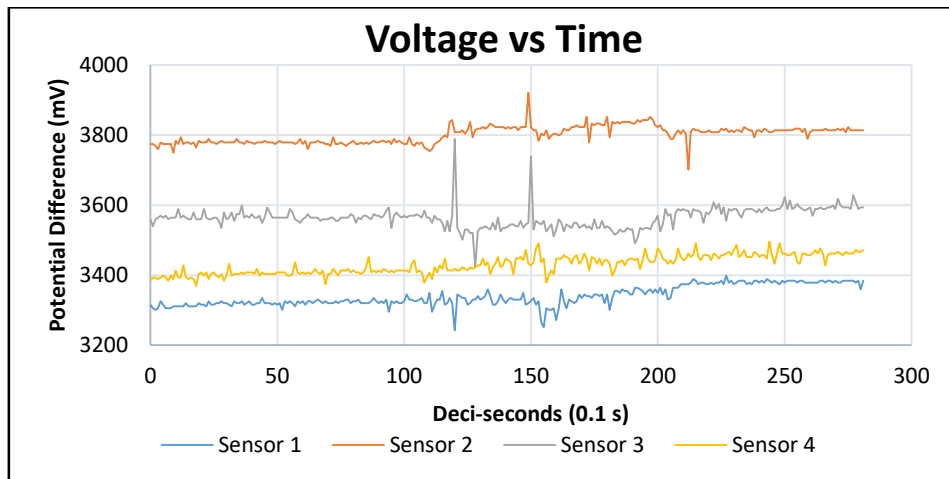
RUN 2



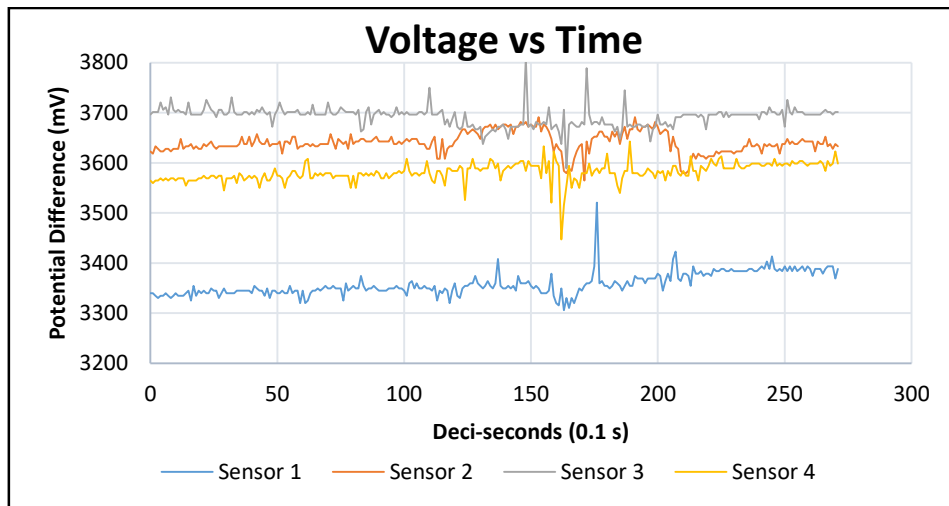
RUN 3



RUN 4

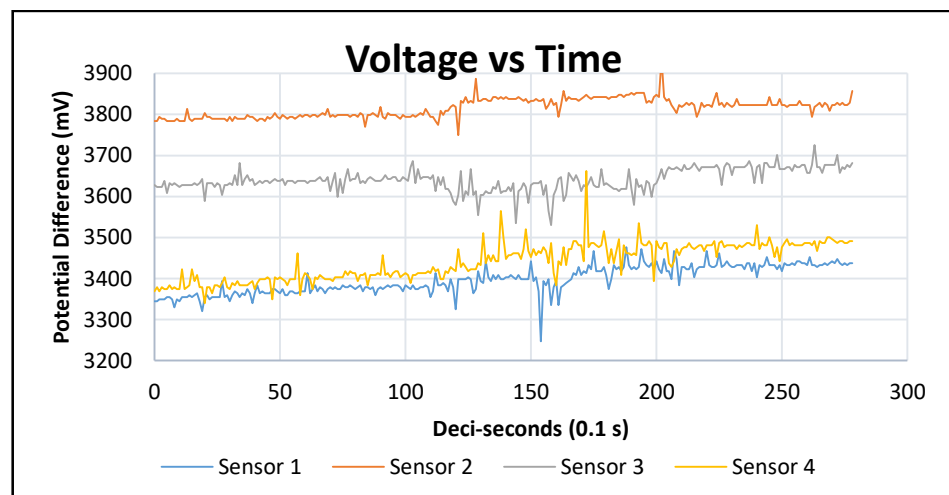


RUN 5

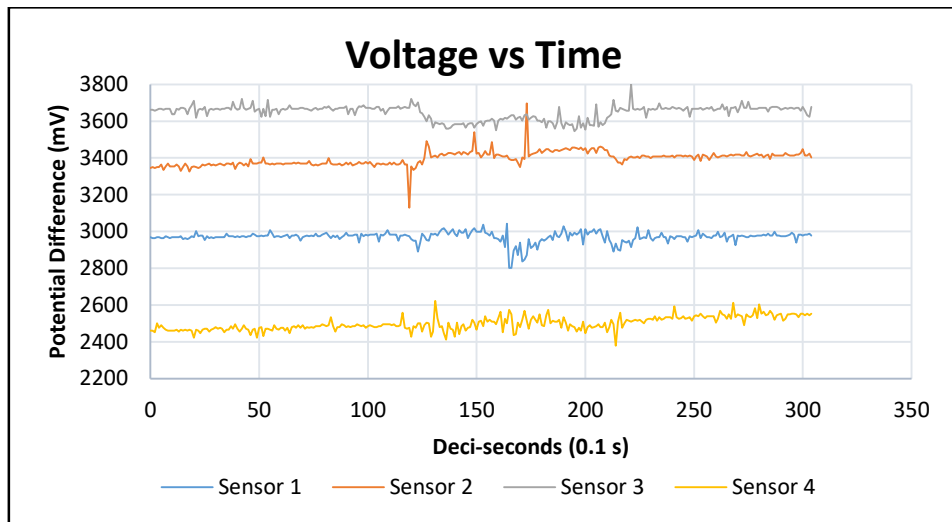


APPENDIX D.18: Test Phase 2: 4-Finger - Geometry 3

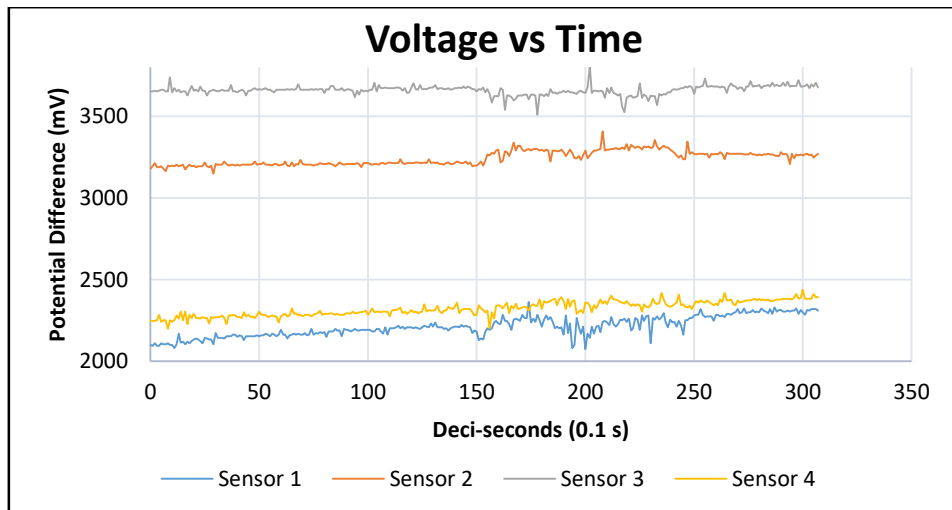
RUN 1



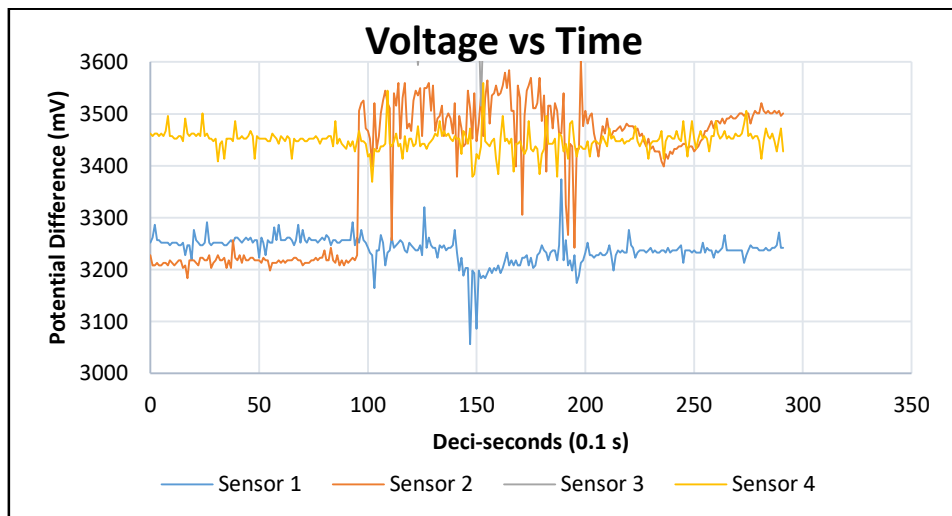
RUN 2



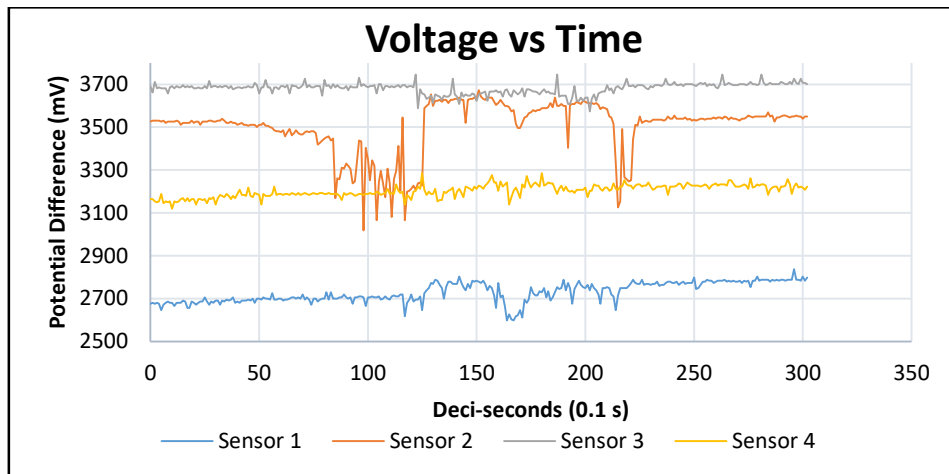
RUN 3



RUN 4

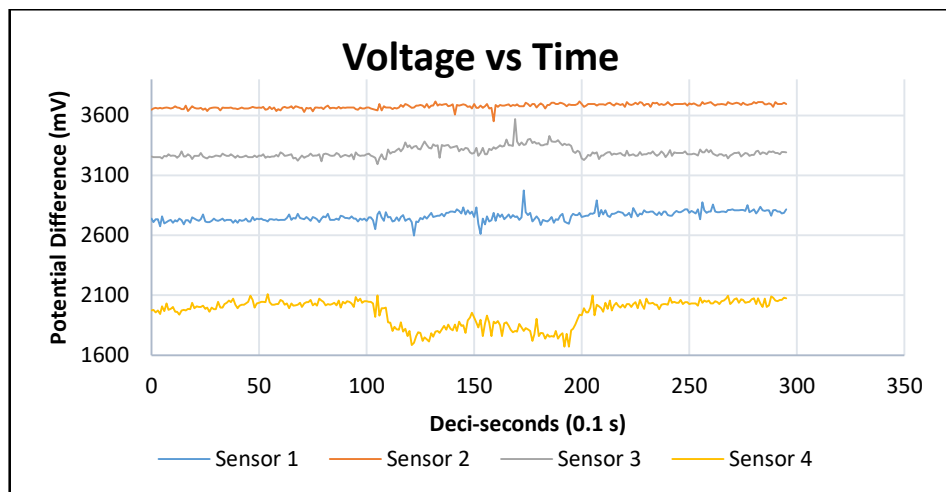


RUN 5

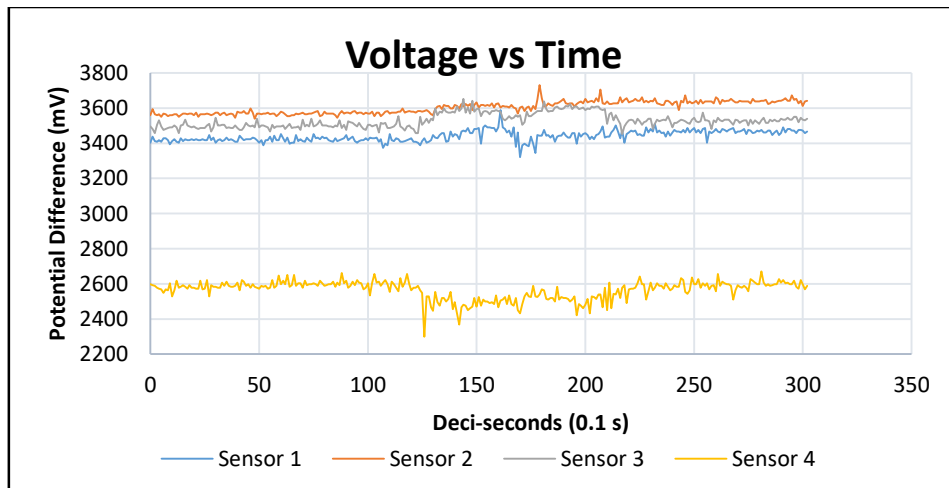


APPENDIX D.19: Test Phase 2: 4-Finger - Geometry 4

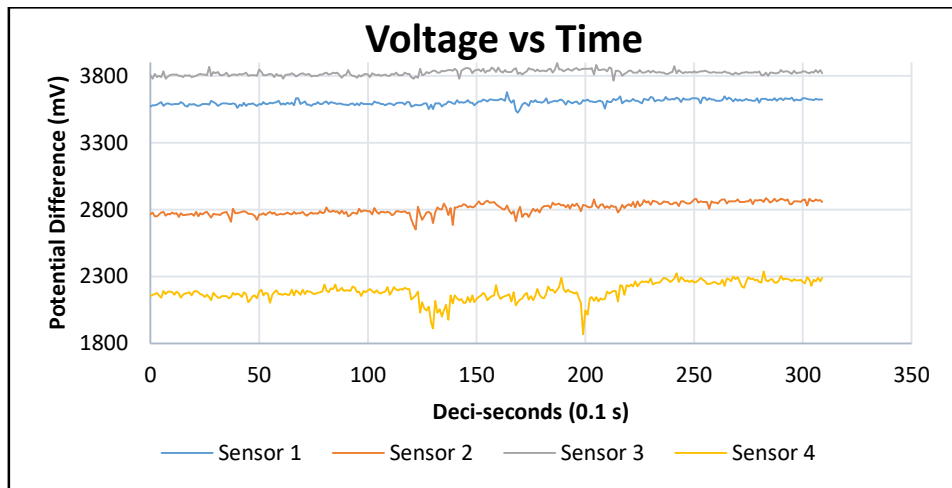
RUN 1



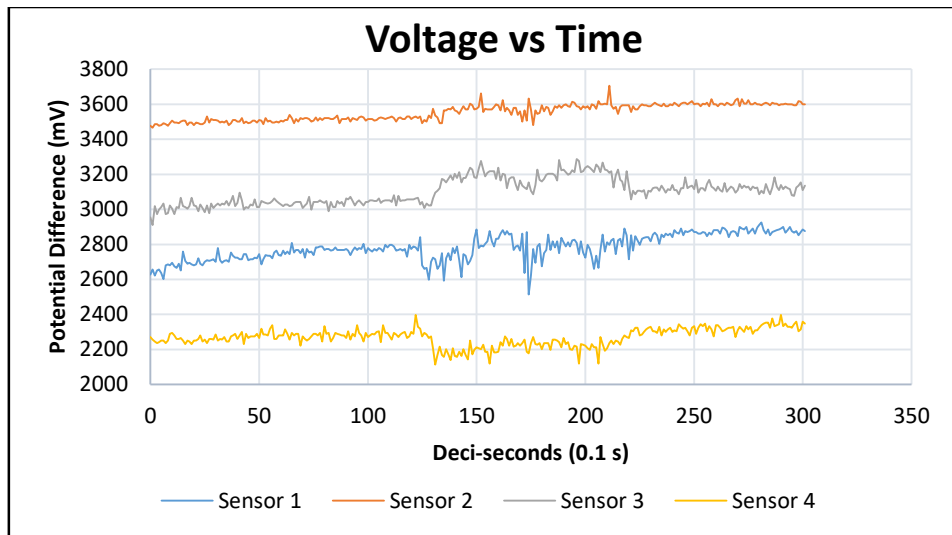
RUN 2



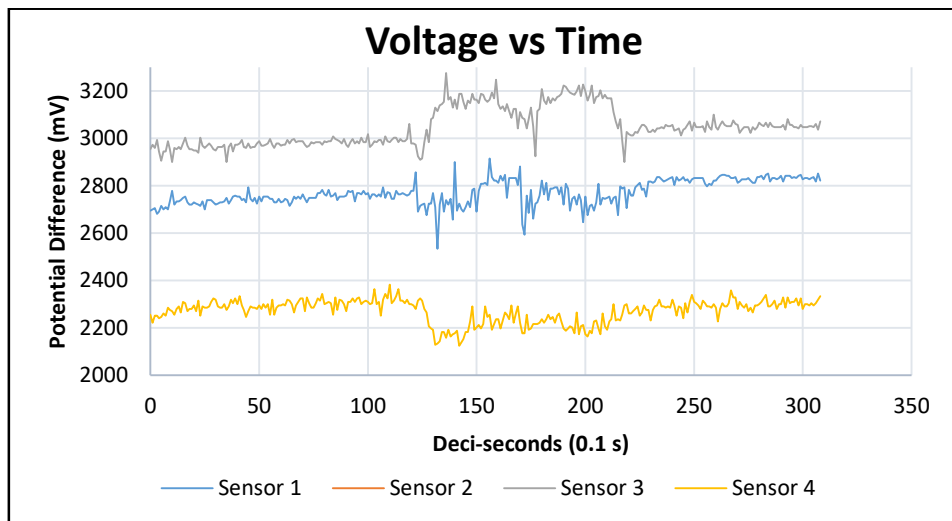
RUN 3



RUN 4



RUN 5



APPENDIX E: System Code

APPENDIX E.1: Conceptual Path Planning Code

The program was written for robotic simulation of the selected arm for path planning for experimentation purposes. The path followed is the path line through which the tool/gripper moves to each target in the conceptual design. The program was generated for programming of a PLC.

```
MEMORY_SIZE = 0;
PROTECT      = READ_WRITE;
TCD: STACK_SIZE = 0,
    TASK_PRIORITY = 50,
TIME_SLICE = 0,
BUSY_LAMP_OFF = 0,
ABORT_REQUEST = 0,
PAUSE_REQUEST = 0;
DEFAULT_GROUP = 1,*,*,*,*,*,*
CONTROL_CODE = 00000000 00000000;
/MN
1: UTOOL_NUM=1;
2: UFRAME_NUM=1;
3: PR[10,1]=0.000 ;
4: PR[10,2]=0.000 ;
5: PR[10,3]=0.000 ;
6: PR[10,4]=0.000 ;
7: PR[10,5]=0.000 ;
8: PR[10,6]=0.000 ;
9: UFRAME[1]=PR[10] ;
10: J P[1] 50% FINE ;
11: J P[2] 50% FINE ;
12: J P[3] 50% FINE ;
13: J P[4] 50% FINE ;
/POS
P[1]{
GP1:
    UF : 1, UT : 1,          CONFIG : 'F U T, 0, 0, 0',
    X = 0.000 mm, Y = -1060.000 mm, Z = 450.000 mm,
    W = -177.109 deg, P = -2.687 deg, R = 0.232 deg
};
P[2]{
GP1:
    UF : 1, UT : 1,          CONFIG : 'F U T, 0, 1, 0',
    X = -1020.000 mm, Y = -0.000 mm, Z = 450.000 mm,
    W = -177.109 deg, P = -2.687 deg, R = 0.232 deg
};
P[3]{
GP1:
    UF : 1, UT : 1,          CONFIG : 'F D T, 0, 1, 0',
    X = -1120.000 mm, Y = 0.000 mm, Z = -390.000 mm,
    W = -177.109 deg, P = -2.687 deg, R = 0.232 deg;
};
P[4]{
GP1:
    UF : 1, UT : 1,          CONFIG : 'F U T, 0, 0, 0',
    X = 0.000 mm, Y = -1060.000 mm, Z = 450.000 mm,
    W = -177.109 deg, P = -2.687 deg, R = 0.232 deg
};
/END
```

APPENDIX E.2: Sensor System Arduino® Code

```
void setup() {  
  // put your setup code here, to run once:  
  Serial.begin(9600);  
}  
  
void loop() {  
  // put your main code here, to run repeatedly:  
  int val = analogRead(0);  // read the input pin  
  
  float newton = (val / 1024.0) * 100;  
  Serial.print(val);  
  
  Serial.print(" ");  
  int val1 = analogRead(1);  // read the input pin  
  
  float newton1 = (val1 / 1024.0) * 100;  
  Serial.print(val1);  
  
  Serial.print(" ");  
  
  int val2 = analogRead(2);  // read the input pin  
  
  float newton2 = (val2 / 1024.0) * 100;  
  Serial.print(val2);  
  
  Serial.print(" ");  
  
  int val3 = analogRead(3);  // read the input pin  
  
  float newton3 = (val3 / 1024.0) * 100;  
  Serial.println(val3);  
  
  delay(100);  
}
```

APPENDIX E.3: Motor Push-Button Control Arduino® Code

```
int Distance = 0; // Record the number of steps we've taken
int flag = 0;
void setup() {
  pinMode(8, OUTPUT);
  pinMode(9, OUTPUT);
  pinMode(10, INPUT);
  pinMode(11, INPUT);
  digitalWrite(8, LOW);
  digitalWrite(9, LOW);
}
void clkwise(){
  digitalWrite(8, LOW);
  digitalWrite(9, HIGH);
  delayMicroseconds(200);
  digitalWrite(9, LOW);
  delayMicroseconds(200);
  Distance++;
  //if(Distance == 3200){
  //  flag = 1;
  //}
}
void ccntclkwise(){
  digitalWrite(8, HIGH);
  digitalWrite(9, HIGH);
  delayMicroseconds(200);
  digitalWrite(9, LOW);
  delayMicroseconds(200);
  Distance--;
  //if(Distance == 0){
  //  flag = 0;
  //}
}
void loop() {
  if(digitalRead(10)==0)
  {
    delay(10);
    if(digitalRead(10)==0){
      for(int i = 0; i < 100; i++){
        clkwise();
      }
    }
  }
  if(digitalRead(11)==0)
  {
    delay(10);
    if(digitalRead(11)==0){
      for(int i = 0; i < 100; i++){
        ccntclkwise();
      }
    }
  }
}
```